Ghent University

Faculty of Pharmaceutical Sciences

EVALUATION OF FAST SPECTROSCOPIC ANALYSIS TECHNIQUES FOR FREEZE-DRIED LIVE, ATTENUATED VIRUS VACCINES

LAURENT HANSEN

Biologist

Thesis submitted to obtain the degree of Doctor in Pharmaceutical Sciences

2016

Promoter: Prof. Dr. Thomas De Beer

Laboratory of Pharmaceutical Process Analytical Technology, Ghent University

Industrial promoter: Dr. Rim Daoussi

VMR&D, Biological Development, Zoetis

Ghent, February 18th, 2016

The author   The promoter   The industrial promoter

Laurent Hansen   Prof. Dr. Thomas De Beer   Dr. Rim Daoussi

ACKNOWLEDGEMENTS

For the nice working atmosphere, the support, the help, and the scientific discussions, I would like to thank all colleagues, former and present, of the PAT lab. Pieter-Jan (PJ), thank you for all your questions. To be honest, I was always afraid of not being able to answer you but luckily I always found something. And please, do not change your laugh...

I also would like to thank all colleagues from the laboratory of Pharmaceutical Technology for having made the lab an enjoyable place to work. Your help, scientific and non-scientific discussions were greatly appreciated. Ilse and Katharine, thank you for having took care of the administrative tasks. A special thank to Marc, my first office-colleague who kept me updated with the latest news of Radio 2 every hour. Thank you also to Christine, my second office-colleague who took well care of me. Your daily Dutch lessons were greatly appreciated and largely contributed to the significant improvement of my Dutch.

My deepest gratitude goes to my family, my grandparents and more particularly to my parents and my brother Christophe. Thank you for everything, your support, confidence, encouragements and all opportunities you have given me.

And now is the time to thank Julie. Where should I start? Thank you for having always been present, for your encouragements during the difficult moments, for your advices, for the little things that brighten up my days and for having built with me the best place of the World. Eléna, my "kapoentje", thank you for entering into my life, thank you for your smiles and laugh, thank you for all happiness you give us every day.

Merci,

Laurent

TABLE OF CONTENTS

Table of contents

LIST OF ABBREVIATIONS

API	active pharmaceutical ingredient
ATR	attenuated total reflectance
BCG	bacillus Calmette-Guerin
CCR	correct classification rate
CD	circular dichroism
CGMPs	pharmaceutical current good manufacturing practices
CJD	Creutzefeld-Jakob disease
CM	capacitance manometer
CMLV	camelpox virus
CPPs	critical process parameters
CQAs	critical quality attributes
DHV	duck viral hepatitis virus
DNA	deoxyribonucleic acid
DOE	design of experiments
DSC	differential scanning calorimetry
EMA	European Medicines Agency
FDA	Food and Drug Administration
FTIR	Fourier transform infrared
HA	haemagglutinin
HBS	hepes buffered saline
HES	hydroxyethyl starch
hPIV3	human parainfluenza virus 3

HSV	Herpes simplex virus
ID	identity
ICH	International Conference on Harmonization
IgG	imunoglobuline G
IMARC	international market analysis research and consulting
IR	infrared
MDSC	modulated differential scanning calorimetry
MTM	manometric temperature measurement
NCE	new chemical entities
NIAD	National Institute of Allergy and Infectious Diseases
NIR	near infrared
OPLS	orthogonal partial least squares
OPV	oral polio vaccine
PAT	process analytical technology
PBS	phosphate buffered saline
PC	principal component
PCA	principal component analysis
PEG	polyethylene glycol
PLSDA	partial least squares discriminant analysis
PPR	*peste des petits ruminants*
PrP^{SC}	scarpie-prion-protein
QbD	quality by design
RGA	residual gas analyzer
RMSEP	root mean square error of prediction
RNA	ribonucleic acid

RP   rinderpest

RSV   respiratory syncytial virus

RTD   resistance temperature detector

Tc   collapse temperature

TDLAS   tunable diode laser absorption spectroscopy

TEMPRIS   temperature remote interrogation system

Teu   eutectic temperature

Tg   glass transition temperature

Tg'   glass transition temperature of the maximally freeze-concentrated

Tm   melting point

SFSTP   Société française des sciences et techniques pharmaceutiques

SG   savitzky golay

SIMCA   soft independent modelling of class analogy

SNV   standard normal variate

WHO   World Health Organization

CHAPTER 1

INTRODUCTION AND OBJECTIVES

CHAPTER 1

INTRODUCTION AND OBJECTIVES

Freeze-drying, also termed "lyophilization", is a low-temperature drying process employed to convert solutions of (heat-)labile materials into solids of sufficient stability for distribution and storage [1]. From a laboratory curiosity, freeze-drying has evolved to an industrial process in the 1930s, when there was a need to stabilize heat-labile antibiotics and blood products at high quantities [2]. During the last half of the twentieth century the freeze-drying process became a well-established method not only employed to preserve biopharmaceuticals [3] but also to stabilize products in the food industry such as coffee, herbs and fruits. Nowadays, lyophilization is still the preferred stabilization method for biopharmaceuticals since approximately 46% of them are freeze-dried [4]. In the future, to overcome the poor solubility and bioavailability of new developed drugs [3], freeze-drying offers a promising alternative.

Despite its wide use within the pharmaceutical industry, freeze-drying formulation and process development is still mainly accomplished empirically resulting in sub-optimal processes [5]. This is also certainly true for the freeze-drying process development of live virus vaccines for which the formulation is designed by trial-and-error [6]. The lack of analytical tools allowing the evaluation of live, attenuated viruses during the process is one reason for this lack of knowledge [7]. However, since 2004, pharmaceutical industries start to move from their traditional way of process development and product manufacturing towards a new approach, encouraged by the Food and Drug Administration's (FDA) Process Analytical Technology (PAT) initiative [8]. The principal objective of PAT is a better fundamental scientific understanding and control of manufacturing processes. In order to achieve these objectives, several new process analytical technologies are now available or being developed. Among these PAT tools, process analyzers able to provide multivariate information related to biological, chemical and physical attributes of the materials being

processed coupled with multivariate data analysis offer new opportunities to increase the process understanding, formulation and process optimization, and hence process control.

In collaboration with an industrial partner, Zoetis (formerly Pfizer Animal Health), this thesis examines the possibility to use fast and non-destructive spectroscopic tools (i.e., Raman, Near Infrared (NIR) and although being destructive, Fourier Transform Infrared (FTIR)) as process analytical techniques for the analysis of freeze-dried veterinary vaccines.

The different objectives of this thesis are listed below:

- Find out if process analytical techniques can be used to evaluate (and hence understand) live, attenuated viruses and their interactions with other compounds (i.e., stabilizers), in freeze-dried vaccine formulations;
- Using process analytical techniques, increase the understanding of virus destabilization mechanisms during storage;
- Develop and validate chemometric models allowing the prediction of the (or some) end product quality attributes making some traditional time-consuming off-line end product analyses superfluous.

At the beginning of the thesis, both Raman and NIR spectroscopy were evaluated but systematically, the Raman spectra were not interpretable due to fluorescent interferences in the samples under investigation. Therefore, it was decided to mainly focus on NIR spectroscopy. Fourier Transform Infrared (FTIR) spectroscopy was also evaluated. Despite its longer analysis time and the need for sample preparation prior to measurement, FTIR spectroscopy offered advantages compared to NIR spectroscopy, mainly its more detailed level of spectral information (useful to study virus destabilization mechanisms or interactions with other formulation components e.g., during storage).

The objectives of this thesis were elaborated in several chapters. In **chapter 2**, an overview of the freeze-drying process and used processing equipment is provided. **Chapter 3** reviews the current knowledge on the freeze-drying process of live, attenuated virus vaccines. The different stresses that viruses may encounter during the different freeze-drying process steps as well as the different formulation and processing strategies applied to withstand

these stresses are presented. **Chapter 4** summarizes the concept of PAT and discusses the process analytical tools used in this thesis.

Chapters 5 to 9 present and discuss the experimental work performed for this PhD thesis. In **chapter 5**, the possibility to use NIR spectroscopy for the distinction between different freeze-dried live, attenuated virus formulations is evaluated. NIR spectra of freeze-dried samples prepared using different virus medium volumes or using different pre-freeze-drying virus treatments are collected and analyzed using principal component analysis (PCA). The possibility to classify new samples according to their pre-freeze-drying virus treatment using partial least squares discriminant analysis (PLSDA) is further assessed. Based on the same approach, **chapter 6** evaluates the possibility to distinguish between freeze-dried samples varying in virus medium volume, pre-freeze-drying virus treatment or virus dose using FTIR spectroscopy. Three amide spectral regions are evaluated using PCA.

By coupling both, process analytical spectroscopic techniques (NIR and FTIR spectroscopy) and traditional tools employed to evaluate freeze-dried vials, **chapter 7** is dedicated to the study of a freeze-dried live, attenuated virus vaccine during an accelerated stability study. Freeze-dried samples stored during four weeks either at 4°C or at 37°C have been weekly analyzed by NIR and FTIR spectroscopy as well as potency assay, Karl Fischer and modulated differential scanning calorimetry (MDSC) and allow to better understand the virus destabilization mechanism upon storage. Chapters 8 and 9 aim at developing practical applications of NIR spectroscopy for the analysis of freeze-dried live, attenuated viruses in vaccine formulations. In **chapter 8**, a model able to classify freeze-dried samples according to their dose content is developed and validated using off-line collected NIR spectra. A soft independent modelling of class analogy (SIMCA) model is first built. Afterwards, using the developed model, new observations can be classified with a correct classification rate (CCR) above 95%. The model is further validated according to the European Medicines Agency (EMA) guideline. As second application (**chapter 9**), the possibility to predict the titer of new freeze-dried vials from off-line collected NIR spectra is evaluated.

REFERENCES

[1]   M. J. Pikal. Freeze-drying. In: J.S. Swarbrick, J.C. Boylan (Ed.) Encyclopedia of Pharmaceutical Technology, Marcel Dekker, New York, USA, 2002, 1807-1833.

[2]   G. Adams. The principles of freeze-drying. In: J. G. Day and G. N. Stacey (Ed.) Methods in Molecular Biology: Cryopreservation and freeze-drying protocols, second ed., Humana Press Inc., Totowa, NJ, USA, 2007, 15-38.

[3]   J.C. Kasper, G. Winter, W. Friess. Recent advance and further challenges in lyophilization. European Journal of Pharmaceutics and Bioopharmaceutics, 2013; 85(2) 162-169.

[4]   H. R. Constantino, M. J. Pikal. Lyophilization of biopharmaceuticals. Arlington (VA): AAPS Press. 2004.

[5]   M.J. Pikal, S. Cardon, C. Bhugra, F. Jameel, S. Rambhatla, W.J. Mascarenhas, H.U. Akay. The nonsteady state modeling of freeze-drying: in-process product temperature and moisture content mapping and pharmaceutical product quality applications. Pharmaceutical Development and Technology, 2005; 10(1): 17-32.

[6]   J.G. Aunins, A.L. Lee, D.B. Volkin. Vaccine Production. The Biomedical Engineering Handbook: 2nd Edition. Ed. Joseph D. Bronzino. Boca Raton: CRC Press LLC, 2000.

[7]   C.J. Burke, T.A. Hsu and D.B. Volkin. Formulation, stability, and delivery of live attenuated vaccines for human use. Critical Reviews in Therapeutic Drug Carrier Systems, 1999; 16(1): 1-83.

[8]   Food and Drug Administration, Process Analytical Technology Initiative, Guidance for Industry; PAT - A Framework for Innovative Pharmaceutical development, Manufacturing and Quality Assurance, 2004.

CHAPTER 2

FREEZE-DRYING AS PHARMACEUTICAL DRYING PROCESS

CHAPTER 2

FREEZE-DRYING AS PHARMACEUTICAL DRYING PROCESS

2.1. THE CONCEPT OF FREEZE-DRYING

Freeze-drying or lyophilization is defined as a low-temperature drying process, based on the principles of heat and mass transfer, employed to improve the stability and long-term storage of (heat-)labile drugs [1]. Although being a complex, costly, energy and time-consuming (from 3-4 up to 7-10 days) multi-step process during which the starting material (solution) undergoes several transformations to yield the end product (dry cake), freeze-drying has established itself as an important drying method in the (bio-)pharmaceutical industry. Accepted by the regulatory authorities as a suitable unit operation in the manufacture of therapeutic products [2], freeze-drying also offers several advantages over other drying techniques as: water is removed without excessive heating, the product sterility can be maintained during processing, the resulting porous cake has an extended shelf life and can be fast, easily reconstituted and handled (shipping and storage) [1, 3, 4].

Freeze-drying starts by freezing the product. Afterwards, the solvent is removed first by sublimation of ice (primary drying) and then by desorption of unfrozen water (secondary drying). This very basic description of the lyophilization process hides a multitude of complex and interacting physical and chemical phenomena related to the formulation and the heat and mass transfers occurring during the process [2]. Formulation and process are interrelated: "A bad formulation can be nearly impossible to freeze-dry, and even with a well designed formulation, a poorly designed process may require more than a week to produce material of suboptimal quality" [1].

2.2.   FREEZE-DRYING EQUIPMENT AND PROCESS

A schematic diagram showing the main components of a freeze-dryer used for (bio-) pharmaceuticals is shown in Figure 2.1. The chamber contains temperature-controlled (coolable or heatable) shelves through which a heat transfer fluid is circulated. Hydraulically movable, the shelves can be compressed in order to fully insert the stoppers into the hexagonally packed vials at the end of the process (prior to aeration). The chamber is connected to the condenser via a valve. The condenser contains series of coils cooled down by a compressor, in order to collect the sublimed water. A vacuum pump is connected to the condenser in order to evacuate the system and provide the necessary pressures for conducting the primary and secondary drying steps [5].
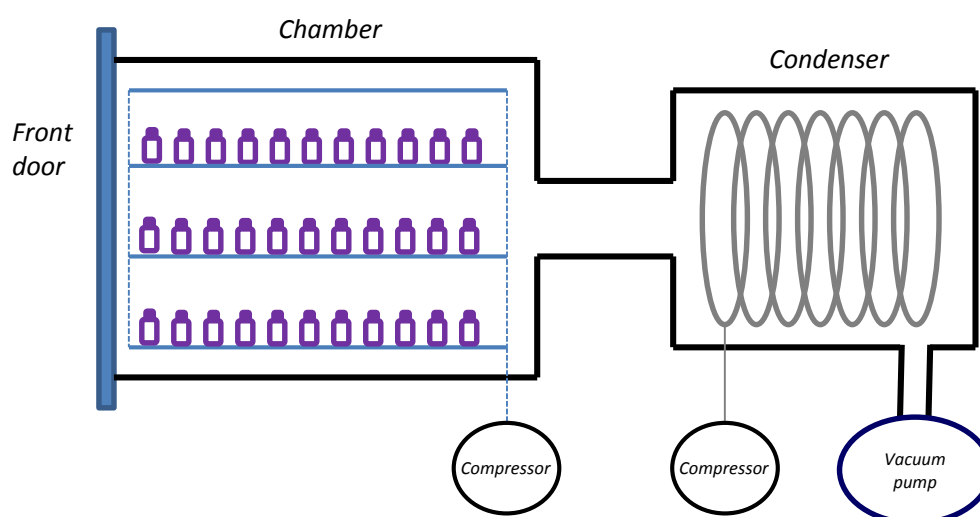
Figure 2.1: Schematic diagram of a typical freeze-dryer.

A freeze-drying cycle consists in three main stages: freezing, primary drying and secondary drying. Three process settings can be varied (being the shelf temperature, the chamber pressure and the time) in a dynamic way in order to obtain a freeze-dried product. During the freezing stage, the shelf temperature is decreased (usually between -40°C to -50°C) in order to convert most of the water into ice. The conversion of liquid water into ice concentrates all solutes into regions between ice crystals. The solutes become more concentrated (i.e., freeze concentration) until they crystallize at the eutectic temperature

(Teu) or until the viscosity sufficiently increases to transform into an amorphous system or glass [1]. The associated temperature with the latter phenomenon is the glass transition temperature Tg' of the maximally freeze-concentrated solution. In some cases, an annealing step is included in the freezing stage to overcome the freezing heterogeneity within a batch and to maximize crystallization of the bulking agent during freezing. The annealing temperature should be between the Tg' of amorphous phase and Teu of bulking agent to give a high crystallization rate and complete crystallization. The optimum annealing time depends on the ratio and properties of the bulking agent used [3].

When the freezing stage is complete, the freeze-drying chamber pressure is decreased below the vapor pressure of ice at the temperature of the product and the shelf temperature is increased in order to provide the energy for ice to sublime. This is the primary drying step [5]. In order to avoid product collapse and maintain an elegant cake structure, the product temperature at the sublimation front must be kept at a temperature 2-5°C below the product collapse temperature (Tc), which is generally a few degrees higher than Tg' [3,6,7]. The collapse temperature is the temperature above which the freeze-dried product loses macroscopic structure and collapse during freeze-drying [8]. Maintaining the temperature below Tg' makes the primary drying phase long (typically > 24 hours) and expensive but is necessary since any cake collapse may result in an inelegant cake (which is inacceptable from a commercial point of view), higher residual moisture content and prolonged reconstitution time. At the end of primary drying, there should be no more ice present in the vial and therefore, no more sublimation. Nevertheless, the amorphous product still contains some dissolved moisture (5-20%) which needs to be removed to values (usually less than 1-2%) allowing optimal product stability during distribution and storage. The objective of secondary drying is to further decrease the moisture by increasing the shelf temperature in order to facilitate the desorption. The product temperature increase from primary drying to secondary drying should be slow (and is in many cases performed gradually) preventing the product temperature exceeding the glass transition temperature (Tg) of the product, hence avoiding product collapse. As the water content of the amorphous phase decreases during secondary drying, the glass transition temperature sharply increases. Therefore, the secondary drying step is usually started at a low shelf temperature followed by a gradual increase to the final secondary drying shelf temperature [1]. At the end of

secondary drying, the water content must be low enough making sure that the glass transition temperature (Tg) is well above (approx. >30°C) the highest temperature relevant for product storage and distribution. The determination of the optimal end product residual moisture is performed empirically and is product dependent [1].

Figure 2.2 visualizes how the freeze-drying conditions are generally set. During most freeze-drying processes, the process settings (e.g., shelf temperature, chamber pressure and time) are rather fixed during each process phase (e.g., constant shelf temperature during primary drying, see Figure 2.2).
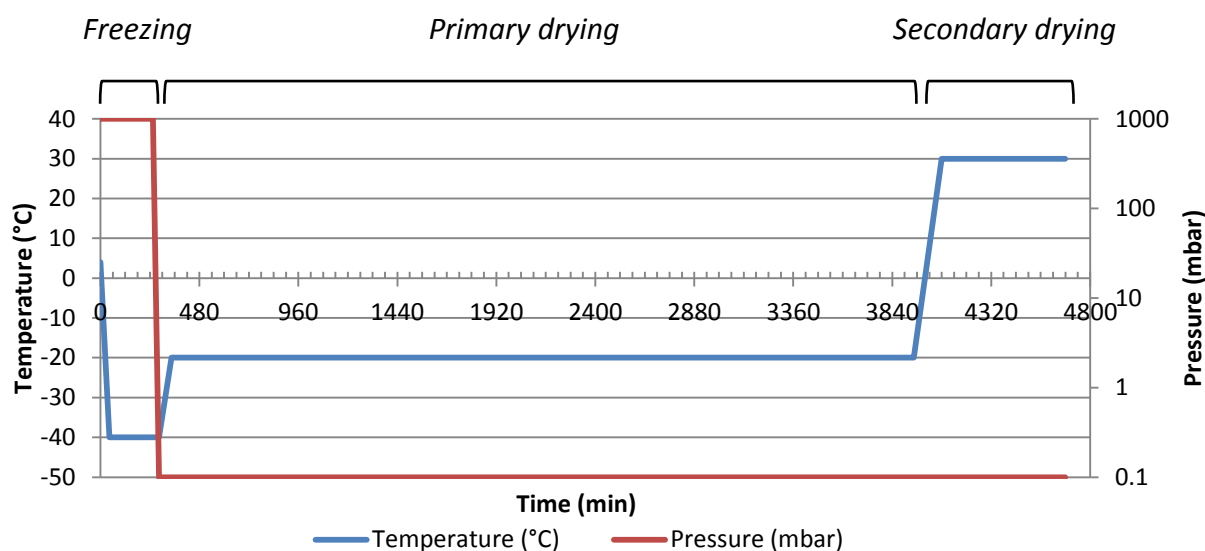
Figure 2.2: Example of traditional temperature and pressure settings of a freeze-drying process

To increase process efficiency, product temperature during primary drying should be as high as possible without inducing collapse. Therefore, the process settings, shelf temperature and chamber pressure, should not be chosen too conservative. During the sublimation phase, the thickness of the dried product layer increases which simultaneously leads to an increase of the dried product mass transfer resistance and product temperature at the sublimation interface. Therefore, the process conditions of an optimal freeze-drying cycle should be modified as primary drying proceeds [9]. Mechanistic modelling, describing the energy and mass transfer during freeze-drying leading to a dried product, can be used to determine the

optimal combination of shelf temperature and chamber pressure in order to keep the product temperature at the sublimation front below the critical temperature during primary drying. Based on mechanistic modelling, the evolution of the optimal chamber pressure and shelf temperature shows a different profile during primary drying compared to a traditional freeze-drying cycle and is presented in Figure 2.3. The high shelf temperature is calculated by the model in order to provide energy for sublimation while keeping the product temperature at the sublimation interface below the critical temperature. As the dry layer thickness increases with the progression of primary drying, the shelf temperature is decreased and adapted accordingly.
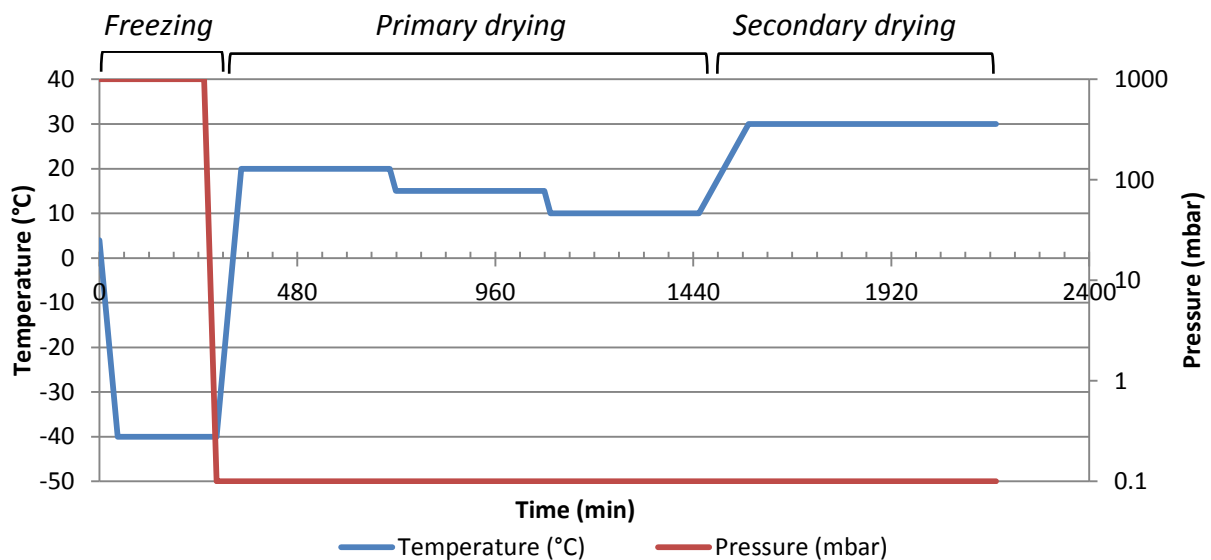
Figure 2.3: Example of temperature and pressure settings based on mechanistic modelling of the primary drying step of a freeze-drying process.

Some years ago, a SMART freeze-drying system was developed [10]. Depending on the input parameters (physical and chemical product properties, vial properties, etc.) for the material to be freeze-dried, the SMART system produces an optimized recipe for freeze-drying. Furthermore, during primary drying the recipe is adjusted in real-time for shelf temperature and chamber pressure based on water vapor content measurements in the freeze-dryer chamber, hence guaranteeing the required product temperature and optimizing the drying step efficiency. However, the SMART system does not allow to control the annealing process

during the freezing step, the product solid state, the dehydration during secondary drying and the residual moisture content.

Therefore, continuous in-line information of the product itself is needed. Critical product information can be continuously monitored using process analyzers (e.g., Raman or NIR spectroscopy) [11-15]. In order to ensure that the process settings are adjusted based on the real-time product behaviour, control algorithms need to be developed (if it is proven that these product characteristics can be linked to the process settings), thereby leading to a fully automatic controlled process based on advanced in-line monitored critical process and formulation information.

REFERENCES

[1]   M. J. Pikal. Freeze-drying. In: J.S. Swarbrick, J.C. Boylan (Ed.) Encyclopedia of Pharmaceutical Technology, Marcel Dekker, New York, USA, 2002, 1807-33.

[2]   F. Franks. Freeze-drying of bioproducts: putting principles into practice. European Journal of Pharmaceutics and Bioopharmaceutics, 1998; 45: 221-9.

[3]   X.C. Tang and M.J. Pikal. Design of freeze-drying processes for pharmaceuticals: practical advice. Pharmaceutical Research, 2004; 21(2): 191-200.

[4]   Food and Drug Administration, Lyophilization of parenteral (7/93): Guide to inspections of lyophilization of parenterals. 2014.

[5]   S.L. Nail, S. Jiang, S. Chongprasert, S.A. Knopp. Fundamentals of freeze-drying. Pharmaceutical Biotechnology, 2002; 14: 281-360.

[6]   M.J. Pikal, S. Shah. The collapse temperature in freeze-drying: dependence on measurement methodology and rate of water removal from the glassy phase. International Journal of Pharmaceutics, 1990; 62: 165-186.

[7]   A.M. Abdul-Fattah, D.S. Kalonia, M.J. Pikal. The challenge of drying method selection for protein pharmaceuticals: product quality implications. Journal of Pharmaceutical Sciences, 2007; 96(8): 1886-1916.

[8]   A.P. Mackenzie. Basic principles of freeze-drying for pharmaceuticals. Bulletin of the Parenteral Drug Association, 1996; 20: 101-130.

[9]   R. Pisano, D. Fissore, A. A. Barresi, P. Brayard, P. Chouvenc,B. Woinet. Quality by design: optimization of a freeze-drying cycle via design space in case of heterogeneous drying behaviour and influence of the freezing protocol. Pharmaceutical Development and Technology, 2013; 18(1): 280–295

[10] X. Tang, S.L. Nail, M.J. Pikal. Freeze-drying process design by manometric temperature measurement: design of a smart freeze-dryer. Pharmaceutical Research, 2005; 22: 685-700.

[11] T. De Beer, M. Allesø, F. Goethals, A. Coppens, Y. Vander Heyden, H. Lopez De Diego, J. Rantanen, F. Verpoort, C. Vervaet, J.P. Remon, W. Baeyens. Implementation of a Process Analytical Technology System in a Freeze-Drying Process Using Raman Spectroscopy for In-Line Process Monitoring. Analytical Chemistry, 2007; 79(21): 7992–8003.

[12] T. De Beer, P. Vercruysse, A. Burggraeve, T. Quinten, J. Ouyang, X. Zhang, C. Vervaet, JP. Remon, W.R. Baeyens. In-line and real-time process monitoring of a freeze-drying process using Raman and NIR spectroscopy as complementary process analytical technology (PAT) tools. Journal of Phamaceutical Sciences, 2009; 98: 3430-3446.

[13] T. De Beer, M. Wiggenhorn, R. Veillon, C. Debacq, Y. Mayeresse, B. Moreau, A. Burggraeve, T. Quinten, W. Friess, G. Winter, JP. Remon, W.R. Baeyens. Importance of using complementary process analyzers for the process monitoring, analysis, and understanding of freeze-drying. Analytical Chemistry, 2009; 15: 7639-7649

[14] S. Pieters, T. De Beer, J.C. Kasper, D. Boulpaep, O. Waszkiewicz, M. Goodarzi, C. Tistaert W. Friess, J.P. Remon, C. Vervaet, Y. Vander Heyden. Near-Infrared Spectroscopy for In-Line Monitoring of Protein Unfolding and Its Interactions with Lyoprotectants during Freeze-Drying. Analytical Chemistry, 2012; 84: 947-955

[15] S. Pieters, Y. Vander Heyden, J.M. Roger, M. D'Hondt, L. Hansen, B. Palagos, B. De Spiegeleer, J.P. Remon, C. Vervaet, T. De Beer. Raman spectroscopy and multivariate analysis for the rapid discrimination between native-like and non-native states in freeze-dried protein formulations. European Journal of Pharmaceutics and Bioopharmaceutics, 2013; 85 (2): 263-271.

CHAPTER 3

FREEZE-DRYING OF LIVE VIRUS VACCINES: A REVIEW

Parts of this chapter are published in:

ABSTRACT

Freeze-drying is the preferred method for stabilizing live, attenuated virus vaccines. After decades of research on several aspects of the process like the stabilization and destabilization mechanisms of the live, attenuated viruses during freeze-drying, the optimal formulation components and process settings are still matter of research. The molecular complexity of live, attenuated viruses, the multiple destabilization pathways and the lack of analytical techniques allowing the measurement of physicochemical changes in the antigen's structure during and after freeze-drying mean that they form a particular lyophilization challenge. The purpose of this chapter is to overview the available information on the development of the freeze-drying process of live, attenuated virus vaccines, herewith focusing on the freezing and drying stresses the viruses can undergo during processing as well as on the mechanisms and strategies (formulation and process) that are used to stabilize them during freeze-drying.

CHAPTER 3

FREEZE-DRYING OF LIVE VIRUS VACCINES: A REVIEW

3.1. INTRODUCTION

Since its discovery over 200 years ago by Edward Jenner, vaccination can be considered as one of the major steps in the fight against infectious diseases. Vaccination aims at controlling and ultimately eliminating infectious agents. The latter objective was obtained for smallpox, which was in 1980 certified as eradicated by the World Health Assembly [1].

Today, vaccines are estimated to avert approximately 2.5 million deaths from diphtheria, tetanus, pertussis (whooping cough), and measles every year and in all age groups. However, millions of people still die from vaccine preventable diseases [2]. This unfortunate finding can directly be linked to the difficulty to distribute vaccines in poorly-served remote rural areas, fragile states and strife-torn regions [3], but also to the often weak thermostability of vaccines [4]. Increasing the stability of vaccines has been at the forefront for decades. Vaccine development scientists aim to provide products preserving adequate quality (potency, titer, activity, and immunogenicity) during storage and after accidental exposure to exceptional conditions, until the vaccines are administered [5].

There are several factors (temperature, pH, suspension medium, exposure to light, freezing, thawing, anti-microbials and inactivating agents) influencing the stability of vaccines. However, the most important factor is the antigen itself as its antigenicity and infectivity are affected differently depending on the antigen's intrinsic stability [5]. According to the U.S. National Institute of Allergy and Infectious Diseases (NIAD), there are seven different types of vaccines, based on their antigen type: live, attenuated vaccines, inactivated vaccines, subunit vaccines, toxoid vaccines, conjugate vaccines, DNA vaccines and recombinant vector vaccines [6].

Live, attenuated vaccines generate both humoral (antibody) and cellular immune responses and are the most successful of all human vaccines because they are able to confer long-term immunity after one or two immunizations [7]. The antigens of such vaccines are bacteria (tuberculosis (BCG), typhoid) or most often viruses (measles, mumps, rubella, polio, yellow fever, varicella and rotavirus) [8]. Live, attenuated virus vaccines consist of viruses that have lost their virulence but that are still able to confer a protective immunity against a virulent virus. Compared to inactivated vaccines, live, attenuated viruses are easier to produce, do not require the use of adjuvants in the formulation and only need minimal downstream processing [9].

The production process of virus vaccines is very complex because it uses living cells that make standardization difficult [9]. Live, attenuated vaccines also form a formulation challenge because of the macromolecular complexity of viruses and bacteria. Viruses can be enveloped or non-enveloped, and have a size ranging (diameter) from 30 (poliovirus) to 300nm (vaccinia (smallpox) virus) [7].

Protected in an adequate cryoprotection medium (e.g., buffer to avoid pH changes, non reducing sugars as cryoprotectants, non ionic surfactants to avoid adsorption and aggregation), most viruses are stable below -60°C. Other viruses are stable at higher temperatures but a temperature above 8°C is always harmful for any virus [5]. To maintain the vaccine temperature between safe margins, from the manufacturing location to the vaccine administration (patient), a cold chain is required.

The cold chain concept is applicable in several industrial fields (e.g., food and pharmaceutical industry) which require to maintain temperature-sensitive products at a protective temperature during processing, storage and distribution. The first significant efforts to ensure a continuous cold chain in the pharmaceutical field were deployed at the beginning of the 1980s with the development of insulated packages, temperature recorders and the improvement in training of the various parties involved in the distribution system [10]. Despite these numerous improvements, keeping the temperature between 2 and 8°C (the temperatures specified by the World Health Organization (WHO), the FDA and other governmental agencies in order to ensure an optimal quality of the vaccines) is not always feasible, even in industrialized countries: breakage of the cold chain due to handling errors occurs frequently [11-14] as well as equipment power failures [10, 15]. However,

maintaining a well-controlled cold chain is of major importance since a disturbance in it can lead to a decrease of the vaccine's therapeutic efficiency. In addition to the presented risks of disturbances, certain vaccines can't be delivered via the cold chain system as the requirements in term of minimal acceptable temperature are not met. This is the case for the oral vaccines against poliomyelitis [16] and the smallpox vaccine in dry form [17], which require a storage at -20°C. Therefore, reducing the dependency on the cold chain of the products would be very useful [18].

The limited stability of viruses in aqueous media above 8°C is well known [5]. This instability results from several types of water-mediated destabilization and degradation pathways.

Therefore, as is the case for proteins [19], the removal of the bulk water (to 1-2% total weight) can significantly increase the stability of viruses by inhibiting or sufficiently decelerating the degradation and destabilization pathways that can occur in aqueous media [7, 8, 9]. Except the oral polio vaccine (OPV), which is a stable vaccine in aqueous formulation [20], all live, attenuated viral vaccines are freeze-dried [4, 21].

Freeze-drying offers many advantages over other drying processes: the low temperatures used during this process allow avoiding high destabilizing drying temperatures, the shelf life of the freeze-dried product is significantly enhanced, the dried product (cake) can be easily reconstituted and the aseptic processing operation meets the finished product sterility requirements without the stress of a terminal sterilization step.

Despite the numerous studies performed, the destabilization mechanisms as well as the protection mechanisms for live, attenuated virus vaccines during lyophilization are not well known. This is attributed to the already mentioned complex structure of viruses, the multiple degradation routes and the lack of analytical techniques allowing the measurement of physicochemical changes in the antigen's structure during and after freeze-drying. Because the destabilization pathways always result in a loss of bioactivity, potency assays are typically used during formulation development [22]. Unfortunately, such assays are characterized by weak accuracy and precision [23], and don't provide direct information to elucidate the mechanisms of destabilization and inactivation.

This chapter focuses on the freeze-drying of live, attenuated virus vaccines. The purpose is to review the available information on the development of the freeze-drying process of live,

attenuated virus vaccines, herewith focusing on the stresses the viruses undergo during processing as well as on the mechanisms and strategies (process and formulation) to stabilize them during freeze-drying.

3.2. LIVE, ATTENUATED VACCINE STRESS AND STABILIZATION MECHANISMS DURING FREEZE-DRYING

To provide solutions for improving the stability of freeze-dried live, attenuated vaccines, understanding of the mechanisms of degradation and destabilization during freeze-drying is needed. A huge amount of information is available on the stress mechanisms and stabilization strategies of pharmaceutical peptides, proteins and DNA during freeze-drying [24-29]. This contrasts to the lack of detailed knowledge on viral-based vaccines. During the past decades, reported improvements of the freeze-drying of live, attenuated virus vaccines (formulation and process) have resulted mainly from empirical discoveries rather than from rational approaches [7]. This chapter aims at providing an overview of the available information.

Firstly, the stresses that can occur during the freezing as well as the drying steps and the strategies that are used to avoid these stresses will be described.

Afterwards, this chapter will focus in more detail on the formulation and more precisely, on the most often used buffers and stabilizers. Finally, the process development strategy will shortly be discussed.

3.2.1. Virus structure

Most live, attenuated viruses possess a lipid bilayer which is considered as the less stable virus component because of its high fragility. The enveloped viruses also have glycosylated or non glycosylated proteins that are essential to infect their host and must be protected [30]. Finally, the viral genome consists either of RNA or DNA and is considered as more stable, but is still subject to both physical and chemical stresses. Considering only this simplified structural description, loss of potency during freeze-drying can be due to protein destabilization (e.g., unfolding, degradation, aggregation), nucleic acid degradation, lipid

layer alteration (e.g., phase transition, mechanical damage) and stresses related to changes in the internal (ice formation, osmolarity change) and external (pH and osmolarity change) virus environment. A schematic overview of the virus and the factors possibly affecting its potency is presented in Figure 3.1.
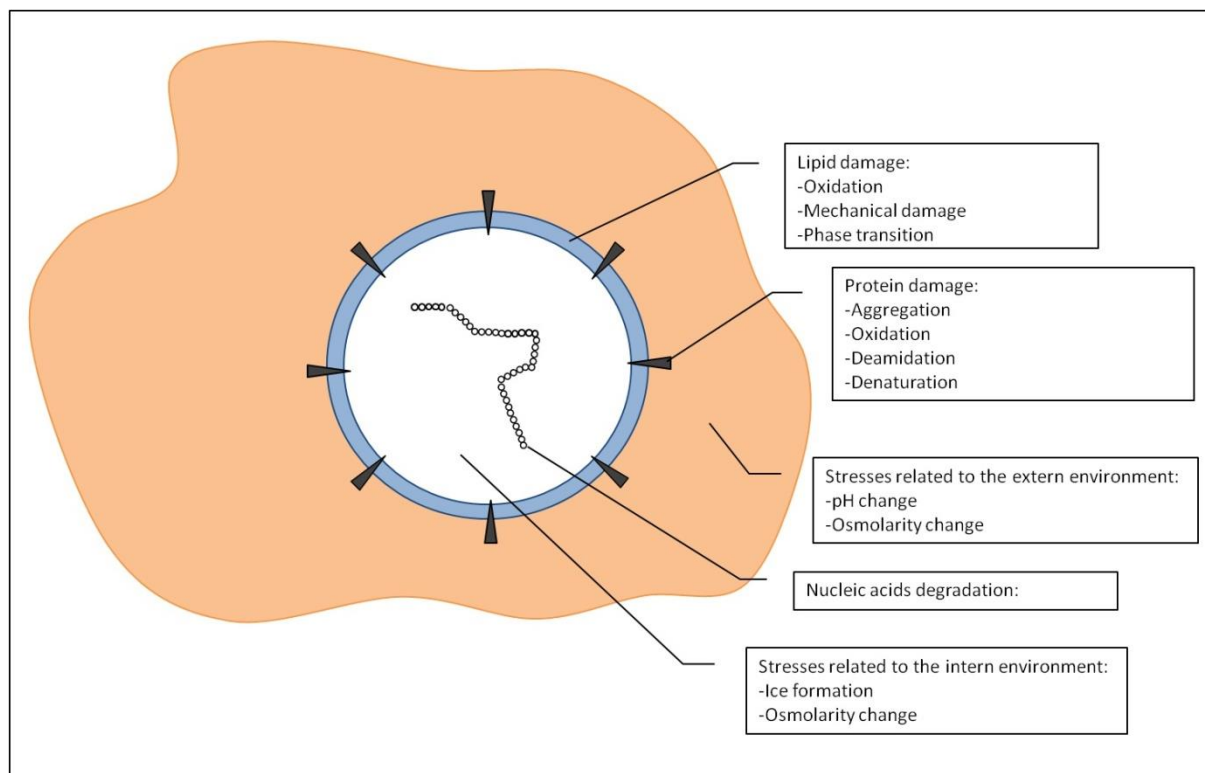
Figure 3.1: Schematic overview of the virus and the factors possibly affecting its potency.

3.2.2. Freezing and associated stresses

During the freezing step, the liquid formulation to be freeze-dried is cooled until ice nucleation starts, which is followed by ice crystal growth. Many biological structures and bio reactions are temperature dependent. Consequently, cooling creates conditions deviating from the normal physiological conditions [31] that might have detrimental effects on the viruses. Freezing can damage the individual virus components (viral coated proteins, viral lipid membrane), change the formulation buffer and osmolarity, all impacting the virus stability. Finally, based on cells cryopreservation knowledge, freezing could also cause intra-virus ice formation. The following paragraphs overviews these possible stresses.

3.2.2.1. Intra-virus ice formation

Compared with viruses, the impact of freezing on cells has been more widely studied [31, 32]. Freezing might damage cells for several reasons (e.g., solution effects, extracellular ice formation, and dehydration), but intracellular ice formation is the most important one [31-33]. Ice formation inside the cells increases the intracellular concentration of electrolytes which in turn affects ionic interactions that can be involved in the stabilization of the native state of intracellular enzymes [31, 32]. Intracellular ice formation occurs when the cell cannot maintain its osmotic equilibrium with the environment, typically at high cooling rate [34]. At low cooling rate, providing water can leave the cells rapidly to maintain thermodynamic equilibrium across the cell membrane, the cytoplasm will not cool below its freezing point [34]. The effect of the cooling rate on cells is well illustrated in [32].

In addition, the interaction of water and ice with the hydrophilic surfaces of intracellular enzymes is different. This is potentially important because the surface tension of water is involved in maintaining the enzymes native state (=hydrophobic effect). If this water is replaced by ice, the stabilizing interaction via the hydrophobic effect can be lost [31]. Intracellular ice crystals can also directly cause mechanical damages to the cellular ultra-structure or the cells can also be affected by the volumetric expansion induced by ice formation [31].

Hence, it can be expected that ice formation within the live, attenuated virus might also result in significant loss of potency for similar reasons under fast cooling. To our best knowledge, there are no publications describing intra-virus ice formation or the consequences of intra-virus ice formation.

3.2.2.2. Changes in osmolarity

Changes in ionic strength as well as in uncharged molecule concentration must be carefully evaluated, especially for vaccines containing antigens with semipermeable membranes like enveloped viruses because of the potential osmotic effects (contraction or swelling) [35].

Marek's disease vaccine can be dramatically affected by the osmolarity. Values of 745mOsm/kg and higher have been proven to markedly reduce the virus survival [36].

The vaccine integrity can be affected by osmotic changes. When grown in culture medium at specific ionic strengths, the virus must reequilibrate when introduced in solutions of

different ionic strengths (e.g. during formulation). This results in osmotic swelling or contraction hence potentially damaging the virus.

When herpes simplex viruses are in a low osmotic pressure (50 mOsm/kg) medium, a dramatic potency decrease (only 26% recovery) is observed, whereas a high osmotic pressure (840 mOsm/kg) medium gives a recovery of 80-92% [37]. The reason for this is that in a hyper-osmotic medium, the internal water of the virus escapes and the protein concentration in the tegument (that anchors the lipid membrane and the capsid) increases. This lowers the nucleation temperature inside the virus membrane and prevents ice crystals formation and growth [37].

Both reported cases were not observed under freezing conditions. However, the freezing step implies the conversion of water into ice and hence might affect the ionic strength of the formulation. Such change could impact the virus integrity but it has, to our best knowledge, never been demonstrated.

3.2.2.3. Effect of the freezing step on pH

During freezing, pH shifts by crystallization of buffer components can occur [38]. This possibility must be properly investigated as both chemical and physical degradations are strongly pH dependent [35].

Brandau and coworkers illustrated the importance of pH on virus activity for several live, attenuated vaccines [35]. The storage stability of the cold-adapted influenza virus liquid is dependent on the pH. At pH 7.1 the formulation retained its titer for 1 month upon storage at 4°C, whereas the same formulation stored at higher or lower pHs showed a significant titer decrease [39]. A pH change can affect viruses by activating or inhibiting certain enzymes (e.g., viral RNA polymerase) and/or by affecting the overall charge of the coated proteins leading to conformational changes of these proteins. The viral RNA polymerase of the live, attenuated oral polio vaccine (OPV) degrades RNA upon storage. However, keeping the formulation at a pH near 5-6 results in a lower enzyme activity [40]. The secondary and tertiary structure of the glycoprotein haemagglutinin (HA) of the influenza subunit virus has been shown to be sensitive to pH drops during freezing [41]. In the study, the magnitude of pH change of a phosphate-buffered solution (PBS) and a Hepes-buffered solution (HBS) was compared and the effects on the glycoproteins were evaluated. The pH change was higher

when using PBS (because of the higher tendency of PBS to crystallize) and led to HA structural changes. The reversibility of HA changes upon acidification and subsequent neutralization is however an indication that structural change isn't caused by pH change (alone) [42, 43] (see next paragraph).

Measles viruses are more stable at neutral pH. In an acidic environment, the physical stability of this virus is highly compromised. Light scattering and circular dichroism (CD) spectroscopy have shown evidence of aggregation at low temperature and precipitation in acidic environments [44].

Numerous studies have revealed that the optimal pH range to limit the loss of activity is generally between 6 and 8 [7, 45, 46] which is a convenient result regarding the needs for parenteral preparations which require a pH close to the physiological pH and confirms the conclusion by Peetermans that most viruses are affected by pH values outside the physiological limits [5]. In most cases, the glycoproteins are affected by a pH shift. Changes in their conformation can be reversible but can also lead to aggregation and precipitation of the viral particles. It is therefore highly recommended to examine with care the impact of pH changes and to select an appropriate buffer system.

3.2.2.4. Effects of the freezing step on the viral coated proteins

The necessity to protect viral coated proteins during freeze-drying was already understood in 1968 in a study evaluating the stability of suspensions of influenza viruses dried to different residual moisture contents [47]. One year later, it was claimed that the surfaces of virus particles, containing coated proteins, were the first exposed to the phasic changes during freezing [48]. The kinds of changes occurring to the viral proteins during freezing, freeze-drying and long term storage are determinant for the activity of the re-hydrated virus particles [48].

Today, it is well known that proteins, in general, are subjected to different freezing stresses [49, 50] during a freeze-drying process. There are three main stress factors: cold denaturation, ice formation and freeze concentration [50].

Change in osmolarity, pH and solute concentration have already been described in the previous paragraphs and are caused by the same stress factor, freeze concentration [24, 25]. This stress factor (freeze concentration) can also lead to liquid-liquid phase separation [50,

51] between incompatible excipients within the freeze concentrate and could negatively influence the preservation of virus by separating the virus from at least one of the protective excipients [50].

A second important stress factor is the formation of large ice-water interfaces due to ice crystallization that can promote surface-induced denaturation of surface-sensitive proteins [28]. High cooling rates result in small ice crystals and large ice-water interface [28]. Even if large ice-water interface has already been demonstrated to result in protein structure change and protein aggregation [24, 52], such a destabilization mechanism has, to the best of our knowledge, never been demonstrated for viruses. The mechanism of protein denaturation at the ice surface is still under discussion [50].

Finally, cold denaturation has been reported for a large number of proteins. This mechanism states that the protein's free energy of unfolding becomes negative at low temperature and may induce spontaneous unfolding of the protein [49]. However the contribution of this stress is frequently considered as negligible in lyophilization because the estimated cold denaturation temperatures are far below the lyophilization temperature especially in the presence of saccharides and polyols [50].

The freezing stresses inducing (possibly irreversible) protein conformation changes have been demonstrated in many case-studies performed on different model proteins [25, 49, 53, 54]. In contrast, only a few studies provide information on the influence of freezing-stress upon viral proteins [41, 55].

For herpes simplex viruses, a lipid-enveloped virus, immunogold labeling experiments have shown that the structural integrity of membrane glycoproteins can be lost during freezing [55].

But the most studied virus glycoprotein is the influenza haemagglutinin (HA). This protein can be found at the surface of several live, attenuated virus vaccines, but can also be used as antigen in the influenza subunit vaccine [41] as well as in influenza virosomes [56]. The secondary and tertiary structures of this viral protein are susceptible to freezing stresses [41]. Demonstrated by a proteolitic assay, the HA conformation might change because of pH change (acid-induced conformation change), but HA structural changes (exposed trypsin cleavage site) can also be observed despite moderate pH shift [41] and can be caused by a

change of the ionic strength resulting from an increase in solute concentration in the non-frozen fraction, recognized as a protein destabilization factor [28].

Fluorescence and CD-spectroscopy of HA after freeze-thawing experiments also confirm that HA conformational changes after freezing are not only caused by a pH shift, but also by freezing-related stress [41]. Finally, haemagglutinin conformation change upon acidification was found to be reversible after subsequent neutralization [42, 43].

3.2.2.5. Effect of the freezing step on the lipid membrane

The lipid membrane is very fragile and an important consideration since the loss of the viral lipid layer automatically results in viral inactivation [57].

Liposomes are considered as model for cell membranes and are extensively studied to understand the effects of lyophilization on the stability of the cell membrane. During the freezing step, the lipid layer must mainly be protected against ice crystal damage [58], fusion and thermotropic phase transitions [59].

More than fifty years ago, Greiff and co-workers observed a titer decrease of influenza A virus during freeze-thawing experiments [60]. According to the authors, the titer decrease was due to mechanical injuries caused by small ice crystals during freezing [60]. The first freeze-thawing cycles caused a relatively limited titer loss, but after the fifth freeze-thawing cycle a marked loss in infectivity titer was observed. These observations were linked to the ice crystal size. Large ice crystals and therefore large interstices (safety zones for the viruses) caused limited damage, whereas the formation of more but smaller ice crystals resulted in more mechanical injury and caused substantial titer decrease.

Conversely, in 2010, Chen and co-workers in their review about liposome lyophilization affirm that fast freezing results in smaller ice crystals which induce little damage to lipid bilayers [58]. In contrast, slow freezing generates bigger ice crystals which are detrimental to the membrane integrity. Other studies confirm the importance to avoid too large ice crystals [61, 62].

However, aiming for the smallest ice crystals can also lead to virus destabilization. Zhai and co-workers compared the effect of three different cooling rates on the retention of the viral infectivity after freeze-drying of a herpes simplex virus [37]. The fastest cooled samples (cooled in melting propane) surprisingly generated the highest virus loss. This loss was

explained by recrystallization of the small ice crystals occurring when the rapidly frozen samples were warmed to a temperature at which lyophilization was practical. Ice recrystallization disrupted the virus, hence resulting in more loss of viral infectivity.

Although there are only a few studies available, it can be concluded that mechanical damages caused by ice crystals leading to viral inactivation can occur. Demonstration of the mechanism of action is lacking, but mechanical degradation is the most often proposed mechanism.

The mechanism of two other effects (fusion and thermotropic phase transitions) during the freezing step is less extensively explained in literature. Both results in an increase of membrane permeability, hence water-soluble molecules that were internally isolated are often leaked to the external medium. Furthermore, thermotropic phase transitions can lead to lateral phase separations of phospholipids and other constituents such as membrane proteins [59].

3.2.3. Formulation and process strategies to protect live, attenuated viruses during freezing

This section overviews the strategies described in literature to protect live, attenuated viruses from the freezing stresses and their consequences discussed above (intra-virus ice formation, change in osmolarity, pH changes, glycoprotein structural changes, lipid membrane mechanical damages and fusion). To avoid these stresses, two protective actions are systematically taken: the use of cryoprotectants and an appropriate cooling rate. The effects of both parameters, especially the cooling rate, must be carefully studied as it might have a positive influence against a determined stress (e.g., a high cooling rate results in small ice crystals that are less detrimental to the membrane [58]) combined with a negative effect on another stress (ice recrystallization of the small ice crystals upon drying [37], larger ice-water interface leading to a larger extent of surface-induced denaturation of surface-sensitive proteins [28] or intra virus ice formation [34]).

Selecting a good cryoprotectant is also very important since this formulation component can protect live, attenuated viruses against: coated protein structural changes,

fusion/aggregation, membrane damages caused by ice crystals, intracellular ice formation and pH shift. However, it should be emphasized that a good cryoprotectant does not necessarily act as a good lyoprotectant. Polyethylene glycol (PEG) is an excellent lactate dehydrogenase and phosphofructokinase protectant during freeze-thawing experiments, however, PEG failed to protect both proteins during freeze-drying unless associated with a supplemental stabilizer (i.e., glucose or trehalose) [63].

Sugars have been demonstrated to protect the HA glycoproteins against changes in secondary and tertiary structure caused by freezing [41]. Currently, in literature, two mechanisms are proposed to explain the stabilization of proteins: thermodynamic and kinetic [49].

The thermodynamic mechanism is related to the ability of the cryoprotectant to thermodynamically shift the equilibrium from the unstable, unfolded conformation toward a stable, native state [49]. The solute exclusion hypothesis is the most widely supported thermodynamic mechanism [49]. It suggests that during freeze concentration, the stabilizer is preferentially excluded from the surface of the protein, i.e., the vicinity of the protein contains a higher amount of water molecules that thermodynamically stabilize the native state of the protein. However, the validity of this solute exclusion hypothesis is questioned [29] in particular because of the low mobility in the glassy state. Thermodynamic stabilization requires a rapid equilibrium between native and unfolded states which isn't possible in the glassy state or even close to the glass transition temperature of the maximally freeze concentrate (Tg') [49].

The kinetic mechanism is rather related to the ability of the cryoprotectant to slow down the rate of inactivation. The vitrification hypothesis is the most widely invoked. During freezing, the solutes concentrate until the freeze-concentrate reaches a maximum and forms a glass at Tg', specific for each formulation.

The exact stabilization mechanism of protein is still under investigation and a subject of research.

In addition to the protection of the coated proteins, other virus structures must be preserved during the freezing step. The vitrification hypothesis during freezing, can also

explain the protection of the viruses against other freezing stresses like aggregation, damages caused by ice crystals and pH shift.

It has been shown that the high viscosity and the limited molecular mobility in a glassy matrix prevents liposomes fusion/aggregation [58, 64, 65] and protects lipid membranes from damage by ice crystals [58].

In addition, cryoprotectants could also prevent aggregation and fusion of live, attenuated viruses by isolating the virus particles in the unfrozen fraction, i.e., the particle isolation hypothesis. When frozen in low sucrose/DNA ratio, aggregation of lipid/DNA complexes was observed despite the glassy state of the sucrose under the experimental conditions. However, when frozen in high sucrose/DNA ratio, aggregation was prevented. The same protection was observed when glucose was used as stabilizer. Whereas a low glucose/DNA ratio did not prevented aggregation, a high glucose/DNA ratio provided particles comparable to unfrozen controls. Nevertheless, in contrast to the sucrose samples, no vitrification was observed when using glucose indicating that the immobilization of particles in a glassy matrix cannot explain the lipid/DNA complexes stabilization and that spatial separation of particles in the unfrozen fraction is sufficient to prevent aggregation [66].   Intra virus ice formation would also be a major concern during freezing of live, attenuated vaccines. Based on freezing studies of cells and liposomes, the use of non-penetrating cryoprotectants such as hydroxyethyl starch (HES) or dextran can inhibit intracellular ice formation [31]. The stabilizers increase the osmotic potential of the extracellular liquid, leading to an escape of water from the cells and thus preventing any intracellular ice formation [67].

To avoid pH shifts during freezing, crystallization of the buffer components in the formulation must be inhibited. This can be done by choosing optimal buffer salts, by keeping the buffer concentration at a minimum, by adding further solutes to maintain all buffer species in the amorphous state or by selecting an appropriate cooling rate [50]. Crystallization of buffer species can also be inhibited by agents, such as sucrose and mannitol [38, 68]. Finally, each buffer salt is characterized by a critical cooling rate, above which crystallization is inhibited and will not result in a pH shift [69].

In cellular cryobiology, the cooling rate is also important in order to manage the volumetric contraction due to the osmotic effect [70]. A slow cooling rate results in a high volumetric

contraction caused by the escape of water from the cell [70]. A fast cooling rate allows little volumetric contraction because the intracellular water has no time to leave the cell rapidly [70]. Water inside the cell implies a less likely vitrification and intracellular ice formation [31]. Slow and high cooling rates depend on the cell and cytoplasm properties. By using a moderate cooling rate, it is possible to allow vitrification with a moderate volume contraction [31].

3.2.4. The drying step and the associated stresses

The lyophilization drying step leads to dehydration of the sample. The consequences on live, attenuated viruses of ice sublimation (primary drying) and water desorption (secondary drying) have not been well studied and are even less described than the effects of freezing upon live, attenuated viruses. Therefore, reviewing the known drying stresses that proteins and liposomes face is the best option to reflect on the potential stresses that coat proteins and the lipid layer of the virus can undergo during the drying steps of freeze-drying.

3.2.4.1. Effects of drying on the viral coated proteins

Proteins in aqueous solution are fully hydrated and are surrounded by a monolayer of water which is termed the hydration shell [71]. Drying removes part of the hydration shell which can disrupt the native state of the protein and lead to denaturation [28]. During dehydration, exposure to a water-poor environment will cause a decrease of the charge density that may facilitate protein-protein hydrophobic interaction and cause aggregation [28] (during dehydration, the hydrated protein tends to transfer protons to the ionized carboxyl groups and thus abolishes as many charges as possible [71]). Water can also play a functional role in the active site of the protein. Removal of these water molecules can inactivate proteins [28].

Even if these stresses are not described in literature for viruses, they could destabilize the proteins in the virus coat, hence affecting the vaccine potency.

3.2.4.2. Effect of drying on the lipid membrane

Similar to proteins, liposomes are also surrounded by a water layer (hydration shell) which is removed during drying and can cause fusion/aggregation of liposomes [58, 72].

Another degradation caused by drying that might lead to viral inactivation is linked to the melting point (Tm) of the lipid layer. Above Tm lipids are in the liquid crystalline phase, while below its melting points, lipids are in the gel phase. During dehydration, water from the lipid headgroup region is removed which causes an increase in van der Waals forces between lipids and results in a higher melting point [41]. When fully hydrated, egg phosphatidylcholine has a Tm of 0°C, but upon dehydration its Tm is 70°C [73, 74]. The changes in Tm between the hydrated and dehydrated state determine whether or not a phase transition will occur during lyophilization and rehydration [58]. The use of carbohydrates can prevent this phase transition which is explained in the next chapter.

If a phase transition from gel to liquid crystalline occurs, it can result in the release of the vesicle content in the environment. This phenomenon has been observed for liposomes, baker's yeast and cells.

3.2.5. Strategies to protect live, attenuated vaccines during drying

The stabilizing capacity of sugars during drying is well known for viruses (see Tables 3.1 and 3.2). However, as for freezing protection, hypotheses related to the protection mechanism of live, attenuated vaccines during drying are not available as such and must be derived from the freeze-drying protection mechanisms of sugars used for liposomes, cells or proteins.

There exist two sugar based drying stabilizing hypotheses: (i) the water-substitution hypothesis and (ii) the kinetic stabilization mechanism (vitrification theory). These two hypotheses can be invoked to explain protein stabilization as well as liposome stabilization.

The water-substitute hypothesis states that the sugar replaces the water molecules (that are removed in the hydration shell) in the hydrogen bonding interactions with the protein and offers a thermodynamic stabilization [75]. This hypothesis is also valid for liposomes and has the effect of reducing Tm of the membrane. By interacting with the phospholipid head group, carbohydrates maintain the spacing and reduce the van der Waals interactions among the acyl chains of the phospholipids. It reduces the interaction between water and phospholipids, replaces water and finally decreases the transition melting temperature [58, 76].

This hypothesis could be relevant for viruses, as a sugar can be hydrogen bonded to the viral coated proteins (providing thermodynamic stabilization) and to the head group of the membrane phospholipids to protect the membrane from phase transition.

The vitrification hypothesis has the same mode of action as during the freezing step. For proteins the isolation into a glassy matrix lowers the molecular mobility needed for the degradation pathways like bimolecular interactions, unfolding and chemical degradation [26]. Similarly, drying can facilitate the aggregation of viral particles by removing the hydration shell surrounding them [77]. The dispersion of the viruses into a glassy matrix can also contribute to the protection by lowering the probability of aggregation.

The viruses appear to be protected by lyoprotectant in three different ways: (a) the dispersion of the virus in a glassy matrix reduces the probability of aggregation and the molecular mobility needed for the degradation pathways, the stabilization of (b) coated proteins and (c) lipid membrane by hydrogen bonding (i.e., water substitution) with the lyoprotectant.

3.3. FORMULATIONS

Freeze-dried live attenuated viruses often require complex formulations existing of numerous excipients [78]. Generally, such freeze-dried vaccines contains one or several antigens, a bulking agent to provide a satisfactory product appearance, a buffer to maintain the pH at a specific value, tonicity modifiers and stabilizers to provide protection to the organism against chemical and physical degradation during processing and storage [75].

Freeze-drying is performed to increase the stability of the vaccine but the freezing and the dehydration steps themselves can be stressful for the product, as described in the first part of this review.

To reduce the negative impact caused by the process, the use of an optimized formulation and process is essential. Optimizing the formulation means finding the best combination of excipients that will have a specific function related either to the process or to the protection of the active component during and after lyophilization.

Several compounds have been used in order to stabilize freeze-dried live, attenuated vaccines. Information gained from databases of licensed vaccines (Table 3.1) as well as from published studies (Table 3.2) reveal some trends and will further be exposed.

Table 3.1: Example of freeze-dried vaccine formulations. Compiled from Physicians Desk Reference and the list of vaccines licensed for immunization and distribution in the U.S. (FDA)

Vaccine *Sponsor*	Description	Virus characteristics	Excipients (not necessarily complete)
ACAM2000 *Sanofi Pasteur Biologics Co*	Live, smallpox (vaccinia) Vaccine	DNA viruses. Envelopped	Mannitol, human serum albumin
Attenuvax *Merck*	Live attenuated measles virus	RNA viruses. Envelopped	Sorbitol, sucrose, gelatin, human albumin, fetal bovine serum
Biavax II *Merck*	Live attenuated rubella and mumps viruses	mumps: RNA viruses. Envelopped rubella: RNA viruses. Envelopped	Sorbitol, gelatin
MMR-II *Merck*	Live attenuated measles, mumps and rubella viruses	measles: RNA viruses. Envelopped mumps: RNA viruses. Envelopped rubella: RNA viruses. Envelopped	Sorbitol, gelatin
M-M-VAX *Merck*	Live attenuated measles and mumps viruses	measles: RNA viruses. Envelopped mumps: RNA viruses. Envelopped	Sucrose, glutamate, human albumin
M-R-VAX *Merck*	Live attenuated measles and rubella viruses	measles: RNA viruses. Envelopped rubella: RNA viruses. Envelopped	Sorbitol, gelatin
Meruvax II *Merck*	Live attenuated rubella virus	RNA viruses. Envelopped	Sorbitol, gelatin
Mumpsvax *Merck*	Live attenuated mumps virus	RNA viruses. Envelopped	Sorbitol, gelatin
Nasovac *Serum institute of India Ltd.*	Live influenza attenuated virus	RNA viruses. Envelopped	Sorbitol, gelatin, phosphate buffer

Table 3.1: Example of freeze-dried vaccine formulations. Compiled from Physicians Desk Reference and the list of vaccines licensed for immunization and distribution in the U.S. (FDA) (continued).

ProQuad *Merck*	Live attenuated measles, mumps, rubella and varicella viruses	measles: RNA viruses. Envelopped mumps: RNA viruses. Envelopped rubella: RNA viruses. Envelopped varicella: DNA viruses. Envelopped	Sorbitol, sucrose, gelatin, human albumin
Varivax *Merck*	Live attenuated varicella virus	DNA viruses. Envelopped	Sucrose, gelatin, glutamate
YF-Vax *Sanofi Pasteur Biologics Co*	Yellow Fever Vaccine	RNA viruses. Envelopped	Sorbitol, gelatin
Zostavax *Merck*	Live attenuated varicella-zoster virus	DNA viruses. Envelopped	Sucrose, gelatin, glutamate

Table 3.2: Compilation of the formulation composition of published studies on virus vaccines stabilization.

Vaccine	Formulations
Respiratory syncytial viruses (RSV) Human vaccine [79]	**SPGA (Sucrose phosphate glutamate albumin)** Sucrose Potassium phosphate buffer Na glutamate Bovine albumin
Rinderpest (RP) Veterinary vaccine [80]	**LGS** Lactobionic acid Hydrolysed gelatin Sorbitol Hepes buffer ------ **BUGS** Potassium phosphate buffer Hydrolysed gelatin Sorbitol ------ **LS** Lactalbumine hydrolysate Sucrose

Table 3.2: Compilation of the formulation composition of published studies on virus vaccines stabilization (continued).

Live, attenuated *peste des petits ruminants* (PPR) vaccine Veterinary vaccine [81]	**LS** Lactalbumine hydrolysate Sucrose HBSS (Hank's balanced salt solution, used to maintain pH and osmotic balance)
	WBM (Weybridge medium) Lactalbumine hydrolysate Sucrose Na glutamate HBSS (Hank's balanced salt solution, used to maintain pH and osmotic balance)
	BUGS Potassium phosphate buffer Hydrolysed gelatin Sorbitol
	TD Trehalose dihydrate
Duck viral hapatitis virus (DHV) vaccines Veterinary vaccine [82]	**SPGA (Sucrose phosphate glutamate albumin)** Sucrose Potassium phosphate buffer Na glutamate Bovine albumin
	LPGG (Lactose phosphate glutamate gelatin) Lactose Potassium phosphate buffer Na glutamate Gelatin
	TPGG (Trehalose phosphate glutamate gelatin) Trehalose Potassium phosphate buffer Na glutamate Gelatin

Table 3.2: Compilation of the formulation composition of published studies on virus vaccines stabilization (continued).

	SPGG (Sorbitol phosphate glutamate gelatin) Sorbitol Potassium phosphate buffer Na glutamate Gelatin
Influenza virus [39]	**SPG (Sucrose phosphate glutamate)** Sucrose Potassium phosphate buffer Glutamate Casitone
Respiratory syncytial viruses (RSV) Human parainfluenza 3 (hPIV3) Human vaccine [83]	Sucrose Phosphate buffer Pluronic F68
Herpes simplex virus (HSV) [37]	Tris-HCL buffer Sucrose Na glutamate
Camelpox virus (CMLV) [85]	**LS (Lactalbumine hydrolysate and sucrose)** Lactalbumine hydrolysate Sucrose HBSS (Hank's balanced salt solution, used to maintain pH and osmotic balance) **BUGS** Potassium phosphate buffer Hydrolysed gelatin Sorbitol **TAA (Trehalose with amino acids and divalent cations)** Trehalose $_L$-Alanine and $_L$-Histidine Ca^{++} and Mg^{++}

Table 3.2: Compilation of the formulation composition of published studies on virus vaccines stabilization (continued).

Mumps virus	**Trehalose**
[86]	Potassium phosphate buffer
	Na glutamate
	Gelatin
	Sucrose
	Sorbitol
	Na glutamate
	Human serum albumin
	Gelatin

Among the different excipients, the buffer and the stabilizers are intended to play a critical role in the protection of the active ingredient and will be the main focus.

- *Formulation pH - Buffer*

In order to stabilize the pH of a vaccine formulation at a specific value (which guarantees an optimal stability of the antigens), buffers are added to the formulation. The buffer choice when developing a formulation to be freeze-dried is critical.

In protein formulation, the most commonly used buffers are phosphate salts [38]. For virus formulations, limited information is available. However, from Table 3.2, it appears that potassium phosphate is the most frequently used buffer. The reason is the pH range of the buffer (6-8) which is particularly suitable to maintain satisfactory virus activity [7, 45, 46], and it is close to physiological pH.

Depending on the salt used, the crystallization tendency and the pH shift magnitude (see paragraph 3.2.2.3, effect of the freezing step on pH) of phosphate buffer will vary. Sodium phosphate buffer demonstrated significant pH changes (increase $\approx$ 4 pH units) during freezing, as a result of crystallization of the buffer component, disodium hydrogen phosphate dodecahydrate, recognized to precipitate at low temperature [84, 87, 88]. The potassium phosphate buffer system was subjected to a smaller pH change due to the crystallization of the monobasic salt which is less soluble than the dibasic form [87].

However, the presence of a phosphate buffer in the formulation will not necessary result in a pH shift. This phenomenon appears to be concentration and freezing-rate dependent. Lower concentrations will result in smaller pH shift [41, 89]. This has been illustrated with a Hepes buffered solution (pH 7.4) in an influenza formulation frozen at -20°C. A drop of 1.4 pH units has been determined for a concentration of 20mM [84], whereas at a concentration of 2mM the pH was reduced by less than 1 unit [41]. Variation in pH for a phosphate buffered saline depended also on the cooling rate with fast cooling (quenching) resulting in a more pronounced pH change compared to slow freezing [41, 88, 91].

Finally, crystallization of buffer species can also be inhibited by agents such as sucrose and mannitol [38, 68]. For sodium phosphate buffer, sucrose and mannitol act by inhibiting the crystallization of dibasic sodium phosphate [92].

Several other buffers (tartrate, succinate, malate and citrate) present interesting properties for lyophilization purposes but are not used for freeze-drying of viruses because of their pH range, which is not appropriate for viruses.

- *Stabilizer*

Stabilizers are added to the formulation to provide protection to the active ingredient against process-induced stress [75]. Because neither the impact of each freeze-drying step on the live, attenuated vaccine, nor the stabilization mechanisms needed to protect the live viruses are fully understood or known, stabilizers are selected by trial-and-error screenings [8, 49].

However, the large variability (size, shape, composition) in nature of antigens can make the optimal lyo- and cryoprotectant formulation difficult. Several classes of compounds (disaccharides, polyols, animal derived compounds, etc) have been used to stabilize freeze-dried live, attenuated vaccines. Information gained from published studies (Table 3.2) as well as from databases of licensed vaccines (Table 3.1) reveal some trends.

Disaccharides (i.e., sucrose and trehalose) are generally good stabilizers and are frequently used. In addition, sorbitol and animal-derived components (gelatin or albumin) seem to provide a satisfactory stability and are also frequently used.

- *Sucrose and trehalose*

Disaccharides like sucrose and trehalose have the capacity to remain amorphous during freeze-drying and are referred to in many publications as good stabilizers [75], with high Tg [90] and higher Tc than monosaccharides [93].

Even if never demonstrated, sucrose and trehalose probably protect the live viruses during freeze-drying by forming a glass (vitrification) and/or hydrogen bonds (water-substitution), hence avoiding several stresses. During the freezing step, dispersion of the antigen into a glass could prevent membrane fusion/aggregation and membrane damage caused by ice crystals. The stabilizers can also protect the viruses indirectly by inhibiting buffer crystallization. During the drying steps, the sugars can act as a water substitution agent by forming hydrogen bonds with the coated proteins or the lipid membrane, hence stabilizing the viruses. By lowering the melting temperature of the lipid membrane, the sugars can also prevent the membrane from phase transition during rehydration of the lyophilized product.

Only two formulations shown in Table 3.2 mention the use of trehalose as a stabilizer despite its more favorable properties. Sucrose is one of the best stabilizers but compared to trehalose, sucrose has been reported to undergo hydrolysis at low pH [75, 94-96], forming reducing monosaccharides whereas no similar report is found for trehalose. Moreover, the viscosity of trehalose in solution has been determined to be nearly 2.5-fold higher than sucrose for all concentrations tested [97]. The viscosity increase during freezing restricts diffusion of reacting molecules [28], minimizing the rate of chemical degradation [29]. The glass transition temperature of trehalose is superior (118°C) [90] to sucrose (75°C) [90] which is particularly important for the long-term stability at ambient temperature. The glass transition temperature of maximally concentrated solutions (Tg') is higher for trehalose (-40°C) in comparison with sucrose (-46°C) [98] allowing a higher primary drying temperature and therefore a shorter primary drying time. For a detailed review on trehalose, readers are referred to [98].

Despite the favorable properties of trehalose, its limited occurrence in vaccine formulation is linked to the following aspects. Firstly, the superiority of trehalose as stabilizer is not universal. Better shelf-stability has been sometimes observed with formulations containing sucrose compared to similar formulations containing trehalose [26, 81, 93]. A combination of

lactalbumin hydrolysate-sucrose was found to be a better thermal protectant of the live, attenuated *peste des petits ruminants* (PPR) vaccine than trehalose alone [78]. Conversely, in a stability study at various temperatures (i.e., 4°C, 25°C, 37°C and 40°C) trehalose, in combination with amino acids and divalent cations has been demonstrated to better protect a camelpox virus vaccine than a combination of sucrose and lactalbumine hydrolysate [85]. Similarly, trehalose in combination with gelatin was demonstrated to be a better stabilizer than sucrose combined with sorbitol for the protection of a live-attenuated mumps vaccine [86]. Using Design of Experiments (DOE), sucrose, in combination with raffinose and compounds frequently observed to accumulate in developing seeds, demonstrated promising long-term stabilization of adenovirus (Ad5) in liquid and freeze-dried formulation stored at various temperatures [99]. Although the use of trehalose in commercial products has been subjected for approval by several governing bodies, this compound has only recently been listed as a pharmaceutical reagent in the United States National Formulary (in 2010), European Pharmacopoeia (in 2010) and the Japanese Pharmacopoeia (in 2011) [98]. These approvals combined with the fact that the use of trehalose to stabilize live attenuated vaccines is recently off-patent, will undoubtedly increase the use of this stabilizer in vaccine formulations.

- *Sorbitol*

Sorbitol is a sugar alcohol which does not easily crystallize [81] despite being an isomer of mannitol (the most commonly used bulking agent) and has been demonstrated, when formulated together with gelatin, to be an effective stabilizer for measles virus [100], rinderpest virus [80], duck viral hepatitis virus [82] and others commercialized vaccines listed in Table 3.1. Different sugars (lactose, sucrose and trehalose) and sorbitol were compared to stabilize duck viral hepatitis virus (DHV). The only formulations able to confer an acceptable stability were the sorbitol-containing formulations [89]. For measles virus, a sorbitol:gelatin ratio of 2:1 is sufficient to preserve the potency of the virus [100]. For DHV, higher sorbitol concentrations (sorbitol:gelatin ratio of 4:1, 8:1 and 16:1) reduce the stability [82]. This could be due to the low Tg of sorbitol (-1.6°C) [101] which implies that sorbitol cannot be used as a main formulation component. The low Tg of sorbitol limits its use, but is probably at the origin of its stabilizing success. Chang and co-workers studied the effect of sorbitol on the stability of lyophilized antibodies [102]. When added to a sucrose formulation, due to its

low Tg, sorbitol acts as plasticizer, increasing the molecular mobility but improving the stability upon storage of an IgG1 (according to Chang, this surprising observation is due to the fact that "mobility" does not control protein stability at storage temperature well below the formulation Tg). In this same study, FTIR results showed that the sucrose formulation containing sorbitol produces a more "native-like structure" than the sucrose formulation without sorbitol [102].

- *Animal-derived components*

Animal-derived components such as gelatin and albumin have also been used as stabilizer in freeze-dried live, attenuated vaccines. Albumin, in combination with sucrose, was employed in 1950 by Bovarnick and coworkers to stabilize rickettsiae [103]. The gelling characteristics of gelatin are frequently used in vaccine formulation (Tables 3.1 and 3.2) to prevent inactivation due to environmental changes such as temperature [82]. However, animal-derived compounds like gelatin represent a potential danger due to the possible contamination with the scarpie-prion-protein (PrP^{SC}) and the new variant of the Creutzefeld-Jakob disease (vCJD) [104] and are therefore more and more requested to be replaced by stabilizers of non-animal origin. In an attempt to substitute gelatin as a stabilizer for a varicella virus liquid vaccine, other components including κ-Carrageenan and different plant proteins have been investigated [105]. Carrageenan, a polysugar synthesized by red algae, was the best choice regarding its capacity to retain the activity of the virus compared to a control formulation with gelatin as stabilizer [105].

A novel promising excipient, silk fibroin, a biologically-derived protein polymer purified from domesticated silkworm (*Bombys mori*) cocoons has recently shown interesting stabilizing properties on a MMR (measles, mumps, rubella) vaccine [106]. The encapsulation of measles, mumps and rubella viral particles in silk film enhanced their storage stability at 25, 37 and 45°C. The mechanism of stabilization seems to act by reducing residual moisture increase during storage at elevated temperatures and by increasing the denaturation temperature of the viral proteins [106].

3.4. PROCESS DEVELOPMENT STRATEGY

The development of a freeze-dying process is very important because of the impact the chosen parameters have on the final product (product appearance, virus potency/stability, residual moisture and freeze-drying cycle duration).

Several studies describing the freeze-drying of virus-based vaccines do not pay attention to the freeze-drying process optimization (process settings) [39, 79-82,107-112]. These studies mainly focus on the formulation optimization by comparing different stabilizers and their effect upon virus titer under different storage conditions and on residual moisture of the finished product. The effects of the process conditions used are often unknown and the rationale behind their settings is almost never described. The choice for a specific set of parameters is often based on previous experience [83], or because it corresponds to a gentle cycle that allows the preservation of a large range of bacteria (for a bacterial vaccine) [113].

Table 3.3 presents some vaccine studies and their freeze-drying process parameters used. Comparing the different process conditions (temperature, pressure and time) between the different studies is impossible because critical product parameters like T_g', T_c, filling volume or filling depth, are formulation dependent. However, Table 3.3 shows a high variability of freeze-drying approach like the use of pre-cooled shelves and the cooling rate, which have a direct effect on the virus.

The use of pre-cooled shelves is conventional when freeze-drying vaccines [83]. However, based on Table 3.3, it is not systematically used (e.g., quench freezing) or when loading on pre-cooled shelves is not desired. The placement of the vials on the shelves that have already been cooled to the desired freezing temperature (typically -40 or -45°C) results in higher nucleation temperature (i.e., low degree of supercooling, -9.5°C), compared to the conventional shelf-ramped freezing (-13.4°C) [114]. With this pre-cooled shelf method, a large heterogeneity in supercooling between vials is observed [114], but this is also the case with the shelf-ramped freezing with differences up to 3°C resulting in important variability in product quality and process performance [115].

In order to obtain a more homogeneous freezing and avoid any ice formation on shelves prior loading, vials can be equilibrated at low shelf temperature (5-10°C) for 15-30min before linearly decreasing the shelf temperature [116].

A thorough study of both shelf-ramp and shelf pre-cooling freezing methods on virus potency could provide valuable process information and is, to our best knowledge, lacking.

As sufficiently demonstrated, the cooling rate is of major importance for virus protection.

Two studies [37, 41] listed in Table 3.3 compared different cooling rates and demonstrated the significant effect of this parameter on virus stabilization. Structural integrity of haemagglutinin of an influenza subunit vaccine is better preserved when the solution is rapidly frozen in liquid nitrogen [37]. Fast freezing allows the system to rapidly vitrify which may prevent the conformational change [37].

Herpes simplex virus-2 was better preserved when frozen in slush nitrogen [41]. In this case, the high cooling rate has a positive impact on the viruses by promoting the formation of small ice crystals.

From the two presented studies [37, 41], it seems that quench freezing offers better preservation of viruses than slow freezing. Another emerging technique during freezing is the use of controlled nucleation, allowing the control of the nucleation temperature [50]. This method results in a more uniform ice crystal structure and maybe virus titer. This method is subjected to investigational studies in the pharmaceutical industry. To date, no study evaluating the impact of controlled ice nucleation on live attenuated viruses has been published.

Finally, Table 3.3 reveals that while the effect of cooling rate on viruses receives limited attention, the impact of primary and secondary drying parameters (temperature, time and pressure) on viruses receives almost no attention. These parameters can be easily calculated to obtain a freeze-drying cycle that promises an elegant product in the shortest time possible [117]. Rules and advice to select appropriate drying steps conditions for protein formulation are largely available in literature [28, 92, 115, 116] and can be applied to viruses.

Primary drying is however very important as demonstrated by Schneid and co-workers on a bacterial vaccine formulation [117]. Whereas conservative primary drying conditions resulted after 28 days storage at 40°C in 50.10^6 living bacteria cells in the product, an increase of the primary drying temperature of 2 and 5°C resulted in 28.10^6 and 20.10^6 living

bacteria cells, respectively [117]. This study highlights the importance of carefully selecting the primary drying temperature as a difference of 2°C can result in a 44% loss.

Residual moisture of the end product can impact vaccine stability and is dictated by the temperature, pressure and duration of secondary drying that are established via empirical studies [75]. Staying within a specified range of residual moisture levels can be vital for product integrity [4]. Whereas overdrying is to be avoided, too high residual moisture levels can cause structural collapse during storage [75] and can increase the product degradation rate as the sorbed water provides molecular mobility [4,75] that can induce chemical degradation (methionine oxidation of human growth hormone [118]) and aggregation (human serum albumin [119]).

Table 3.3: Process parameters of some vaccine studies.

Pre-cooled shelves	Cooling rate	Freezing (Temperature / Time)	Annealing (Temperature / Time)	Primary drying (Temperature / Pressure / Time)	Secondary drying (Temperature / Pressure / Time)	Organism	Remarks	Reference
-45°C	Unk	-45°C / 90min	-15°C / 33h	-30°C / 0.1mbar / 48h	2 steps: 1) 0°C / 0.1mbar / 30min 2) 10°C / 0.1mbar / 280min	Medi 534 Live attenuated virus vaccine	Annealing step not for all samples	[83]
No	Unk	-20°C / 24h (refrigerator) Liquid nitrogen / 5 - 10min	No	-35°C / 0.220mbar / 24h	20°C / 0.060mbar / 24h	Influenza subunit vaccine	Transferred to a vacuum dessicator at RT for 2 days	[41]
No	Unk	-75°C / unk. (cold air chamber)	No	-10°C / 0.15mbar / 18h	20°C / 0.15mbar / 15h	Bacteria		[113]
-50°C	10°C.sec^{-1}	-50°C / ~25sec	No	-50°C / 0.067mBar / 1000min	5°C / 0.067mBar / 120min	HSV-2 virus		[37]
No	20-50°C.sec^{-1}	Slush nitrogen / ~25sec	No	-180 to 20°C / 1.10^{-5}mBar / 14h				
No	200-400°C.sec^{-1}	Melting propane / ~25sec	No					

Table 3.3: Process parameters of some vaccine studies (continued).

No	Unk	Liquid nitrogen / 5 - 10min	No	-35°C / 0.220mbar / 24h	20°C / 0.060mbar / 24h	Virosomes	Same research group as [41]	[56]
No	1°C/min	-50°C / 3h	No	2 Steps: 1) -50°C / 3Pa / 60h 2) 0°C / 3Pa / 4h	20°C / 3Pa / 8h	Adenovirus		[119]
No	1°C/min	-40°C / 3h	No	2 Steps: 1) -35°C / 0.045mbar / 25h 2) -20°C / 0.045mbar / 10h	20°C / 0.045mbar / 10h	Virus like particles		[120]
			No	-15°C / 0.045mbar / 20h	40°C / 0.007mbar / 10h			
			-15°C / 2h	-15°C / 0.045mbar / 20h	40°C / 0.007mbar / 10h			
No	Unk	-40°C / 3h	No	-40 to 37°C / 60mTorr / 40h		Duck viral hepatitis vaccine		[82]

Unk= unknown.

3.5. CONCLUSION

Despite the high dependence on freeze-drying to stabilize live virus vaccines, their lyophilization process and especially their (de)stabilization mechanisms are still not well elucidated. The complexity of these formulations as well as the lack of techniques to evaluate the different virus degradation pathways are responsible for this gap [4, 7, 83]. Moreover, the large financial issues behind vaccine development and stabilization make that the available information is rarely published. However, other biopharmaceuticals like proteins, liposomes and cells have been well studied and provide valuable knowledge. Knowing the different stresses that can occur during freeze-drying is essential to provide stabilization solutions.

During the freezing step, the stresses that viruses can face are numerous and summarized in Table 3.4. Although the stresses and their causes are different, there are two strategies that can be used to protect the virus: an appropriate cooling rate and the use of a cryoprotectant that acts via the solid exclusion hypothesis and/or the vitrification hypothesis.

Table 3.4: Summary of the possible virus stresses during the freezing step, their cause and the strategy that can be used to avoid the stress.

Stress	Cause	Strategy to protect
Intra-virus ice formation	Fast freezing	Cryoprotectant and adequate cooling rate
Osmolarity change	Conversion of water into ice	Cryoprotectant and adequate cooling rate
pH shift	Buffer crystallization	Cryoprotectant Low buffer concentration Adequate cooling rate
Coated proteins destabilization	Freeze concentration	Cryoprotectant
Lipid destabilization -mechanical damage -fusion and phase transition	Ice formation	Cryoprotectant

Information related to the destabilization mechanisms during the drying steps are less numerous. The lipid membrane and the coated viral proteins are the main attributes

susceptible to degradation. Both can be protected by the use of a stabilizer via the vitrification hypothesis and the water replacement hypothesis. A typical property of lipids is their melting temperature (Tm) that must be taken into account in order to avoid phase transition. Disaccharides, via the water substitute hypothesis, can decrease the Tm and avoid such phase transition [73, 74].

Examination of the formulations used to stabilize viruses reveals a relatively constant use of sorbitol, sucrose and animal-derived components such as gelatin. However, other compounds (like trehalose and silk fibroin) are gaining interest in the freeze-drying field because of their superior stabilizing properties.

Finally, process parameters, despite being of high importance (cooling rate, primary and secondary drying temperatures) are not subjected to extensive studies. During optimization studies, the formulation parameters often receive priority over the process settings while they however should be considered together.

REFERENCES

[1]   D.A. Henderson, and F. Fenner. Smallpox and vaccinia. In: Plotkin, S.A. and Mortimer, E.A. editors. Vaccines, 2nd ed., Philadelphia, PA: W.B. Saunders, 1994.

[2]   WHO/UNICEF, Global Immunization Data. 2010. p. 4.

[3]   WHO, UNICEF, World bank. State of the world's vaccines and immunization, 3rd ed. Geneva, World Health Organization, 2009

[4]   J. Rexroad, C.M. Wiethoff, L.S. Jones, C.R. Middaugh. Lyophilization and the thermostability of vaccines. Cell preservation technology, 2002; 1(2)

[5]   J. Peetermans, Factors affecting the stability of viral vaccines. Developments in biological standardization, 1996; 87:97-101.

[6]   NIAID, 2012. http://www.niaid.nih.gov/topics/vaccines/understanding/pages/ typesvaccines.aspx (accessed on September 12, 2012)

[7]   C.J. Burke, T.A. Hsu, and D.B. Volkin. Formulation, stability, and delivery of live attenuated vaccines for human use. Critical Reviews in Therapeutic Drug Carrier Systems, 1999. 16(1): 1-83.

[8]   J.G. Aunins, A.L. Lee, D.B. Volkin. Vaccine Production. In: Bronzino Joseph D. Editor. The Biomedical Engineering Handbook: 2nd Edition. Boca Raton: CRC Press LLC, 2000.

[9]   P. Van Gelder, B. Makoschey. Production of viral vaccines for veterinary use. Berl. Munch. Tierarztl. Wochenschr., 2012. 125(3-4):103-109

[10]   J.P. Emond. The cold chain, In: Stephen S.E.S., Miles B., and Williams John R. Editors. RFID Technology and new studies applications, Cambridge University Press 2008.

[11]   H. Briggs, S. Ilett. Weak link in vaccine cold chain. British medical journal, 1993; 306:557-558.

[12] S. Hunter. Storage of vaccines in general practice. British medical journal, 1989; 299:661-662

[13] R.B. Haworth, L. Stirzaker, S. Wilkes, A. Battersby. Is the cold chain maintained in general practice? British medical journal, 1993; 307:242-244

[14] T. Yogini, S. Woods. Storage of vaccines in the community: Weak link in the cold chain? British medical journal, 1992; 304:756-758

[15] S. Setia, H. Mainzer, M.L. Washington, G. Coil, R. Snyder, B.G. Weniger. Frequency and causes of vaccine wastage. Vaccine, 2002; 20(7-8): 1148-1156.

[16] S. Jaspal, C. Kanta Gupta, B. Sharma, H. Singh. Stability of oral polio vaccine at different temperatures. Vaccine, 1988; 6:12-13

[17] P.A. Pipkin, P.D. Minor. Studies on the loss of infectivity of live type 3 polio vaccine on storage. Biological, 1998; 26:17-23

[18] J.P. Amorij, A. Huckriede, J. Wilschut, H. Frijlink, W.L.J. Hinrichs. Development of Stable Influenza Vaccine Powder Formulations: Challenges and Possibilities. Pharmaceutical Research, 2008; 25(6): 1256-1273.

[19] J.F. Carpenter, M.J. Pikal, B.S. Chang, T.W. Randolpf. Rational design of stable lyophilized protein formulations: some pratical advice. Pharmaceutical research, 1997; 14:969-975.

[20] J. Sokhey, C.K. Gupta, B. Sharma, H. Singh. Stability of oral polio vaccine at different temperatures. Vaccine, 1988;6(1):12-3

[21] D. Chen, D. Kristensen. Opportunities and challenges of developing thermostable vaccines. Expert Review Vaccines, 2009; 8(5): 547-557

[22] D.B. Volkin, C.R. Middaugh. Vaccines as physically and chemically well-defined pharmaceutical dosage forms. Expert Review of Vaccines, 2010; 9(7): 689-691.

[23] D.B. Volkin, C.J. Burke, G. Sanyal, C.R. Middaugh. Analysis of vaccine stability. Developments in biological standardization 1996; 87:135-142.

[24] J-M. Sarciaux, S. Mansour, M.J. Hageman, S.L. Nail. Effects of buffer composition and processing conditions on aggregation of bovine IgG during freeze-drying. Journal of Pharmaceutical Sciences, 1999; 88(12): 1354-1361.

[25] T.J. Anchordoquy, J.F. Carpenter. Polymers Protect Lactate Dehydrogenase during Freeze-Drying by Inhibiting Dissociation in the Frozen State. Archives of Biochemistry and Biophysics, 1996; 332(2): 231-238.

[26] L. Chang, J. Shepherd, J. Sun, D. Ouellette, K.L. Grant, X.C Tang, M.J. Pikal. Mechanism of protein stabilization by sugars during freeze-drying and storage: Native structure preservation, specific interaction, and/or immobilization in a glassy matrix? Journal of Pharmaceutical Sciences, 2005; 94(7): 1427-1444.

[27] L.L. Chang, M.J. Pikal. Mechanisms of Protein stabilization in the solid state. Journal of Pharmaceutical sciences, 2009; 98(9):2886-2908.

[28] W. Wang. Lyophilization and development of solid protein pharmaceuticals. International Journal of Pharmaceutics, 2000; 203(1-2): 1-60.

[29] M.J. Pikal. Mechanisms of protein stabilization during freeze-drying and storage: the relative importance of thermodynamic stabilization and glassy state relaxation dynamics., In: Rey L., May J.C., Editors. Freeze-Drying/Lyophilization of Pharmaceutical and Biological Products, New York. Marcel Dekker; 1999, 161-198.

[30] D.O. White, F.J. Fenner. Medical Virology, 3rd ed. Academic, Orlando, FL, 1987.

[31] J.Wolfe, G. Bryant. Cellular cryobiology: thermodynamic and mechanical effects. International Journal of Refrigeration, 2001; 24(5): 438-450.

[32] D.E. Pegg. Principles of cryopreservation, in Cryopreservation and freeze-drying protocols, J.G. Day, Stacey, G.N, Editor. 2007: New Jersey.

[33]   S.J. Paynter. Principles and practical issues for cryopreservation of nerve cells. Brain Research Bulletin, 2008; 75(1): 1-14.

[34]   P. Mazur. Kinetics of water loss from cells at subzero temperatures and the likelihood of intracellular freezing. The Journal of general physiology, 1963; 47: 347-369.

[35]   D.T. Brandau, L.S. Jones, C.M. Wiethoff J. Rexroad, C.R. Middaugh. Thermal stability of vaccines. Journal of Pharmaceutical Sciences, 2003; 92(2): 218-231.

[36]   W.M. Colwell, D.G. Simmons, J.R., Harris, T.G. Fulp, J.H. Carrozza, T.A. Maag. Influence of some physical factors on survival of Marek's disease vaccine virus. Avian Diseases, 1975; 19: 781-790.

[37]   S. Zhai, R.K. Hansen, R. Taylor, J.N. Skepper, R. Sanches, N.K.H. Slater. Effect of freezing rates and excipients on the infectivity of a live viral vaccine during lyophilization. Biotechnology Progress, 2004; 20: 1113-250.

[38]   S.L. Nail, S. Jiang, S. Chongprasert, S.A. Knopp. Fundamentals of freeze-drying. Pharmaceutical Biotechnology, 2002; 14: 281-360.

[39]   D.A. Yannarell, K.M. Goldberg, R.N. Hjorth, Stabilizing cold-adapted influenza virus vaccine under various storage conditions. Journal of Virological Methods, 2002; 102(1-2): 15-25.

[40]   J.F.E. Newman, S. Tirrell, C. Ullman, P.G. Piatti, F. Brown. Stabilising oral poliovaccine at high ambient temperatures. Vaccine, 1995; 13(15): 1431-1435.

[41]   J.P. Amorij, J. Meulenaar W.L.J. Hinrichs, T. Stegmann, A. Huckriede, F. Coenen H.W. Frijlink. Rational design of an influenza subunit vaccine powder with sugar glass technology: Preventing conformational changes of haemagglutinin during freezing and freeze-drying. Vaccine, 2007; 25(35): 6447-6457.

[42]   R.W. Ruigrok, S.R. Martin, D.C. Wiley, P.M. Bayley, S.A. Wharton, J.J. Skehel. Conformation changes in the haemagglutinin of influenza virus which accompany heat-induced fusion of virus with liposomes. Virology, 1986; 155(2): 484-97.

[43] M. Krumbiegel, A. Herrmann, R. Blumenthal. Kinetics of the low pH-induced conformational changes and fusogenic activity of the influenza hemagglutinin. Biophysical Journal, 1994;67(6):2355-60.

[44] J. Kissmann, S.F. Ausar, A. Rudolph, C. Braun, S.P. Cape, R.E. Sievers, M.J. Federspiel, S.B. Joshi, C.R. Middaugh. Stabilization of measles virus for vaccine formulation. Human vaccine, 2008; 4(5): 350-359.

[45] F.L. Black, Growth and stability of measles virus. Virology, 1959; 7(2): 184-192.

[46] R.J. Salo, and D.O. Cliver, Effect of acide pH, salts, and temperature on infectivity and physical integrity on enteroviruses. Archives of Virology, 1976; 52(4): 269-282.

[47] D. Greiff, W.A. Rightsel. Stability of suspension of inluenza virus dried to different contents of residual moisture by sublimation in vacuo. Applied Microbiology, 1968; 16 (6): 835-840.

[48] D. Greiff, W.A. Rightsel. Stabilities of dried suspensions of influenza virus sealed in a vacuum of under different gases. Applied Microbilogy, 1969; 17(6): 830-835.

[49] B.S. Bhatnagar, R.H. Bogner, and M.J. Pikal, Protein Stability During Freezing: Separation of Stresses and Mechanisms of Protein Stabilization. Pharmaceutical Development and Technology, 2007; 12(5): 505-523.

[50] J.C. Kasper, and W. Friess, The freezing step in lyophilization: Physico-chemical fundamentals, freezing methods and consequences on process performance and quality attributes of biopharmaceuticals. European Journal of Pharmaceutics and Biopharmaceutics, 2011; 78(2): 248-263.

[51] T.W. Randolph, Phase separation of excipients during lyophilization: Effects on protein stability. Journal of Pharmaceutical Sciences, 1997; 86(11): 1198-1203.

[52] G.B. Strambini, E. Gabellieri. Proteins in frozen solutions: evidence of ice induced partial unfolding, Biophysical journal 1996; 70: 971–976.

[53] B.S. Bhatnagar, M.J. Pikal, R.H. Bogner. Study of the individual contibutions of ice formation and freeze-concentration on isothermal stability of lactate dehydrogenase during freezing. Journal of Phamraceutical Sciences, 2008; 97: 798-814.

[54] S. Nema, K.E. Avis. Freeze-thaw studies of a model protein, lactate dehydrogenase, in presence of cryoprotectants. Journal of parenteral and science technology, 1993; 47: 76-83.

[55] R.K. Hansen, S. Zhai, J.N. Skepper, M.D. Johnston, H.O. Alpar, N.K.H. Slater. Mechanisms of Inactivation of HSV-2 during Storage in Frozen and Lyophilized Forms. Biotechnology Progress, 2005; 21(3): 911-917.

[56] J. de Jonge, J.P. Amorij, W.L.J. Hinrichs, J. Wilschut, A. Huckriede, H.W. Frijlink. Inulin sugar glasses preserve the structural integrity and biological activity of influenza virosomes during freeze-drying and storage. European Journal of Pharmaceutical sciences, 2007; 32: 33-34.

[57] C. Grose, W.E. Friedrichs, K.O. Smith. Cryopreservation of varicella-zoster virions without loss of structural integrity of infectivity. Intervirology, 1981; 15(3): 156-160.

[58] C. Chen, D. Han, C. Cai, X. Tang. An overview of liposome lyophilization and its future potential. Journal of Controlled Release, 2010; 142(3): 299-311.

[59] J.H. Crowe, J.F. Carpenter, L.M. Crowe, T.J. Anchordoguy. Are freezing and dehydration similar stress vectors? A comparison of modes of interaction of stabilizing solutes with biomolecules. Cryobiology, 1990; 27: 219-231.

[60] D. Greiff, H. Blumenthal, M. Chiga, H. Pinkerton. The effects on biological materials of freezing and drying by vacuum sublimation. II. Effect on influenza virus. The Journal of Experimental Medicine, 1954; 100(1): 89-101.

[61] W.F. Wolkers, F. Tablin, J.H. Crowe. From anhydrobiosis to freeze-drying of eukaryotic cells. Comparative biochemistry and physiology A, 2002; 131 (3): 535-543.

[62]   M. Pieters, J.C. Jerling, J.W. Weisel. Effect of freeze-drying, freezing and frozen storage of blood plasma on fibrin network characteristics. Thrombosis Research, 2002; 107(5): 263-269.

[63]   J.F. Carpenter, S.J. Prestrelski, T. Arakawa. Separation of Freezing- and Drying-Induced Denaturation of Lyophilized Proteins Using Stress-Specific Stabilization: I. Enzyme Activity and Calorimetric Studies. Archives of Biochemistry and Biophysics, 1993; 303: 456-464.

[64]   A. Engel, G. Bendas, F. Wilhelm, M. Mannova, M. Ausborn, P. Nuhn. Freeze-drying of liposomes with free and membrane-bound cryoprotectants — the background of protection and damaging processes, International Journal of Pharmaceutics, 1994; 107(2): 99-110.

[65]   P.R. Harrigan, T.D. Madden, P.R. Cullis. Protection of liposomes during dehydration or freezing. Chemistry and Physics of Lipids, 1990; 52(2): 139-149

[66]   S.D. Allison, M.d.C. Molina, T.J. Anchordoquy. Stabilization of lipid/DNA complexes during the freezing step of the lyophilization process: the particle isolation hypothesis. Biochimica and Biophysica Acta, 2000; 1468: 127-138.

[67]   L.F. Siow, T. Rades, M.H. Lim. Cryo-responses of two types of large unilamellar vesicles in the presence of non-permeable or permeable cryoprotecting agents. Cryobiology, 2008; 50: 276-285.

[68]   E.Y. Shalaev, and F. Franks. Changes in the Physical State of Model Mixtures during Freezing and Drying: Impact on Product Quality. Cryobiology, 1996; 33(1): 14-26.

[69]   B.S. Chang, C.S. Randall. Use of subambient thermal analysis to optimize protein lyophilization. Cryobiology, 1992; 29: 632-656.

[70]   P. Mazur. Kinetics of water loss from cells at subzero temperatures and the likelihood of intracellular freezing. Journal of General Physiology, 1963;47:347-369.

[71] J.A. Rupley, G. Careri. Protein hydration and function. Advances in Protein Chemistry, 1991; 41: 37-173.

[72] J.H. Crowe, L. M. Crowe, J.F. Carpenter. Preserving dry biomaterials: the water replacement hypothesis. Biopharm, 1993; 6(1): 28.

[73] J. H. Crowe, and L. M. Crowe. Preservation of liposomes by freeze-drying. In G. Gregoriadis, Editor. Liposome Technology, 2nd ed. CRC Press, Boca Raton, FL, 1992.

[74] L. M. Crowe, and J. H. Crowe. Freeze-dried liposomes. In: Puisieux F, Editor. Liposomes Paris, Editions de Sante, 1995, 237–272.

[75] M.J.Pikal. Freeze-drying. Encyclopedia of Pharmaceutical Technology: 1807 - 1833.

[76] J.H. Crowe, L.M. Crowe, A.E. Olivier, N. Tsvetkova, W. Wolkers, F. Tablin. The Trehalose Myth Revisited: Introduction to a Symposium on Stabilization of Cells in the Dry State. Cryobiology, 2001; 43(2): 89-105.

[77] P.M. Precausta, D. Simatos, M. Le Pemp, B. Devaux, F. Kato. Influence of residual moisture and sealing atmosphere on viability of two freeze-dried viral vaccines. Journal of Clinical Microbiology, 1980; 12(4): 483-489.

[78] O.S. Kumru, S.B. Joshi, D.E. Smith, C.R. Middaugh, T. Prusik, D.B. Volkin. Vaccine instability in the cold chain: Mechanisms, analysis and formulation strategies. Biologicals, 2014; 42: 237-259.

[79] G.A. Tannock, J.C. Hierholzer, D.A. Bryce, C-F. Chee, J.A. Paul. Freeze-drying of respiratory syncytial viruses for transportation and storage. Journal of Clinical Microbiology, 1987, 25(9): 1769-1771.

[80] J.C. Mariner, J.A. House, A.E. Sollod, C. Stem, M. Van Den End, C.A. Mebus. Comparison of the effect of various chemical stabilizers and lyophilization cycles on the thermostability of a vero cell-adapted rinderpest vaccine. Veterinary Microbiology, 1990; 21(3): 195-209.

[81] J. Sarkar, B.P. Sreenivasa, S.P. Dhar, S.K. Bandyopadhyay. Comparative efficacy of various chemical stabilizers on the thermostability of a live-attenuated peste des petits ruminants (PPR) vaccine. Vaccine, 2003; 21(32): 4728-4735.

[82] M.S. Kang, H. Jang, M.C. Kim, M.J. Kim, S.J. Joh, J.H. Kwon, Y.K. Kwon. Development of a stabilizer for lyophilization of an attenuated duck viral hepatitis vaccine. Poultry Sciences, 2010; 89(6): 1167-1170.

[83] A. Abdul-Fattah, V. Truong-Le, L. Yee, E. Pan, Y. Ao, D.S. Kalonia, M.J. Pikal. Drying-Induced Variations in Physico-Chemical Properties of Amorphous Pharmaceuticals and Their Impact on Stability II: Stability of a Vaccine. Pharmaceutical Research, 2007; 24(4): 715-727.

[84] M.A. Croyle, B.J. Roessler, B.L. Davidson, J.L. Hilfinger, G.L. Amidon. Factors that Influence Stability of Recombinant Adenoviral Preparations for Human Gene Therapy. Pharmaceutical Development and Technology, 1998; 3(3): 373-383.

[85] M. Prabhu, V. Bhanuprakash, G. Venkatesan, R. Yogisharadhya, D.P. Bora, V. Balamurugan. Evaluation of stability of live attenuated camelpox vaccine stabilized with different stabilizers and reconstituted with various diluents. Biologicals, 2014; 42(3):169-75.

[86] R.K. Jamil, M. Taqavian, Z.A. Sadigh, M.K. Shahkarami, F. Esna-Ashari, R. Hamkar, S.M. Hosseini, A. Hatami. Evaluation of the thermal stability of a novel strain of live-attenuated mumps vaccine (RS-12 strain) lyophilized in different stabilizers. Journal of virological methods, 2014; 199:35-8.

[87] N. Murase, and F. Franks. Salt precipitation during the freeze-concentration of phosphate buffer solutions. Biophysical Chemistry, 1989; 34(3): 293-300.

[88] G. Gomez, M.J. Pikal, and N. Rodríguez-Hornedo. Effect of Initial Buffer Composition on pH Changes During Far-From-Equilibrium Freezing of Sodium Phosphate Buffer Solutions. Pharmaceutical Research, 2001; 18(1): 90-97.

[89] G. Gomez, M.J. Pikal. Effect of freezing on the pH of sodium phosphate buffer solutions. Pharmaceutical Research, 1994; 11.

[90] L.S. Taylor, and G. Zografi. Sugar–polymer hydrogen bond interactions in lyophilized amorphous mixtures. Journal of Pharmaceutical Sciences, 1998; 87(12): 1615-1621.

[91] L. van den Berg, D. Rose. Effect of freezing on the pH and composition of sodium and potassium phosphate solutions: The reciprocal system KH2PO4-Na2HPO4-H2O. Archives of Biochemistry and Biophysics, 1959; 81: 319-329.

[92] J.J. Schwegman, L.M. Hardwick, M.J. Akers. Practical formulation and process development of freeze-dried products. Pharmaceutical development and technology, 2005; 10:151-173

[93] G.D. Adams, Lyophilization of Vaccines, In: Robinson A., Hudson M.J., Cranage M.P., Editors. Vaccine Protocols, 2nd ed, Totowa, NJ, Humana Press, 1996. 167-185.

[94] M. Karel, and T.P. Labuza. Nonenzymic browning in model systems containing sucrose. Journal of Agricultural and Food Chemistry, 1968; 16(5): 717-719.

[95] T. Schoebel, S.R. Tannenbaum, and T.P. Labuza. Reaction at Limited Water Concentration 1. Sucrose Hydrolysis. Journal of Food Science, 1969; 34(4): 324-329.

[96] J.M. Flink, Nonenzymatic Browning of Freeze-Dried Sucrose. Journal of Food Science, 1983; 48(2): 539-542.

[97] M. Sola-Penna, and J.R. Meyer-Fernandes. Stabilization against Thermal Inactivation Promoted by Sugars on Enzyme Structure and Function: Why Is Trehalose More Effective Than Other Sugars? Archives of Biochemistry and Biophysics, 1998; 360(1): 10-14.

[98] Y. Roos. Melting and glass transitions of low molecular weight carbohydrates. Carbohydrate Research, 1993; 238: 39-48.

[99] M. Stewart S.J. Ward, J. Drew. Use of adenovirus as a model system to illustrate a simple method using standard equipment and inexpensive excipients to remove live virus dependence on the cold-chain. Vaccine, 2014; 32: 2931-2938.

[100] E. de Rizzo, E.C. Tenorio, I.F. Mendes, F.L. Fang, M.M. Pral, C.S. Takata, C. Miyaki, N.M. Gallina, H.N. Tuchiya and O.K. Akimura. Sorbitol-gelatin and glutamic acid-lactose solutions for stabilization of reference preparations of measles virus. Bulletin of the Pan American Health Organisation, 1989; 23: 299-305.

[101] L. Yu, D.S. Mishra, and D.R. Rigsbee, Determination of the glass properties of D-mannitol using sorbitol as an impurity. Journal of Pharmaceutical Sciences, 1998; 87(6): 774-777.

[102] L.L. Chang, D. Shepherd, J. Sun, X. Tang, M.J. Pikal. Effect of sorbitol and residual moisture on the stability of lyophilized antibodies: implications for the mechanism of protein stabilization in the solid state. Journal of Pharmaceutical Sciences, 2005; 94:1445-1455

[103] M.R. Bovarnick, J.C. Miller, and J.C. Snyder. The influence of certain salts, amino acids, sugars, and proteins on the stability of Riskettsiae. Journal of bacteriology, 1950; 59(4): 509-522.

[104] T. Nemoto, M. Horiuchi, N. Ishiquro, M. Sinagawa. Detection methods of possible prion contaminants in collagen and gelatin. Archives of Virology, 1999; 144(1): 177-184.

[105] B.-H. Chun, Y.K. Lee, B.C. Lee, N. Chung. Development of a varicella virus vaccine stabilizer containing no animal-derived component. Biotechnology Letters, 2004; 26(10): 807-812.

[106] J. Zhang, E. Pritchard, X. Hu, T. Valentin, B. Panilaitis, F. G. Omenetto, & D. L. Kaplan. Stabilization of vaccines and antibiotics in silk and eliminating the cold chain. Proceedings of the National Academy of Sciences of the United States of America, 2012; 109(30): 11981–11986.

[107] B.W. Calnek, S.B. Hitchner, and H.K. Adldinge. Lyophilization of cell-free Mareks disease herpesvirus and a herpesvirus from Turkeys. Applied Microbiology, 1970; 20(5): 723-726

[108] E.M. Scott, and W. Woodside. Stability of pseudorabies virus during freeze-drying and storage-effect of suspending media. Journal of Clinical Microbiology, 1976; 4(1): 1-5.

[109] D.K. Sood, R.K. Aggarwal, S.B. Sharma, J. Sokhey, H. Singh. Study on tha stability of17D-204 Yellow-fever vaccine before and after stabilization. Vaccine, 1993; 11(11): 254-258.

[110] O.N. Fellowes. Freeze-drying of foot-and-mouth disease virus and storage stability of infectivity of dried virus at 4C. Applied Microbiology, 1965; 13(3): 496-499.

[111] W.B. Beardmore, T.D. Clark, and K.V. Jones. Preservation of influenza virus infectivity by lyophilization. Applied Microbiology, 1968; 16(2): 362-365

[112] J. Kissmann, S.F. Ausar, A. Rudolph, C. Braun, S.P. Cape, R.E. Sievers, M.J. Federspiel, S.B. Joshi, C.R. Middaugh. Stabilization of measles virus for vaccine formulation. Human Vaccines, 2008; 4(5): 350-359.

[113] F. Fonseca, S. Passot, O. Cunin, M. Marin. Collapse temperature of freeze-dried Lactobacillus bulgaricus suspensions and protective media. Biotechnology Progress, 2004; 20: 229-238.

[114] J.A. Searles, J.F. Carpenter, T.W. Randolph. The ice nucleation temperature determines the primary drying rate of lyophilization for samples frozen on a temperature-controlled shelf. Journal Pharmaceutical Sciences, 2001; 90: 860-871.

[115] F. Franks. Freeze-drying of bioproducts: putting principles into practice. European Journal of Pharmaceutics and Biopharmaceutics, 1998; 45(3): 221-229.

[116] X. Tang, M.J. Pikal. Design of freeze-drying processes for pharmaceuticals: practical advice. Pharmaceutical Research, 2004; 21: 191-200.

[117] S.C. Schneid, P.M. Stärtzel, P. Lettner, H. Gieseler. Robustness testing in pharmaceutical freeze-drying: Inter-relation of process conditions and product quality attributes studied for a vaccine formulation. Pharmaceutical Development and Technology, 2011; 16(6): 583-590.

[118] T. Moreira, L. Cabrera, A. Gutierrez, A. Cadiz, M. Castellano. Role of temperature and moisture on monomer content of freeze-dried human albumin. Acta Pharm. Nord, 1992; 4: 59-60.

[119] S. Chen, D. Guo, B. Guo, J. Liu, Y. Shen, X. Xu, W. Huang, S. Guo. Investigation on formulation and preparation of adenovirus encoding human endostatin lyophilized powders. International journal of Pharmaceutics, 2012; 427: 145-152.

[120] R. Lang, G. Winter, L. Vogt, A. Zürcher, B. Dorigo, B. Schimmele. Rational Design of a Stable, Freeze-Dried Virus-Like Particle-Based Vaccine Formulation. Drug Development and Industrial Pharmacy, 2009; 35(1): 83-97.

CHAPTER 4

PROCESS ANALYTICAL TECHNOLOGY FOR FREEZE-DRYING

CHAPTER 4

PROCESS ANALYTICAL TECHNOLOGY FOR FREEZE-DRYING

4.1. PROCESS ANALYTICAL TECHNOLOGY

4.1.1. Introduction

In September 2003, the Wall Street Journal stated: 'The pharmaceutical industry has a little secret: even as it invents futuristic new drugs, its manufacturing techniques lag far behind those of potato-chip and laundry-soap makers' [1]. Still partially applicable today, conventional pharmaceutical manufacturing is generally accomplished using batch processing. Often considered as uncomprehended inefficient black-boxes, the batch processes are monitored with univariate sensors measuring e.g., pH, temperature and pressure. At the end of the process, end product quality is assessed off-line with time-consuming and less efficient laboratory testing conducted on randomly collected samples.

However, significant opportunities exist to improve pharmaceutical development, manufacturing, and quality assurance. In many other industries (e.g., chemical, food, agricultural, etc), real time fast and non-destructive process analyzers have replaced traditional off-line laboratory techniques [2]. The low analysis time (seconds or minutes) of the process analyzers compared to the traditional laboratory techniques (hours or days) offers the opportunity of live feedback (i.e., during processing). In addition, by eliminating the manual sampling handling, the sample integrity is retained and the risk of operator error is reduced [3].

Unfortunately, the pharmaceutical manufacturing industry has been hesitant to introduce such innovative systems. The highly regulated environment of the pharmaceutical industry was considered as rigid and unfavorable to innovation [4]. Therefore, in 2002, in order to eliminate the hesitancy to innovate, the Food and Drug Administration (FDA) launched a new initiative entitled "Pharmaceutical Current Good Manufacturing Practices (CGMPs) for

the 21st Century: A Risk-Based Approach" [5]. Aiming to a global improvement and the modernization of pharmaceutical manufacturing, this initiative was followed by the launch of several other guidelines written by the FDA [4, 6] and the International Conference of Harmonization (ICH) [7-9]. Process Analytical Technology (PAT) is a key element of the CGMPs for the 21st Century initiative [10] and is intended to encourage the development and implementation of effective and efficient innovative approaches in pharmaceutical development, manufacturing and quality assurance.

4.1.2. The PAT framework

The FDA has defined PAT as a system for designing, analyzing and controlling manufacturing through timely measurements (i.e., during processing) of critical quality and performance attributes of raw and in-process materials and processes, with the goal of ensuring final product quality. The term analytical in PAT is viewed broadly to include chemical, physical, microbiological, mathematical and risk analysis conducted in an integrated manner. One of the most important statements within the PAT concept is that 'quality cannot be tested into products; it should be built-in' [4]. By using the approach of building quality into products, the PAT guidance highlights the necessity to fundamentally understand the process. The design and development of well understood processes that will consistently ensure a predefined quality at the end of the manufacturing process is a desired goal of the PAT framework [4]. Several criteria must be fulfilled to consider a process well understood: (i) all critical sources of variability are identified and explained, (ii) variability is managed by the process, and (iii) product quality attributes can be accurately and reliably predicted over the design space established for materials used, process parameters, manufacturing, environmental and other conditions.

Several PAT tools are available to enable process understanding for scientific, risk-managed pharmaceutical development, manufacture, and quality assurance. An appropriate combination of some, or all, of these tools may be applicable to a single-unit operation, or to an entire manufacturing process and its quality assurance. These tools are subdivided in four categories [4].

- Multivariate tools for design, data acquisition and analysis

Pharmaceutical products and processes are complex multi-factorial systems. Structured experiments conducted during product and process development can provide scientific understanding of the relevant multi-factorial relationships and serve as building blocks of knowledge. Together with other development projects, they can become part of an overall institutional knowledge system for a particular product and its processes and support the development of process simulation models. An appropriate use of these tools enables identification and evaluation of product and process variables that may be critical to product quality and performance. The identification of potential failure modes and the evaluation of their effects may also be possible.

- Process analyzers

From univariate process measurement tools (e.g., pH, temperature, and pressure) to multivariate tools able to measure (sometimes non-destructively) biological, chemical and physical attributes, process analysis has advanced significantly during the past several decades. The measurement can be performed at-line (the sample is removed, isolated from and analyzed close to the process stream), on-line (the sample is removed for analysis from process stream and returned to process stream again), in-line (the sample is not removed but analyzed in the process stream), and off-line (the sample is removed and analyzed away from process stream) (Figure 4.1). In the context of freeze-drying, several in-line monitoring analytical techniques are available (Table 4.1). Some of these tools are applicable at the production scale but some of them are restricted to the laboratory scale. Moreover, within the group of PAT tools, one can distinguish between process analyzers measuring directly the product or measuring the entire batch progress (based on gas composition in the chamber).

In order to be implemented, the process analyzers should be compatible with the extreme conditions of the freeze-drying process (vacuum, low temperature, and sterility) [11]. It is also possible to extract samples out of the freeze-dryer during the process via a sampling thief and perform at-line measurements [11, 12]. Conversely, on-line monitoring appears to be incompatible with the freeze-drying process as performed today.
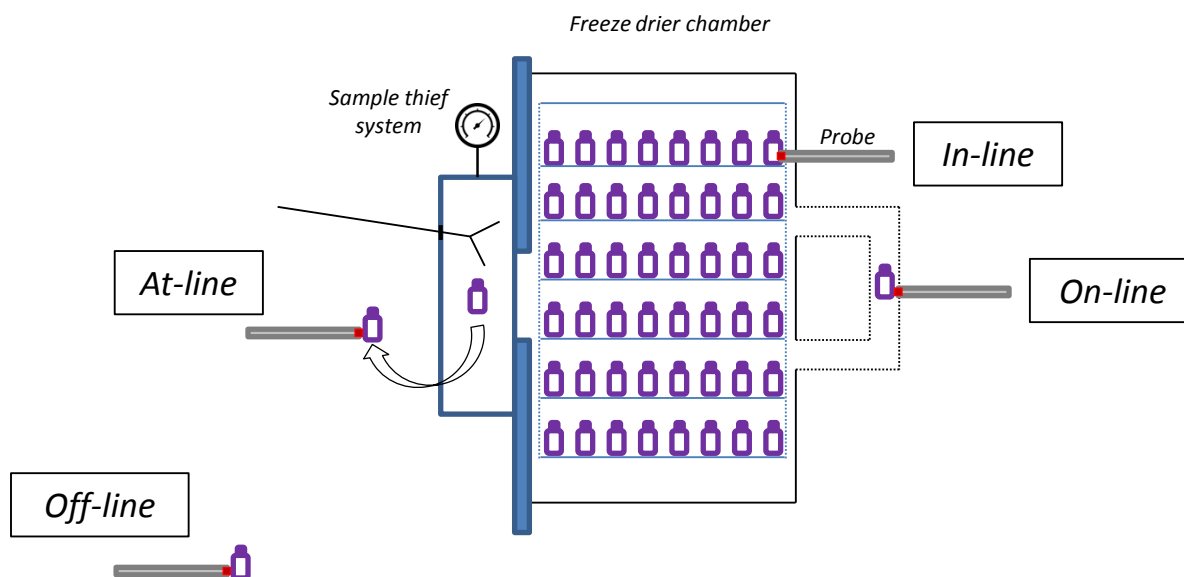
Figure 4.1: Schematic overview of a freeze-dryer chamber illustrating the difference between in-line, at-line, on-line and off-line measurements.

- Process control tools

Based on the (critical) material attributes of the input materials and the continuously obtained critical process and product information, process monitoring and control tools enable to steer the process settings, hence guiding the freeze-drying process towards it's desired state, providing a consistent end product quality. As already described in chapter 2, a SMART system has been developed some years ago [13]. Based on water vapor content measurements in the freeze-dryer chamber (during primary drying) the recipe is adjusted in real-time for shelf temperature and chamber pressure, hence guaranteeing the required product temperature and optimizing the primary drying step efficiency. However, the SMART system does not allow to control all aspects of the freeze-drying process (e.g., the annealing process during the freezing step, the product solid state, the dehydration during secondary drying and the residual moisture content) and is not yet applied at production scale.

- Continuous improvement and knowledge management tools

Over the life cycle of a product, data collection and analysis contribute to continuous learning and can be used to justify proposals for post-approval changes.

Table 4.1: Available in-line freeze-drying process monitoring tools compiled from [11].

In-line tools	Application to production freeze-dryer	Measured parameter(s)	Advantages	Disadvantages
Product monitoring tools				
Thermocouples	Yes	- Product temperature		- Invasive - Influence product behaviour - Measurement depends on position
Resistance temperature detectors (RTD)	Yes	- Product temperature		- Invasive - Influence product behaviour
Temperature Remote Interrogation System (TEMPRIS)	Yes	- Product temperature	- Wireless and battery-free - Compatible with automatic loading system - Can be placed anywhere on the shelf	- Invasive - Huge size of the probe - Influence product behaviour - Practically difficult to implement
The Microbalance technique	No	- Sublimation rate	- Suitable to study effect of cooling rate on sublimation rate	- Interruption of heat transfer during measurement - Measurement heavily depends on vial location
Near Infrared (NIR) spectroscopy	No	- Residual moisture determination - Primary drying endpoint - Product monitoring (protein)	- Non-destructive - Non invasive - Fast	- Single vial technique (except if use NIR with multiprobe) - Difficult or impossible to implement at production scale (conventional batch process) - Only a fraction of vial is analyzed

Table 4.1: Available in-line freeze-drying process monitoring tools compiled from [11] (continued).

Raman spectroscopy	No	- Product monitoring (physical phenomena, protein behaviour) - Freezing and primary drying end point	- Non-destructive - Non invasive - Fast	- Single vial technique - Difficult or impossible to implement at production scale (conventional batch process) - Only a fraction of vial is analyzed
Batch monitoring tools				
Capacitance manometer (CM)	Yes	- Pressure - Primary drying end point (when combined to Pirani)	- Wide pressure range - Withstand steam sterilization	
Pirani	Yes	- Pressure - Primary drying end point (when combined to CM)	- Withstand steam sterilization	- Inaccurate pressure measurement when gas composition change (end of Primary drying)
Gas Plasma Spectroscopy (Lyotrack)	Yes	- Primary drying endpoint	- Withstand steam sterilization	- Potential risk to product stability (via free radical oxidation)
Manometric Temperature Measurement (MTM)	Yes	- Product temperature - Ice sublimation interface temperature - Primary drying end point - Vial heat transfer coefficient - Sublimation rate - Product resistance	- Provides parameters useful for process monitoring and control	- Require a minimum ice sublimation area - Briefly impact the process (when closing the valve) - Does not work for formulations with high amorphous solid content - Temperature biased towards colder running vials - Require a fast closing valve (may be difficult for production scale)

Table 4.1: Available in-line freeze-drying process monitoring tools compiled from [11] (continued).

Tunable Diode Laser Absorption Spectroscopy (TDLAS)	Yes	- Sublimation rate - Potential to measure primary and secondary drying end point - Potential to measure product temperature - Potential to determine residual moisture		- Applicability depends on duct length between the chamber and the condenser - Needs further improvement in both the hardware and the analysis (for residual moisture determination)
Residual Gas Analyzer (RGA)	Yes	- End of primary and secondary drying - Residual moisture (Calibration) - Detection of leaks and contaminants		- Cannot withstand steam sterilization - Can be applied in sterile environment

4.2. PROCESS ANALYTICAL TECHNOLOGY FOR BIOPHARMACEUTICAL PROCESSES

Compared to the implementation of PAT in the chemical and pharmaceutical industries, some unique considerations come into play with biotechnological processes and products [10, 14, 15].

1) Biopharmaceutical products (e.g., proteins, viruses) are large, complex and heterogeneous molecules [10].

2) Biotechnological processes are more complex than typical chemical or small-molecule drug-manufacturing processes (with regard to number of batch records, number of product quality tests, number of critical process steps, and the amount and complexity of process data generated) [10].

3) Biopharmaceutical products are extremely sensitive to the manufacturing process (batch to batch variability is commonly observed in product quality) [14, 16].

4) Raw materials can be complex and often variable [14, 17]

5) The function/clinical significance of product variants, small changes in molecular structure in the product or profile of impurities is often incompletely understood [14].

6) In-process intermediates can be complex mixtures where the desired product may be a small fraction of the bulk liquid [14]

All these differences make the implementation of PAT in biopharmaceutical manufacturing more challenging than in chemical or pharmaceutical processes.

Biotechnological manufacturing can be divided into four segments being upstream (e.g., microbial fermentation, mammalian cell culture), harvest, downstream (e.g., refolding, precipitation, filtration) and drug product processing (e.g., formulation, filling, lyophilization) [10]. The monitoring of critical quality attributes (CQAs) and critical process parameters (CPPs) with PAT tools is possible in each segment. Upstream unit operations can be monitored with PAT tools (e.g., FTIR spectroscopy, NIR spectroscopy, conductance and capacitance-based biomass probe, gas sensors, and many others) providing information on substrate, biomass, product and metabolite concentrations [18, 19]. The harvest step is less investigated from a PAT point of view, because of its limited effect on final product quality

[10]. Relatively under-explored compared to the possible opportunities [10], PAT implementation in downstream processes and particularly in process chromatography, might present a lot of gain (e.g., to facilitate the pooling of the chromatography columns) [20, 21]. Freeze-drying is a commonly used unit operation in biotechnological drug products processing. Several freeze-drying PAT applications have been developed for small molecules and can easily be extended to their biotechnological counterparts. Today, PAT sensors can be used to monitor several quality attributes during freeze-drying (e.g., residual moisture [22-25], protein unfolding [26-28], mannitol phase [29], lipid content [30], virus state [31, 32]) as well as process attributes (e.g., step endpoint [33-35], heat and mass transfer [36], product layer resistance [37], sublimation rate [38]).

4.3. MEASUREMENT PRINCIPLES OF THE APPLIED PROCESS ANALYZERS

4.3.1. NIR spectroscopy

Near infrared (NIR) spectroscopy is a fast, non-destructive and non-invasive analytical tool that can be implemented during pharmaceutical development, in production processes for monitoring or in quality control laboratories [39]. The possibility to measure samples fast and directly through transparent containers (e.g., glass vials [40]) enables the monitoring of large numbers of samples in the production line, without affecting the throughput of the production. This advantage contributed to the wide acceptance of this spectroscopic tool in the pharmaceutical industry [41]. A single NIR spectrum may contain qualitative and quantitative physical and chemical information [42]. Therefore, when associated with chemometrics, NIR spectroscopy becomes a powerful tool to analyze solid, liquid and biotechnological pharmaceutical forms.

NIR spectroscopy studies the absorption of electromagnetic radiation in the NIR region (i.e., 800-2500nm or 4000-12 500cm^{-1}) [43, 44]. All NIR absorption bands result from overtones and combinations of fundamental vibrations from the mid-infrared (Figure 4.2).

Visible

UV		Infrared	Microwave	Radio

Overtones and combination bands	Fundamental
Near-infrared spectroscopy (NIR)	mid-infrared spectroscopy

800nm	2500nm	25.000nm
-	-	-
12.500cm^{-1}	4000cm^{-1}	400cm^{-1}
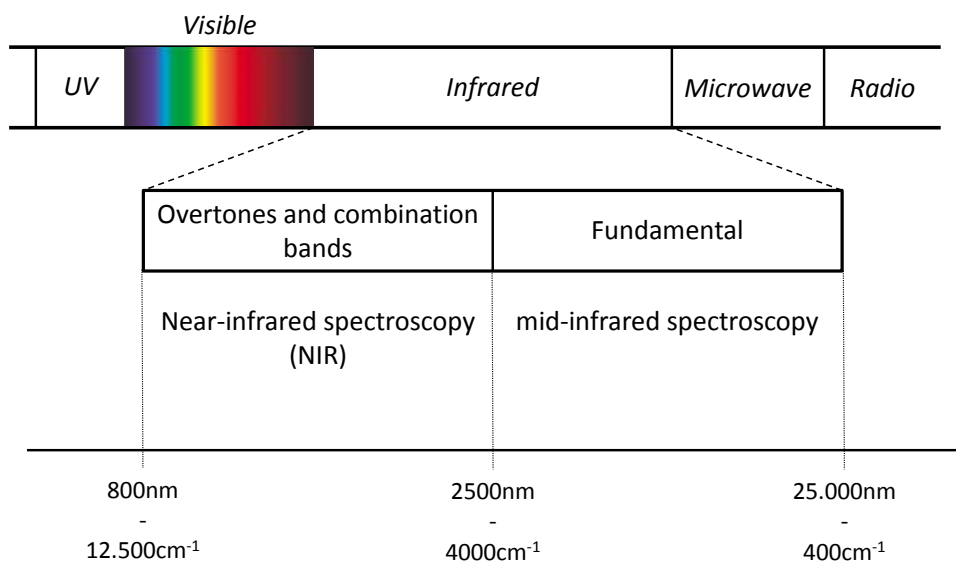
Figure 4.2: Electromagnetic spectrum.

When a sample is measured by NIR spectroscopy, the sample is irradiated by NIR light. Some of this NIR light is absorbed by the molecules, bringing them to a higher vibrational state (Figure 4.3) [42].
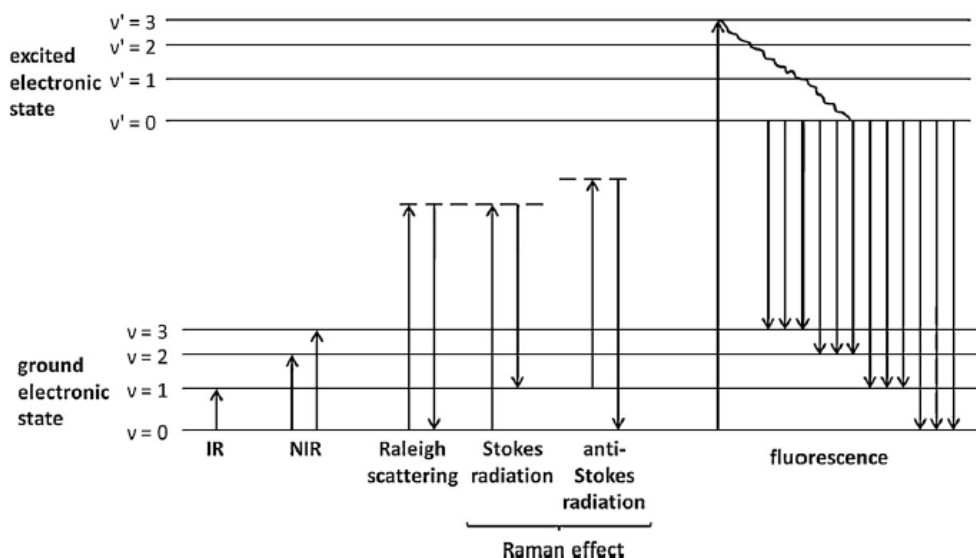
Figure 4.3: Schematic overview of the energy level transition associated with IR and NIR absorption, the Raman effect and fluorescence [42]

80

Molecules that absorb NIR energy vibrate in two modes: stretching and bending. Stretching is defined as a continuous change in the interatomic distance along the axis of the bond between two atoms. Bending corresponds to a change in bond angle. Only vibrations resulting in changes in molecule dipole moment can absorb NIR radiation. A dipole is the product of charge (positive and negative) and distance. While no change in dipole moment occurs during the stretch vibration of an X_2 molecule, a change in dipole moment can be observed during the stretch vibration of an XY molecule (Figure 4.4). Consequently, R-H, O-H, N-H, C-H and S-H bonds are strong NIR absorbers whereas diatomic molecules like H_2 do not absorb NIR radiation.
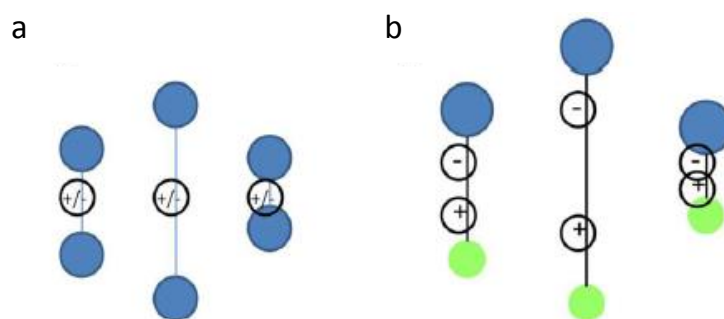
Figure 4.4: Schematic overview of the possible changes in dipole moment during the stretch vibration of an X_2 (a) and a XY (b) molecule, respectively. Adapted from [42]

The NIR spectrum contains overtones and combinations of the fundamental mid-infrared bands. The overtones occur at about two and three times the frequency of the fundamental vibration. For example, the absorption band of the C-H stretch fundamental vibration occurs at a frequency of 2960cm^{-1}, the first overtone at 5920cm^{-1} and the second overtone at 8880cm^{-1}. Combination bands are the sum of several fundamentals from different vibrations. Therefore, a C-H combination band, which is the sum of a C-H stretch (2960cm^{-1}) and a C-H bend (1460cm^{-1}) will occur near 4420cm^{-1}.

 NIR spectra are difficult to interpret due to their complexity [43]. NIR absorption bands are broad, overlapping and weaker than the corresponding mid-infrared band [43, 45]. Therefore, direct interpretation of the NIR raw spectra is difficult and might require chemometrics in order to relate the NIR spectral information to the sample properties [39, 43]. Besides the different sample properties, undesired sample variation (e.g., particle size,

sample density, sample-to-sample measurement variations, etc.) can also be reflected in spectral differences. Therefore, spectral preprocessing methods are commonly used to reduce the effect of this interfering variance sources, thereby increasing the part of the variance due to the parameters of interest [46].

4.3.1.1. Integrating sphere

The integrating sphere is a powerful, fast and easy-to-use tool for diffuse-reflection sampling of solids and powders (Figure 4.5). When directed onto a surface, the infrared radiation will interact with the surface by alternately passing through it and reflecting. This causes the light to scatter, or "diffuse", as it makes its way through the sample.

The integrating sphere allows to measure extended sample area (depending on the sample port size) and provide uniform light collection independent of the sample orientation [47].

Diffuse-reflection measurements are simplified by using an integrating sphere. The NIR beam is directed onto the sphere and travels directly through the center of the sphere, through the optical window, and into the sample. The beam scatters off of the sample and the reflected light beams re-enter the sphere. The inside of the sphere is coated with diffuse gold, which collects the light beams and directs them into the detector (Figure 4.5).
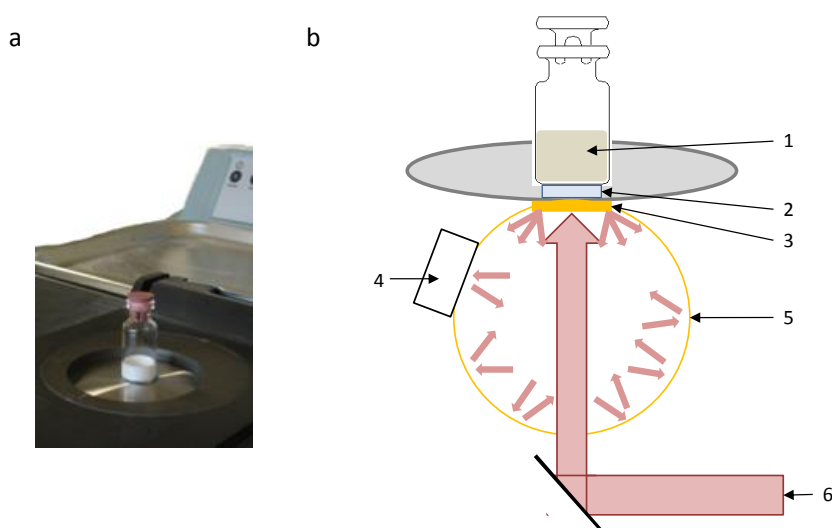
Figure 4.5: Integrating sphere sample interface picture (a) and schematic overview (b). 1: sample. 2: sapphire window. 3: Internal gold reference flag, computer controlled. 4: detector. 5: Gold coated sphere. 6: Infrared radiation.

4.3.1.2. NIR application in freeze-drying

Since the demonstration of the suitability of NIR spectroscopy to determine the residual moisture content in lyophilized sucrose through the glass vial [40], several studies of freeze-dried products monitored with NIR spectroscopy have been published and are presented in Table 4.2. The first studies were performed off-line and focused on the residual moisture content determination [22, 23, 48-50]. Fifteen years later, a study aiming to detect and evaluate the protein conformation was published [26] and several other off-line studies conducted to study biopharmaceutical products followed [31, 51, 52]. The possibility to monitor a freeze-dried mannitol formulation in-line was demonstrated in 2009 [35] and allowed to evaluate the mannitol behaviour during the different freeze-drying steps. Other in line experiments were performed and studied the protein stabilization mechanisms during the freeze-drying process [27] or monitored the residual moisture content at different positions of the freeze-dryer shelves [25].

Table 4.2: Applications of NIR spectroscopy for the freeze-drying process

In-process interfacing	Monitored critical information	Formulation type	Reference
Off-line	Moisture content	Pharmaceutical - sucrose	[40]
Off-line	Moisture content	Undisclosed	[48]
Off-line	Moisture content: method transfer	Undisclosed	[49]
Off-line	Moisture content determination	Pharmaceutical - mannitol	[22]
Off-line	Moisture content: comparison between LOD and NIR	Biopharmaceutical - hepatitis A virus, porcine parvovirus and pseudorabies virus	[50]
Off-line	Distinction between surface and hydrate water	Pharmaceutical - mannitol	[23]
Off-line	Protein conformation	Biopharmaceutical - Bovine chymotrypsinogen A and horse cytochrome C	[26]
Off-line	Protein secondary structure analysis	Biopharmaceutical - Various proteins	[51]
In-line	Product monitoring and process step endpoint determination	Pharmaceutical - mannitol	[35, 53]
Off-line	Moisture content determination with different stabilizer ratios	Pharmaceutical - mannitol/sucrose	[54]
Off-line	Hydrogen bond between protein and stabilzer	Biopharmaceutical – Ribonuclease A (RNase A)	[52]
Off-line	Trehalose crystallization monitoring	Pharmaceutical - Trehalose	[55]
Off-line	Classification of freeze-dried products according to composition, water content and solid-state properties	Pharmaceutical - mannitol/sucrose	[24]
Off-line	Solid state analysis of protein formulation	Biopharmaceutical - Insulin and human growth hormone	[56]
Off-line	Phenol quantification	Biopharmaceutical - Phenol/Insulin formulation	[57]
Off-line	Moisture content determination	Pharmaceutical - mannitol	[58]

Table 4.2: Applications of NIR spectroscopy for the freeze-drying process (continued)

In-line	Product monitoring: protein unfolding	Biopharmaceutical - imunoglobuline G (IgG)	[27]
Off-line	Virus evaluation	Biopharmaceutical - Trehalose/live, attenuated virus	[31]
In-line, multipoint	Moisture content monitoring	Pharmaceutical - sucrose	[25]
In-line	Monitoring of a multicomponent formulation	Pharmaceutical - Mannitol, fenofibrate and tertiary-butyl alcohol	[59]

4.3.2. FTIR spectroscopy

Fourier Transform Infrared (FTIR) spectroscopy has been successfully used in several scientific and technical applications [60]. The expansion of the use of this technique (since 2001) can be in part explained by the Fast Fourier Transform algorithm [61]. The idea is to split the light into two beams and measure the interference of their radiation. The detector measures a signal that is a function of the change in path length between these two beams. This obtained signal will finally be converted by a mathematical method, called Fourier Transformation (FT), to the normal output, i.e., frequencies [62]. In addition, the use of chemometric tools and the versatility of the spectroscopic technique which allows to analyze different types of samples (liquids, pastes, polymers, gases) contributed to the popularity of this technique [60, 61].

FTIR spectroscopy studies the absorption of the electromagnetic radiation in the mid IR region (i.e., 2500-25.000nm or 4000-400cm^{-1}) [60, 61]. Similarly to NIR spectroscopy, FTIR spectroscopy measures molecular vibrations (which vibrate in two modes: stretching and bending). The selection rule for molecules to be FTIR active is identical to NIR, being a change in dipole moment during their normal modes [60]. The principal difference between FTIR and NIR spectroscopy is that, FTIR spectroscopy mainly measures the fundamental vibrations of molecules (Figure 4.3) whereas NIR spectroscopy measures overtones and combinations of the fundamental vibrations [44, 61]. Fundamental vibrations are significantly higher in absorption than overtones and combination bands [44]. Therefore, the ability of FTIR spectroscopy to detect low levels of analyte is higher. Higher absorption also confers an advantage for the identification of molecules via their "fingerprint" region. Indeed, all mid-infrared fundamental absorptions bands in the FTIR fingerprint region (roughly below 1700cm^{-1}), are already in their second or third overtone above 4000cm^{-1} and hence too weak to significantly contribute in the NIR [44].

4.3.2.1. Attenuated Total Reflectance (ATR)

A wide range of sample interfaces (sampling accessories) have been developed for infrared spectroscopy over the past 20 to 30 years [60]. The attenuated total reflectance (ATR) unit allows to measure samples in different conditions (liquid, pastes, polymers, dehydrated samples) and also offers the advantage to require little or no sample preparation [61].

In ATR, the sample is placed onto an optically dense crystal of relatively higher refractive index. When light transits between materials with different refractive indices, refraction occurs (Figure 4.6). If the transition is from a high refractive index material (crystal) to a low refractive index material (sample), the incident angle is smaller than the transmitted angle. When the internal angle reaches a critical level, the external angle is 90 degrees and the propagation of light is parallel to the surface of the interface between the materials and constitutes the critical angle. With ATR, the infrared beam enters the crystal at an angle greater than the critical angle of the crystal. This causes the IR energy to internally reflect off the parallel surfaces of the crystal.
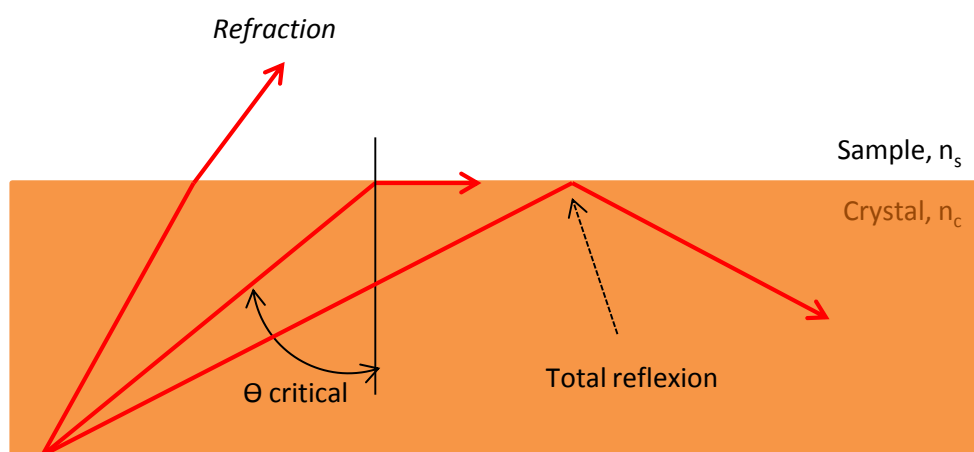
Figure 4.6: Light pathways between a crystal of high refractive index (n_c) and a sample of lower refractive index (n_s) in function of the incident angle [63].

In ATR measurement, the IR beam reflects from the internal surface of the crystal and creates a small amount of radiation, an evanescent wave, which extends beyond the surface of the crystal and interacts with the sample in close contact with the ATR crystal (Figure 4.7). Some of the energy of the evanescent wave is absorbed by the sample and the reflected radiation is passed to the detector in the IR spectrometer as it exits the crystal [61]. Penetration depth at each reflection point (~ 2.0μm for a ZnSe crystal) depends on many factors and is wavelength-dependant. Longer wavelength waves penetrate deeper than shorter wavelength waves.
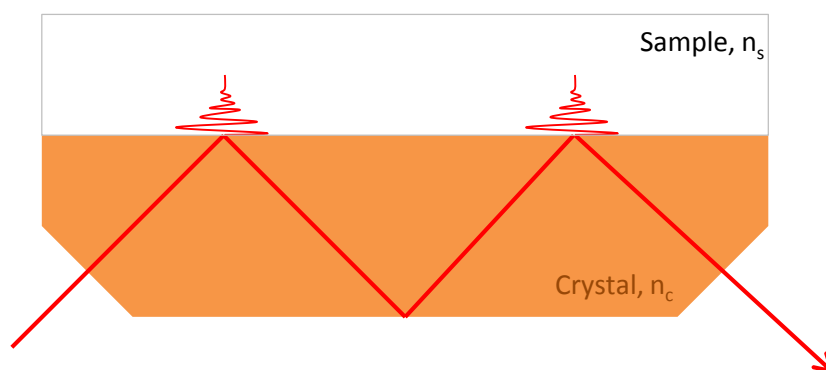
Figure 4.7: ATR sample measurement [64].

4.3.2.2. FTIR applications in freeze-drying

FTIR spectroscopy is recognized to be a tool of choice for the study of protein secondary structure [65]. It is therefore not surprising to find this tool in several studies dedicated to the freeze-drying process of proteins (Table 4.3). FTIR spectroscopy is a sensitive tool but the in-line measurements are not straightforward [66]. Indeed, in all cited studies of Table 4.3 (except [67]), the FTIR spectra collection was performed off-line. As can also be observed in Table 4.3, the amide I band is the most often used to assess different proteins secondary structure. The amide I band is a characteristic band for proteins and polypeptides. The band arises from the amide bonds linking the different amino acids and is associated to stretching vibrations of the C=O bond of the amide with minor contributions from the out-of-phase CN stretching vibration [65]. Since the C=O is involved in the hydrogen bonds responsible for the protein secondary structure, frequency shifts of this amide I is associated to protein secondary structure changes and is therefore used in the different studies as a reference to assess the stability/conformation of proteins.

Table 4.3: Applications of FTIR spectroscopy in the freeze-drying process.

In process interfacing	Monitored critical information	Used as reference technique?	Formulation type	Reference
In-line	Amide I monitoring	No	Biopharmaceutical - Lysozyme/sucrose	[67]
Off-line	Amide I evaluation	Yes	Biopharmaceutical - Actin	[68]
Off-line	Amide I evaluation	Yes	Biopharmaceutical - Bovine chymotrypsinogen A and horse cytochrome C	[26]
Off-line	Amide I evaluation	Yes	Biopharmaceutical - Imunoglobuline G (IgG) and recombinant human serum albumin	[69]
Off-line	Amide I evaluation	Yes	Biopharmaceutical - Imunoglobuline G (IgG)	[70]
Off-line	Amide I evaluation	Yes	Biopharmaceutical - Various proteins	[51]
Off-line	Amide I evaluation	Yes	Biopharmaceutical - Imunoglobuline G (IgG)	[71]
Off-line	Amide I evaluation	Yes	Biopharmaceutical - Human growth hormone (hGH)	[72]
Off-line	Asparagine side chain (Amide I)	No	Biopharmaceutical - Ribonuclease A (RNase A)	[52]
Off-line	Phenol quantification	No	Biopharmaceutical - Phenol/Insulin formulation	[57]
Off-line	Amide I and II evaluation	Yes	Biopharmaceutical - β-galactosidase	[73]
Off-line	Amide I evaluation	Yes	Biopharmaceutical - Imunoglobuline G (IgG)	[27]
Off-line	Amide I evaluation	Yes	Biopharmaceutical - Imunoglobuline G (IgG)	[74]
Off-line	Amide I evaluation	Yes	Biopharmaceutical - Lactic Dehydrogenase (LDH)	[28]
Off-line	Amide I, II & III	No	Biopharmaceutical - Live, attenuated virus vaccine	[32]

REFERENCES

[1]   L. Aboud, S. Hensley. New prescription for drug makers: Update the plants, The Wall Street Journal, September 3, 2003

[2]   T. Kourti. The Process Analytical Technology Initiative and Multivariate Process Analysis, Monitoring and Control Analytical and Bioanalytical Chemistry, 384 (2006) 1043-1048.

[3]   R. Guenard, G. Thurau, in: K.A. Bakeev (Ed.), Process Analytical Technology, John Wiley & Sons Ltd, United Kingdom, 2010, 17-36.

[4]   Food and Drug Administration, Guidance for Industry; PAT - A framework for innovative pharmaceutical development, manufacturing and quality assurance, (2004)

[5]   Food and Drug Administration, Pharmaceutical cGMPs for the 21st century - a risk-based approach, 2004

[6]   Food and Drug Administration, PAT - A framework for innovative pharmaceutical manufacturing and quality assurance, 2004

[7]   International Conference on Harmonisation, Pharmaceutical Development Q8, (2009)

[8]   International Conference on Harmonisation, Quality Risk Management Q9, (2005)

[9]   International Conference on Harmonisation, Pharmaceutical Quality System Q10, (2008)

[10]   A.S. Rathore, R. Bhambure, V. Ghare. Process Analytical Technology (PAT) for biopharmaceutical products. Analytical and Bioanalytical Chemistry, 2010;398:137-154.

[11]   S.M. Patel, M.J. Pikal. Process Analytical Technologies (PAT) in freeze-drying of parenteral product. Pharmaceutical development and technology, 2009;14(6): 567-587.

[12]   A. Kauppinen M. Toiviainen, M. Lehtonen, K. Järvinen, J. Paaso, M. Juuti, J. Ketolainen Validation of a multipoint near-infrared spectroscopy method for in-line moisture content analysis during freeze-drying. Journal of Pharmaceutical and Biomedical analysis, 2014; 95:229-37.

[13] X. Tang, S.L. Nail, M.J. Pikal. Freeze-drying process design by manometric temperature measurement: design of a smart freeze-dryer. Pharmaceutical Research, 2005;22: 685-700.

[14] E.K. Read, J.T. Park, R.B. Shah, B.S. Riley, K.A. Brorson, A.S. Rathore. Process analytical technology (PAT) for Biopharmaceutical products: Part I. Concepts and applications. Biotechnology and Bioengineering, 2010;105(2): 276-284.

[15] J. Glassey, K.V. Gernaey, C. Clemens, T.W. Schulz, R. Oliveira, G. Striedner, CF. Mandenius. Process analytical technology (PAT) for biopharmaceuticals. Biotechnology Journal, 2011;6: 369-377.

[16] A.S. Rathore Follow-on protein products: scientific issues, developments and challenges. Trends Biotechnology, 2009;27(12): 689-705.

[17] A.O. Kirdar, G. Chen, J. Weidner, A.S. Rathore. Application of near-infrared (NIR) spectroscopy for screening of raw materials used in the cell culture medium for the production of a recombinant therapeutic protein. Biotechnology Progress, 2010; 26:527-531

[18] A. E. Cervera, N. Petersen, A. E. Lantz, A. Larsen, K. V. Gernaey. Application of near-infrared spectroscopy for monitoring and control of cell culture and fermentation. Biotechnology Progress, 2009; 25(6): 1561–81

[19] N. Petersen, P. Odman, A. E. C. Padrell, S. Stocks, A. E. Lantz, K. V. Gernaey. In situ near infrared spectroscopy for analyte-specific monitoring of glucose and ammonium in streptomyces coelicolor fermentations. Biotechnology Progress, 2009;26(1): 263–71.

[20] R.A. Fahrner, G.S. Blanks. Real-time control of antibody loading during protein A affinity chromatography using an on-line assay. Journal of Chromatography A, 1999;849(1): 191-6.

[21] A.S. Rathore, M. Yu, S. Yeboah, A. Sharma. Case study and application of process analytical technology (PAT) towards bioprocessing: use of on-line high-performance liquid chromatography (HPLC) for making real-time pooling decisions for process chromatography. Biotechnology and Bioengineering, 2008; 100(2):306-316.

[22] M. W. Derksen, P. J. van de Oetelaar, F. A. Maris. The use of near-infrared spectroscopy in the efficient prediction of a specification for the residual moisture content of a freeze-dried product. Journal of Pharmaceutical and Biomedical Analysis, 1998;17(3): 473–80.

[23] W. Cao, C. Mao, W. Chen, H. Lin, S. Krishnan, N. Cauchon. Differentiation and Quantitative Determination of Surface and Hydrate Water in Lyophilized Mannitol Using NIR Spectroscopy, Journal of Pharmaceutical sciences, 2006;95(9): 2077–2086.

[24] H. Grohganz, D. Gildemyn, E. Skibsted, J. M. Flink, J. Rantanen. Towards a robust water content determination of freeze-dried samples by near-infrared spectroscopy. Analytica Chimica Acta, 2010;676(1-2): 34–40.

[25] A. Kauppinen, M. Toiviainen, O. Korhonen, J. Aaltonen, J. Paaso, M. Juuti, J. Ketolainen. In-Line Multipoint Near-Infrared Spectroscopy for Moisture Content Quantification during Freeze-Drying. Analytical Chemistry, 2013;85: 2377-2384.

[26] S. Bai, R. Nayar, J. F. Carpenter, M. C. Manning. Noninvasive determination of protein conformation in the solid state using near infrared (NIR) spectroscopy. Journal of Pharmaceutical Sciences, 2005;94(9): 2030–2038.

[27] S. Pieters, T. De Beer, J.C. Kasper, D. Boulpaep, O. Waszkiewicz, M. Goodarzi, C. Tistaert W. Friess, J.P. Remon, C. Vervaet, Y. Vander Heyden. Near-Infrared Spectroscopy for In-Line Monitoring of Protein Unfolding and Its Interactions with Lyoprotectants during Freeze-Drying. Analytical Chemistry, 2012;84:947-955

[28] S. Pieters, Y. Vander Heyden, J.M. Roger, M. D'Hondt, L. Hansen, B. Palagos, B. De Spiegeleer, J.P. Remon, C. Vervaet, T. De Beer. Raman spectroscopy and multivariate analysis for the rapid discrimination between native-like and non-native states in freeze-dried protein formulations. European Journal of Pharmaceutics and Biopharmaceutics, 2013; 85 (2): 263-271.

[29] S. Romero-Torres, H. Wikstrom, E.R. Grant, L.S. Taylor. Monitoring of mannitol phase behaviour during freeze-drying using non-invasive Raman spectroscopy. PDA Journal of Pharmaceutical SciencesTechnol 2007;61: 131– 145

[30] D. Christensen, M. Allesø, I. Rosenkrands, J. Rantanen, C. Foged, E.M. Agger, P. Andersen, H.M. Nielsen. NIR transmission spectroscopy for rapid determination of lipid and lyoprotector content in liposomal vaccine adjuvant system CAF01. European Journal of Pharmaceutics and Biopharmaceutics, 2008;70(3): 914–920.

[31] L. Hansen, S. Pieters, R. Daoussi, J.P. Montenez, Y. Vander Heyden, C. Veravaet, J.P. Remon, T. De Beer. Near-infrared spectroscopic evaluation of lyophilized viral vaccine formulations. Biotechnology progress, 2013; 29 (6): 1573-1586.

[32] L. Hansen, K. Pierre, S. Pastoret, A. Bonnegarde-Bernard, R. Daoussi, C. Vervaet, J.P. Remon, T. De Beer. FTIR spectroscopy for the detection and evaluation of live attenuated viruses in freeze-dried vaccine formulations. Biotechnology Progress, 2015; 31(4): 1107-1118

[33] M. Brülls, S. Folestad, A. Sparén, A. Rasmuson. In-situ near-infrared spectroscopy monitoring of the lyophilization process. Pharmaceutical Research, 2003;20(3): 494–9.

[34] T. De Beer, M. Allesø, F. Goethals, A. Coppens, Y. Vander Heyden, H. Lopez De Diego, J. Rantanen, F. Verpoort, C. Vervaet, J.P. Remon, W. Baeyens. Implementation of a Process Analytical Technology System in a Freeze-Drying Process Using Raman Spectroscopy for In-Line Process Monitoring. Analytical Chemistry, 2007;79(21): 7992–8003.

[35] T. De Beer, P. Vercruysse, A. Burggraeve, T. Quinten, J. Ouyang, X. Zhang, C. Vervaet, JP. Remon, W.R. Baeyens. In-line and real-time process monitoring of a freeze-drying process using Raman and NIR spectroscopy as complementary process analytical technology (PAT) tools. Journal of Phamaceutical Sciences, 2009;98:3430-3446.

[36] X. Tang, S.L. Nail, M.J. Pikal. Evaluation of manometric temperature measurement (MTM), a process analytical technology tool in freeze-drying. Part III: Heat and mass transfer measurement. AAPS Pharm Sci Tech 2006;7:97.

[37] X. Tang, S.L. Nail, M.J. Pikal. Evaluation of manometric temperature measurement, a process analytical technology tool for freeze-drying. Part II: Measurement of dry-layer resistance. AAPS Pharm Sci Tech, 2006;7: 93

[38] H. Gieseler, W.J. Kessler, M. Finson, S.J. Davis, P.A. Mulhall, V. Bons, D.J. Debo, M.J. Pikal. Evaluation of tunable diode laser absorption spectroscopy for in-process water vapor mass flux measure- ments during freeze-drying. Journal of Pharmaceutical Sciences, 2007;96: 1776–1793.

[39] Y. Roggo, P. Chalus, L. Maurer, C. Lema-Martinez, A. Edmond, N. Jent. A review of near infrared spectroscopy and chemometrics in pharmaceutical technologies. Journal of Pharmaceutical and Biomedical Analysis, 2007, 44, 683-700.

[40] M.S. Kamat, R.A. Lodder, P.P. DeLuca. Near-infrared spectroscopic determination of residual moisture in lyophilized sucrose through intact glass vials. Pharmaceutical Research, 1989; 6(11):961-5.

[41] G. Reich. Near-infrared spectroscopy and imaging: basic principles and pharmaceutical applications, Advanced Drug Delivery Reviews 2005;57: 1109–1143.

[42] T. De Beer, A. Burggraeve, M. Fonteyne, L. Saerens, J.P. Remon, C. Vervaet. Near infrared and Raman spectoscopy for the in-process monitoring of pharmaceutical production porcesses. International Journal of Pharmaceutics, 2011; 417: 32-47.

[43] J. Luypaert, D.L. Massart,Y. Vander Heyden. Near-infrared spectroscopy applications in pharmaceutical analysis. Talanta, 2007; 72:865-883.

[44] M.B. Simpson, in: K.A. Bakeev (Ed.), Process Analytical Technology, John Wiley & Sons Ltd, United Kingdom, 2010, 17-36.

[45] D. Burns, E. Ciurczak. Handbook of Near-infrared Analysis. second ed., Marcel Dekker, Inc., New York, 2001

[46] J. Luypaert, S. Heureding, Y. Vander Heyden, D.L. Massart. The effect of preprocessing methods in reducing interfering variability from near-infrared measurements of creams. Journal of Pharmaceutical and Biomedical Analysis, 2004; 36: 495-503.

[47]   L.M. Hanssen, K.A. Snail. In J.M. Chalmers and P.R. Griffiths (Eds.) Integrating sphere for mid- and near-infrared reflection spectroscopy. Handbook of Vibrational Spectroscopy, John Wiley & Sons, United Kingdom, 2002, 1175-1191.

[48]   I.R. Last, K.A. Prebble. Suitability of near-infrared methods for the determination of moisture in a freeze-dried injection product containing different amounts of the active ingredient. Journal of Pharmaceutical and Biomedical analysis, 1993;11: 1071-1076.

[49]   J.A. Jones, I.R. Last, B.F. MacDonald, K.A. Prebble. Development and transferability of near-infrared methods for determination of moisture in a freeze-dried injection product. Journal of Pharmaceutical and Biomedical analysis, 1993;11: 1227-1231.

[50]   M. Savage, J. Torres, L. Franks, B. Masecar, J. Hotta. Determination of adequate moisture content for efficient dry-heat viral inactivation in lyophilized factor VIII by loss on drying and by near infrared spectroscopy. Biologicals, 1998;26(2): 119-24.

[51]   K. Izutsu, Y. Fujimaki, A. Kuwabara, Y. Hiyama, C. Yomota, N. Aoyagi. Near-infrared analysis of protein secondary structure in aqueous solutions and freeze-dried solids. Journal of Pharmaceutical Sciences, 2006;95(4): 781-789.

[52]   D.S. Katayama, J.F. Carpenter, K.P. Menard, M.C. Manning, T.W. Randolph. Mixing properties of lyophilized protein systems: a spectroscopic and calorimetric study. Journal of Pharmaceutical Sciences, 2009; 98(9):2954-69.

[53]   T. De Beer, M. Wiggenhorn, R. Veillon, C. Debacq, Y. Mayeresse, B. Moreau, A. Burggraeve, T. Quinten, W. Friess, G. Winter, JP. Remon, W.R. Baeyens. Importance of using complementary process analyzers for the process monitoring, analysis, and understanding of freeze-drying. Analytical Chemistry, 2009; 15:7639-7649

[54]   H. Grohganz, M. Fonteyne, E. Skibsted, T. Falck, B. Palmqvist, J. Rantanen. Role of excipients in the quantification of water in lyophilised mixtures using NIR spectroscopy. Journal of Pharmaceutical and Biomedical analysis, 2009;49(4): 901-907.

[55]   B. Connolly, T. W. Patapoff , J. Wang, J. M. Moore, T. J. Kamerzell. Vibrational spectroscopy and chemometrics to characterize and quantitate trehalose crystallization. Analytical Biochemistry, 2010;399:48–57

[56] H. Groghanz, D. Gildemyn, E.Skibsted, J.M. Flink, J. Rantanen. Rapid solid-state analysis of freeze-dried protein formulations using NIR and Raman Spectroscopies. Journal of Pharmaceutical Sciences, 2011; 100(7): 2871-75.

[57] M.J. Maltesen, S. Bjerregaard, L. Hovgaard, S. Havelund, M. van de Weert, H. Grohganz, Multivariate analysis of phenol in feeze-dried and spray-dried insulin formulations by NIR and FTIR. AAPS PharmSciTech, 2011; 12(2): 627-635.

[58] W.L. Yip, I. Gausemel, S.A. Sande, K. Dyrstad. Strategies for multivariate modeling of moisture content in freeze-dried mannitol-containing products by near-infrared spectroscopy. Journal of Pharmaceutical and Biomedical analysis, 2012;70: 202-211.

[59] J.G. Rosas, H. de Waard, T. De Beer, C. Vervaet, JP. Remon, W.L.J. Hinrichs, H. W. Frijlink, M. Blanco. NIR spectroscopy for the in-line monitoring of a multicomponent formulation during the entire freeze-drying process. Journal of Pharmaceutical and Biomedical Analysis, 2014;97: 39–46

[60] J.P. Coates, in: K.A. Bakeev (Ed.), Process Analytical Technology, John Wiley & Sons Ltd, United Kingdom, 2010, 17-36.

[61] A. Alvarez-Ordonez, D.J.M. Mouwen, M. Lopez, M. Prieto. Fourier transfom infrared spectroscopy as a tool to characterize molecular composition and stress response in foodborne pathogenic bacteria. Journal of Microbiological Methods, 2011;84: 369-378.

[62] B.H. Stuart, Infrared spectroscopy: fundamentals and applications, John Wiley & Sons, Chichester, United Kingdom, 2004, 244.

[63] P. Larkin, Infrared and raman spectroscopy: principles and spectral interpretation. Elsevier, 2011

[64] Thermo Scientific, Nicolet iS5 Spectrometer Fast Facts. 2010 Revision B269-269400

[65] A. Barth, C. Zscherp, What vibrations tell us about proteins. Quarterly Review of Biophysics, 2002; 35: 363-430

[66] A.P. Teixeira, R. Oliveira, P.M. Alves, M.J. Corrondo. Advances in on-line monitoring and control of mammalian cell cultures: Supporting the PAT initiative. Biotechnology Advances, 2009; 27(6):726-32.

[67] R.L. Remmele, C. Stushnoff, J.F. Carpenter. Real-time in situ monitoring of lysozyme during lyophilization using infrared spectroscopy: dehydration stress in the presence of sucrose. Pharmaceutical Research, 1997;14(11):1548-55

[68] S. D. Allison, M. C. Manning, T.W. Randolph, K.I.M. Middleton, A. Davis, J.F. Carpenter. Optimization of Storage Stability of Lyophilized Actin Using Combinations of Disaccharides and Dextran, Journal of Pharmaceutical Sciences, 2000;89(2): 199–214.

[69] L. L. Chang, D. Shepherd, J. Sun, D. Ouellette, K.L. Grant, X.C. Tang, M.J. Pikal. Mechanism of protein stabilization by sugars during freeze-drying and storage: native structure preservation, specific interaction, and/or immobilization in a glassy matrix? Journal of Pharmaceutical Sciences, 2005; 94(7), 1427–44.

[70] L. L. Chang, D. Shepherd, J. Sun D, X.C. Tang, M.J. Pikal. Effect of Sorbitol and Residual Moisture on the Stability of Lyophilized Antibodies: Implications for the Mechanism of Protein Stabilization in the Solid State. Journal of Pharmaceutical Sciences, 2005, 94(7), 1445–1455.

[71] A. M. Abdul-fattah, V.U. Truong-le, L. Yee, L. Nguyen, D.S. Kalonia, M.T. Cicerone, M.J. Pikal. Drying-Induced Variations in Physico-Chemical Properties of Amorphous Pharmaceuticals and Their Impact on Stability (I): Stability of a Monoclonal Antibody, Journal of Pharmaceutical Sciences, 2007; 96(8), 1983–2008.

[72] M.J. Pikal, D. Rigsbee, M.L. Roy, D. Galreath, K.J. Kovach, B.S. Wang, J.F. Carpenter, M.T. Cicerone. Solid State Chemistry of Proteins: II. The Correlation of Storage Stability of Freeze-Dried Human Growth Hormone (hGH) with Structure and Dynamics in the Glassy Solid. Journal of Pharmaceutical Sciences, 2008; 97(12): 5106–5121.

[73] V.P. Heljo, K. Jouppila, T. Hatanpää, A.M. Juppo. The Use of Disaccharides in Inhibiting Enzymatic Activity Loss and Secondary Structure Changes in Freeze-Dried β-Galactosidase during Storage. Pharmaceutical Research, 2011; 28: 540–552.

[74] J. Park, K. Nagapudi, C. Vergara, R. Ramachander, J.S. Laurence, S. Krishnan. Effect of pH and Excipients on Structure , Dynamics , and Long-Term Stability of a Model IgG1 Monoclonal Antibody upon Freeze-Drying. Pharmaceutical Research, 2013;30(4): 968-984.

CHAPTER 5

NEAR-INFRARED SPECTROSCOPIC EVALUATION OF LYOPHILIZED VIRAL VACCINE FORMULATIONS

Parts of this chapter are published in:

ABSTRACT

This chapter examines the applicability of NIR spectroscopy to evaluate the virus state in a freeze-dried live, attenuated vaccine formulation. Therefore, this formulation was freeze-dried using different virus volumes and after applying different pre-freeze-drying virus treatments (resulting in different virus states): (i) as used in the commercial formulation; (ii) without antigen (placebo); (iii) concentrated via a centrifugal filter device; and (iv) stressed by 96h exposure to room temperature. Each freeze-dried product was measured directly after freeze-drying with NIR spectroscopy and the spectra were analyzed using principal component analysis (PCA). Herewith, two NIR spectral regions were evaluated: (i) the 7300-4000cm^{-1} region containing the amide A/II band which might reflect information on the coated proteins of freeze-dried live, attenuated viruses; and (ii) the C-H vibration overtone regions (10,000-7500 and 6340-5500cm^{-1}) which might supply information on the lipid layer surrounding the freeze-dried live, attenuated viruses. The different pre-freeze-drying treated live, attenuated virus formulations (different virus states and virus volumes) resulted in different groups in the scores plots resulting from the PCA of the collected NIR spectra. Secondly, partial least squares discriminant analysis models (PLSDA) were developed and evaluated, allowing classification of the freeze-dried formulations according to virus pre-freeze-drying treatment. The results of this chapter suggest the applicability of NIR spectroscopy for evaluating live, attenuated vaccine formulations with respect to their virus pre-freeze-drying treatment and virus volume.

CHAPTER 5

NEAR-INFRARED SPECTROSCOPIC EVALUATION OF LYOPHILIZED VIRAL VACCINE FORMULATIONS

5.1. INTRODUCTION

The limited stability of many biopharmaceutical products in aqueous solutions is a well-known problem. Drying these formulations prior to storage is a solution to overcome this instability issue.

Therefore, freeze-drying has become a well-established and preferred technique in the pharmaceutical industry (despite the disadvantages of cost and process time) since approximately 46% of biopharmaceuticals are freeze-dried [1]. The freeze-drying process consists of 3 main consecutive steps: freezing, primary drying and secondary drying. During the freezing step, the temperature is decreased in order to convert most of the water into ice. Herewith, the solutes are crystallized or transformed into an amorphous system. During primary drying, vacuum is introduced in the freeze-drying chamber and the ice is removed by sublimation. The secondary drying step, occurring under deep vacuum, ends the process by removing the unfrozen water by desorption [2].

Although freeze-drying is performed to stabilize a product for long term storage and distribution, the freezing and dehydration steps themselves can be stressful and damaging for the biopharmaceutical product, hence reducing the therapeutic activity. Therefore, understanding the product behaviour and the mechanisms of stabilization and destabilization during freeze-drying are of crucial importance for optimal product and process design.

According to the National Institute of Allergy and Infectious Diseases (NIAID), there are up to seven different types of vaccines: live attenuated vaccines, inactivated vaccines, subunit vaccines, toxoid vaccines, conjugate vaccines, DNA vaccines and recombinant vector

vaccines [3]. Because of their manufacturing simplicity and the strong immune response they generate, live, attenuated vaccines have been favored in many cases. The organisms of such vaccines can be bacteria (Tuberculosis (BCG), typhoid) or - most often - viruses (measles, mumps, rubella, polio, yellow fever, varicella and rotavirus) [4]. Due to their low stability in aqueous solution, most of the live, attenuated vaccines are freeze-dried.

Studies elucidating the (de)stabilization mechanisms of live, attenuated viruses in vaccine formulations during freeze-drying are lacking. This lack of knowledge is a major barrier to the development of more thermally stable vaccines [5] and can be attributed to two main reasons: (i) measuring the destabilization mechanisms is complex because of the multiple destabilization pathways (such as oxidation, light-catalyzed reaction, change in ionic strength, pH shift due to buffer crystallization and possibly mechanical membrane damage due to ice crystal growth)[6,7], and (ii) the analytical tools allowing the evaluation of live, attenuated viruses during freeze-drying are lacking.

As a consequence, biological potency assays after processing are the currently applied methods to evaluate whether the activity of the viruses is maintained [6, 8, 9].

Today, the stabilization strategies applied for live, attenuated viruses, their coated proteins and their surrounding lipid bilayer during freeze-drying are derived from the stabilizing actions taken for other biopharmaceutical products like proteins, cells and liposomes.

However, the stabilization mechanisms during freeze-drying of proteins and biologicals in general, are currently still a matter of research and debate. Several hypotheses have been proposed but no full satisfactory explanation has yet been demonstrated [10-12]. The vitrification hypothesis states that the protein is molecularly dispersed into a glassy matrix which limits the molecular mobility needed for unfolding and other destabilization mechanisms [13]. This vitrification stabilization mechanism can also be helpful during freeze-drying of live, attenuated virus formulations since the isolation of viruses into a glassy matrix can contribute to its protection by reducing the probability of unfolding and, as a consequence, aggregation of its coated proteins. The water-substitute hypothesis states that water removed from the environment of proteins (i.e., water shell) during drying is replaced by a lyoprotectant, which is hydrogen bonded to the protein hence thermodynamically stabilizing the protein. It is hypothesized that a lyoprotectant can also be hydrogen bonded

to the viral coated proteins hence stabilizing the live, attenuated virus. Furthermore, studies have also demonstrated that multiple hydrogen bonds can be formed between lyoprotectants and lipids [14, 15] via the phospholipid polar group at the surface of lipid bilayer vesicles [16] and liposomes [17]. This interaction might also be formed between lyoprotectants and the lipid layer of live, attenuated viruses.

Furthermore, because of the more complex structure of live, attenuated viruses compared to e.g., proteins and liposomes, other destabilization sources must be avoided during freeze-drying e.g., mechanical damages due to ice crystals and intra-cellular ice formation. As for cells and bacteria, the freezing step might destroy viruses via mechanical damage to the membrane, and via ice formation in the virus particle which may lead to its destruction. Compared to viruses, the impact of freezing on cells is much more studied [18, 19].

Freezing can damage cells for several reasons but intracellular ice formation is mostly fatal [18, 19]. Ice formation inside the cell (under fast cooling [19]) increases the concentration of electrolytes which affects the ionic interactions that can be involved to stabilize cellular enzymes. It can also change the osmotic potential of the cell or directly cause mechanical damages to the cellular ultra-structure [18, 19].

De Beer et al., [20, 21] and Pieters et al., [22] recently proposed the first process analytical techniques (NIR and Raman spectroscopy) allowing the monitoring and evaluation of the product behaviour itself (excipients and proteins) during the entire freeze-drying process. These non-invasive analytical tools allow fast and non-destructive analysis of samples before, during and after freeze-drying. Determination of the residual moisture content through intact glass vials was the first application of NIR analysis of freeze-dried formulations [23-26]. Afterwards, focus has moved to the real time monitoring of product behaviour (APIs and excipients) during freeze-drying [20-22, 27, 28]. Protein dehydration and denaturation has been monitored using NIR spectroscopy by evaluating the amide A/II frequency (near 4850cm^{-1}) which represents the strength of the hydrogen bonds of the amide group of proteins [22, 29, 30]. Liposomes were monitored by looking at the lipid layer via the analysis of the C-H overtones in NIR spectra [28]. Finally, FTIR spectroscopy has been used off-line to study the effect of different protectants on the membrane phase behaviour and the overall protein secondary structure of air-dried *Lactobacillus bulgaricus* by

evaluating the C-H stretching region (3000-2800cm^{-1}) and the amide I and II bands (1655 and 1545cm^{-1}, respectively) [31].

To our best knowledge, it has never been demonstrated whether NIR spectroscopy can evaluate viruses in vaccine formulations and distinguish intact from non-intact live, attenuated viruses. The aim of this chapter is to examine the applicability of NIR spectroscopy to evaluate the virus in a freeze-dried live, attenuated vaccine formulation. Therefore, this formulation was freeze-dried using different virus volumes and after applying different pre-freeze-drying virus treatments (resulting in different virus states): (i) as used in the commercial formulation; (ii) without antigen (placebo); (iii) concentrated via a centrifugal filter device; and (iv) stressed by 96h exposure to room temperature.

5.2. MATERIALS AND METHODS

5.2.1. Materials

The live, attenuated virus used as vaccine in this chapter was obtained from Zoetis.

For the first experiments performed to study the capability of NIR to evaluate the virus state, the live, attenuated viruses were differently pre-freeze-drying treated. Depending on the applied pre-freeze-drying treatment (further termed 'pretreatment'), the virus quality, integrity or state might vary. The resulting formulations were named after their pretreatment: 'normal' (i.e., as used in the commercial formulations), 'absent' (i.e., placebo formulations), 'concentrated' via a centrifugal filter device (Millipore, Amicon® Ultra) and 'stressed' (by storage at room temperature for 96hours). For clarity, the 'concentrated' virus samples were prepared using a similar virus culture medium volume as the 'normal' virus samples, but because of the centrifugation pretreatment process they contain more viral particles in that volume. The other formulation components (stabilizers and buffer) were similar as in the commercial formulation and thus kept constant for these four classes. Detailed information on the composition of the commercial formulation cannot be given because of confidentiality reasons.

For a second series of experiments, the stabilizers from the commercial formulation were replaced by trehalose (Cargill, Krefeld, Germany) in order to make the formulation less

complex for the NIR spectral interpretation (see results section). Trehalose is a well-known cryo-/lyoprotectant used in many freeze-dried formulations. Its ability to maintain a satisfying titer (i.e., similar to the commercial formulation) after lyophilization and to provide a freeze-dried cake with sufficient elegance was investigated and confirmed in preliminary experiments. The same four classes (normal, concentrated, placebo, stressed) as for the commercial formulation were freeze-dried and an additional placebo formulation which only contained the culture medium of the virus was also freeze-dried. This placebo formulation is further called 'flow through' formulation since the culture medium, free from virus, is obtained by collecting the flow through after the centrifugation.

An overview of all formulations used for this study is given in Table 5.1a.

Besides examining whether NIR spectroscopy is able to evaluate viruses differently pretreated, also its ability to detect differences in added volume of virus culture medium to the formulations was studied. This study was only done for the trehalose formulation. Four virus formulations varying in virus volume were prepared (Table 5.1b). Stabilizer and buffer were kept constant (concentration and volume).

An overview of all formulations used in this chapter is presented in Figure 5.1.

Table 5.1: Overview of the studied live, attenuated virus formulations.

	Virus pretreatment	Virus medium (µl)	Buffer (µl)	Stabilizer (µl)		*qsp* filling volume (µl)	Total volume (µl)
				If commercial formulation	If Trehalose formulation		
a	Normal	x	y	z	9% w/v	j	800
	Stressed	x	y	z	9% w/v	j	800
	Concentrated	x	y	z	9% w/v	j	800
	Without	0	y	z	9% w/v	j + x	800
	Flow through	x	y	NA	9% w/v	j	800
b	Normal	0	y	NA	9% w/v	i + 400	800
	Normal	30	y	NA	9% w/v	i + 370	800
	Normal	100	y	NA	9% w/v	i + 300	800
	Normal	400	y	NA	9% w/v	i + 0	800

a) Virus pretreatment study. b) Virus volume study.
All symbols (x, y, z and j) represent absolute values in µl.

(a) Virus pretreatment study
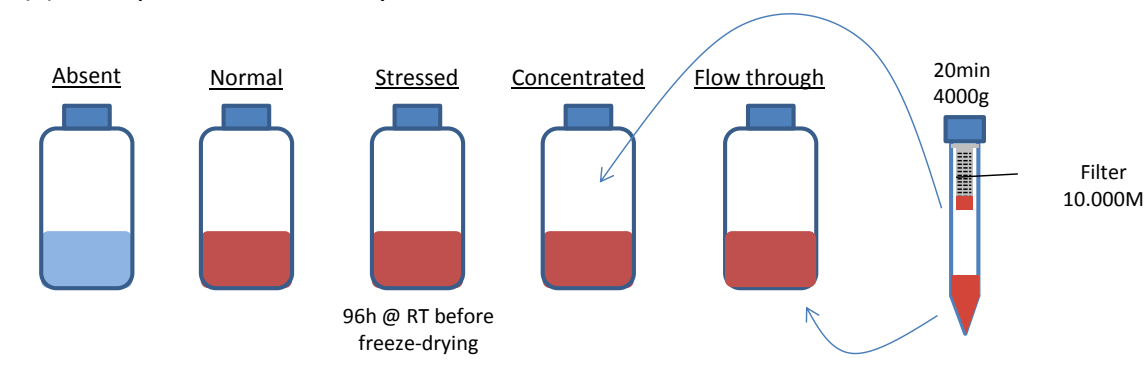
(b) Virus volume study
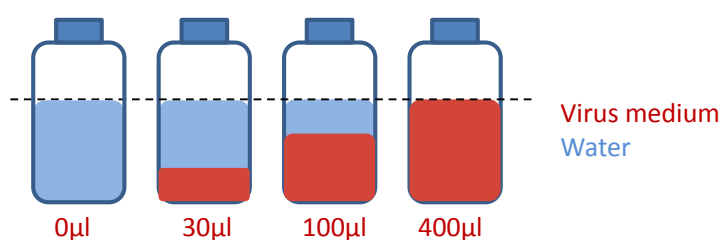
Figure 5.1: Overview of the formulations used in the (a) virus pretreatment study and (b) virus volume study.

The virus pretreatment study was performed independently from the virus volume study. The difference between both studies is the volume of virus culture medium that has been used. A constant volume was used for the virus pretreatment study (Table 5.1a) whereas different virus volumes were used for the virus volume study (Table 5.1b).

The studied formulations (Table 5.1) were freeze-dried multiple times, resulting in several batches (Table 5.2).

Table 5.2: Overview of the freeze-dried batches of each used live, attenuated virus formulation.

Batches	Batch ID	Formulation	Study	Sample types per batch & number of samples per type	Number of titrated samples	Analyzed spectral regions	
						7300-4000 cm^{-1}	10,000-7500 & 6340-5500cm^{-1}
Commercial formulation 1	Com1	Table 5.1a	Virus pretreatment	Normal: 20 samples Stressed: 20 samples Concentrated: 20 samples Without: 20 samples Total: 80 samples	Normal: 6/20 Stressed: 8/20 Concentrated: 6/20 Without: 0/20 Total: 20 samples	X	X
Commercial formulation 2	Com2	Table 5.1a	Virus pretreatment	Normal: 19 samples Stressed: 19 samples Concentrated: 20 samples Without: 20 samples Total: 78 samples	Normal: 5/19 Stressed: 0/19 Concentrated: 5/20 Without: 0/20 Total: 10 samples	X	
Trehalose formulation 1	Treha1	Table 5.1a	Virus pretreatment	Normal: 20 samples Concentrated: 20 samples Without: 19 samples Total: 59 samples	Normal: 0/20 Concentrated: 0/20 Without: 0/19 Total: 0 sample		X

Table 5.2: Overview of the freeze-dried batches of each used live, attenuated virus formulation (continued).

Trehalose formulation 2	Treha2	Table 5.1b	Virus volume	0µl: 10 samples 30µl: 10 samples 100µl: 10 samples 400µl: 10 samples Total: 40 samples	0µl: 0 samples 30µl: 4 samples 100µl: 4 samples 400µl: 4 samples Total: 12 samples	X	X
Trehalose formulation 3	Treha3	Table 5.1a	Virus pretreatment	Normal: 10 samples Concentrated 1min: 10 samples Concentrated 10min: 10 samples Concentrated 20min: 10 samples Flow through: 10 samples Without: 10 samples Total: 60 samples	Normal: 6/10 Concentrated 1min: 8/10 Concentrated 10min: 8/10 Concentrated 20min: 8/10 Flow through: 0/10 Without: 0/10 Total: 30 samples	X	X
Trehalose formulation 4	Treha4	Table 5.1a	Virus pretreatment	Normal: 29 samples Concentrated: 27 samples Flow through: 30 samples Without: 30 samples Total: 116 samples	Normal: 17/29 Concentrated: 7/27 Flow through: 0/30 Without: 0/30 Total: 24 samples		X
Trehalose formulation 5	Treha5	Table 5.1a	Virus pretreatment	Normal: 30 samples Concentrated: 30 samples Flow through: 30 samples Without: 30 samples Total: 120 samples	Normal: 0/30 Concentrated: 14/30 Flow through: 0/30 Without: 0/30 Total: 14 samples		X

Table 5.2: Overview of the freeze-dried batches of each used live, attenuated virus formulation (continued).

Trehalose formulation 6	Treha6	Table 5.1a	Virus pretreatment	Normal: 20 samples Concentrated: 20 samples Flow through: 20 samples Without: 20 samples Total: 80 samples	Normal: 12/20 Concentrated: 12/20 Flow through: 0/20 Without: 0/20 Total: 24 samples		X

5.2.2. Freeze-Drying

Freeze-drying experiments were performed using an Amsco FINN-AQUA GT4 freeze-dryer (GEA, Köln, Germany).

Different freeze-drying process settings were used depending on the formulation. For confidentiality reason, these freeze-drying cycle settings are not detailed. All freeze-dried cakes had an elegant appearance without signs of collapse.

5.2.3. NIR spectroscopy

NIR spectra of all freeze-dried samples from each batch were collected off-line using a Fourier-Transform NIR spectrometer (Thermo Fisher Scientific, Nicolet Antaris II near-IR analyzer) equipped with an InGaAs detector and a quartz halogen lamp. One NIR spectrum per freeze-dried sample was recorded in the $10000\text{-}4000\text{cm}^{-1}$ region with a resolution of 8cm^{-1} and averaged over 16 scans through the bottom of the glass vial in random order with the integrating sphere device. The NIR spectra were collected immediately after freeze-drying.

5.2.4. Data analysis

NIR spectral data analysis was done using SIMCA P+ v.12.0.1 (Umetrics, Umeå, Sweden). Two spectral regions were evaluated: (i) the amide A/II band ($7300\text{-}4000\text{cm}^{-1}$) which might reflect information on the coated proteins (Haemagglutinin and Neuraminidase) from the studied

freeze-dried live, attenuated viruses; and (ii) the C-H vibration overtone regions (10,000-7500 and 6340-5500cm^{-1}) which might supply information on the lipid layer surrounding the freeze-dried live, attenuated viruses. In order to avoid the influence of water in the 7300-4000cm^{-1} region, this spectral range has also been reduced to 5029-4000cm^{-1}. The 10000-7500 & 6340-5500cm^{-1} spectral ranges were selected based on the work from Christensen et al., [28] and contains the 1st and 2nd overtone of the CH- group. This spectral range has the advantage not to be influenced by water. Table 5.2 overviews the analyzed spectral ranges for each freeze-dried batch. All collected NIR spectra were preprocessed using standard normal variate (SNV) and second derivatives with Savitzky-Golay smoothing (37 points) (the latter only for the 7300-4000cm^{-1} spectral region). The use of SNV preprocessing eliminates the additive baseline offset variations and multiplicative scaling effects in the spectra which may be caused by possible differences in sample density and different-sample-to-sample measurement variations. Second derivatives have been selected for (a) spectral discrimination, as a qualitative fingerprinting technique to accentuate small structural differences between similar spectra; and for (b) spectral resolution enhancement, as a technique for increasing the apparent resolution of overlapping spectral bands in order to more easily determine the number of bands and their wavelengths.

All collected NIR spectra per batch were analyzed as one data matrix (**D**) using principal component analysis (PCA), allowing to examine the spectral differences between the different sample types per batch (Table 5.2). PCA produces an orthogonal bilinear data matrix (**D**) decomposition, where principal components (PCs) are obtained in a sequential way to explain maximum variance:

$$\mathbf{D}=\mathbf{TP}^{\mathbf{T}} + \mathbf{E}$$

$$= t_1p'_1 + t_2p'_2 +...+t_Qp'_Q + \mathbf{E}$$

Where **T** is the *M x Q* score matrix, **P** is the *N x Q* loading matrix, **E** is the *M x N* model residual matrix, i.e., the residual variation of the data set that it is not related to any chemical contribution. **Q** is the selected number of PCs, each describing a non-correlated physical phenomenon in the data set, and **N** is the number of collected spectra at **M** wavelengths [32]. Each principal component consists of two vectors, the score vector **t** and

the loading vector **p**. The score vector contains a score value for each spectrum, and this score value informs how the spectrum is related to the other spectra in that particular component. The loading vector indicates which spectral features in the original spectra are captured by the component studied. These abstract, unique, and orthogonal PCs are helpful in deducing the number of different sources of variation present in the data. However, these PCs do not necessarily correspond to the true underlying factors causing the data variation, but are orthogonal linear combinations of them, since each PC is obtained by maximizing the amount of variance it can explain [33].

Furthermore, partial least square discriminant analysis (PLSDA) models were developed based on the NIR spectra from the different sample types (normal, placebo, concentrated and stressed). PLSDA models are able to accomplish a rotation of the projection to give latent variables a focus on class separation ("discrimination"). This model takes into account the class membership of observations and is developed from a training set of observations of known classes (sample pretreatments) [34]. The aim was to use the PLSDA models to predict the class membership of future samples. To evaluate the well known risk that the PLSDA model is spurious, i.e., the model just fits the training set well but doesn't predict the new observations correctly, a permutation test was used. The idea of this validation is to compare the goodness of fit and the goodness of prediction (R^2 and Q^2, respectively) of the original model with the goodness of fit and the goodness of prediction of several models based on data where the class membership has been randomly permuted, while the X-matrix has been kept intact. The ability of each created PLSDA model to classify observations was evaluated using a misclassification table. Such table shows the proportion of correct classification of the tested new observation set. The calculated misclassification rates are considered as good indicators of model performance [35].

5.2.5. Titration

Titration was done according the company internal SOP. Each titer is the average of triplicate measurements and is expressed in $\log_{10}$ CCID$_{50}$ (Cell Culture Infection Dose 50 – Inverse of the highest dilution which produces a cytopathogenic effect in 50% of the cells). Titration provides information regarding the number of viral particles contained in each vial.

Statistical analysis for comparing the significant titer differences between the different pretreated samples was performed using the non-parametric Kruskal-Wallis analysis of variance test (Minitab (R) 15.1.1.0 software). In addition, in order to determine which group of pretreated samples differs significantly, Dunn's test was performed using a Matlab m-file [41] as follow-up test (Matlab 7.12, The Mathworks, Natick, MA). For practical reason, only some samples from each batch could be titrated and are presented in Table 5.2.

5.2.6. Karl Fischer

The residual moisture content was determined on 24 samples from batch Treha2 (Table 5.2) using Karl Fischer titration. A Mettler Toledo V30 volumetric Karl Fischer titrator (Schwerzenbach, Switzerland) with Hydranal® titration solvent from Sigma Chemical Company was used. A known volume of dried methanol was added to the sampled vial, and left to equilibrate for a few minutes. From the solution, a known volume was then removed volumetrically using a syringe and injected into the titration cell. The water content of pure methanol was determined in duplicate prior to the measurement and subtracted from the result. All titrated vials were measured in duplicate.

5.3. RESULTS AND DISCUSSION

The discussion of the results is divided into two parts, based on the column 'study' in Table 5.2: (i) virus pretreatment; (ii) virus volume. Furthermore, each study is subdivided into two parts being the results obtained by analyzing the spectral region (7300-4000cm^{-1}) corresponding to the coated proteins and the results obtained by analyzing the spectral region (10000-7500 & 6340-5500 cm^{-1}) corresponding to the lipid layer covering the live, attenuated viruses.

5.3.1. Virus pretreatment study

5.3.1.1. Spectral region 7300-4000cm^{-1}

- *Principal component analysis (PCA)*

Principal component analysis was performed on all collected spectra from batch Com1 (Table 5.2) (i.e., 80 spectra, 1 spectrum per sample, 20 samples per virus pretreatment class). All preprocessed NIR spectra were decomposed into four principal components (PCs) explaining 80.9% of the spectral variance, where PC1 accounted for 30.5%, PC2 28.8%, PC3 13.1% and PC4 8.5% of the spectral variance, respectively. The PC1 versus PC2 scores plot (Figure 5.2a) showed no separation along PC1 according to the sample pretreatment. A peak around 5280cm^{-1}, representing water [36] in the PC1 loadings (Figure 5.2b), indicated that PC1 differentiates between the samples according to moisture content. The residual moisture variability in the samples was hence independent from the sample pretreatment since the spectra from the samples differently pre-treated were randomly spread along PC1. Interestingly, the PC2 versus PC3 scores plot (Figure 5.2c) distinguished the samples according the pretreatment. Examination of the PC2 and PC3 loadings to identify the spectral variability responsible for this separation revealed that many NIR signals (except water bands since these were captured by PC1) contributed to this separation (data not shown). This is most probably due to the complexity of the commercial formulation which contains e.g., more than three stabilizers. However, the excipients were similar in each differently pretreated sample from batch Com1. The only difference between the samples types from batch Com1 (Table 5.2) was the pretreatment. Although the spectra were separated according to pretreatment, it was not possible to explain this from the spectral contributions because of the complexity of the loadings and the formulation.
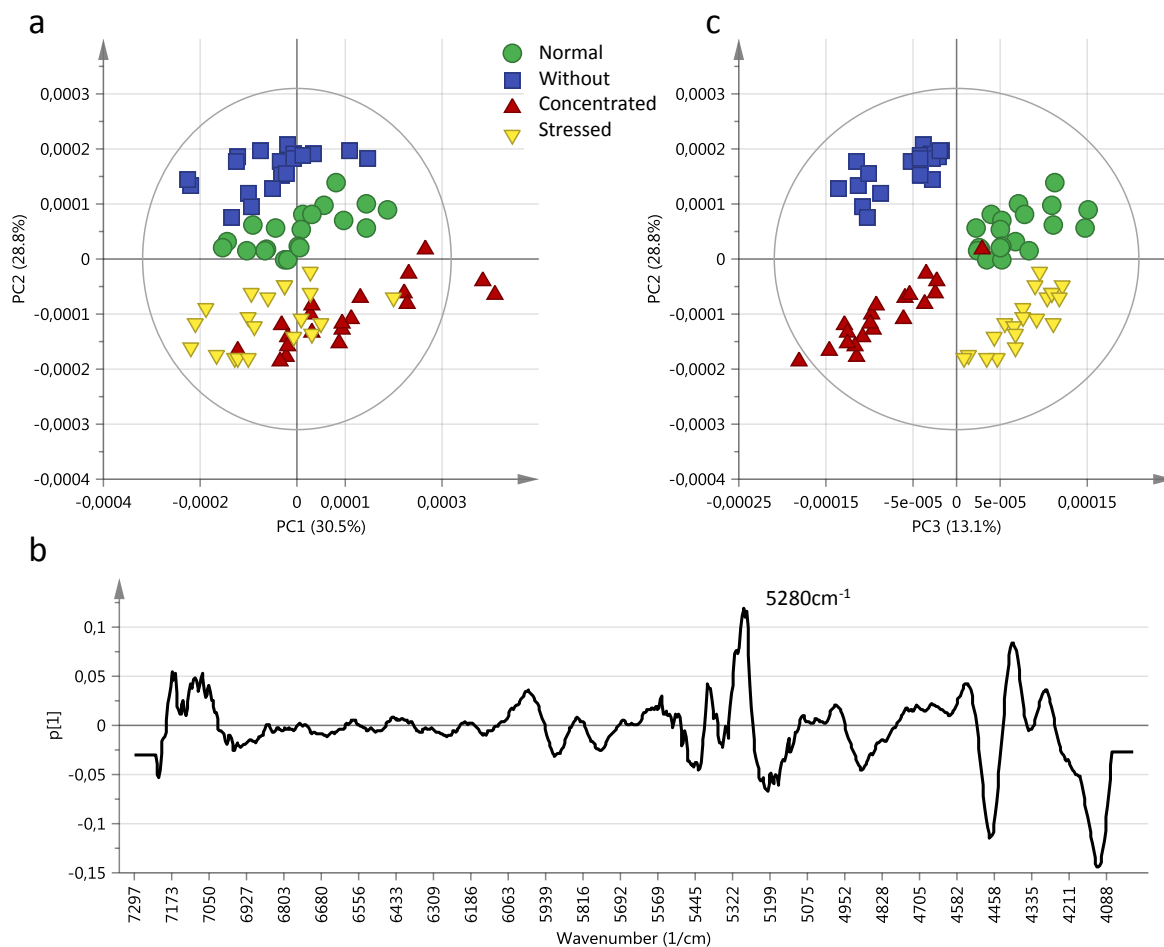
Figure 5.2: Scores plots obtained after PCA of the spectra collected from batch Com1 (7300-4000cm^{-1} spectral region) a) PC1 versus PC2 scores plot b) PC1 loadings line plot c) PC2 versus PC3 scores plot. Each point represents one different vial and each symbol represents a different sample pretreatment.

To ensure that the observed groups in the PC2 versus PC3 scores plot was related to the sample pretreatment, several verifications were done.

Undoubtedly, examination of the virus itself gained the first attention. As mentioned in the introduction, only biological potency assays after freeze-drying were possible. These assays are not of high precision [8] and only result in a titer (quantitative information) without qualitative information.

Titration of the samples revealed that the 'stressed' samples having a mean titer of 5.46±0.2 (n=8), were significantly different from the mean titer (6.91±0.09, n=6) of the 'concentrated' samples (Kruskal-Wallis, p<0.05). Having a titer of 6.56±0.14 (n=6), the 'normal' samples

were not significantly different from the 'stressed' or the 'concentrated' samples even if the 'normal' samples were distinguished from the other samples by NIR spectroscopy. This can be a confirmation of the low precision of the assay [8] to detect the differences between pretreated samples.

Fourteen weeks after freeze-drying of batch Com1, NIR spectra were collected again. PCA was done combining these spectra and the spectra collected directly after freeze-drying, resulting in a four components PCA model explaining 94.3% of the spectral variance. The PC1 versus PC4 scores plot is presented in Figure 5.3a. In this scores plot, PC1 (explaining 82.9% of the spectral variance) showed a separation according to storage time while PC4 (2.4% of the spectral variance) showed a separation according virus pretreatment. PC2 and PC3 explained respectively 6% and 2.9% of the spectral variance and did not show any separation anymore. The examination of the PC1 and PC4 loadings (Figure 5.3b) revealed that the clustering according storage time along PC1 was attributed to differences in water content whereas the separation according virus pretreatment along PC4 was due to many NIR signals, which were difficult to interpret because of the complexity of the commercial formulation. Increase in residual moisture content during storage can be observed and was most probably caused by moisture release from the stopper [37].

When analyzing by PCA the spectra collected after 14 weeks of storage individually, the PC2 versus PC3 scores plot (model explaining 83.4% of the total spectral variance, PC2= 15.4% and PC3=13.6%) also showed clustering according virus pretreatment (Figure 5.3c), although less clear compared to the scores plot from the spectra collected before storage (Figure 5.2c).
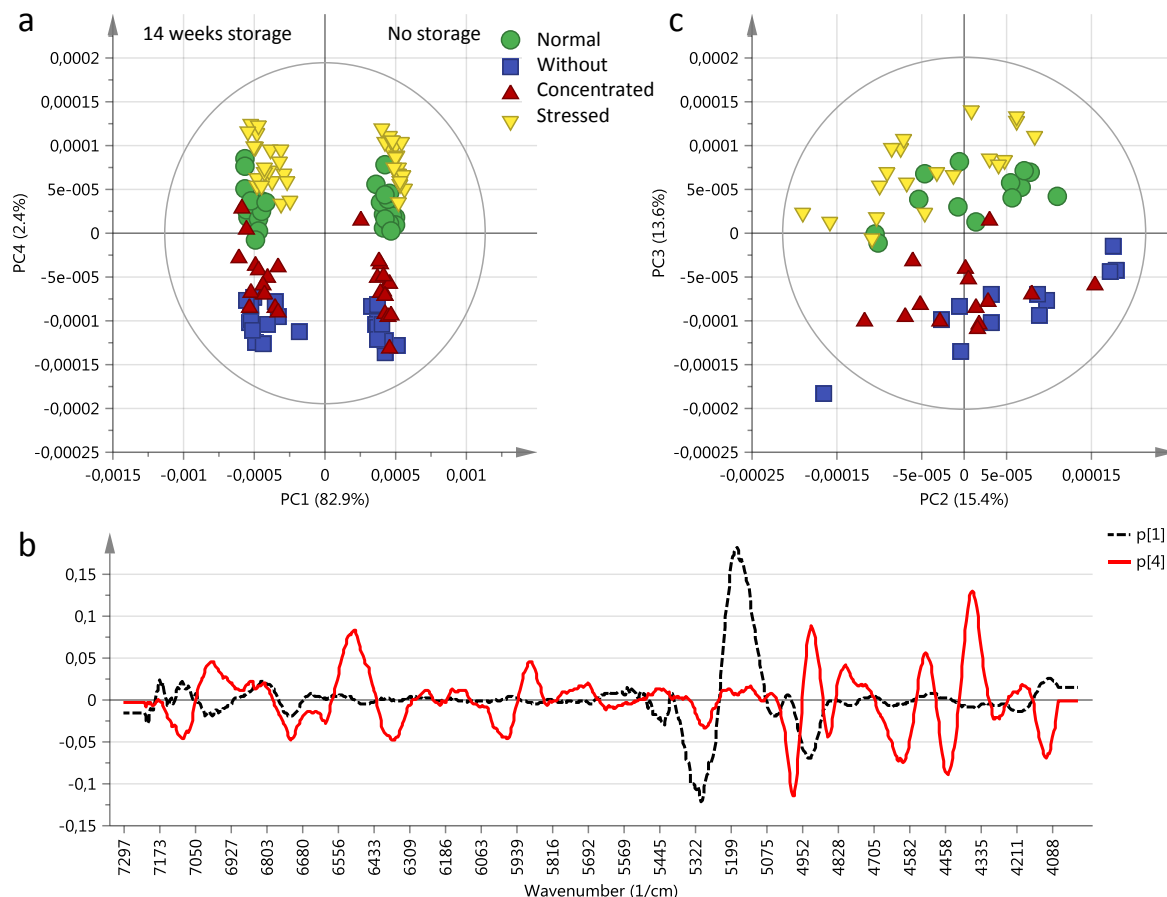
Figure 5.3: Impact of storage time. a) PC1 versus PC4 scores plot obtained after PCA of the spectra collected before and after storage. b) Corresponding PC1 (black dotted) and PC4 (red) loadings line plot c) PC2 versus PC3 scores plot obtained after PCA on the spectra collected only after storage. Each point represents one sample and each symbol represents a different virus pretreatment.

Finally, as it can be seen in Table 5.1a, the viruses are contained in a culture medium (inherent to virus production, culture). The viruses and the culture medium hence form the virus medium (Table 5.1a). In order to ensure that the observed NIR spectral differentiation according to pretreatment (Figure 5.2c) were not due to culture medium changes but due to viruses changes, a batch identical to batch Com1 but only containing culture medium was differently pretreated (normal, stressed, concentrated) and then freeze-dried. These samples were then measured using NIR spectroscopy and analyzed by PCA. The obtained scores plots did not show any spectral differentiation among these differently pretreated samples of this 'culture medium' batch (data not shown). This confirmed that the higher

116

observed NIR spectral differences according to virus medium pretreatment were due to virus modifications and not culture medium changes.

Exploratory analysis with PCA suggests that NIR spectroscopy is able to distinguish between the four different 'virus pretreatments' in the commercial vaccine formulations. However, it was not possible to interpret the spectral variability (from the loadings) which is responsible for the clustering in the scores plots. Therefore, in new experiments less complex formulations, (i.e., formulations having less different excipients) were used (see further).

- *Partial least square discriminant analysis (PLSDA)*

Since the formulations subjected to different pretreatments could be distinguished from the NIR data, the possibility to classify future freeze-dried samples according to their pretreatment was evaluated. Therefore, a PLSDA model was built using batch Com1 (Table 5.2), excluding the placebo samples (without viruses). The 60 collected spectra (20 normal, 20 concentrated and 20 stressed) were divided into a training and a test set. The training set contained 39 spectra (13 spectra per sample pretreatment) and was used to develop the model. The test set was then used to evaluate the model. The developed PLSDA model existed of five components (R^2Y= 0.963 and Q^2Y= 0.938). The Q^2 parameter expresses the predictive ability of the model and is obtained by cross validation [34]. Special attention should be paid to the validation of PLSDA models. The Q^2 value can provide over-optimistic results [35]. Therefore, combination with other model evaluation techniques such as permutation tests [35, 39], and model performance evaluation via misclassification tables are advised [35] and have been used in this study.

For the permutation test, a total of 20 permutations of the class membership (Y-block) was done while the spectra in the X-block were not permutated. For each permutation, a PLSDA model was fitted and the new estimates of R^2Y and Q^2Y values were computed. These values were afterwards plotted in a permutation plot and compared to the original Q^2Y and R^2Y values (Figure 5.4). If the original values are outside the distribution of the permuted values, a high validity of the original model may be assumed [40]. Analysis of the permutation plot (Figure 5.4) hence contributed to validating the original model since all the permuted Q^2 values were clearly lower than the original Q^2 value (top right Figure 5.4) and since the regression line of the Q^2 values intersected the vertical axis below zero [34]. Moreover,

when all permuted R^2 values are lower to the original R^2 value, this is also an indication for the validity of the original model [34].
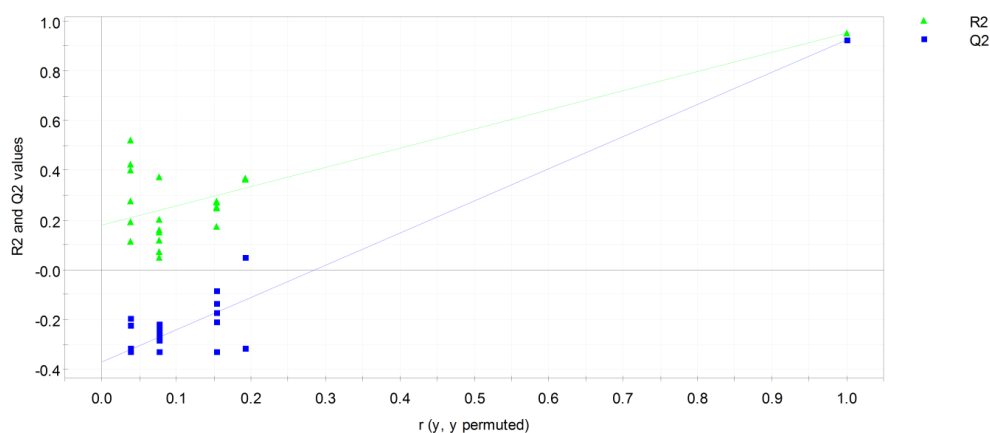
Figure 5.4: Validation plot obtained by performing a permutation test. The plot shows, for a selected y-variable ('normal' variable), on the vertical axis the values of R^2 (green triangle) and Q^2 (blue square) for the original model (far to the right) and of the Y-permuted models further to the left. The horizontal axis shows the correlation between the permuted y-vectors and the original y-vector for the selected y ('normal' variable). Two regression lines have been fitted, one among the R^2Y points and another one among the Q^2Y points (Intercepts: R^2 = (0.0, 0.163) and Q^2 = (0.0, - 0.361)).

The predictability of the PLSDA model was finally evaluated using a misclassification table in which the spectra from the test set - spectra not used for the model development - were classified by the model and in which the proportion of misclassification of the test set samples is given. As can be seen from the misclassification table (Table 5.3), the prediction of the test set was 100% correct. The test set samples were from the same batch as the training set samples (batch Com1). The number of correct classifications is presented for each class.

Table 5.3: Misclassification table overviewing the predictions of the test samples using the PLSDA model.

	Members	Correct classification rate (CCR, %)	Normal	Stressed	Concentrated
Normal	7	**100%**	**7**	0	0
Stressed	7	**100%**	0	**7**	0
Concentrated	7	**100%**	0	0	**7**
No class	0		0	0	0
Total	21	**100%**	7	7	7

In a next step, the classification ability of the PLSDA model was evaluated using samples from another freeze-dried batch; i.e., batch Com2 (Table 5.2) containing similar formulations as batch Com1: 19 'normal ' samples, 19 'stressed' samples and 20 'concentrated' samples.

Table 5.4: Misclassification table overviewing the predictions of the external test set (batch Com2) using the PLSDA model.

	Members	Correct classification rate (CCR, %)	Normal	Stressed	Concentrated
Normal	19	100%	19	0	0
Stressed	19	0%	19	0	0
Concentrated	20	65%	7	0	13
No class	0		0	0	0
Total	58	55.17%	45		13

The misclassification table (Table 5.4) showed that all 'normal' samples were correctly classified. The stressed samples were all wrongly classified as normal. There is a possibility that these samples were not enough stressed to be classified as stressed viruses and that they were therefore classified as normal samples. In order to stress the viruses, they were exposed 96hours at room temperature. However, this stressing condition is subject to variation of the surrounding environment resulting in uncontrolled stressing and hence possibly not enough stressed viruses in case of batch Com2. Unfortunately, due to a titration problem, no titers were obtained for these stressed samples. It was therefore impossible to confirm that the viruses exposed to stressing conditions had similar titers as the unstressed samples. The PLSDA model claimed that there was no difference between the stressed and normal samples from batch Com2. Finally, 65% of the 'concentrated' samples were correctly classified. The other 35% were classified as 'normal'.

Five concentrated samples were titrated from batch Com2. Among these, samples C4 and C5 were misclassified by the model (i.e., as normal samples). However, from the titration results (Figure 5.5) it can be seen that concentrated samples C4 and C5 had a titer similar to the titers of the 'normal' samples (N1-N5) whereas the titers of the correctly classified 'concentrated' samples (C1, C2 and C3) were higher.
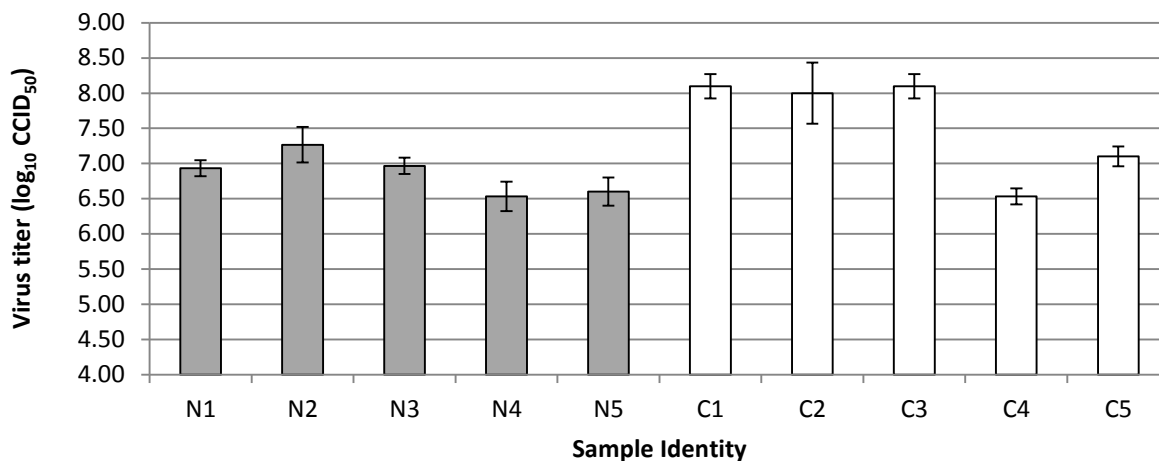
Figure 5.5: Titration results of batch Com2. In gray, normal samples and in white, concentrated samples. Titers are expressed as $\log_{10}$ $CCID_{50}$ (Cell Culture Infection Dose 50). Each titer is the mean of 3 determinations ± standard deviation.

5.3.1.2. <u>Spectral region 10000-7500 & 6340-5500cm^{-1}</u>

To evaluate the live, attenuated virus samples via the surrounding lipid bilayer, another NIR spectral region (10000-7500 & 6340-5500cm^{-1}) was selected. Compared to the above analyzed protein region, this spectral region offers the advantage that it does not include the NIR spectral water band regions [28]. PCA using this spectral region of the NIR spectra collected from batch Com1 (Table 5.2) did not allow to distinguish between the samples according virus pretreatment (PCA scores plot not shown).

To simplify the NIR spectral analysis (i.e., to avoid disturbing NIR spectral signals from the different excipients in the commercial formulation in the NIR spectral ranges used to evaluate the virus pretreatment), and based on the fact that Christensen and co-workers [28] were able to detect liposomes in a trehalose formulation using the spectral ranges 10000-7500 & 6340-5500cm^{-1}, trehalose 9% w/v was used to replace the stabilizers from the commercial formulation (Table 5.1a).

- *Principal component analysis (PCA)*

Principal component analysis was performed on the NIR spectra from all samples of batch Treha1 (Table 5.2) and allowed clear distinction between the different virus pretreatments (data not shown). This was more extensively studied using batch Treha3 (Table 5.2). This batch contained 60 samples in total having 6 different virus pretreatments (10 samples per

120

virus pretreatment): normal, absent (i.e., placebo formulations), concentrated via a centrifugal filter device using different centrifugation times (1 minute, 10 minutes or 20 minutes) and the flow through pretreatment (see materials and methods).

Within batch Treha3, different PCA were performed using the two spectral ranges (10000-7500 & 6340-5500cm^{-1}) individually and combined. The PCA of the NIR spectra from the samples 'normal', 'concentrated 20min', 'flow through', and 'without' using the 10,000-7500cm^{-1} spectral region consisted of 2 PCs explaining 95.3% of the spectral variability. The first PC explained 89.4% of the spectral variability and was responsible for the separation according virus pretreatment (Figure 5.6a). PCA using the 6340-5500 cm^{-1} NIR spectral region also resulted in separation according to virus pretreatment (Figure 5.6b). These 2 PCs explained 96.5% of the spectral variability, where the first principal component accounted for 93.4% and allowed differentiation according to the virus pretreatment (Figure 5.6b). Separation was also seen along the second component, where the placebo samples were isolated from the samples containing virus medium. The groups in both scores plots in Figure 5.6 are explained in their corresponding PC1 loadings in Figures 5.6c and 5.6d. For both spectral regions, the NIR signal responsible for the separation corresponded to the 1st and 2nd C-H overtones from the lipids surrounding the live, attenuated viruses.
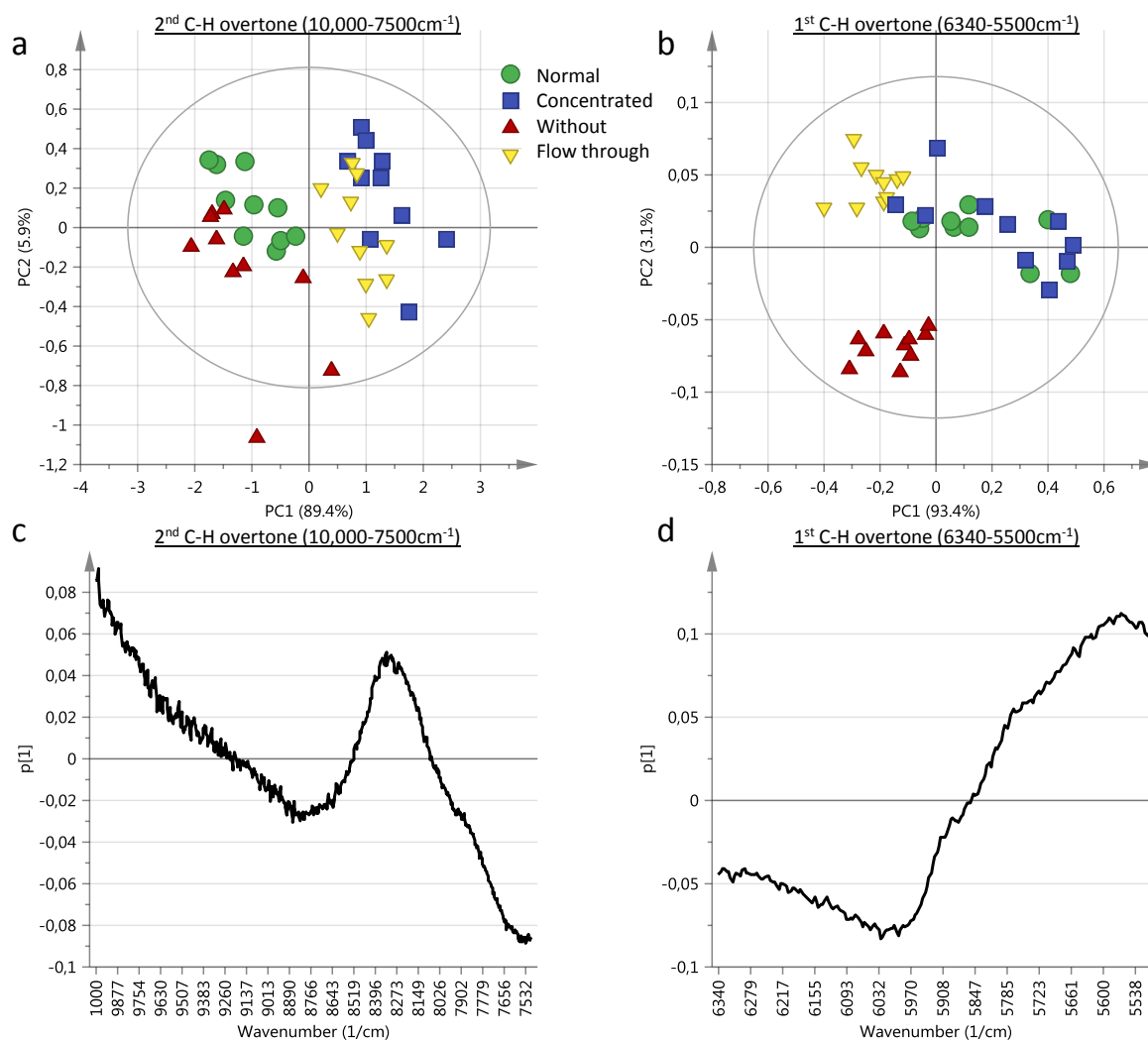
Figure 5.6: Scores and loadings plots obtained after PCA of the NIR spectra from the samples normal, concentrated 20min, flow through and without of batch Treha3 using the 10,000-7500cm^{-1} and 6340-5500 cm^{-1} spectral regions. a) PC1 versus PC2 scores plot (10,000-7500cm^{-1}) b) PC1 versus PC2 scores plot (6340-5500cm^{-1}). c) PC1 loadings plot (10,000-7500cm^{-1}) d) PC1 loadings plot (6340-5500cm^{-1}).

Another PCA was performed for evaluating the differently concentrated samples from batch Treha3 (Table 5.2), prepared using different centrifugation times (i.e., 1 minute, 10 minutes and 20 minutes). The titration results of these differently concentrated samples showed that the highest centrifugation time (20 minutes) resulted in the highest titer (Figure 5.7d). PCA analysis was performed to evaluate whether these concentration differences could also be derived from the NIR spectra.
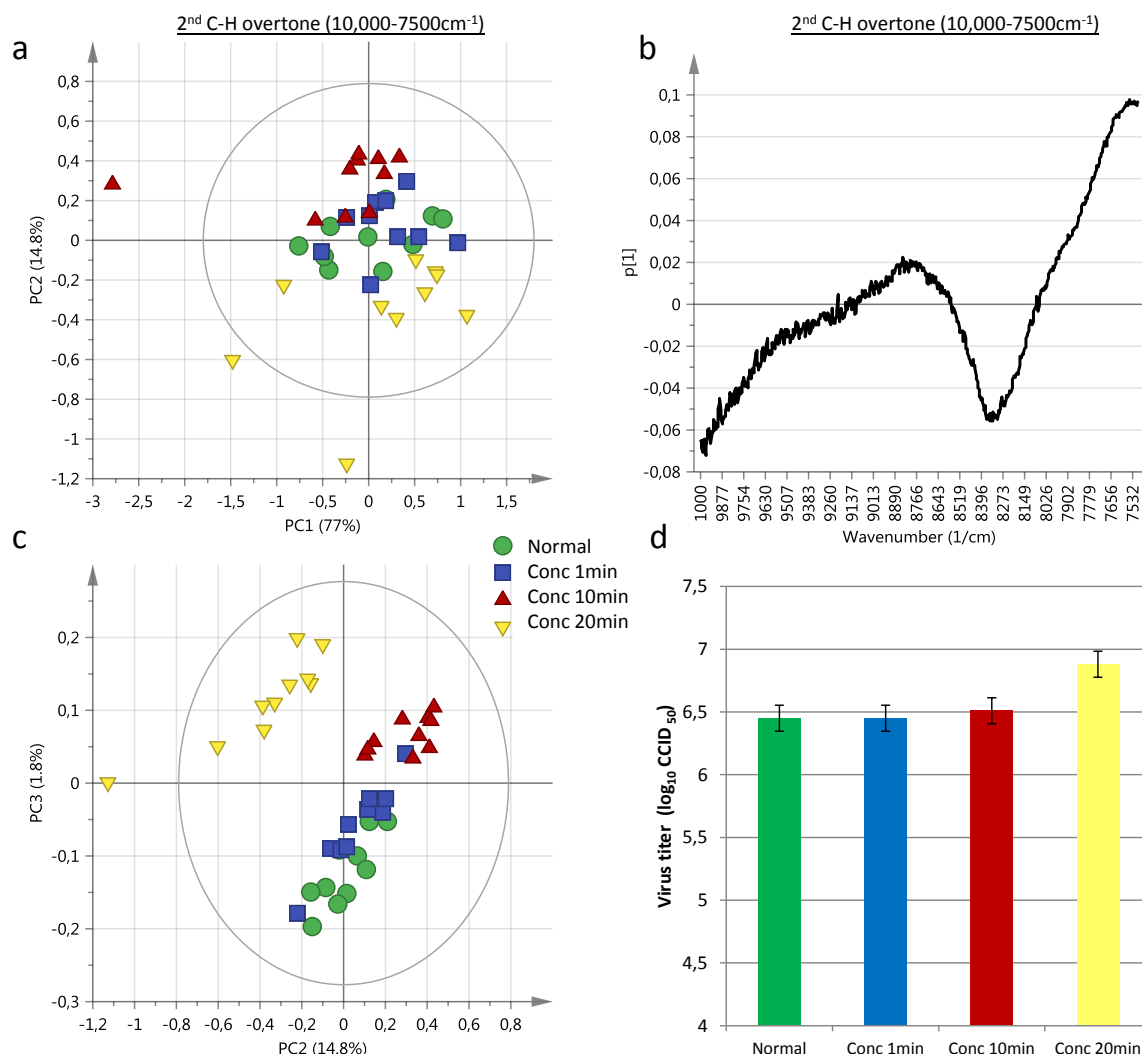
Figure 5.7: PC1 versus PC2 and PC2 versus PC3 scores plots obtained after PCA of the NIR spectra from the samples obtained after applying different centrifugation times. (Normal = no centrifugation, concentrated 1min, concentrated 10min and concentrated 20min = centrifugation times of 1 minute, 10 and 20 minutes respectively. Each color in the scores plots represents the samples subjected to a different centrifugation time. a) PC1 versus PC2 scores plot. b) PC 1 loadings plot. c) PC2 versus PC3 scores plot. d) Titration results.

The PCA of the NIR spectra collected from the differently concentrated samples in batch Treha3 consisted of 3 PCs explaining 93.6% of the spectral variance. The first principal component accounted for 77% of the spectral variability and did not distinguish between the differently concentrated samples (Figure 5.7a). The analysis of the loadings of this component showed the C-H overtone corresponding to the lipid layer (Figure 5.7b). The PC2 versus PC3 scores plot (Figure 5.7c) clearly differentiated between the viruses centrifugated

for 20 minutes and the other samples. The differences in titration results might explain this clustering (Figure 5.7d). The 20 minutes concentrated samples had a titer (6.88±0.29, n=8) which was significantly higher (Kruskal-Wallis, p<0.05) than the 10 minutes and 1 minute concentrated samples and the normal samples (6.52±0.31 n=8, 6.45±0.31 n=8 and 6.45±0.33 n=6), respectively.

- *Partial least square discriminant analysis (PLSDA).*

Using different independent trehalose batches (Treha 1-4-5-6, Table 5.2), a PLSDA model was built to evaluate the possibility to classify the different virus pretreatment samples using the lipid spectral range.

The training set to develop the PLSDA model consisted of the NIR spectra from 375 samples of batches Treha 1-4-5-6, representing 4 different virus pretreatments (normal, concentrated, flow through and without). The developed PLSDA model consisted of five components (R^2Y= 0.778 and Q^2Y= 0.682). Similarly to the PLSDA model built for batch Com1, a permutation test was performed. A total of 20 permutations of the class membership were done and the analysis of the permutation plot validated the model (data not shown). The PLSDA model was further evaluated using the Treha3 batch (as independent test batch) containing 10 normal, 10 concentrated for 20 minutes, 10 flow through and 10 without samples.

Table 5.5: Misclassification table overviewing the predictions of the external test set (batch Treha3) using the PLSDA model.

	Members	Correct classification rate (CCR, %)	Normal	Concentrated	FT	Without
Normal	10	**50%**	5	5	0	0
Concentrated	10	**90%**	0	9	1	0
FT	10	**90%**	0	1	9	0
Without	10	**100%**	0	0	0	10
No class	0		0	0	0	0
Total	40	**82,50%**	5	10	15	10

In total, 82.5% of the samples from the test batch were well classified (Table 5.5). The without samples were 100% correctly attributed, the concentrated and flow through samples had a score of 90%. The normal samples were less correctly classified: 50% were classified as normal but 50% were wrongly classified as concentrated. However, the titration results of the samples from batch Treha3 revealed that several normal samples had a high titer (N1 and N2) (Figure 5.8). This might be the reason why they were classified as concentrated samples by the model. Moreover, several concentrated samples from the batches used to build the model were probably not enough concentrated which can also explain that normal samples with high titers were misclassified and considered as concentrated samples.
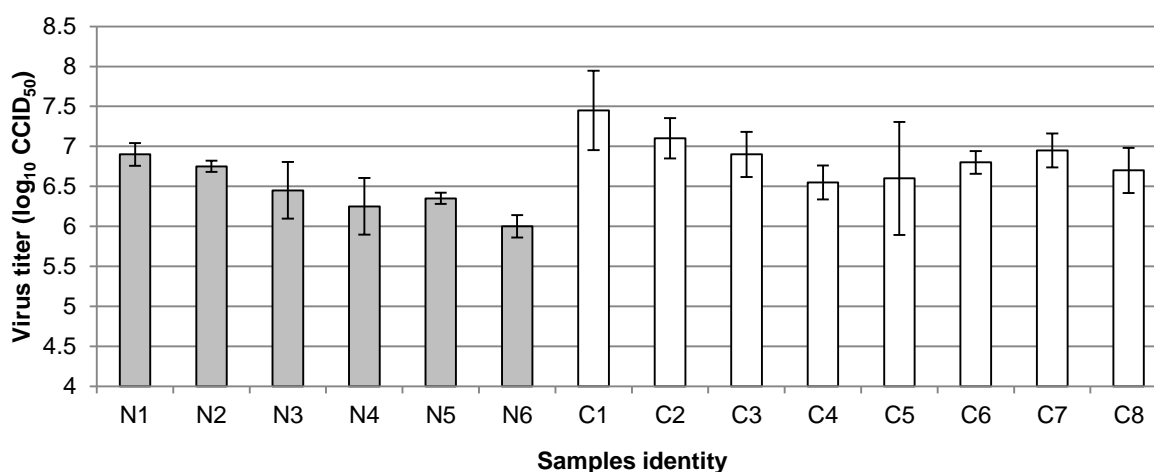
Figure 5.8: Titration results of the normal and 20 minutes concentrated samples from the independent test batch (Treha3).

5.3.2. Virus volume study

This part of the study evaluates the ability of NIR spectroscopy to distinguish differences in applied virus volume in freeze-dried live, attenuated vaccine formulations. Four trehalose formulations varying in virus volume were prepared as described in Table 5.1b. The stabilizer and buffer were kept constant (concentration and volume) as well as the virus pretreatment (normal). The added water volume was varied depending on the applied virus volume in order to guarantee an equal total volume in each formulation. One batch (Treha2, Table 5.2)

was freeze-dried for this study. The residual moisture and titer of some samples from each volume class were determined. The vials containing 0µl of virus were not titrated as they did not contain the antigen. The 30µl virus volume vials had a titer of 6.56±0.1 (n=4), which differed significantly from the 400µl virus volume samples which had a titer of 8.3±0.5 (n=4) (Kruskal-Wallis, $p < 0.05$) (Figure 5.9a). The 100µl virus volume samples had a titer of 7.52±0.35 (n=4) which did not significantly differ from the 30µl and 400µl virus volume samples.

The Karl Fischer analysis revealed an increase of the residual moisture with the virus volume (Figure 5.9b). The 0µl vials had a residual moisture of 1.22±0.1% (n=6), the 30µl, 100µl and 400µl had a residual moisture content of 1.49±0.1% (n=6), 2.31±0.3% (n=6) and 4.92±0.3% (n=6), respectively.
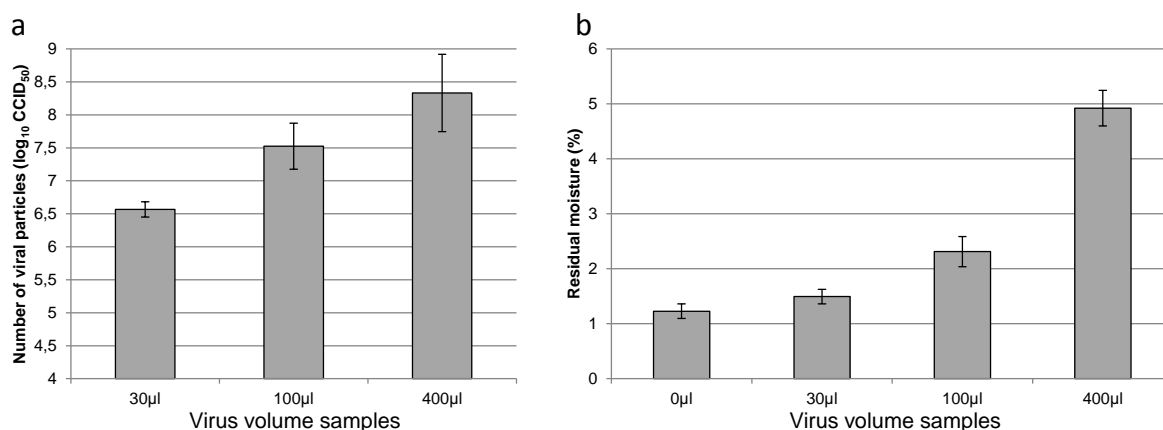
Figure 5.9: Titration and residual moisture results of the Treha2 batch. a) Titration results. b) Residual moisture results.

After freeze-drying, NIR spectra were collected from each sample (i.e., 40 spectra) of batch Treha2. The NIR spectra were analyzed using PCA for both the 7300-4000cm^{-1} and the 10,000-7500 cm^{-1} spectral ranges.

5.3.2.1. Spectral region 7300-4000cm^{-1}

The PCA performed on the 40 spectra described 97.7% of the spectral variability (composed by 2 PCs). The PC1 versus PC2 scores plot showed that the first PC (explaining 95.3% of the spectral variability) distinguished the samples according to their virus volume (Figure 5.10a). Analysis of the PC1 loadings plot clearly revealed two major contributions : the water bands

(~7000cm^{-1} and ~5200cm^{-1}) and the amide A/II band (4850cm^{-1}) (Figure 5.10b). These two involved spectral contributions were confirmed by the titration results as well as by the residual moisture analysis: the higher the virus volume, the higher the titer and residual moisture. To avoid the contribution of the water bands, the spectral region was reduced to 5029-4000cm^{-1}. The new 2-components PCA model explained 98.3% of the spectral variance. The PC1 versus PC2 scores plot revealed again that the first PC (explaining 93.5% of the spectral variability) distinguished the samples according to their virus volume (Figure 5.10c). Analysis of the PC1 loadings plot showed that the NIR signal at 4850cm^{-1} was responsible for this separation. This NIR signal corresponded to the amide A/II band (Figure 5.10d) [22].
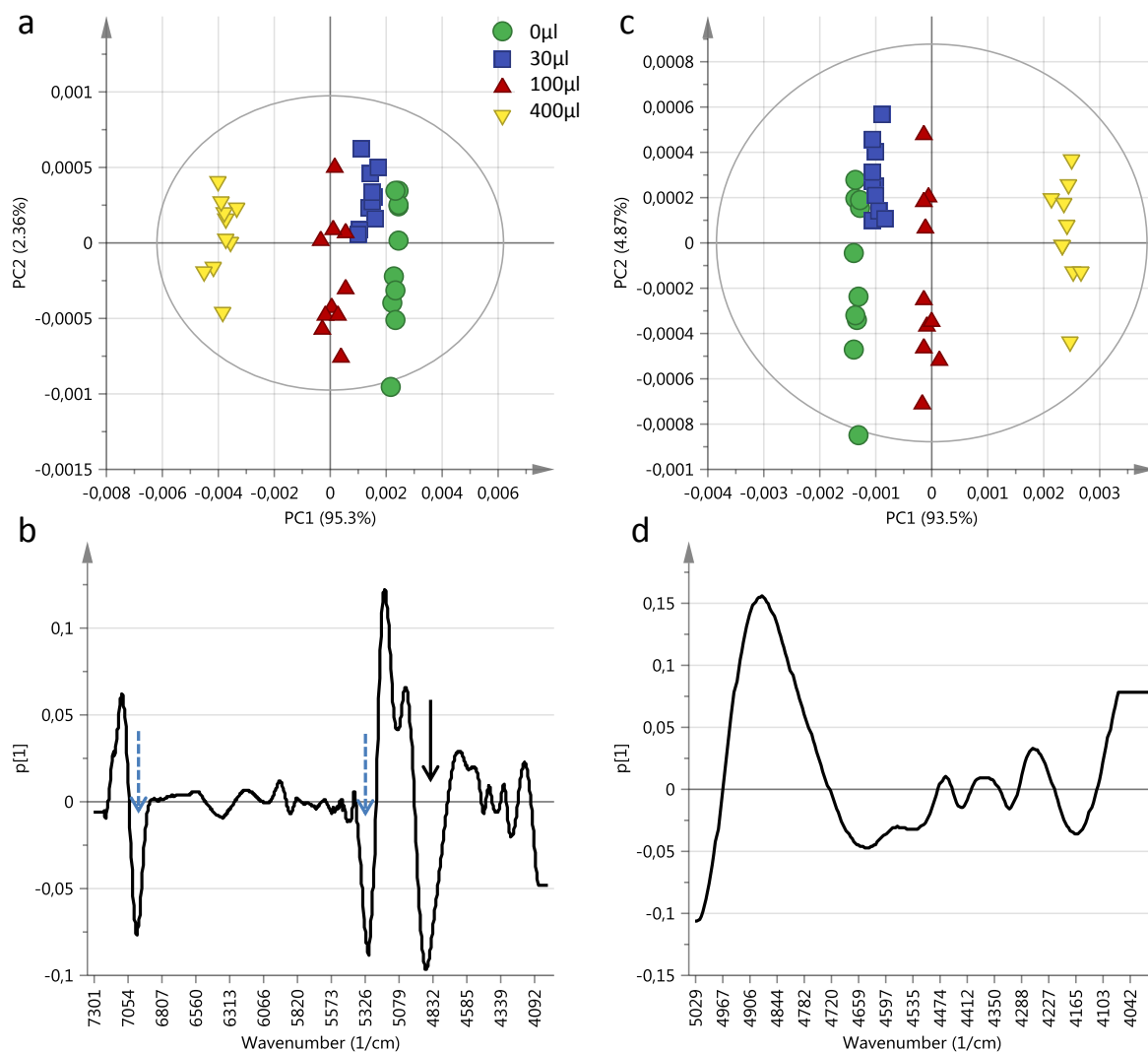
Figure 5.10: Scores and loadings plots a) PC1 versus PC2 scores plot obtained after PCA of the NIR spectra from the virus volume samples using the 7300-4000cm^{-1} spectral region. b) Corresponding PC1 loadings plot (7300-4000cm^{-1} spectral region) the blue dashed arrows represent water and the black solid arrow represents the amide A/II band c) PC1 versus PC2 scores plot obtained after PCA of the NIR spectra from the virus volume samples using the 5029-4000cm^{-1} spectral region. d) Corresponding PC1 loadings plot (5029-4000cm^{-1} spectral region). Each symbol represents a different virus volume sample.

5.3.2.2. Spectral region 10,000-7500cm^{-1}

The 40 NIR spectra from the Treha2 batch were further analyzed using the 10,000-7500cm^{-1} spectral region. This spectral range has the advantage not to be influenced by water [28]. The PCA consisted of 2PCs, explaining 87.6% of the overall spectral variability. The PC1 versus PC2 scores plot indicated that PC1, describing 76.9% of the spectra variability,

distinguished between the samples according to virus volume (Figure 5.11a). The PC1 loadings plot confirmed that the 2nd C-H overtone was responsible for the separation along PC1 in the scores plot (Figure 5.11b).
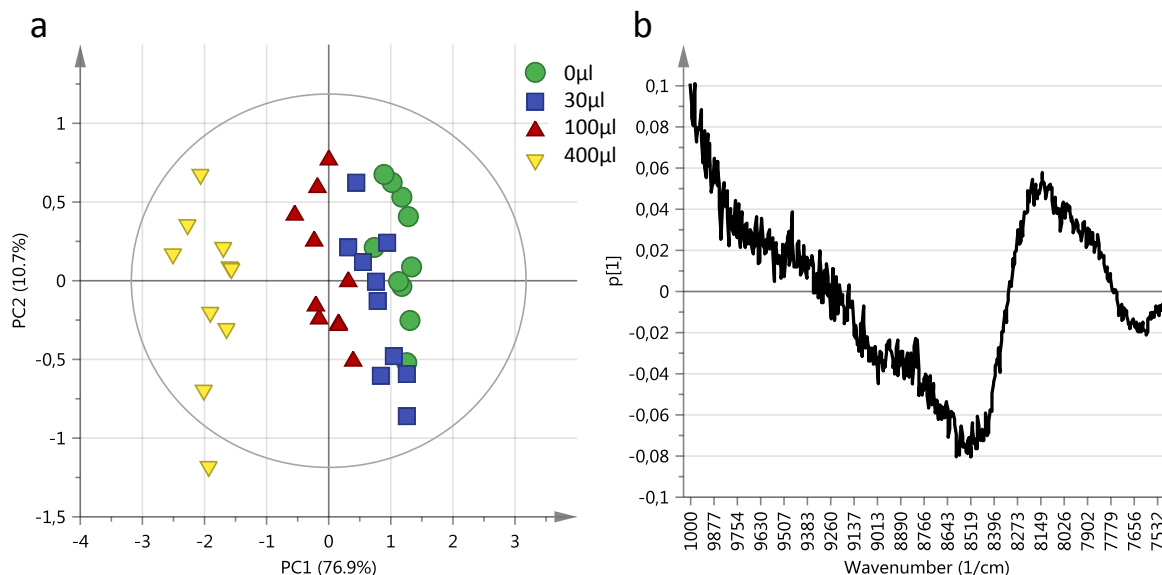
Figure 5.11: Scores and loadings plots obtained after PCA on the NIR spectra of the virus volume samples using the 10,000-7500cm^{-1} spectral range a) PC 1 versus PC2 scores plot, each color represents a different virus volume. b) PC1 loadings plot.

In addition to the ability of NIR spectroscopy to distinguish between different virus pretreatments, these results suggest that NIR is also able to distinguish differences in virus volume. The distance between the different classes within the scores plot (Figure 5.10c and 5.11a) corresponded to the virus volume increase but also to the water volume increase (Figure 5.9b). However, the absence of water band within the analyzed spectral region prevents the possibility that the clustering was due to residual moisture differences between the different virus volume samples [28] and ensure that the clustering was rather due to the virus volume.

5.4. CONCLUSION

This study is - to our best knowledge - the first one evaluating and demonstrating the suitability of NIR spectroscopy to detect live, attenuated viruses in a freeze-dried formulation. NIR spectroscopy was able to distinguish between formulations varying in terms of 'virus pretreatment' as well as 'virus volume'. This was possible using two specific spectral ranges; (1) 7300-4000cm^{-1} containing the amide A/II region (2) 10,000-7500 and 6340-5500cm^{-1} containing the first and second overtones of CH vibrations.

In order to evaluate the possibility to classify the freeze-dried vaccine formulations according to their virus pretreatment, two PLSDA models were built, each model based on one of the two different studied spectral regions. Both models were validated using a permutation test and the models were systematically evaluated with an internal and an external independent test set using misclassification tables. The prediction of the internal data set was successful whereas the prediction of the external independent batch was not optimal. However, the pretreatment variability could explain the misclassifications as well as the batch-to-batch variability. By in the future increasing the number of batches to update the models, it should be possible to better cover the batch-to-batch variability.

REFERENCES

[1]   H.R. Constantino, M.J. Pikal Lyophilization of biopharmaceuticals. Arlington (VA): AAPS Press.   2004.

[2]   M.J. Pikal. Freeze-drying.In:Swarbrick JS, Boylan JC. Encyclopedia of Pharmaceutical Technology. New York: Marcel Dekker, 2002:1807-33.

[3]   National Institute of Allerfy and Infectious Diseases.Types of vaccines. Available at: www.niaid.nih.gov/topics/vaccines/understanding/pages/typesvaccines.aspx. Accessed on September 12, 2012.

[4]   J.G. Aunins, A.L. Lee, D.B. Volkin. Vaccine Production. In: Bronzino JD. The Biomedical Engineering Handbook: 2nd Edition. CRC Press LLC, 2000.

[5]   J. Rexroad, C.M. Wiethoff, L.S. Jones, C.R Middaugh. Lyophilization and the Thermostability of Vaccines. Cell Preservation Technology, 2002;1: 91-104.

[6]   D.T. Brandau, L.S. Jones, C.M. Wiethoff, J. Rexroad, C.R. Middaugh. Thermal stability of vaccines. Journal of Pharmaceutical Sciences, 2003;92: 218-231.

[7]   A. Abdul-Fattah, V. Truong-Le, L.Yee, E. Pan, Y. Ao, D.S. Kalonia, M.J. Pikal. Drying-Induced Variations in Physico-Chemical Properties of Amorphous Pharmaceuticals and Their   Impact on Stability II: Stability of a Vaccine. Pharmaceutical Research, 2007;24: 715-727.

[8]   D.B. Volkin, C.J. Burke, G. Sanyal, C.R. Middaugh. Analysis of vaccine stability. Development in biological standardization, 1996;87: 135-142.

[9]   N.R. Maddux, S.B. Joshi, D.B. Volkin, J.P. Ralston, C.R. Middaugh. Multidimensional methods for the formulation of biopharmaceuticals and vaccines. Journal of Pharmaceutical Sciences, 2011;100: 4171-4197.

[10]   J.J. Hill, E.Y. Shalaev, G.Zografi. Thermodynamic and dynamic factors involved in the stability of native protein structure in amorphous solids in relation to levels of hydration. Journal of Pharmaceutical Science, 2005;94: 1636-1667.

[11] V. Ragoonanan and A. Aksan. Protein stabilization. Transfusion medicine and homeotherapy, 2007;34: 246-252.

[12] L. Chang, M.J. Pikal. Mechanisms of protein stabilization in the solid state. Journal of Pharmaceutical Sciences, 2009;98: 2886-2908.

[13] L. Chang, D. Shepherd, J. Sun, D. Ouellett, K.L. Grant, X.C. Tang, M.J. Pikal. Mechanism of protein stabilization by sugars during freeze-drying and storage: native structure preservation, specific interaction, and/or immobilization in a glassy matrix? Journal of Pharmaceutical Sciences 2005, 94: 1427-1444.

[14] L.M. Crowe and J.H. Crowe. Trehalose and dry dipalmitoylphosphatidylcholine revisited, Biochemica et Biophysica Acta, 1988;946: 193–201.

[15] J.H. Crowe, F.A. Hoekstra, K.H. Nguyen, L.M. Crowe. Is vitrification involved in depression of the phase transition temperature in dry phospholipids? Biochemica et Biophysica Acta, 1996;1280: 187–196.

[16] G. Strauss, P. Schurtenberger, H. Hauser. The interaction of saccharides with lipid bilayer vesicles: stabilization during freeze-thawing and freeze-drying. Biochemica et Biophysica Acta. 1986;858: 169-180.

[17] A.K. Sum, R. Faller R, J.J. de Pablo. Molecular simulation study of phospholipid bilayers and insights of the interactions with disaccharides. Biophysical Journal, 2003;85:2830–2844.

[18] J. Wolfe, G. Bryant. Cellular cryobiology: thermodynamic and mechanical effects. International. Journal of Refrigeration, 2001;24: 438-450.

[19] D.E. Pegg. Principles of cryopreservation. In: Day JG, Stacey GN. Cryopreservation and freeze drying protocols. New Jersey: 2007.

[20] T.R. De Beer, M. Wiggenhorn, R. Veillon, C. Debacq, Y. Mayeresse, B. Moreau, A. Burggraeve, T. Quinten, W. Friess, G. Winter, J.P. Remon, W.R. Baeyens. Importance of using complementary process analyzers for the process monitoring, analysis, and understanding of freeze-drying. Analytical Chemistry, 2009; 15: 7639-7649

[21] T.R. De Beer, P. Vercruysse, A. Burggraeve, T. Quinten, J. Ouyang, X. Zhang, C. Vervaet, J.P. Remon, W.R. Baeyens. In-line and real-time process monitoring of a freeze-drying process using Raman and NIR spectroscopy as complementary process analytical technology (PAT) tools. Journal of Pharmaceutical Sciences, 2009;98: 3430-3446.

[22] S. Pieters, T. De Beer, J.C. Kasper, D. Boulpaep, O. Waszkiewicz, M. Goodarzi, C. Tistaert, W. Friess, J.P. Remon, C. Vervaet, Y. Vander Heyden. Near-Infrared Spectroscopy for In-Line Monitoring of Protein Unfolding and Its Interactions with Lyoprotectants during Freeze-Drying. Analytical Chemistry, 2012;84: 947-955

[23] I.R. Last, K.A. Prebble. Suitability of near-infrared methods for the determination of moisture in a freeze-dried injection product containing different amounts of the active ingredient. Journal of Pharmaceutical and Biomedical analysis, 1993;11: 1071-1076.

[24] M.S. Kamat, R.A. Lodder, P.P. DeLuca. Near-infrared spectroscopic determination of residual moisture in lyophilized sucrose through intact glass vials. Pharmaceutical Research, 1989;6: 961-965.

[25] J.A. Jones, I.R. Last, B.F. MacDonald, K.A. Prebble. Development and transferability of near-infrared methods for determination of moisture in a freeze-dried injection product. Journal of Pharmaceutical and Biomedical analysis, 1993;11: 1227-1231.

[26] M. Savage, J. Torres, L. Franks, B. Masecar, J. Hotta. Determination of adequate moisture content for efficient dry-heat viral inactivation in lyophilized factor VIII by loss on drying and by near infrared spectroscopy. Biologicals, 1998;26: 119-124.

[27] M. Brülls, S. Folestad, A. Sparén, A. Rasmuson. In-situ near-infrared spectroscopy monitoring of the lyophilization process. Pharmaceutical Research, 2003;20: 494-499.

[28] D. Christensen , M. Allesø, I. Rosenkrands, J. Rantanen, C. Foged, E.M. Agger, P. Andersen, H.M. Nielsen. NIR transmission spectroscopy for rapid determination of lipid and lyoprotector content liposomal vaccine adjuvant system CAF01. European journal of Pharmaceutics and Biopharmaceutics. 2008;70: 914-920.

[29] Y. Liu, R.K. Cho, K. Sakuri, T. Miura, Y. Ozaki. Studies on Spectra-Structure Correlations in Near-Infrared Spectra of Proteins and Polypeptides. A Marker Band for Hydrogen-Bonds. Applied Spectroscopy, 1994;48: 1249-1254.

[30] K. Murayama, Y. Ozaki. Two-dimensional near-IR correlation spectroscopy study of molten globule-like state of ovalbumin in acidic pH region: simultaneous changes in hydration and secondary structure. Biopolymers, 2002;67: 394-405

[31] H. Oldenhof, W.F. Wolkers, F. Fonseca, S. Passot, M. Marin. Effect of sucrose and maltodextrin on the physical properties and survival of air-dried Lactobacillus bulgaricus: an in situ fourier transform infrared spectroscopy study. Biotechnology Progress, 2005;21: 885-892.

[32] L. Zhang, M.J. Henson, S.S. Sekulic. Multivariate data analysis for Raman imaging of a model pharmaceutical tablet. Analytica Chimica Acta, 2005;545: 262-278.

[33] A. de Juan, R. Tauler. Chemometrics applied to unravel multicomponent processes and mixtures: Revisiting latest trends in multivariate resolution. Analytica Chimica Acta, 2003;500: 195-210.

[34] L. Eriksson, E. Johansson, N. Kettaneh-Wold, J. Trygg, C. Wikström, S. Wold. Multi- and Megavariate Data Analysis. Part I: Basic Principles and Applications. Umea: Umetrics, 2006.

[35] K. Kjeldahl and R. Bro. Some common misunderstandings in chemometrics. Journal of Chemometrics, 2010;24: 558-564.

[36] G.X. Zhou, Z. Ge, J. Dorwart, B. Izzo, J. Kukura, G. Bicker, J. Wyvratt. Determination and differentiation of surface and bound water in drug substances by near infrared spectroscopy. Journal of Pharmaceutical Sciences, 2003;92: 1058-1065.

[37] M.J. Pikal, S. Shah. Moisture transfer from stopper to product and resulting stability implications. Development in biological standardization, 1991;74: 165-179.

[38] J.A. Westerhuis, H.C.J. Hoefsloot, S. Smit, D.J. Vis, A.K. Smilde, E.J.J van Velzen, J.P.M. van Duijnhoven, F.A. van Dorsten. Assessment of PLSDA cross validation. Metabolomics, 2008;4: 81-89.

[39] S. Mazzara, S. Cerutti, S. Iannaccone, A. Conti, S. Olivieri, M. Alessio, L. Pattini. Application of Multivariate Data Analysis for the Classification of Two Dimensional Gel Images in Neuroproteomics. Proteomics & Bioinformatics, 2011;4: 16-21.

[40] L. Eriksson, J. Jaworska, A.P. Worth, M.T.D. Cronin, R.M. McDowell, P. Gramatica. Methods for reliability and uncertainty assessment and for applicability evaluations of classification- and regression-based QSARs. Environmental Health Perspectives, 2003;111: 1361-1375.

[41] Cardillo G. Dunn's Test: a procedure for multiple, not parametric comparisons. 2006, http://www.mathworks.com/matlabcentral/fileexchange/12827

CHAPTER 6

FTIR SPECTROSCOPY FOR THE DETECTION AND EVALUATION OF LIVE ATTENUATED VIRUSES IN FREEZE-DRIED VACCINE FORMULATIONS

137

ABSTRACT

This chapter examines the applicability of Fourier Transform Infrared (FTIR) spectroscopy to detect the applied virus medium volume (i.e., during sample filling), to evaluate the virus state and to distinguish between different vaccine doses in a freeze-dried live, attenuated vaccine formulation. Therefore, different formulations were freeze-dried after preparing them with different virus medium volumes (i.e., 30µl, 100µl and 400µl) or after applying different pre-freeze-drying sample treatments (resulting in different virus states); i.e., (i) as done for the commercial formulation; (ii) samples without virus medium (placebo); (iii) samples with virus medium but free from antigen; (iv) concentrated samples obtained via a centrifugal filter device; and (v) samples stressed by 96h exposure to room temperature; or by using different doses (placebo, 25-dose vials, 50-dose vials and 125-dose vials). Each freeze-dried product was measured directly after freeze-drying with FTIR spectroscopy. The collected spectra were analyzed using principal component analysis (PCA) and evaluated at three spectral regions which might provide information on the coated proteins of freeze-dried live, attenuated viruses: (i) 1700-1600cm^{-1} (amide I band), 1600-1500cm^{-1} (amide II band) and 1200-1350cm^{-1} (amide III band). The latter spectral band does not overlap with water signals and is hence not influenced by residual moisture in the samples. It was proven that FTIR could distinguish between the freeze-dried samples prepared using different virus medium volumes, containing different doses and using different pre-freeze-drying sample treatments in the amide III region.

138

CHAPTER 6

FTIR SPECTROSCOPY FOR THE DETECTION AND EVALUATION OF LIVE ATTENUATED VIRUSES IN FREEZE-DRIED VACCINE FORMULATIONS

6.1. INTRODUCTION

Live, attenuated viruses are used in many vaccines because of the strong immune response they generate [1]. However, their potency is severely compromised by their low stability in aqueous solutions. To overcome this, most live, attenuated virus formulations are freeze-dried [2].

After freeze-drying, the potency of live, attenuated viruses measured by titration is generally evaluated in a few randomly collected samples by assays measuring their biological response *in vitro* (i.e., cell-based assays). These tests are often considered imprecise, labor-intensive and time-consuming [3-5].

Near infrared (NIR) and Raman spectroscopy are frequently used as non-invasive, non-destructive and fast analytical techniques for pharmaceutical products [6-8]. One of the first freeze-drying related applications of NIR spectroscopy was the determination of residual moisture content in the end products (i.e., through the glass vials) [9-12]. Afterwards, NIR and Raman in-process monitoring of excipient [13-15] and protein [16] behaviour during freeze-drying was performed.

Recently, also the possibility of NIR spectroscopy to evaluate live, attenuated virus vaccine formulations has been examined [17]. For a freeze-dried live, attenuated virus vaccine formulation, NIR spectroscopy was able to distinguish between samples prepared using different virus medium volumes or using different pre-freeze-drying treatments. This

distinction could be made by evaluating two NIR spectral regions: (i) the 7300-4000cm^{-1} region containing the amide A/II band which might reflect information on the coated proteins of the freeze-dried live, attenuated viruses; and (ii) the C-H vibration overtone regions (10,000-7500 and 6340-5500cm^{-1}) which might supply information on the lipid layer surrounding the freeze-dried live, attenuated viruses.

Fourier transform infrared (FTIR) spectroscopy is a reference technique frequently used to obtain information about the secondary structure of proteins [18]. The amide I and amide II bands are two characteristic bands for proteins and polypeptides. Both arise from the amide bonds linking the different amino acids. The amide I (~ 1650cm^{-1}) is associated to stretching vibrations of the C=O bond of the amide with minor contributions from the out-of-phase CN stretching vibration, whereas the amide II (~ 1550cm^{-1}) is associated to bending vibrations of the N-H bond and stretching vibrations of the C-N bond [18]. Since both, the C=O and N-H bonds, are involved in the hydrogen bonds responsible for the protein secondary structure, frequency shifts of these amide I and II bands are associated to protein secondary structure changes. The amide III band (1400 to 1200cm^{-1}) is the combination of the N-H bending and the C-N stretching vibration [18, 19]. The amide III is also influenced by side-chain vibrations that vary considerably making this band less suited for secondary structure analysis [18]. However, in contrast to the amide I and II bands the amide III band offers the advantage not to show overlap with water signals, which is important when analyzing freeze-dried samples [20-22].

Several studies have evaluated freeze-dried proteins secondary structure [16, 23-25] and bacteria (lactic acid bacteria protein secondary structure and lipid CH_2 vibration) [26] using FTIR spectroscopy. However, to our best knowledge, there is no paper demonstrating the possibility of FTIR spectroscopy to evaluate live, attenuated viruses in freeze-dried formulations.

The selection rule for molecules to be FTIR and NIR active is identical, being a change in dipole moment during their normal modes. However, FTIR spectroscopy mainly measures the fundamental vibrations of molecules, whereas NIR spectroscopy mainly measures overtones and combinations of fundamental vibrations. Overtones and combinations bands have a lower intensity than fundamental bands, resulting in detection sensitivity differences

at low levels of analyte (FTIR being more sensitive). Because of the anharmonicity of the atomic vibrations, the NIR bands related to particular functional groups of an analyte are often broad and overlapping [27] making their analysis complex and requiring chemometrics.

The aim of this study was to examine the suitability of FTIR spectroscopy to evaluate live, attenuated viruses in freeze-dried vaccine formulations. Two different formulations provided by a pharmaceutical company were studied. Being available in large quantities, product 1 was freeze-dried after preparing it with different virus medium volumes (i.e., 30µl, 100µl and 400µl) or after applying different pre-freeze-drying sample treatments (resulting in different virus states); i.e., (i) as done for the commercial formulation; (ii) samples without virus medium (placebo); (iii) samples with virus medium but free from antigen; (iv) concentrated samples obtained via a centrifugal filter device; and (v) samples stressed by 96h exposure to room temperature. Product 2, containing another live attenuated virus, was provided by the company in its freeze-dried form. These freeze-dried samples varied in the number of viral particles present in the virus medium, resulting in different multidose vials (i.e., placebo, 25-dose vials, 50-dose vials and 125-dose vials).

6.2. MATERIALS AND METHODS

6.2.1. Materials

The live, attenuated viral vaccines were provided by Zoetis.

Trehalose (Cargill, Krefeld, Germany), a well-known cryo-/lyoprotectant used in many freeze-dried formulations, was used as stabilizer at a concentration of 9% (w/v) in product 1.

To study the capability of FTIR spectroscopy to evaluate the virus state, live, attenuated viruses were differently pre-treated (Table 6.1b). Depending on the applied pre-freeze-drying-treatment (further termed 'pretreatment'), the virus quality, integrity or state might vary. The resulting formulations were named after their pretreatment: 'normal' (i.e., as used in the commercial formulations,), 'absent' (i.e., placebo formulations without virus medium), 'concentrated' via a centrifugal filter device (Millipore, Amicon® Ultra), 'medium' (i.e.,

placebo formulations where virus medium without viruses was used) and 'stressed' (by storage at room temperature for 96hours). For clarity, the 'concentrated' virus samples were prepared using a similar virus culture medium volume as the 'normal' virus samples. However due to the centrifugation pretreatment process, the 'concentrated' samples contain more viral particles in that volume. The other formulation components (stabilizers and buffer) were kept constant (Table 6.1b).

Besides investigating whether FT-IR is able to evaluate the differently pretreated viruses, its ability to detect differences in added virus culture medium volume was studied as well. Three virus formulations varying in virus medium volume were prepared (Table 6.1a). Stabilizer and buffer were kept constant (concentration and volume).

Table 6.1: Product 1: Formulations used in the (a) virus volume study and (b) virus pretreatment study.

	Virus pretreatment	Virus medium containing viruses (µl)	Medium without viruses (µl)	Buffer (µl)	Trehalose	*qsp* filling volume (µl)	Total volume (µl)
a	Normal	30	0	y	9% w/v	i + 370	800
	Normal	100	0	y	9% w/v	i + 300	800
	Normal	400	0	y	9% w/v	i + 0	800
b	Normal	x	0	y	9% w/v	j	800
	Stressed	x	0	y	9% w/v	j	800
	Concentrated	x	0	y	9% w/v	j	800
	Medium	0	x	y	9% w/v	j	800
	Absent	0	0	y	9% w/v	j + x	800

All symbols (x, y, i and j) represent absolute values in µl.

The stabilizer of product 2, containing another live, attenuated virus, is more complex as it contains several components. Three formulations containing different doses (125, 50 and 25 doses) and one placebo formulation were prepared and freeze-dried by Zoetis (Table 6.2).

Table 6.2: Product 2: Dose study

Virus pretreatment	Doses	Virus medium volume (ml)	Stabilizer solution	*qsp* filling volume, medium free from viruses (ml)	Total volume (ml)
Normal	125	e	33% (v/v)	h-e	5
Normal	50	f	33% (v/v)	h-f	5
Normal	25	g	33% (v/v)	h-g	5
Absent	0	0	33% (v/v)	h	5

All symbols (e, f, g and h) represent absolute values in ml.

An overview of all formulations used in this study is presented in Figure 6.1.
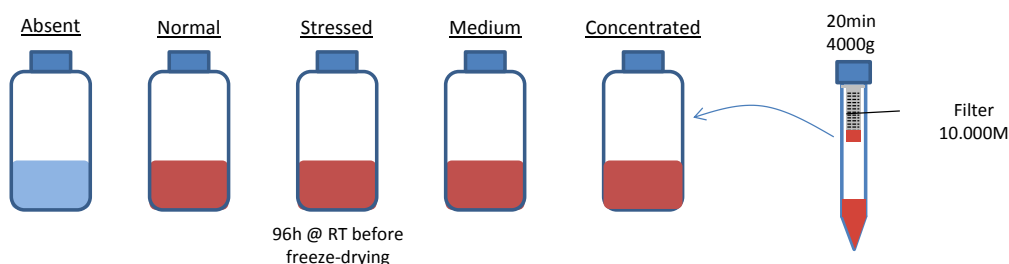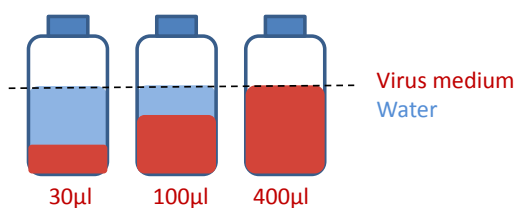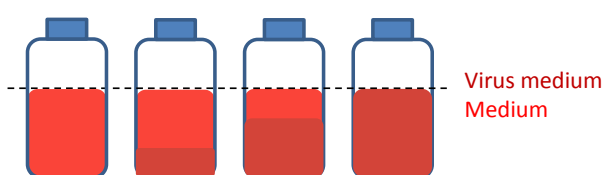
Figure 6.1: Overview of the formulations used in the (a) virus pretreatment study (b) virus volume study and (c) virus dose study.

6.2.2. Freeze-Drying

Product 1 was freeze-dried using an Amsco FINN-AQUA GT4 freeze-dryer (GEA, Köln, Germany).

A conservative cycle resulting in elegant cakes, without any signs of collapse, was used (The process settings can't be disclosed for confidentiality reasons). All product 1 formulations (virus volume study and virus pretreatment study) were freeze-dried together.

Product 2 was freeze-dried using a Lyostar 3 (SP scientific, Stone Ridge, NY, USA) with a conservative cycle providing elegant cakes without signs of collapse (The process settings can't be disclosed for confidentiality reasons). The different dose formulations and the placebo formulation were freeze-dried together.

6.2.3. FTIR spectroscopy

FTIR spectra were recorded using an ATR FTIR spectrometer (Thermo Fisher Scientific, Nicolet iS5 ATR FT-IR spectrometer). The sample was grinded in the vial and then pressed against a diamond ATR crystal. One spectrum per freeze-dried vial was collected in the 4000 - 550 cm^{-1} spectral range with a resolution of 8 cm^{-1} and averaged over 32 scans.

6.2.4. NIR spectroscopy

 Besides the traditional applied reference method (titration, see further), NIR spectroscopy was also used as additional tool to evaluate the different freeze-dried formulations [17] and to compare with the FT-IR observations. NIR spectra of all freeze-dried samples were collected off-line using a Fourier-Transform NIR spectrometer (Thermo Fisher Scientific, Nicolet Antaris II near-IR analyzer) equipped with an InGaAs detector and a quartz halogen lamp. All NIR spectra were recorded in the 10000-4000cm^{-1} region with a resolution of 8cm^{-1} and averaged over 16 scans. One NIR spectrum per freeze-dried sample (in random order) was collected through the bottom of the glass vial using the integrating sphere device immediately after freeze-drying.

6.2.5. Data analysis

FTIR and NIR spectral data analysis was performed using SIMCA P+ v.13.0.3 (Umetrics, Umeå, Sweden).

Depending on the spectroscopic tool (FTIR or NIR spectroscopy) and analyzed spectral region, different pre-processing methods were applied (Table 6.3). The evaluated spectral regions were selected in order to reflect information about the coated proteins (Haemagglutinin and Neuraminidase) from the freeze-dried live, attenuated viruses (see introduction). Therefore, the three amide bands (amide I, II and III) in the FTIR spectra and the amide A/II band in the NIR spectra were analyzed.

Table 6.3: Analyzed spectral ranges and corresponding applied pre-processing

	Preprocessing	Spectral region	Wavenumbers (cm^{-1})
FTIR spectroscopy	SNV	Amide I	1700-1600
	SNV	Amide II	1600-1500
	SNV	Amide III	1200-1350
	SNV and 2nd derivative (17 Savitzky-Golay points)		
NIR spectroscopy	SNV and 2nd derivative (37 Savitzky-Golay points)		7300-4000

FTIR spectra were analyzed using principal component analysis (PCA), allowing to examine the spectral differences between for instance the different sample types per batch (Table 6.2). PCA produces an orthogonal bilinear data matrix (**D**) decomposition, where principal components (PCs) are obtained in a sequential way to explain maximum variance:

$$D=TP^T + E$$

$$= t_1p'_1 + t_2p'_2 + \ldots + t_Qp'_Q + E$$

Where **T** is the *M x Q* score matrix, **P** is the *N x Q* loading matrix, **E** is the *M x N* model residual matrix, i.e., the residual variation of the data set that it is not captured by the model. Q is the selected number of PCs, each describing a non-correlated source of variation in the data set, and N is the number of collected spectra at M wavelengths [28]. Each principal component consists of two vectors, the score vector **t** and the loading vector **p**. The

score vector contains a score value for each spectrum, and this score value informs how the spectrum is related to the other spectra in that particular component. The loading vector indicates which spectral features in the original spectra are captured by the component studied. These abstract, unique and orthogonal PCs are helpful in deducing the number of different sources of variation present in the data. However, these PCs do not necessarily correspond to the true underlying factors causing the data variation, but are orthogonal linear combinations of them, since each PC is obtained by maximizing the amount of variance it can explain [29].

The number of PC included to describe the model was determined by cross validation. Each PC resulting on an increase of the predictive ability (Q^2) of the model was kept.

The collected NIR spectra were also evaluated using principal component analysis (PCA).

6.2.6. Titration

Titration of product 1 and 2 was done according to Zoetis internal SOPs. Each titer is expressed in $\log_{10}$ CCID$_{50}$ (Cell Culture Infection Dose 50 – Inverse of the highest dilution which produces a cytopathogenic effect in 50% of the cells). Titration provides information about the number of living viral particles contained in each vial. For each study (virus pretreatment, virus volume and virus dose), statistical analysis was performed to evaluate if the titers of different vial populations (e.g. 125-dose, 50 and 25-dose vials or 'stressed virus', 'normal virus' and 'concentrated virus') were significantly different. Minitab® 15.1.1.0 software was used to perform the statistical analysis.

When the titer distribution was normal (evaluated using a Kolmogorov-Smirnov test) and the variance equal (Levene's test) an Anova I test was performed. When the distribution was determined as not normal or when the number of observation in each population was low, a non-parametric Kruskal-Wallis analysis of variance was used. In addition to the Kruskal-Wallis test, in order to determine which population is significantly different from the others, Dunn's test was performed using a Matlab m-file [30] as follow-up test (Matlab 7.12, The Mathworks, Natick, MA).

6.2.7. Karl Fischer

The residual moisture content of freeze-dried samples was determined by Karl Fischer titration. For product 1, a Mettler Toledo V30 volumetric Karl Fischer titrator (Schwerzenbach, Switzerland) with Hydranal® titration solvent from Sigma Chemical Company was used. A known volume of dried methanol was added to the sampled vial, and left to equilibrate for a few minutes. From the solution, a known volume was then removed volumetrically using a syringe and injected into the titration cell. The water content of pure methanol was determined in duplicate prior to the measurement and subtracted from the result.

Product 2 was measured with a Metrohm 860 KF Thermoprep (oven) coupled to a Metrohm 852 Titrando (Herisau, Switzerland).

6.3. RESULTS AND DISCUSSION

The discussion of the results is divided into three parts: (i) virus volume study (Table 6.1a); (ii) virus pretreatment study (Table 6.1b) and (iii) dose study performed using product 2 (Table 6.2).

6.3.1. Virus volume study

To evaluate the ability of FTIR spectroscopy to distinguish between applied live, attenuated virus medium volume in the freeze-dried samples, three formulations were prepared containing 30µl, 100µl and 400µl of virus medium volume, respectively (Table 6.1a). The 30µl virus medium volume vials had a titer of 6.93±0.2 (n=3) which differed significantly from the 400µl virus medium volume vials having a titer of 8.67±0.56 (n=3) (Kruskal-Wallis, $p<0.05$, Figure 6.2). The 100µl virus volume vials had a titer of 7.82±0.21 (n=3) which did not significantly differ from the 30µl and 400µl virus volume samples (Kruskal-Wallis, $p<0.05$, Figure 6.2). Regarding the titration results Figure 6.2(left), a significant difference between all groups of sample was expected. This surprising result obtained via Kruskal-Wallis analysis

(selected because of the small amount of titrated samples), might be due to the fact that this statistical analysis consider the population medians instead of the population means.

The Karl Fischer analysis revealed an increase in residual moisture with increasing virus medium volume. The 30, 100 and 400µl virus medium volume samples had a residual moisture of 1.28%±0.05 (n=3), 1.83%±0.13 (n=3) and 3.68%±0.89 (n=3), respectively (Figure 6.2).
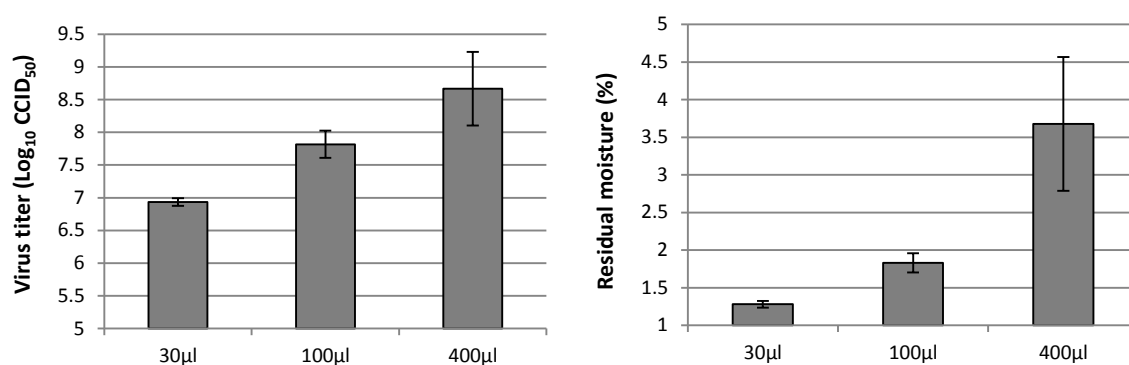
Figure 6.2: (left) Titration results of the different virus medium volume samples. Titers are expressed as $\log_{10}$ $CCID_{50}$ (Cell Culture Infection Dose 50). Each titer is the average of three determinations (Figure 6.2, right). Residual moisture results of the different virus medium volume samples. Each result is the average of three determinations.

After freeze-drying, FTIR spectra of 10 vials per virus medium volume class (i.e., 30 spectra in total) were collected.

As described in the materials and method section, the aim was to evaluate the three amide spectral regions (I, II and III) in the FTIR spectra. Figure 6.3 shows an FTIR spectrum of a freeze-dried product from this virus volume study and the FTIR spectrum of water. The amide I (1700-1600cm^{-1}) and II (1600-1500cm^{-1}) bands clearly overlap with the strong water signal. As the residual moisture varies between the three different virus medium volume sample types (Figure 6.3), the FTIR spectra of the virus volume study were not analyzed in the amide I and II regions. However, since water does not overlap with the amide III region (Figure 6.3), the FTIR spectra of the virus volume study were analyzed using the amide III (1350-1200cm^{-1}) spectral region using PCA.
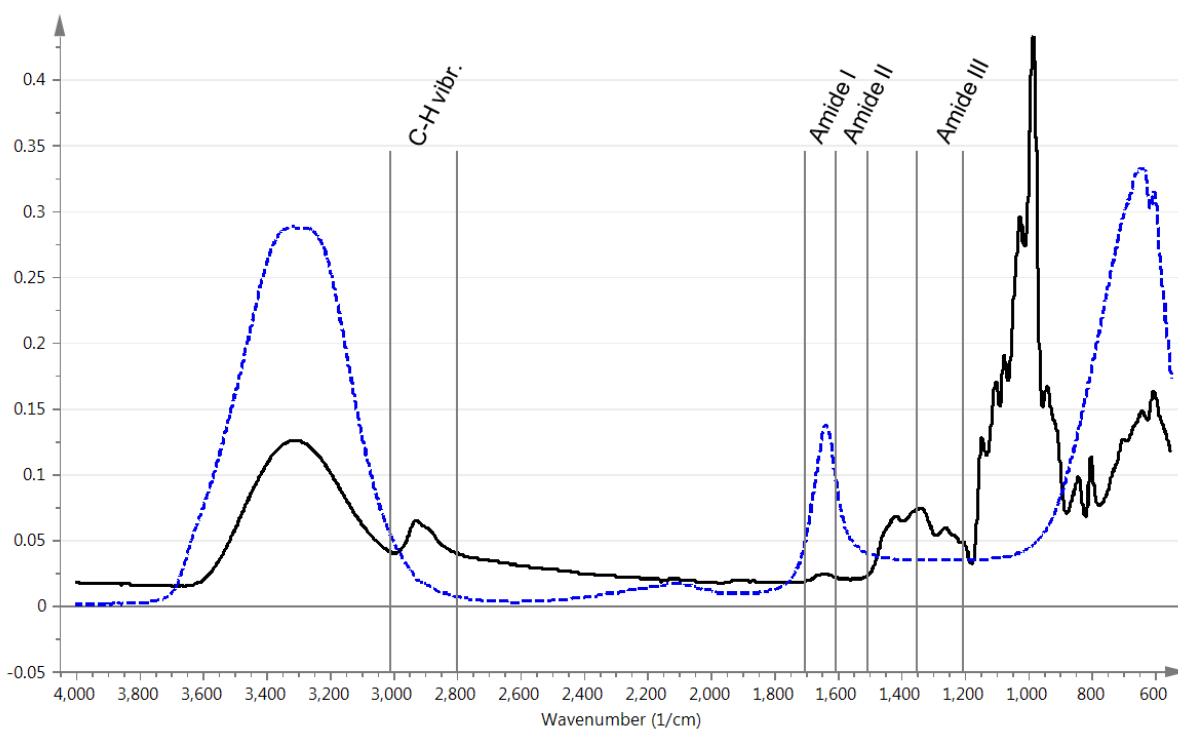
Figure 6.3: Spectra of water (blue dashed line) and a freeze-dried virus volume study sample (black line).

The resulting PCA model (composed of two components) described 99.6% of the spectral variability. The first PC explained almost all the spectral variability (99.3%) and distinguished the samples according their virus medium content (Figure 6.4a). The distances in the scores plot between the virus medium volume groups were in agreement with the differences in virus medium content. Analysis of the loadings of the first principal component revealed one major peak at 1290cm^{-1} (Figure 6.4b). This peak is located in a spectral range (1300-1270cm^{-1}) typical for α-helix [19]. Analysis of the SNV corrected spectra (Figure 6.4c) clearly showed a difference in peak intensity between the three virus medium volumes and confirmed the observation of the scores and loadings plots.
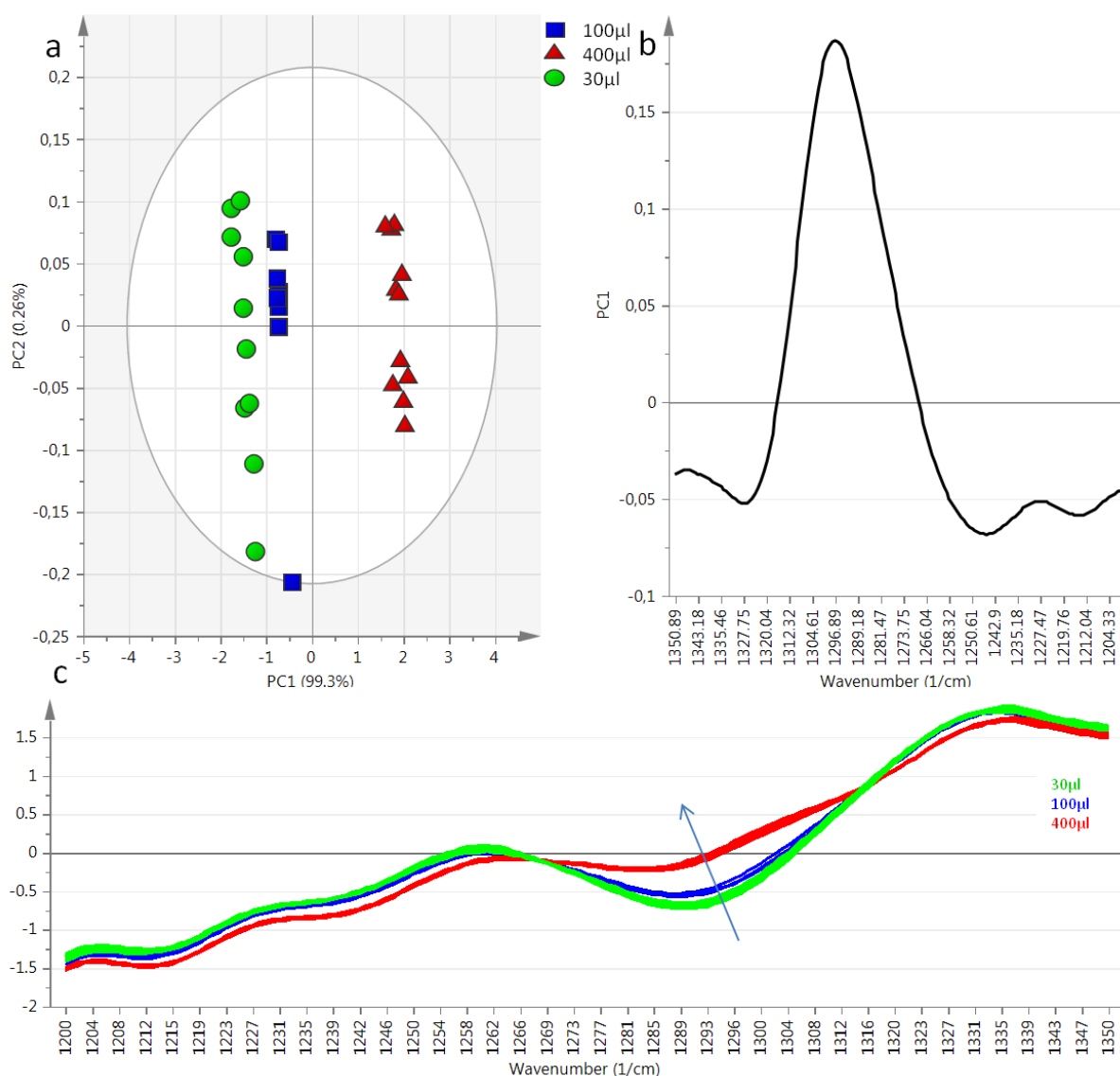
Figure 6.4: Scores (a) and loadings (b) plots obtained after PCA on the FTIR spectra (1200-1350cm^{-1} spectral region) from the virus volume samples 30, 100 and 400μl. (c) SNV corrected FTIR spectra of the 1200-1350cm^{-1} spectral region (the arrow indicates the positive direction of PC1).

The scores plot of the FTIR PCA models allowed the distinction of the three different virus volumes (30μl, 100μl and 400μl).

To confirm this FTIR analysis, also NIR spectra of twenty vials per virus medium volume class were collected and analyzed using the 7300-4000cm^{-1} spectral region (after SNV and 2nd derivative preprocessing), as demonstrated in our previous study [17]. The PCA model (composed of two components) developed from the 60 spectra, described 84.3% of the spectral variability. The PC1 versus PC2 scores plot showed that the first PC (explaining

63.8% of the spectral variability) distinguished the samples according to their virus medium volume (Figure 6.5a). Similarly as previously described in [17], analysis of the PC1 loadings plot revealed two major contributions: the water bands (~7000 and ~5200cm^{-1}) and the amide A/II band (4850cm^{-1}) (Figure 6.5b).
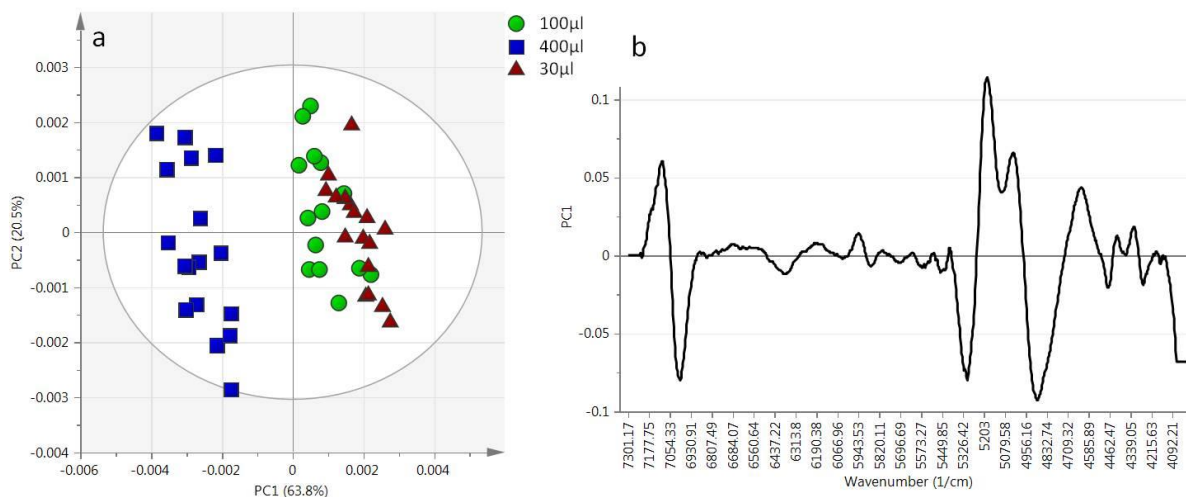
Figure 6.5: Scores (a) and loadings plots (b) obtained after PCA on the NIR spectra from the samples 30, 100 and 400µl using the 7300-4000cm^{-1} spectral region.

To avoid the contribution of the water bands on the principal component analysis of the NIR spectra, a new PCA model was built for the 5029-4000cm^{-1} spectral range. The new two component PCA model explained 76.4% of the spectral variance and also distinguished between the different virus volumes (data not shown).

These results described above confirm that FTIR spectroscopy is able to distinguish between different virus medium volumes in the freeze-dried formulations. Analysis of the loadings plot has shown that this distinction was caused by a difference in α-helix between the different virus medium volumes. The variation of this protein secondary structure between the different virus medium volumes was not detected with NIR spectroscopy. To avoid the impact of the residual moisture variation on the virus volume determination, the amide III spectral region should be used, since this spectral band does not overlap with water bands.

6.3.2. Virus pretreatment study

To evaluate the ability of FTIR spectroscopy to distinguish between differently pre-freeze-drying treated live, attenuated virus samples, five formulations were prepared as overviewed in Table 6.1b. The three formulations containing viruses were titrated. The 'stressed virus' samples had a titer of 6.12±0.1 (n=3) which significantly differed from the 'concentrated virus' samples having a titer of 7.72±0.06 (n=3) (Kruskal-Wallis, $p < 0.05$, Figure 6.6 left). The 'normal virus' samples had a titer of 6.93±0.2 (n=3) which did not significantly differ from the 'stressed' and 'concentrated' virus samples. A significant titer difference between all groups of sample was expected. The analysis of the population medians performed by the Kruskal-Wallis procedure might explain this surprising statistical results.

Karl Fischer analysis revealed no significant difference in residual moisture between the different pre-treated samples. The normal, stressed, concentrated, absent and medium had a residual moisture of 1.28±0.05 (n=3), 1.26±0.18 (n=3), 1.42±0.1 (n=3), 1.19±0.11 (n=3) and 1.30±0.2 (n=3), respectively (Figure 6.6 right).
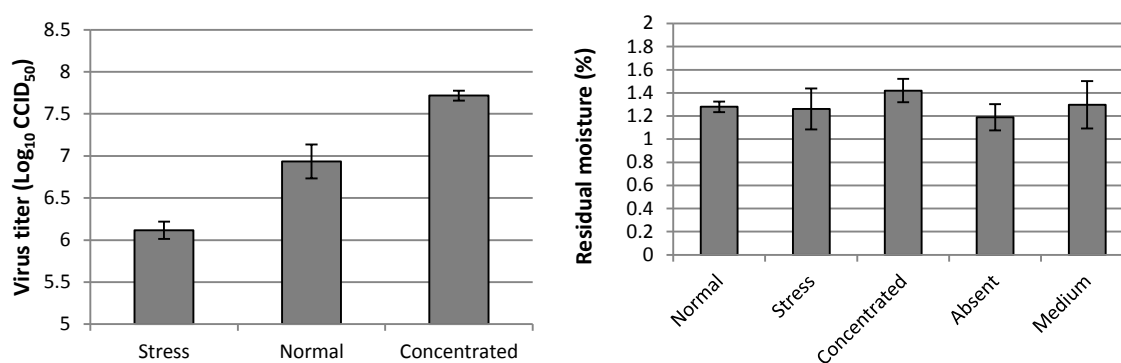
Figure 6.6: Titration results of the different pre-treated samples (left). Titers are expressed as $\log_{10}$ $CCID_{50}$ (Cell Culture Infection Dose 50). Each titer is the average of three determinations. Residual moisture results of the different pretreated virus samples (right). Each result is the average of three determinations.

After freeze-drying, ten FTIR spectra per pretreatment group (i.e., 50 spectra in total) were collected. Because the residual moisture was not significantly different between the different pretreatment groups, the FTIR spectra were analyzed using PCA for different

spectral ranges, i.e., the 1700-1600cm^{-1} (amide I band), the 1600-1500cm^{-1} (amide II band) and the 1200-1350cm^{-1} (amide III band). According to the titration results, only two groups containing viruses have significantly different titers, being the 'stressed' and 'concentrated' samples. Therefore, PCA models were first built using the spectra of these both groups.

6.3.2.1. Spectral region 1700-1600cm^{-1}, amide I band

The PCA model (composed of three principal components) developed from the 20 FTIR spectra of the 'stressed' and 'concentrated' samples described 95% of the overall spectral variability. It was not possible to distinguish between concentrated and stressed samples using the amide I band (data not shown).

6.3.2.2. Spectral region 1600-1500cm^{-1}, amide II band

The PCA model (composed of five principal components) developed using the 20 spectra described 99.2% of the spectral variability. Using the amide II band, it was also not possible to distinguish between concentrated and stressed samples (data not shown).

6.3.2.3. Spectral region 1200-1350cm^{-1}, amide III band

The PCA model (composed of four principal components) developed using the 20 spectra (from the 'stressed' and 'concentrated' samples) described 95.3% of the overall spectral variability. The first principal component (capturing 68.7% of the spectral variability) was able to distinguish between both groups (stressed and concentrated) (Figure 6.7a). Analysis of the loadings plot revealed a broad peak at 1290cm^{-1} (α-helical structure) responsible for the grouping according virus pretreatment (Figure 6.7b).
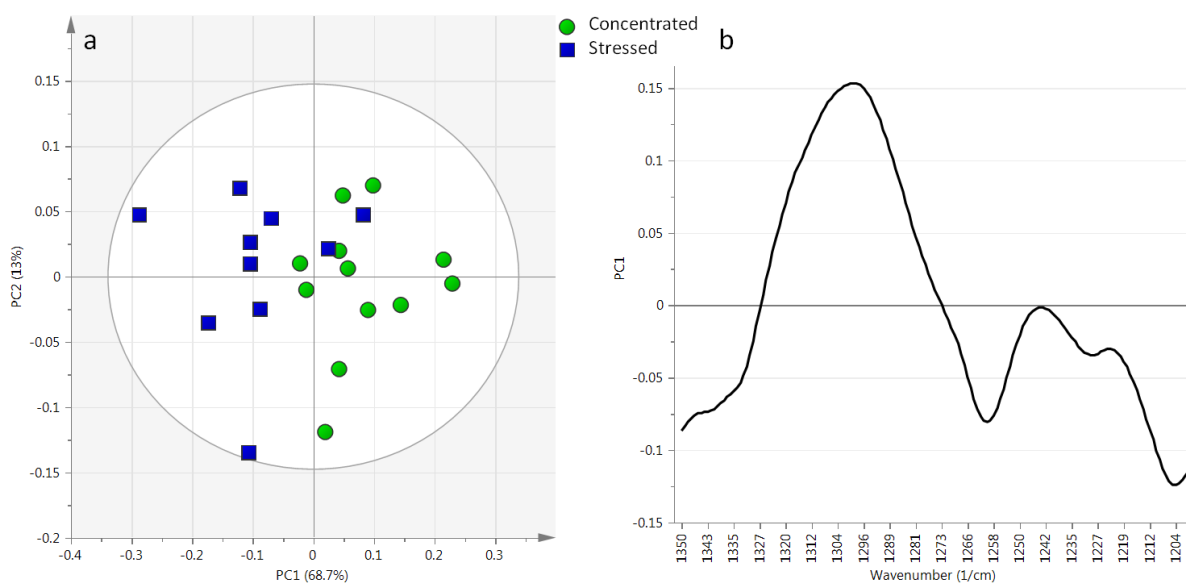
Figure 6.7: Scores (a) and loadings plots (b) obtained after PCA of the FTIR spectra from the concentrated and stressed samples using the 1350-1200cm^{-1} spectral region.

Besides FTIR, NIR spectra of 40 vials (20 stressed and 20 concentrated pretreated samples) were also collected and analyzed using the 7300-4000cm^{-1} spectral region [17] to confirm the FTIR findings. The two component PCA model developed from these 40 spectra described 75.8% of the overall spectral variability. The PC1 versus PC2 scores plot showed that the first PC (explaining 45.9% of the spectral variability) and the second PC (explaining 29.9% of the spectral variability) allowed distinguishing the samples according their pretreatment (Figure 6.8).
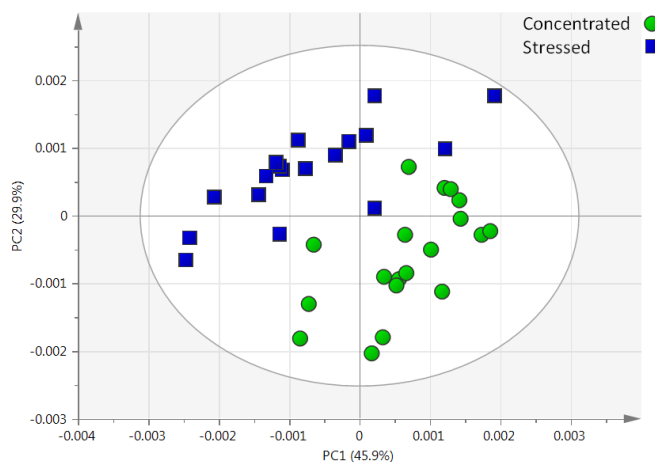
Figure 6.8: Scores plot obtained after PCA on the NIR spectra collected from the stressed and concentrated pre-treated samples using the 7300-4000cm^{-1} spectral region.

In addition to the evaluation of 'stressed' and 'concentrated' pretreated samples, characterized by a significantly different virus titer, the class 'medium' was also studied. This class was interesting to analyze since the only difference between these samples and the other pretreated samples (i.e., 'normal', 'stressed' and 'concentrated') is the absence of virus particle in the vials (Table 6.1b).

Using the amide III spectral range, different PCA models were built using: (i) the FTIR spectra from the 'normal' and 'medium' samples, (ii) the FTIR spectra from the 'concentrated' and 'medium' samples and (iii) the FTIR spectra from the 'stressed' and 'medium' samples (Figure 6.9). The first model ('normal' and 'medium' samples) was composed of five PCs describing 98.3% of the spectral variability. The PC1 versus PC2 scores plot distinguished between both groups of samples (Figure 6.9a). The loadings of the first and second principal component are presented in Figure 6.9d. The first principal component distinguished between the spectra by a large peak around $1290cm^{-1}$. The second principal component distinguished between the spectra by a peak at $1315cm^{-1}$. Both peaks are located in a spectral range typical for α-helical structure [21, 22]. A difference between the 'normal' and 'medium' samples in this spectral range was also visible in the SNV and 2nd derived spectra (Figure 6.9e). The second PCA model was built using the 'medium' and 'concentrated' spectra and consisted of five PCs describing 97.2% of the spectral variability. The first principal component (73.3% of the spectral variability) clearly distinguished between the two groups (Figure 6.9b). The PC1 loadings plot revealed one peak at $1290cm^{-1}$ (α-helical structure) (data not shown). The last PCA model ('stressed' and 'medium' samples) was composed of six PCs explaining 97.7% of the spectral variability. Loadings of the second principal component showed different peaks, one located at $1280cm^{-1}$ typical for β-turn [21,22] and another one located at $1233cm^{-1}$ typical for β-sheet [21,22] (data not shown).

155
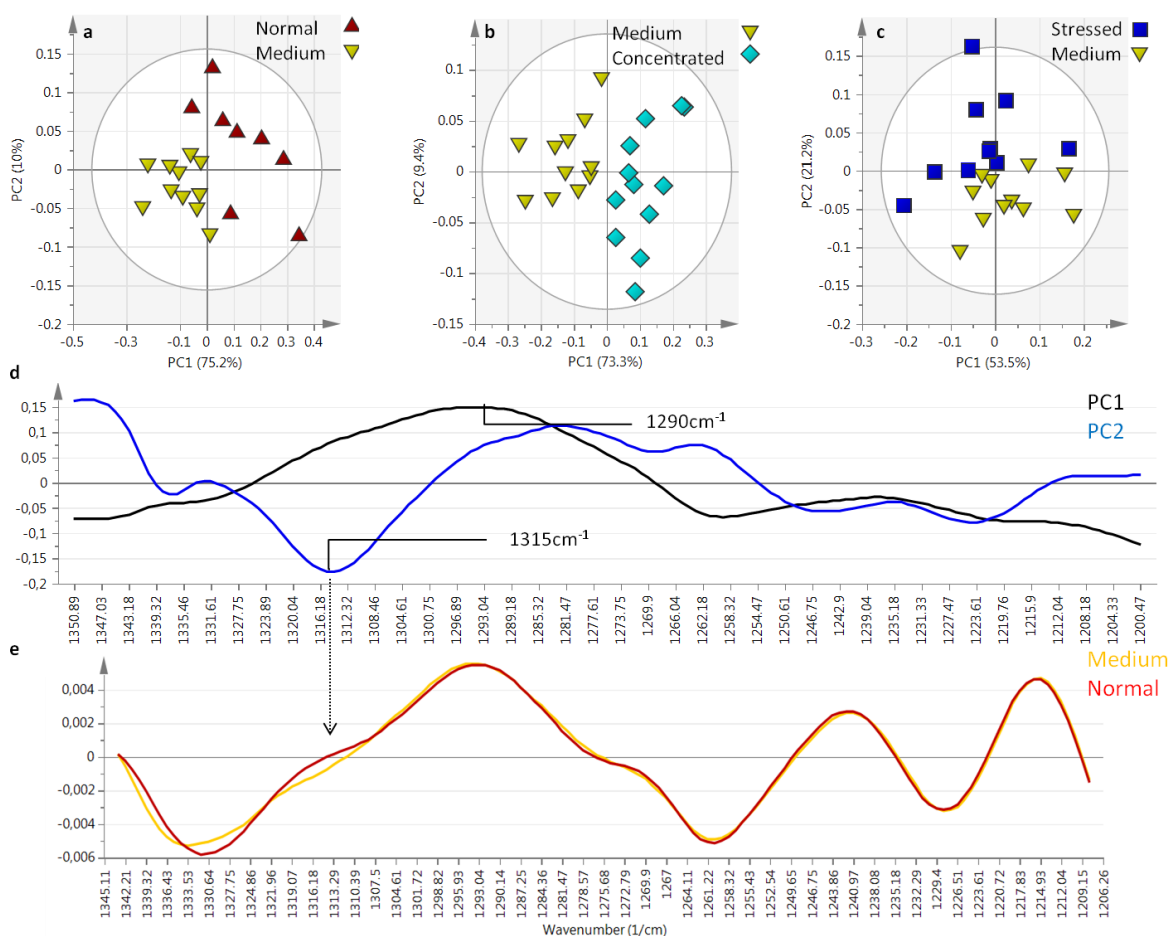
Figure 6.9: Scores plots obtained after PCA using the 1350-1200cm^{-1} (Amide III) spectral region of the FTIR spectra of; a) normal and medium samples, b) concentrated and medium samples, c) stressed and medium samples. The loadings plot of the PCA using normal and medium samples (d) (PC1 black and PC2 blue) and the spectra of the medium (yellow) and normal (red) samples (snv and 2nd derived) (e) are also presented.

These PCA models developed from 'medium' samples containing no viruses on the one hand and the differently pretreated samples on the other hand, allowed distinguishing between the presence and absence of viruses. As can be derived from the loadings plots, one peak around 1290cm^{-1} and typical for α-helical protein secondary structure was involved in the spectral distinction between normal and medium samples as well as concentrated and medium samples. Loadings of the principal component distinguishing between stressed and medium samples showed two different peaks, located at 1280cm^{-1} (β-turn) and at 1233cm^{-1} (β-sheet).

6.3.3. Virus dose study

In this part of the study, the ability of FTIR spectroscopy to detect another live, attenuated virus as well as to distinguish between vaccines containing different doses was evaluated.

The three formulations, different in virus dose (Table 6.2), were titrated. The 125 doses samples had a titer of 5.09 ± 0.16 (n=8), the 50 doses samples had a titer of 4.73 ± 0.08 (n=8) and the 25 doses had a titer of 4.41 ± 0.18 (n=8). These titers were significantly different (Anova I, $p<0.05$, Figure 6.10 left).

Unlike the virus volume study, Karl Fischer analysis revealed no significant difference in residual moisture between the different dose samples. The 125, 50, 25 and placebo samples had a residual moisture of 1.44 ± 0.33 (n=3), 1.31 ± 0.16 (n=3), 1.44 ± 0.21 (n=3), and 1.36 ± 0.07 (n=3), respectively (Figure 6.10, right).
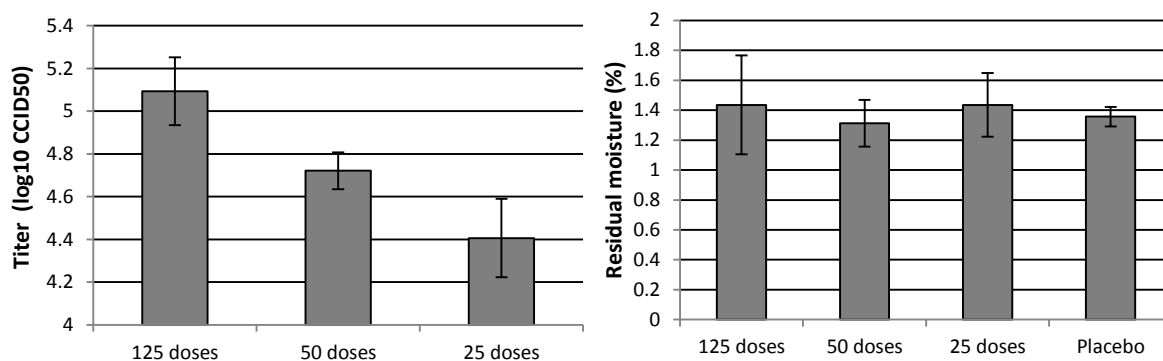
Figure 6.10: Titration results of the different dose samples (left). Titers are expressed as $\log_{10}$ $CCID_{50}$ (Cell Culture Infection Dose 50). Each titer is the average of eight determinations. Residual moisture results of the different pre-freeze-drying treated virus samples (right) (n = 3).

After freeze-drying, ten FTIR spectra per dose group and five FTIR spectra of the placebo group (i.e., 35 spectra in total) were collected. The FTIR spectra, SNV preprocessed, were analyzed using PCA applying different spectral ranges, i.e., the 1700-1600cm^{-1} (amide I band), the 1600-1500cm^{-1} (amide II band) and the 1200-1350cm^{-1} (amide III band).

6.3.3.1. Spectral region 1700-1600cm^{-1}, amide I band

The PCA model (composed of two principal components) developed from the 35 spectra described 97.7% of the overall spectral variability. The first PC capturing 78.2% of spectral

variability distinguished between the samples according to their doses (Figure 6.11a). The distances in the scores plot between the dose groups is in agreement with their actual dose difference. Among the different peaks observed in the PC1 loadings plot (1632 cm^{-1}, 1645 cm^{-1}, 1660 cm^{-1}, 1680 cm^{-1}, 1695cm^{-1}) (Figure 6.11b), the two peaks located at 1632 cm^{-1} and 1645 cm^{-1} also clearly varied in the SNV preprocessed spectra (Figure 6.11c). These two peaks might represent turn/β sheet (1638cm^{-1}) [26] and α-helix (1645cm^{-1}) [26], respectively.

6.3.3.2. Spectral region 1600-1500cm^{-1}, amide II band

The PCA model (composed of three principal components) developed using the 35 spectra described 99.3% of the spectral variability. No PCs combination was able to distinguish between the different doses using the amide II band (data not shown).

6.3.3.3. Spectral region 1200-1350cm^{-1}, amide III band

The PCA model (composed of two components) developed from the 35 spectra using the amide III spectral region described 91.4% of the spectral variability. The first PC explained 63.6% of the spectral variability and distinguished between the samples according to their dose (Figure 6.12a). In contrast to the amide I band, the separation between the different doses was less clear. Nevertheless, the placebo was better separated from the other samples. Analysis of the loadings of the first principal component revealed one major peak at 1290cm^{-1} (Figure 6.12b). This peak is located in a spectral range (1300-1270cm^{-1}) typical for α-helix [19]. Analysis of the SNV corrected spectra (Figure 6.12c) clearly showed a difference in peak intensity between the different doses and confirmed the observation of the scores and loadings plots.
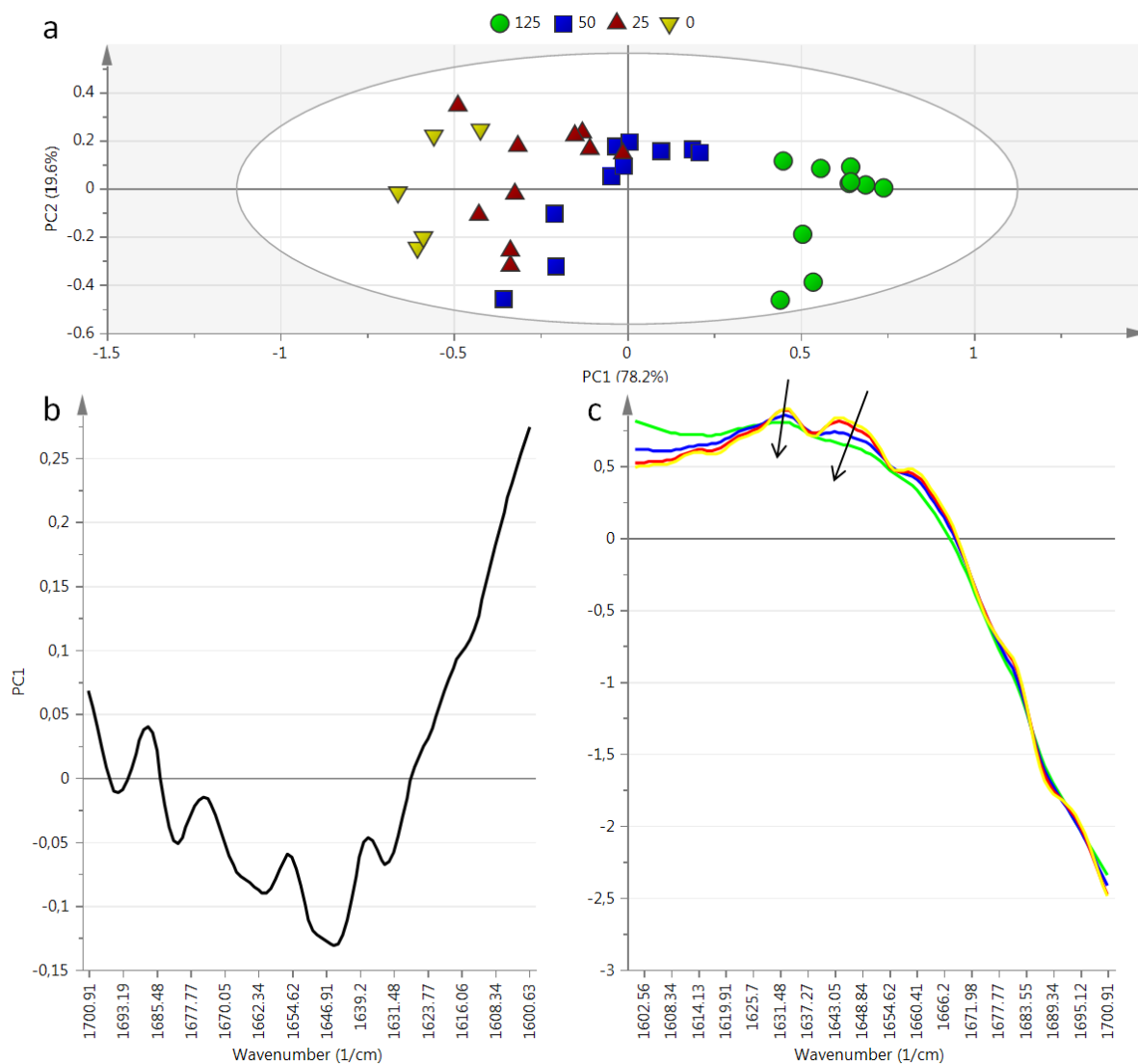
Figure 6.11: PC1 versus PC2 scores (a) and PC1 loadings (b) plots obtained after PCA of the FTIR spectra from the samples 0 (placebo), 25, 50 and 125 doses using the 1600-1700cm^{-1} spectral region. (c) SNV corrected spectra of the 1600-1700cm^{-1} spectral region (the arrow indicates the positive direction of PC1).
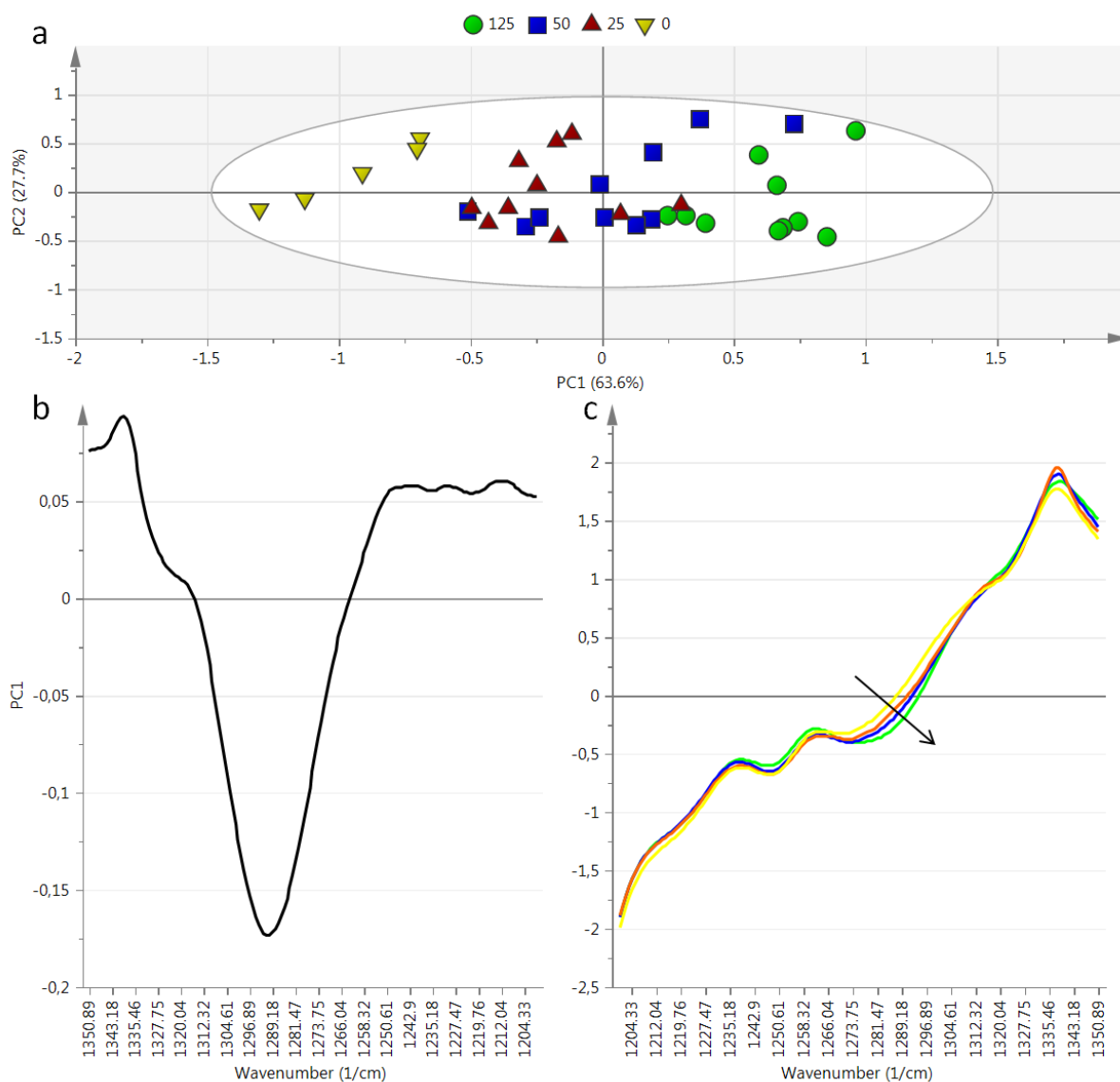
Figure 6.12: PC1 versus PC2 scores (a) and PC1 loadings (b) plots obtained after PCA of the FTIR spectra from the 0, 25, 50 and 125 dose samples using the 1350-1200cm^{-1} spectral region. (c) SNV corrected spectra of the 1350-1200cm^{-1} spectral region (the arrow indicates the positive direction of PC1).

NIR analysis was also performed using the virus dose samples. Spectra from 18 vials per virus dose were collected and analyzed using the 7300-4000 cm^{-1} spectral regions (after SNV and 2nd derivative pre-processing), as demonstrated in [17]. The PCA model (composed of four components) developed from the 72 spectra described 93.3% of the spectral variability. The PC2 (18.2% of the spectral variability) versus PC4 (8.48% of spectral variability) scores plot allowed distinguishing the samples according to their virus dose (Figure 6.13).
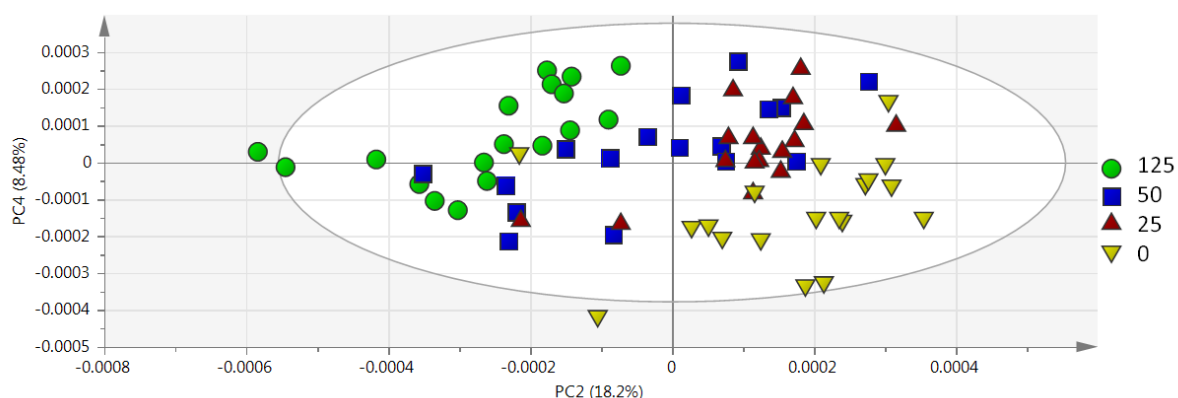
Figure 6.13: Scores plot obtained after PCA on the NIR spectra from the virus dose samples using the 7300-4000cm^{-1} spectral region.

6.4.   CONCLUSION

This study is, to our best knowledge, the first one evaluating and demonstrating the ability of FTIR spectroscopy to detect live, attenuated viruses in a freeze-dried formulation. FTIR was able to distinguish between freeze-dried formulations varying in "virus volume", "virus pretreatment" and "virus dose".

In the virus volume study, the amide III spectral region was used hence avoiding the influence of the residual moisture which was different for the different virus medium volume samples. Using this spectral region, it was possible to distinguish between the different virus medium volume samples.

No residual moisture difference was detected for the samples of the virus pretreatment study. Among the three amide (I, II, III) spectral ranges studied, the amide III spectral range was the most appropriate one to distinguish the different pretreated samples.

Finally, in the virus dose study, the three amide spectral ranges were also compared (as no difference in residual moisture was seen between the different doses). Both, the amide I and III spectral ranges distinguished the samples according to their doses. Using the amide I spectral range, the distance between the different groups in the scores plot was in agreement with the dose content. Using the amide III spectral range, the placebo samples

were better separated from the samples containing doses but the distinction between the different dose samples was less clear.

The presented results demonstrate the ability of FTIR spectroscopy to evaluate live, attenuated viruses in freeze-dried formulations.

REFERENCES

[1] J.G. Aunins, A.L. Lee, D.B. Volkin. Vaccine Production. In: Bronzino JD. The Biomedical Engineering Handbook: 2nd Edition. CRC Press LLC, 2000.

[2] J. Rexroad, C.M. Wiethoff, L.S. Jones, C.R Middaugh. Lyophilization and the Thermostability of Vaccines. Cell Preservation Technology, 2002;1: 91-104.

[3] C.J. Burke, T.A. Hsu, and D.B. Volkin. Formulation, stability, and delivery of live attenuated vaccines for human use. Critical Reviews in Therapeutic Drug Carrier Systems, 1999; 16(1): 1-83.

[4] D.B. Volkin, C.J. Burke, G. Sanyal, C.R. Middaugh. Analysis of vaccine stability. Development in biological standardization, 1996;87: 135-142.

[5] D.T. Brandau, L.S. Jones, C.M. Wiethoff, J. Rexroad, C.R. Middaugh. Thermal stability of vaccines. Journal of Pharmaceutical Sciences, 2003;92: 218-231.

[6] T.R. De Beer, A. Burggraeve, M. Fonteyne, L. Saerens, J.P. Remon, C. Vervaet. Near infrared and Raman spectoscopy for the in-process monitoring of pharmaceutical production porcesses. International Journal of Pharmaceutics, 2011; 417: 32-47.

[7] B. Berry, J. Moretto, T. Matthews, J. Smelko, K. Wiltberger. Cross-scale predictive modeling of CHO cell culture growth and metabolites using Raman spectroscopy and multivariate analysis. Biotechnology Progress, 2015;31(2): 566-577.

[8] H. Mehdizadeh, R. Procopio-Melino, D. Lauri, K.M. Karry, D. Drapeau, M. Moshgbar. Generic Raman-based Calibration Models Enabling Real-time Monitoring of Cell Culture Bioreactors. Biotechnology Progress, 2015; 31(4): 1004-1013.

[9] M.S. Kamat, R.A. Lodder, P.P. DeLuca. Near-infrared spectroscopic determination of residual moisture in lyophilized sucrose through intact glass vials. Pharmaceutical Research, 1989;6: 961-965.

[10] I.R. Last, K.A. Prebble. Suitability of near-infrared methods for the determination of moisture in a freeze-dried injection product containing different amounts of the active ingredient. Journal of Pharmaceutical and Biomedical analysis, 1993;11: 1071-1076.

[11] J.A. Jones, I.R. Last, B.F. MacDonald, K.A. Prebble. Development and transferability of near-infrared methods for determination of moisture in a freeze-dried injection product. Journal of Pharmaceutical and Biomedical analysis, 1993;11: 1227-1231.

[12] M. Savage, J. Torres, L. Franks, B. Masecar, J. Hotta. Determination of adequate moisture content for efficient dry-heat viral inactivation in lyophilized factor VIII by loss on drying and by near infrared spectroscopy. Biologicals, 1998;26: 119-124.

[13] M. Brülls, S. Folestad, A. Sparén, A. Rasmuson. In-situ near-infrared spectroscopy monitoring of the lyophilization process. Pharmaceutical Research, 2003;20:494-499.

[14] T.R. De Beer, M. Wiggenhorn, R. Veillon, C. Debacq, Y. Mayeresse, B. Moreau, A. Burggraeve, T. Quinten, W. Friess, G. Winter, J.P. Remon, W.R. Baeyens. Importance of using complementary process analyzers for the process monitoring, analysis, and understanding of freeze-drying. Analytical Chemistry, 2009; 15: 7639-7649

[15] T.R. De Beer, P. Vercruysse, A. Burggraeve, T. Quinten, J. Ouyang, X. Zhang, C. Vervaet, J.P. Remon, W.R. Baeyens. In-line and real-time process monitoring of a freeze-drying process using Raman and NIR spectroscopy as complementary process analytical technology (PAT) tools. Journal of Pharmaceutical Sciences, 2009;98: 3430-3446.

[16] S. Pieters, T. De Beer, J.C. Kasper, D. Boulpaep, O. Waszkiewicz, M. Goodarzi, C. Tistaert, W. Friess, J.P. Remon, C. Vervaet, Y. Vander Heyden. Near-infrared spectroscopy for in-line monitoring of protein unfolding and its interactions with lyoprotectants during freeze-drying. Analytical Chemistry, 2012;84: 947-955

[17] L. Hansen, S. Pieters, R. Daoussi, J.P. Montenez, C. Vervaet, J.P. Remon, T. De Beer. Near-infrared spectroscopic evaluation of lyophilized viral vaccine formulations. Biotechnology progress, 2013; 29 (6): 1573-1586.

[18] A. Barth, C. Zscherp, What vibrations tell us about proteins. Quarterly Review of Biophysics, 2002; 35: 363-430.

[19] G. Socrates. Infrared and Raman Characteristic Group Frequencies: Tables and Charts (tird ed.) John Wiley and Sons Ltd., UK (2001)

[20] F-N. Fu, D.B. DeOlivera, W. Trumble, H.K. Sarkar, B.R. Singh. Secondary structure estimation of proteins using the amide III region of Fourrier transform infrared spectroscopy: application to analyze calcium-binding-induced structural changes in calsequestrin. Applied Spectroscopy, 1994; 48, 1432-1441.

[21] Cai S, Singh BR. Identification of β-turn and random coil amide III infrared bands for secondary structure estimation of proteins. Biophysical Chemistry, 1999; 80: 7-20.

[22] S. Cai, B.R. Singh. A distinct utility of the Amide III infrared band for secondary structure estimation of Aqueous protein solutions using partial least squares methods. Biochemistry, 2004; 43: 2541-2549.

[23] K.W. Ward, G.D.J Adams, H.O. Alpar, W.J. Irwin. Protection of the enzyme L-asparaginase during lyophilization-a molecular modeling approach to predict required level of lyoprotectant. International journal of Pharmaceutics, 1999; 187: 153-162.

[24] M.J. Maltesen, S. Bjerregaard, L. Hovgaard, S. Havelund, M. van de Weert, H. Grohganz. Multivariate analysis of phenol in feeze-dried and spray-dried insulin formulations by NIR and FTIR. AAPS PharmSciTech, 2011; 12(2): 627-635.

[25] S. Pieters, T. De Beer, J.C. Kasper, D. Boulpaep, O. Waszkiewicz, M. Goodarzi, C. Tistaert, W. Friess, J.P. Remon, C. Vervaet, Y. Vander Heyden. Near-Infrared Spectroscopy for In-Line Monitoring of Protein Unfolding and Its Interactions with Lyoprotectants during Freeze-Drying. Analytical Chemistry, 2012;84: 947-955

[26] H. Oldenhof, W.F. Wolkers, F. Fonseca, S. Passot, M. Marin. Effect of sucrose and maltodextrin on the physical properties and survival of air-dried Lactobacillus bulgaricus: an in situ fourier transform infrared spectroscopy study. Biotechnology Progress, 2005;21: 885-892.

[27] D. Burns, E. Ciurczak. Handbook of Near-infrared Analysis. second ed., Marcel Dekker, Inc., New York, 2001

[28] L. Zhang, M.J. Henson, S.S. Sekulic. Multivariate data analysis for Raman imaging of a model   pharmaceutical tablet. Analytica Chimica Acta, 2005;545: 262-278.

165

[29]   A. de Juan, R. Tauler. Chemometrics applied to unravel multicomponent processes and mixtures: Revisiting latest trends in multivariate resolution. Analytica Chimica Acta, 2003;500: 195-210.

[30]   G. Cardillo. Dunn's Test: a procedure for multiple, not parametric comparisons. 2006, http://www.mathworks.com/matlabcentral/fileexchange/12827

CHAPTER 7

SPECTROSCOPIC EVALUATION OF A FREEZE-DRIED VACCINE DURING AN ACCELERATED STABILITY STUDY

Parts of this chapter are submitted in :

ABSTRACT

This chapter evaluates a freeze-dried live, attenuated virus vaccine during an accelerated stability study using Near Infrared (NIR) and Fourier Transform Infrared (FTIR) spectroscopy in addition to the traditional quality tests (i.e., potency assay, residual moisture analysis) and Modulated Differential Scanning Calorimetry (MDSC). Therefore, freeze-dried live, attenuated virus vaccines were stored during four weeks at 4°C (i.e., recommended storage condition) and at 37°C (i.e., accelerated storage condition) and weekly analyzed using these techniques. The potency assay showed that the virus titer decreased in two phases when the samples were stored at 37°C. The highest titer loss occurred during the first week storage at 37°C after which the degradation rate decreased. Both the residual moisture content and the relaxation enthalpy also increased according to this two-phase pattern during storage at 37°C. In order to evaluate the virus and its interaction with the amorphous stabilizer in the formulation (trehalose), the NIR spectra were analyzed via principal component analysis (PCA) using the amide A/II band (5029-4690cm^{-1}). The FTIR spectra were also analyzed via PCA using the amide III spectral range (1350-1200cm^{-1}). Analysis of the amide A/II band in the NIR spectra revealed that the titer decrease during storage was probably linked to a change of the hydrogen bonds (i.e., interaction) between the virus proteins and the amorphous trehalose. Analyzing the amide III band (FTIR spectra) showed that the virus destabilization was coupled to a decrease of the coated proteins β-turn and an increase of α-helix. During storage at 4°C, the titer remained constant, no enthalpic relaxation was observed and neither the amide A/II band (NIR spectra) nor the amide III band (FTIR spectra) varied.

CHAPTER 7

SPECTROSCOPIC EVALUATION OF A FREEZE-DRIED VACCINE DURING AN ACCELERATED STABILITY STUDY

7.1.   INTRODUCTION

Worldwide, the success of immunization programs is partly dependent on the stability of vaccines [1]. The stability of a vaccine is its ability to retain its chemical, physical, microbiological and biological properties within specified limits throughout its shelf-life [1]. The potency of live, attenuated virus vaccines is severely compromised by their low stability in aqueous solution. Therefore, freeze-drying is often applied to remove the bulk water and improve the vaccine stability during distribution and storage.

Freeze-drying consists of 3 main consecutive steps: freezing, primary drying and secondary drying. During the freezing step, the temperature is decreased to convert most of the water into ice. Herewith, the solutes are crystallized or transformed into an amorphous system. During primary drying, vacuum is introduced in the freeze-drying chamber and the ice is removed by sublimation. The secondary drying step, usually occurring under deep vacuum, ends the process by removing the unfrozen water by desorption [2].

Most often, the stability of freeze-dried vaccines is evaluated in long-term stability studies and under accelerated and stress conditions. Long term stability studies are performed under the conditions (temperature and humidity) specified for the product storage and serve as a base to attribute an expiration date to the product. Accelerated and stress stability testing, under conditions carefully selected on a case-by-case basis, are strongly suggested by the regulatory authorities [3]. Studies under accelerated conditions are performed at higher temperatures than those recommended for storage [1] and are useful to provide product stability information for future development. Furthermore, studies under

accelerated conditions assist in the validation of analytical methods for the stability program, and provide information that may help to understand the degradation profile of the product [3]. Studies under stress conditions, on the other hand, are useful to evaluate whether accidental exposures to conditions other than those intended (such as light and extreme temperature [1]) are detrimental, which is also useful to develop product stability knowledge [3].

The stabilization mechanisms of live, attenuated viruses during freeze-drying and in the dried state (i.e., during storage) are not clearly described in literature and hence elucidated. This lack of information can be attributed to two main reasons: (i) measuring the destabilization mechanisms is complex because of the multiple potential destabilization pathways (such as oxidation, light-catalyzed reaction, change in ionic strength, pH shift due to buffer crystallization and possibly mechanical membrane damage due to ice crystal growth) [4,5], and (ii) the analytical tools allowing the evaluation of live, attenuated viruses during freeze-drying are lacking.

A review describing the current knowledge on the freeze-drying process of live attenuated virus vaccines, the potential destabilization mechanisms occurring during the freezing and the drying steps and the strategies used to protect viruses during freeze-drying has been recently published [6].

Near Infrared (NIR) and Fourier Transform Infrared (FTIR) spectroscopy have been demonstrated to have potential to evaluate freeze-dried live, attenuated viral vaccines [7, 8]. NIR spectroscopy was able to distinguish between samples prepared using different virus medium volumes or using different pre-freeze-drying treatments [7]. This distinction was possible by evaluating two NIR spectral regions: (i) the $7300\text{-}4000\text{cm}^{-1}$ region containing the amide A/II band which might reflect information on the coated proteins of the live, attenuated viruses; and (ii) the C-H vibration overtone regions ($10,000\text{-}7500$ and $6340\text{-}5500\text{cm}^{-1}$) which might supply information about the lipid layer surrounding the live, attenuated viruses.

FTIR spectroscopy was also able to distinguish between lyophilized samples prepared using different virus medium volumes or using different pre-freeze-drying treatments as well as

between samples containing different doses of viruses [8]. Among the three amide bands (i.e., amide I, amide II, amide III) in FTIR spectra, the amide III band (1350-1200cm^{-1}) showed to be the most suitable one for analysis since this band is not influenced by water.

The aim of this chapter is to evaluate freeze-dried live, attenuated virus vaccines during an accelerated stability study using NIR and FTIR spectroscopy. Both spectroscopic tools were used to potentially clarify the observations made using traditional quality tests (i.e., potency assay, residual moisture analysis and modulated differential scanning calorimetry (MDSC)), and to increase the knowledge about the viability decrease of live, attenuated virus vaccines during storage. For this study, freeze-dried samples from a live, attenuated virus vaccine formulation were stored at 4°C (i.e., recommended storage condition) and at 37°C (i.e., accelerated storage condition) during four weeks and weekly evaluated using all analytical techniques described above.

7.2. MATERIALS AND METHODS

7.2.1. Materials

The live, attenuated viruses were provided by Zoetis. Trehalose (Cargill, Krefeld, Germany), a well-known cryo-/lyoprotectant utilized in many freeze-dried formulations, was used as stabilizer at a concentration of 9% (w/v).

7.2.2. Freeze-Drying

The vaccines were freeze-dried using an Amsco FINN-AQUA GT4 freeze-dryer (GEA, Köln, Germany), resulting in elegant cakes, without any signs of collapse (the freeze-drying process settings cannot be disclosed for confidentiality reasons). At the end of the process, the vials were stoppered under inert gas atmosphere and sealed with aluminum crimps.

7.2.3. Study design

Unless explicitly mentioned, the term 'stability study' in this chapter refers to both storage conditions used for the study described in this chapter, i.e., storage at 4°C (i.e., recommended storage conditions) and storage at 37°C (i.e., accelerated storage conditions). The stability study setup is presented in Figure 7.1. After freeze-drying and before starting the stability study (i.e., at time 0, T0), the following measurements were done: NIR and FTIR spectra collection, titration (i.e., viability evaluation), MDSC and Karl Fischer (i.e., residual moisture determination). Afterwards, the stability study started and identical measurements as at T0 were performed weekly during 4 weeks. In addition, during the first week of storage, NIR spectra were collected every day.
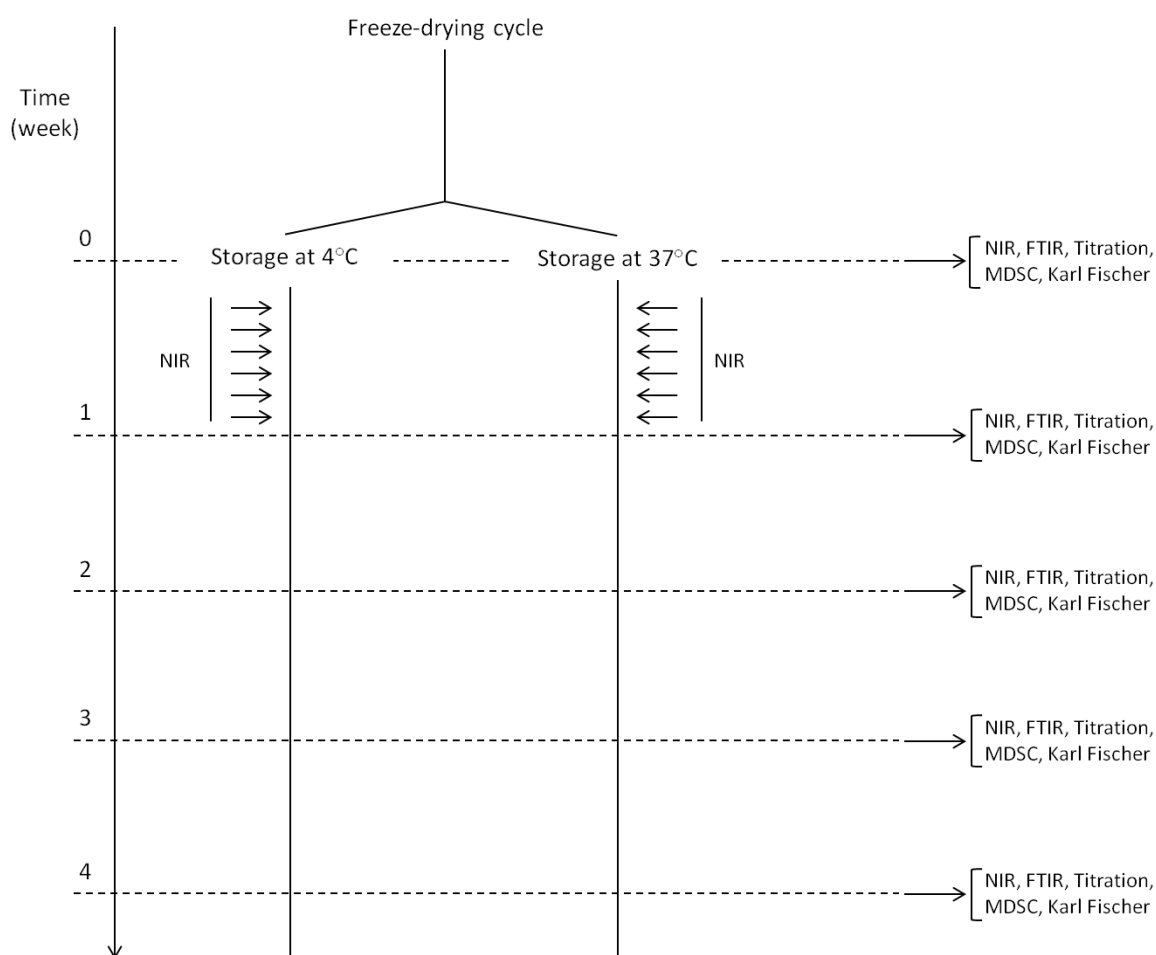
Figure 7.1: Schematic overview of the stability study.

The number of freeze-dried samples (vials) used for each analysis at each time point is presented in Table 7.1. In total, 207 vials were analyzed in this study. In contrast to all other applied analytical techniques, NIR spectroscopy offers the advantage of not requiring sample preparation and being non-destructive, hence allowing to evaluate the same vials throughout the entire study. Twenty vials stored at 4°C and twenty other vials stored at 37°C were hence monitored using NIR spectroscopy during the entire stability study. Every week, five vials were analyzed using FTIR spectroscopy, Karl Fischer and titration while three vials were analyzed via MDSC for both storage temperatures.

Table 7.1: Repartition of the freeze-dried samples used during the stability study.

Storage time	NIR[a]		FTIR		MDSC		Karl Fischer		Titration	
	4°C	37°C	4°C	37°C	4°C	37°C	4°C	37°C	4°C	37°C
0	20	20	5		3		5		10	
1day - 6days	20	20	NA	NA	NA	NA	NA	NA	NA	NA
1 week	20	20	5	5	3	3	5	5	5	5
2 weeks	20	20	5	5	3	3	5	5	5	5
3 weeks	20	20	5	5	3	3	5	5	5	5
4 weeks	20	20	5	5	3	3	5	5	5	5
Total vials	20	20	45		27		45		50	

[a] NIR analysis is non-destructive, allowing analysis of the same vials throughout the entire stability study

7.2.4. NIR spectroscopy

NIR spectra of the freeze-dried samples were collected off-line using a Fourier-Transform NIR spectrometer (Thermo Fisher Scientific, Nicolet Antaris II near-IR analyzer) equipped with an InGaAs detector and a quartz halogen lamp. All NIR spectra were recorded in the 10000-4000cm^{-1} region with a resolution of 8 cm^{-1} and averaged over 16 scans. One NIR spectrum per freeze-dried sample was collected through the bottom of the glass vial using the integrating sphere device. All measured vials were systematically kept at room temperature for 30 min prior the collection of the spectra.

7.2.5. FTIR spectroscopy

FTIR spectra were recorded using an ATR FT-IR spectrometer (Thermo Fisher Scientific, Nicolet iS5 ATR FT-IR spectrometer). Prior to analysis, the freeze-dried sample was grinded in the vial and then pressed against a diamond ATR crystal. One spectrum per freeze-dried sample was collected in the 4000 - 550 cm^{-1} spectral range with a resolution of 8 cm^{-1} and averaged over 32 scans.

7.2.6. Data analysis

NIR and FTIR spectral analysis was performed using SIMCA 14 (Umetrics, Umeå, Sweden).

Depending on the spectroscopic tool (FTIR or NIR spectroscopy) and the analyzed spectral range, different spectral pre-processing methods were applied (Table 7.2). The evaluated spectral regions (Table 7.2) were selected since they might reflect information on the coated proteins (Haemagglutinin and Neuraminidase) of the freeze-dried live, attenuated viruses (see introduction).

Table 7.2: Analyzed spectral ranges and applied spectral pre-processing

	Preprocessing	Analyzed bands	Spectral range (cm^{-1})
FTIR spectroscopy	SNV	Amide III	1200-1350
NIR spectroscopy	SNV	Water band and Amide A/II	7300-4000
	SNV and 2nd derivative (37 Savitzky-Golay points)	Amide A/II	5029-4690

Both, FTIR and NIR spectra were separately analyzed using principal component analysis (PCA). PCA produces an orthogonal bilinear data matrix (**D**) decomposition, where principal components (PCs) are obtained in a sequential way to explain maximum variance:

$$D=TP^T + E$$

$$= t_1p'_1 + t_2p'_2 + ... + t_Qp'_Q + E$$

Where **T** is the $M \times Q$ score matrix, **P** is the $N \times Q$ loading matrix, **E** is the $M \times N$ model residual matrix, i.e., the residual variation of the data set that it is not captured by the model. Q is the selected number of PCs, each describing a non-correlated source of variation in the data set, and N is the number of collected spectra at M wavelengths [9]. Each principal component consists of two vectors, the score vector **t** and the loading vector **p**. The score vector contains a score value for each spectrum, and this score value informs how the spectrum is related to the other spectra in that particular component. The loading vector indicates which spectral features in the original spectra are captured by the component studied. These abstract, unique and orthogonal PCs are helpful in deducing the number of different sources of variation present in the data. However, these PCs do not necessarily correspond to the true underlying factors causing the data variation, but are orthogonal linear combinations of them, since each PC is obtained by maximizing the amount of variance it can explain [10].

The number of PCs included in the PCA model was determined by cross validation using the approach of Krzanowski [11]. The spectral data of the dataset was divided into 7 groups and a model was generated for the data devoid of one group. The deleted group was predicted by the model and the squared differences between the predicted and observed values were summed to form the Predictive Residual Sum of Squares (PRESS). This procedure was then repeated 7 times, followed by the summation of all partial PRESS-values in terms of an overall PRESS-value. If a new PC_i enhanced the predictive power compared with the preceding PC_{i-1}, the new PCi was kept in the model [12].

7.2.7. Titration

Titration was done according to a Zoetis internal SOPs. Each titer is expressed in $\log_{10}$ CCID$_{50}$ (Cell Culture Infection Dose 50 – Inverse of the highest dilution which produces a cytopathogenic effect in 50% of the cells). Titration provides information about the number of living viral particles in a freeze-dried vial.

7.2.8. Karl Fischer

The residual moisture content of the freeze-dried samples was determined via Karl Fischer titration. A Mettler Toledo V30 volumetric Karl Fischer titrator (Schwerzenbach, Switzerland) with Hydranal® titration solvent from Sigma Chemical Company was used. A known volume of dried methanol was added to the sampled vial, and left to equilibrate for a few minutes. From the solution, a known volume was then removed volumetrically using a syringe and injected into the titration cell. The water content of pure methanol was determined in duplicate prior to the measurement and subtracted from the result.

7.2.9. MDSC

The thermal behaviour of the freeze-dried samples was evaluated using a differential scanning calorimeter Q2000 (TA Instruments, Zellik, Belgium) equipped with a refrigerated cooling system. The DSC was calibrated for temperature and enthalpy using an indium standard. Tzero calibration was performed in 2 steps; baseline calibration (without samples or pans) and sapphire calibration (using large sapphire disks on both the sample and reference positions). Small sapphire disks, placed in a Tzero pan, were used for the heat capacity calibration. For the MDSC experiments, samples (±3 mg) were run in Tzero pans (TA Instruments, Zellik, Belgium) with an underlying heating rate of 5 °C/min (from -20°C to 120°C). The modulation period and amplitude were set at 40 s and 0.531 °C, respectively. Data were analyzed using the Universal Analysis software (TA Instruments). Glass transition

temperature was determined in the reverse heat flow signal and the enthalpic recovery peaks were integrated in the non reverse heat flow signal.

7.3. RESULTS

7.3.1. Evaluation of the virus titer

The titration results are presented in Figure 7.2. At T0, prior to storage, the samples had a titer of 6.39±0.21 (n=10). No titer difference was observed between the T0 samples and the samples stored during 1, 2 and 3 weeks at 4°C having titers of 6.32±0.05 (n=5), 6.33±0.2 (n=5) and 6.15±0.22 (n=5), respectively. At a storage temperature of 37°C, the titer was found to decrease in two phases. After one week storage, the titer decreased from 6.39±0.21 (n=10) at T0 to 5.2±0.22 (n=5) at T1 corresponding to a titer loss of 1.17 log. Afterwards, the titer loss slowed down and the vials stored 2 and 3 weeks at 37°C had titers of 4.82±0.08 (n=5) and 4.47±0.22 (n=5), respectively. This second phase of titer decrease is characterized by a titer loss of 0.4 log. Unfortunately, the virus titers obtained for the vials stored during four weeks are not valid because a cytopathogenic effect was detected in the negative controls of the potency assay.

This two-phase degradation profile has also been observed during the accelerated stability study of the same virus using other stabilizers (data not shown). Similarly, accelerated stability studies of pseudorabies virus [13], canine distemper vaccine [14], measles vaccine [15] and Rinderpest vaccine [16] showed the same two phase titer loss trend. Their degradation curves were analyzed using a two-phase model that separates the degradation process into a rapid initial decay followed by a gradual linear decrease [15, 16]. Regression modelling of the gradual linear decrease (i.e., the second phase) offered the advantage to provide additional information (degradation constant (i.e., the slope), the y-intercept (obtained from linear regression analysis beginning at T1) and the shelf life (calculated from the regression analysis, and function of the desired minimum titer)) to characterize the product stability and was used to compare the effect of different stabilizers, formulations or process settings on the product stability.
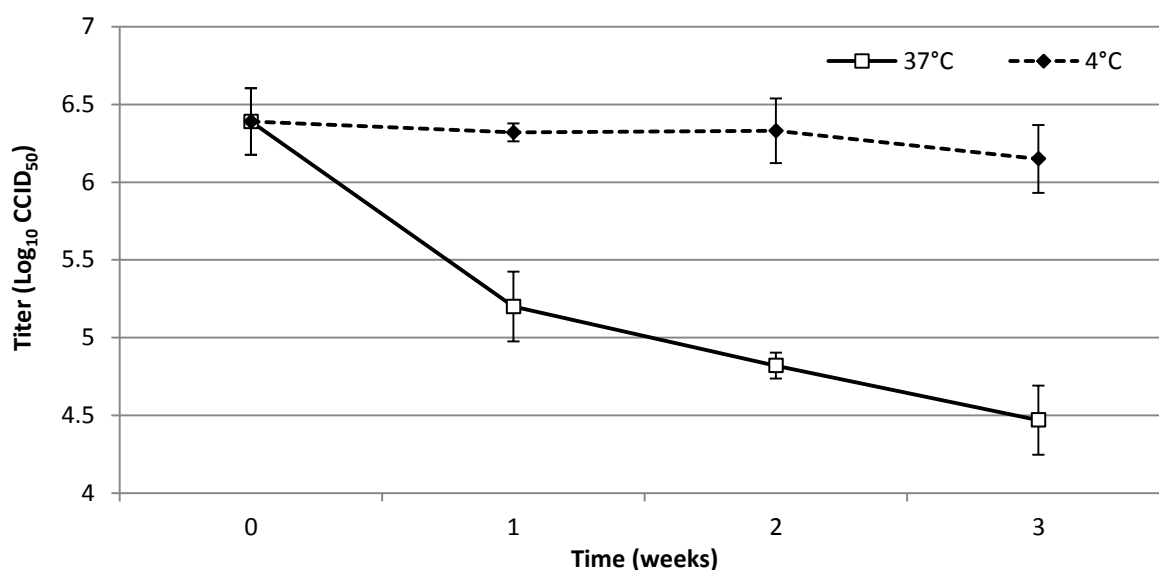
Figure 7.2: Titration results of the freeze-dried samples stored at 4°C and 37°C. Titers are expressed as $\log_{10}$ $CCID_{50}$ (Cell Culture Infection Dose 50). The initial titer (T0) is the average of 10 determinations in duplicate and each titer of the stored samples is the average of 5 determinations in duplicate.

7.3.2. Evaluation of the residual moisture

Residual moisture analysis by Karl Fischer (Figure 7.3) was also performed weekly (see Figure 7.1). Before the stability study (T0), the samples had a residual moisture content of 1.86±0.3 (n=5). After 1, 2, 3 and 4 weeks storage at 4°C, residual moisture values of 1.82±0.16 (n=5), 1.95±0.25 (n=5), 1.73±0.39 (n=5) and 1.92±0.12 (n=4) respectively were obtained. The residual moisture hence remained similar during storage at 4°C. During storage at 37°C, the residual moisture increased gradually (above 2%) with values of 2.09±0.24 (n=5), 2.18±0.15 (n=5), 2.45±0.25 (n=5) and 2.30±0.15 (n=5) after 1, 2, 3 and 4 weeks storage, respectively. In contrast to the observed titer decrease during storage at 37°C, the residual moisture increase did not show a two-phase pattern.
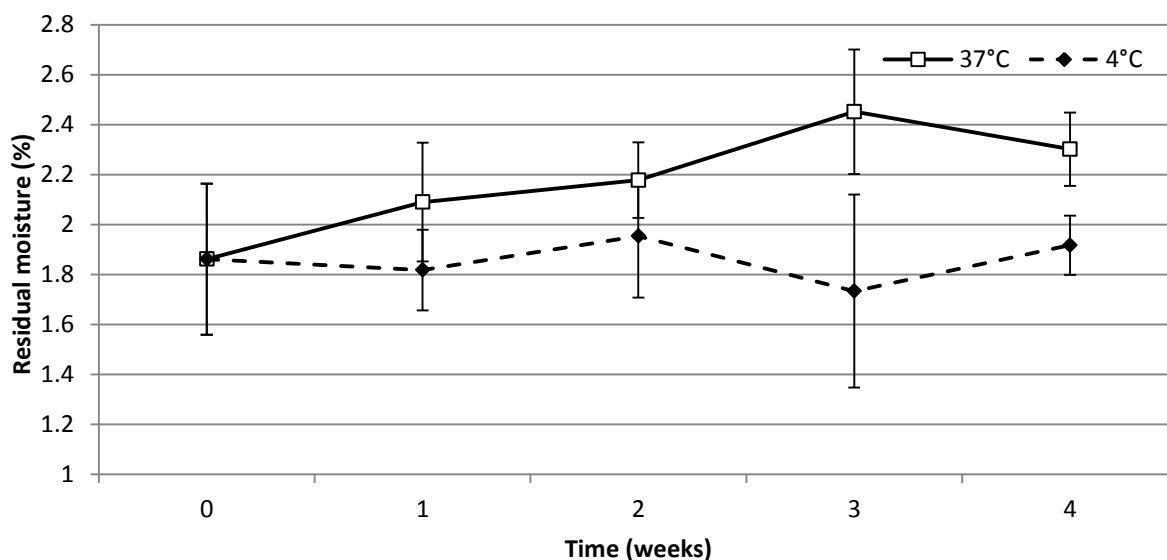
Figure 7.3: Residual moisture content of the freeze-dried samples stored at 4°C and 37°C. Each result is the average of three measurements.

NIR spectra were also collected at each time point during the stability study (Figure 7.1). NIR spectroscopy offers the advantage (among others) of providing multivariate information related to biological, chemical and physical attributes of the materials being processed [17] and has been demonstrated several times to be an effective tool for the determination of the residual moisture content in freeze-dried end products [18-21].

Twenty samples stored at 37°C were monitored with NIR spectroscopy every week. Principal component analysis was performed on these spectra (i.e., 100 spectra, 1 spectrum per sample, 20 samples per week, 5 time points). All SNV preprocessed NIR spectra were decomposed into two principal components (PCs) explaining 95.6% of the spectral variance, where PC1 accounted for 90.7% of the spectral variance and PC2 for 4.9% of the spectral variance. The PC1 scores versus storage time plot (Figure 7.4a) clearly showed a two-phase variation in the first principal component.
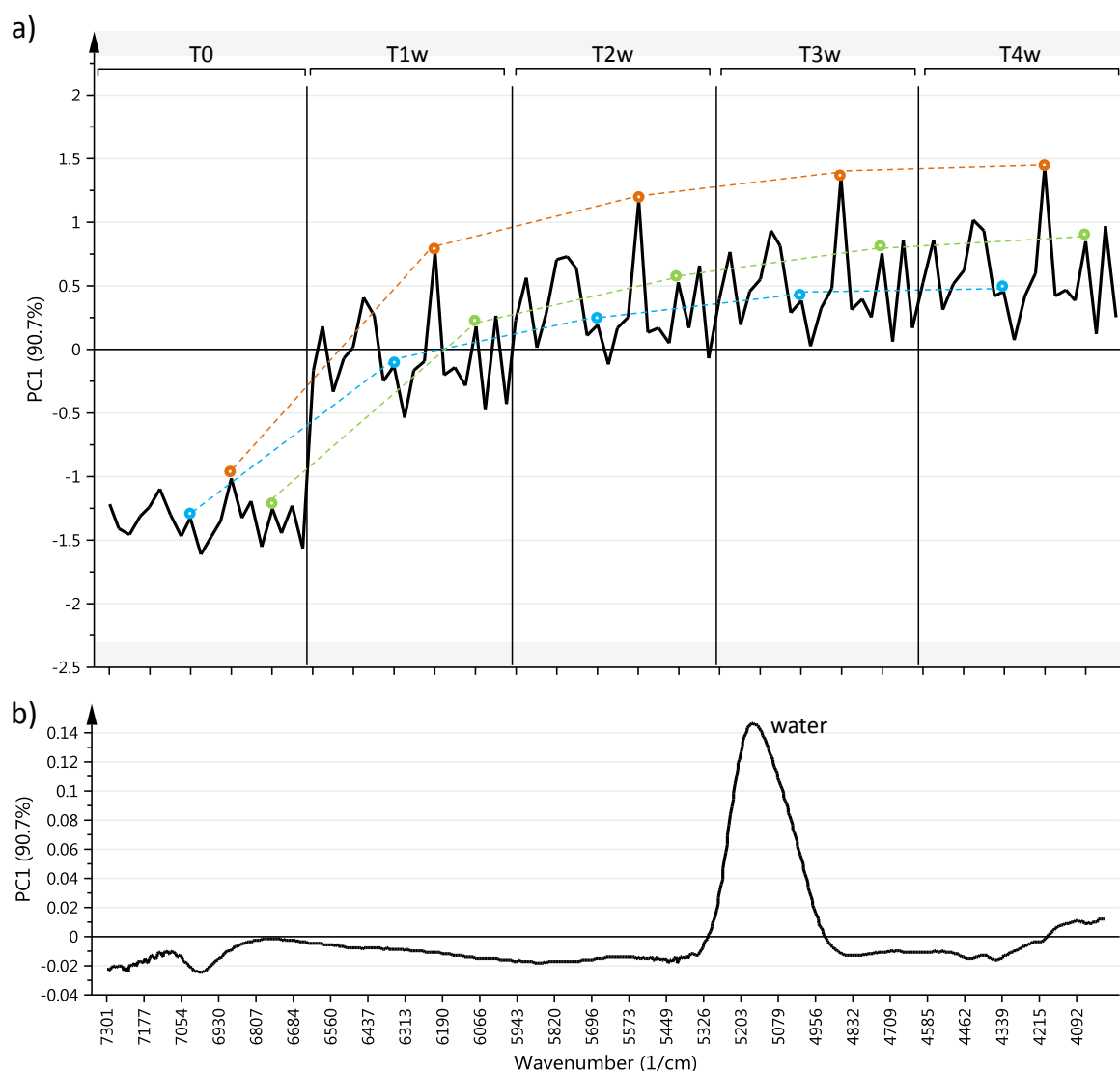
Figure 7.4: Scores and loadings plots obtained after principal component analysis of the NIR spectra collected on the samples stored at 37°C. a) PC1 scores versus storage time plot. The dashed colored lines visualize the evolution of three (out of the 20) samples. T1w, T2w, T3w and T4w represent 1 week, 2 weeks, 3 weeks and 4 weeks storage respectively b) PC1 loadings plot.

The broad peak around 5100-5200cm^{-1} in the corresponding PC1 loadings plot representing water [22] (Figure 7.4b), indicated that PC1 differentiated between the samples according to their moisture content. Moreover, the loadings plot indicated that the intensity of the water band increased during storage, (positive values of PC1 in the scores plot are characterized by an increase of peak intensity) confirming that the residual moisture increased during storage. Interestingly, the sample moisture content trend detected by NIR spectroscopy

followed the same two-phase pattern as the virus titer decrease trend during storage at 37°C (Figure 7.2).

The evaluation of the SNV preprocessed spectra (Figure 7.5) confirmed the intensity increase of the water band (5100-5200cm^{-1}) upon storage at 37°C.
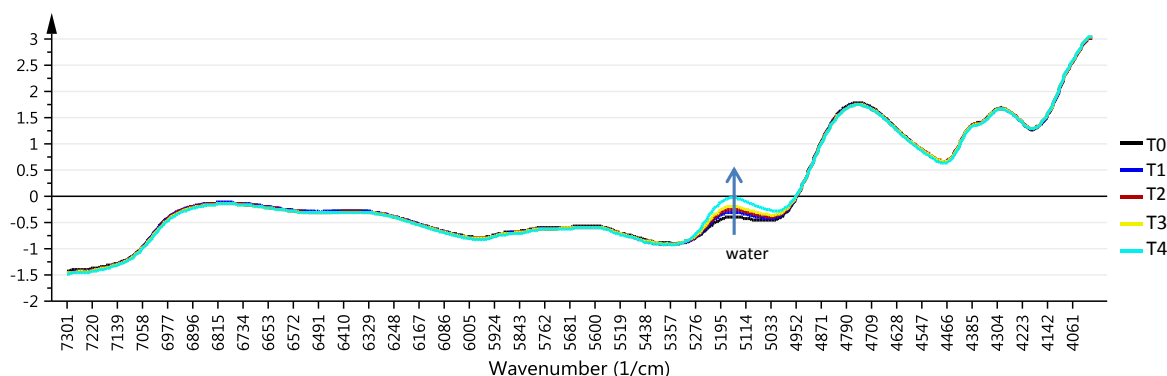
Figure 7.5: NIR SNV preprocessed spectra of the freeze-dried samples stored at 37°C, collected weekly. Arrow indicates the evolution of the spectral signals during storage time.

During the first week of the stability study, NIR spectra were collected every day (Figure 7.1) and PCA was also performed on these spectra (i.e., 120 spectra, 1 spectrum per sample, 20 samples per storage time point). All SNV preprocessed NIR spectra were decomposed into two principal components (PCs) explaining 91.9% of the spectral variance. The PC1 (covering 81.9% of the spectral variance) scores versus storage time plot (Figure 7.6a) clearly showed a two-phase trend. The peak around 5100-5200cm^{-1} in the corresponding PC1 loadings plot representing water [22] (Figure 7.6b), indicated that PC1 differentiated between the samples according to their water content.
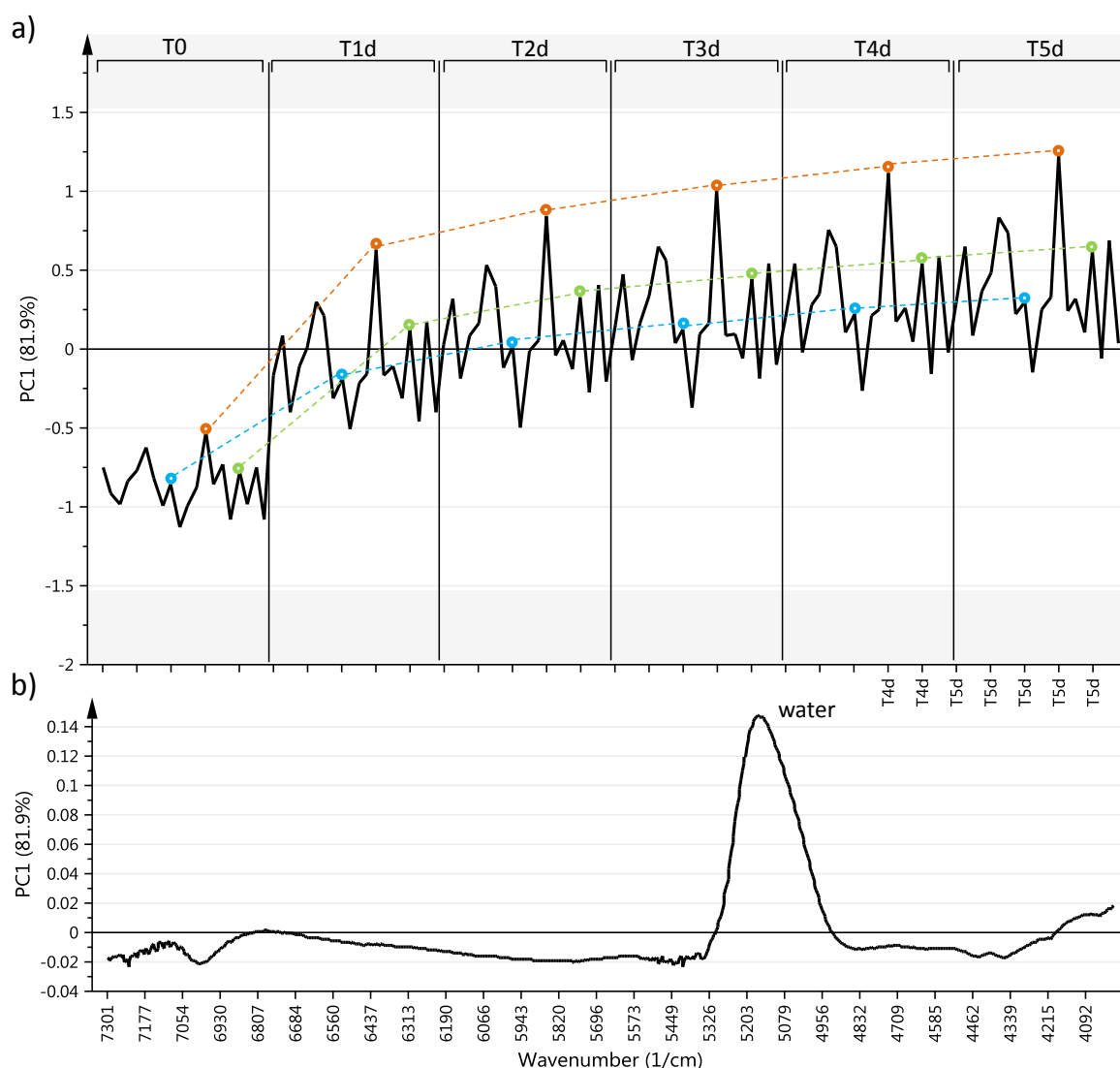
Figure 7.6: a) PC1 scores versus storage time plot obtained after principal component analysis of the NIR spectra collected daily during the first week of storage at 37°C. The dashed colored lines help to visualize the evolution of three (out of the 20) samples daily analyzed. T1d, T2d, T3d, T4d and T5d represent 1day, 2 days, 3 days, 4 days and 5 days storage respectively. b) PC1 loadings plot.

Similarly, twenty samples stored at 4°C were also monitored with NIR spectroscopy every week. PCA was performed on the collected spectra (i.e., 100 spectra, 1 spectrum per sample, 20 samples per storage time point). All SNV preprocessed NIR spectra were decomposed into three principal components (PCs) explaining 93.8% of the spectral variance. The PC1 (explaining 68.7% of the spectral variance) scores versus storage time plot (Figure 7.7a) and the PC1 loadings plot (Figure 7.7b) showed a slight increase of the water content upon storage at 4°C. This residual moisture increase detected by NIR was not detected by Karl

Fischer analysis (Figure 7.3) and did not follow the same two-phase pattern as seen during storage at 37°C.

a)

b)
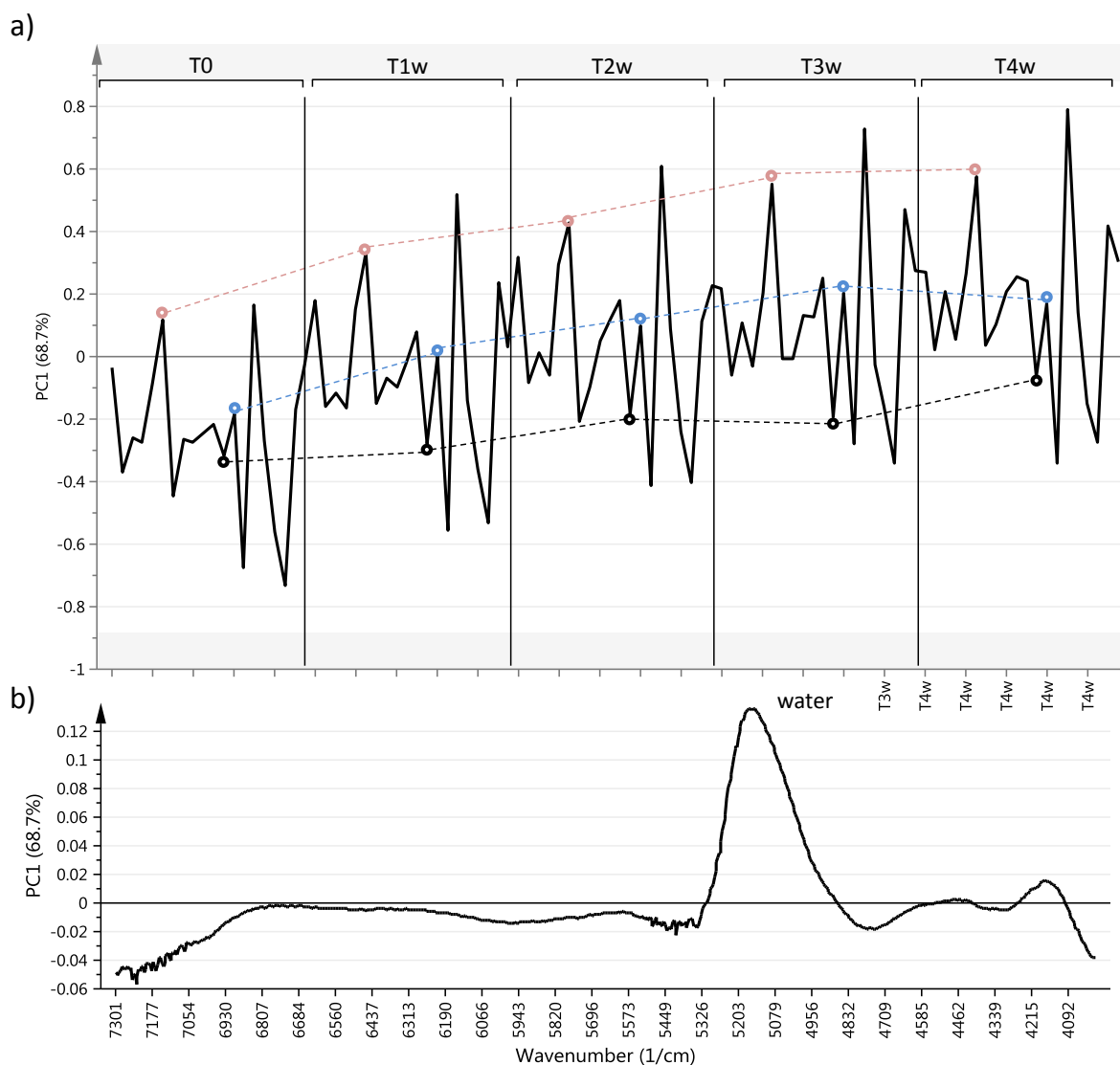
Figure 7.7: a) PC1 scores versus storage time plot obtained after principal component analysis of the NIR spectra collected weekly during storage at 4°C. The dashed colored lines visualize the evolution of three (out of the 20) samples. T1w, T2w, T3w and T4w represent 1 week, 2 weeks, 3 weeks and 4 weeks storage, respectively. b) PC1 loadings plot.

To conclude, NIR spectroscopy demonstrated that the moisture content of the samples stored at 37°C increased in two phases. The moisture increased already sharply after one day storage and then increased more linearly during the further four weeks of storage. At

183

4°C storage, NIR spectroscopy demonstrated that the moisture content in the samples slightly increased (without following a two-phase pattern).

The residual moisture increase patterns observed by NIR spectroscopy are similar to observations made by Pikal and Shah [23]. In their study, both at 40°C and 25°C storage temperature, the moisture content of a freeze-dried lactose formulation first increased sharply but then reached a plateau. At 5°C storage, the cake residual moisture also increased but gradually and almost approached the same residual moisture values as 40°C and 25°C storage after 24 months storage. This residual moisture increase observed upon storage was caused by moisture release by the stopper, equilibrating the moisture content between the stopper and the freeze-dried cake. The rate of reaching the moisture equilibrium was shown to be strongly storage temperature dependent [23].

To decrease this moisture release by the stopper, either high temperature vacuum drying of the stoppers after steam sterilization or the use of stoppers which are less prone to water release is advised [2].

Moisture release by the stopper most probably explains the residual moisture increase observed by NIR spectroscopy in our study.

7.3.3. Thermal behaviour of the stored samples

According to the NIR observations, the residual moisture increased upon storage at 4°C and 37°C. The moisture content increase was higher at 37°C than at 4°C storage. Interestingly, at 37°C storage, the sample moisture content trend detected by NIR followed the same two-phase pattern as the virus titer decrease trend observed during storage at 37°C. In contrast, at 4°C storage, the titer remained constant and the moisture content only slightly increased (only detected by NIR) without following the two-phase pattern observed at 37°C. These observations suggested the link between storage temperature, moisture content increase and virus stability. To understand these observations in more detail, thermal analysis of the stored samples using MDSC was performed (Table 7.1).

Thermal analysis of the samples stored at 37°C showed two events: both the enthalpic recovery (Figure 7.8) and the glass transition temperature (T_g) (Figure 7.9) increased in

function of storage time. Interestingly, this increase followed the same two-phase pattern (Figure 7.10) as the titer decrease and the residual moisture increase observed by NIR spectroscopy.
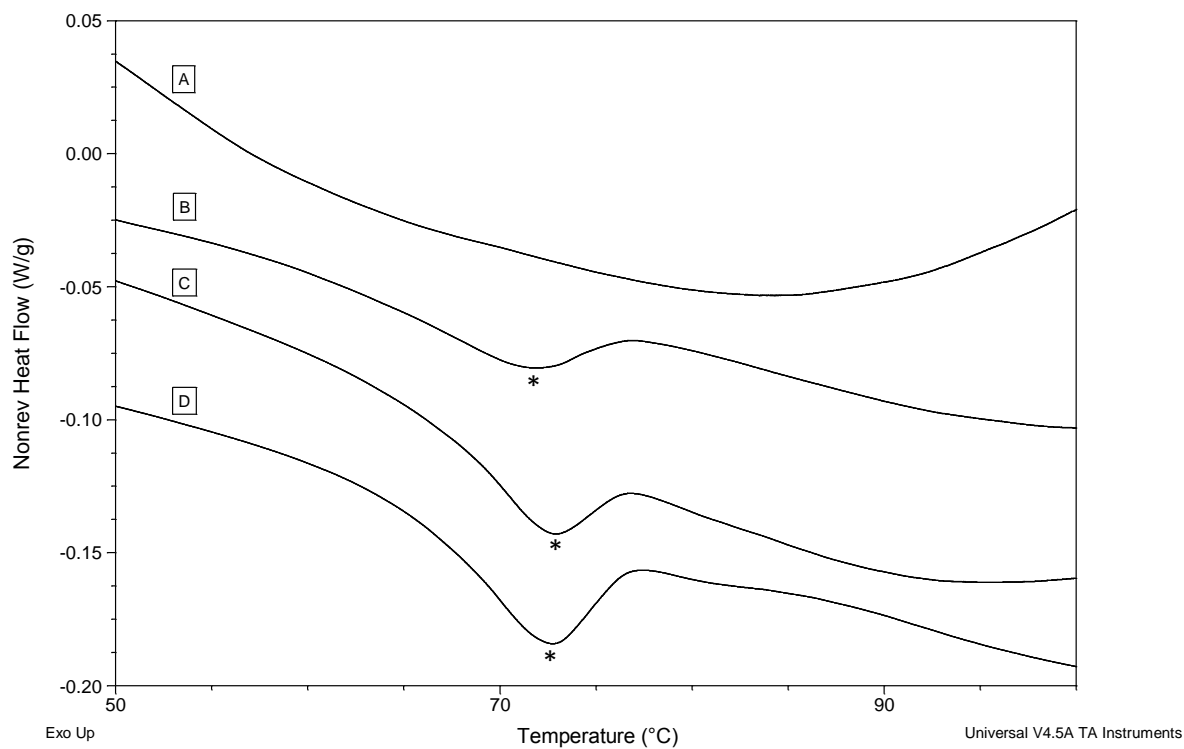
Figure 7.8: MDSC curves: Non reverse heat flow in function of the temperature of samples stored at 37°C. A, B, C and D represent 0 week, 1 week, 2 weeks and 3 weeks of storage, respectively. Enthalpic recovery peaks are marked with an asterisk.
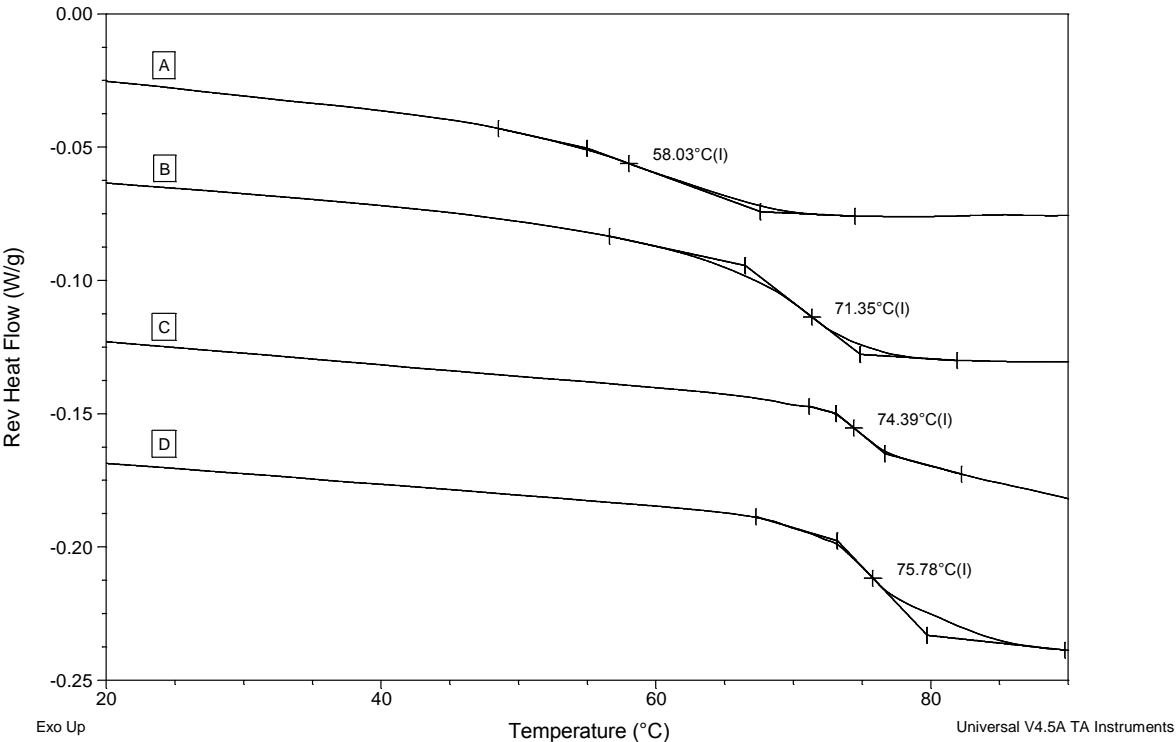
Figure 7.9: MDSC curves: Reverse heat flow in function of the temperature of samples stored at 37°C. A, B, C and D represent 0 week, 1 week, 2 weeks and 3 weeks of storage, respectively.
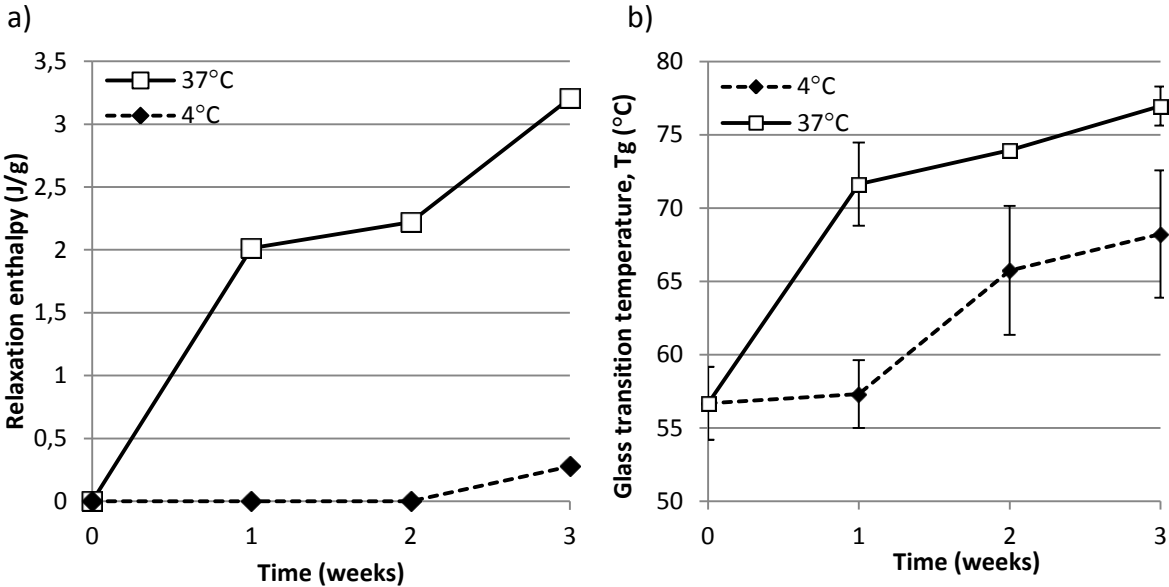
Figure 7.10: a) Relaxation enthalpy and b) Glass transition temperature in function of storage time of samples stored at 4°C and 37°C.

The enthalpic recovery detected with MDSC is a measure of the relaxation enthalpy. When an amorphous material is stored at a temperature near below its glass transition temperature (Tg), it might undergo "relaxation" and spontaneously lose enthalpy and free volume. The rate of this loss is considered to reflect the level of molecular mobility in the non equilibrium glassy amorphous sample [24]. Kawai and co-workers suggested that the activation energy for enthalpy relaxation decreases with increasing molecular mobility [25].

The first observation, the two-phase pattern of the relaxation enthalpy increase, can be explained by the residual moisture increase detected by NIR spectroscopy which (by increasing the molecular mobility – moisture has a plasticizing effect) decreased the activation energy of relaxation enthalpy. The second observation, the Tg increase according to a two-phase pattern is an effect of the relaxation enthalpy. Similar increases of the Tg and enthalpic recovery have already been reported for amorphous trehalose and amorphous lactose [26, 27]. The Tg increase was suggested to be caused by the lactose molecules becoming closer (i.e., the free volume decreased) and forming a rigid matrix with low molecular movement (i.e., relaxation) [27].

In freeze-dried samples, sorption of water causes plasticization of the amorphous phase thereby lowering the Tg [2, 26]. However, in this study, despite the residual moisture increase observed by NIR spectroscopy, the Tg of the samples stored at 37°C increased. This can be explained by the fact that the residual moisture increase upon storage was rather low (approx. 0.5%), which seems to be not sufficient enough to combat the Tg increasing effect caused by the enthalpic recovery. Hence, the effect of relaxation on Tg was superior to the plasticization effect of water.

Upon storage at 4°C, no relaxation enthalpy (Figure 7.10) was observed. The absence of relaxation upon storage at 4°C can be explained by the fact that the relaxation rate is maximal close to Tg (e.g., at a storage temperature of 37°C) while negligible relaxation occurs at temperatures far below Tg (e.g., at a storage temperature of 4°C) [26]. In addition, the activation energy of the relaxation enthalpy remained high since only a slight increase of residual moisture was observed by NIR spectroscopy (Figure 7.7), which was even not detected with Karl Fischer. Finally, the Tg of the samples stored at 4°C remained constant during the first week of storage and then increased (Figure 7.10). This Tg increase was not

coupled to an increase of the relaxation enthalpy in the MDSC thermogram. Nevertheless, the T_g increase might be caused by secondary relaxation undetectable by MDSC. Supplemental analysis with other equipment (e.g., by broadband dielectric spectroscopy) should be performed to verify this hypothesis.

According to the glass dynamic hypothesis (a well-known stabilization hypothesis of proteins in glassy systems, thoroughly described in [24]), instability requires molecular mobility in the amorphous solid. The detection of relaxation enthalpy in the samples stored at 37°C indicates that the glass is subjected to molecular mobility [28]. A correlation has already been shown between molecular mobility and protein aggregation [29, 30] as well as chemical stability [31].

Similarly as the relaxation enthalpy, the virus titer was shown to decrease according a two-phase pattern (Figure 7.2) suggesting that the virus destabilization is linked to the molecular mobility increase. Therefore, the virus titer decrease via virus particles aggregation, virus coated proteins unfolding or any other destabilization mechanism already described for proteins and requiring mobility are likely.

7.3.4. FTIR and NIR spectroscopic evaluation of the live, attenuated virus during storage.

Recently, NIR and FTIR spectroscopy have been demonstrated to be useful to evaluate live, attenuated viruses in freeze-dried formulations [7, 8]. In order to further clarify the observed titer decrease during storage in this study, both spectroscopic tools were used to provide direct information about the viruses and their interaction with the stabilizer (trehalose) in function of the storage temperature.

7.3.4.1. NIR spectroscopy

To evaluate the impact of the storage temperature on the viruses, two PCA models were built. The first model was developed with the NIR spectra collected directly after the freeze-drying process (i.e., T0 samples) and the NIR spectra collected after one day storage at 37°C. The second PCA model was built using the NIR spectra of the T0 samples and the NIR spectra

of the samples stored 1 day at 4°C. To avoid the influence of the water bands and moisture variability between spectra on the PCA, a small spectral range (5029-4690cm^{-1}) only containing the amide A/II band (4850cm^{-1}) (i.e., not influenced by water), was used to build the PCA models.

The first PCA model built from the SNV and 2nd derivative preprocessed NIR spectra of the T0 samples and the samples stored during one day at 37°C was developed from 40 spectra and consisted of two principal components covering 91.8% of the spectral variability. The PC1 (explaining 76.3% of the spectral variability) versus PC2 (explaining 15.5% of the spectral variability) scores plot showed that the model distinguished the T0 samples from the samples stored during one day at 37°C (Figure 7.11a). Interestingly, the loadings plot of the second principal component revealed two peaks at 4980cm^{-1} and 4800cm^{-1} (Figure 7.11c). The band at 4800cm^{-1} can be identified in the spectra (Figure 7.11d) as the amide A/II band and its intensity was different between T0 and T1d samples.

The PCA model built from the SNV and 2nd derivative preprocessed NIR spectra of the T0 samples and the samples stored during one day at 4°C was also developed from 40 spectra. This model consisted of three principal components describing 97.1% of the spectral variability and did not allow distinguishing between the T0 samples and the samples stored one day at 4°C (PC1 versus PC2 scores plot is presented in Figure 7.11b).

Protein dehydration and denaturation has been monitored using NIR spectroscopy by evaluating the amide A/II frequency which represents the strength of the hydrogen bonds of the amide group of proteins [32-34]. At 37°C, a change in the amide A/II band has been observed (Figure 7.11) whereas no change was observed upon storage at 4°C (Figure 7.11) indicating that hydrogen bonds strength of the virus proteins amide group is affected at 37°C storage.
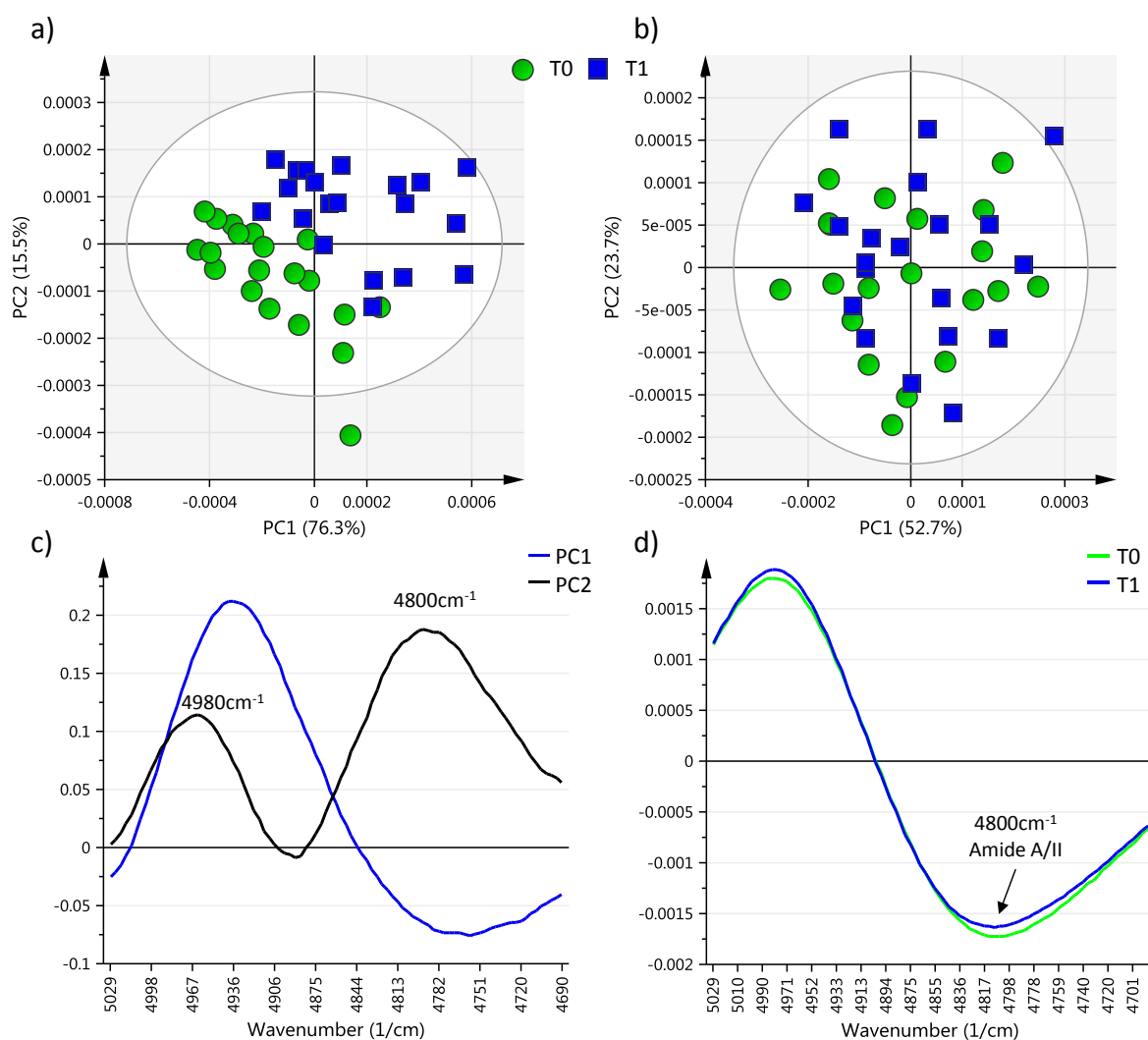
Figure 7.11: Principal component analysis of the preprocessed NIR spectra collected of the T0 samples and the samples stored one day at 37°C or one day at 4°C (5029-4690cm^{-1} spectral range). a) PC1 versus PC2 scores plot of T0 samples and samples stored one day at 37°C.   b) PC1 versus PC2 scores plot of T0 samples and samples stored one day at 4°C. c) PC1 and PC2 loadings plot of T0 samples and the samples stored one day at 37°C. d) NIR SNV and 2nd derivative spectra of a T0 sample and a sample stored 1 day at 37°C.

7.3.4.2. FTIR spectroscopy

Hydrogen bonding influences the protein secondary structure [28]. Therefore, in order to evaluate whether the virus coated protein secondary structure is influenced by storage at 37°C, FTIR spectroscopy, recognized to be an excellent tool to study protein secondary structure, was used. Two PCA models were built using the FTIR spectra collected during the stability study (Figure 7.1). All time points were used in these PCA models because only five

FTIR spectra per time point were available. In order to avoid the contribution of the water bands on the principal component analysis, the PCA models were built using the SNV preprocessed amide III spectral range (1350-1200cm^{-1}) which is not disturbed by water [8].

The first PCA model was built using the FTIR spectra of the T0 samples and the samples stored during 1, 2, 3 and 4 weeks at 37°C. This PCA model, developed from 24 spectra and composed of two principal components, described 93.2% of the spectral variability. The PC1 (explaining 74.2% of the spectral variability) versus PC2 (explaining 19% of the spectral variability) scores plot showed that the model distinguished between the T0 samples and the samples stored at 37°C (Figure 7.12a). Analysis of the loadings plot of the first principal component (Figure 7.12b) revealed two peaks at 1297cm^{-1} (α-helix) and 1262cm^{-1} (β-turn) being responsible for the distinction between the T0 samples and the samples stored during 1, 2, 3 and 4 weeks at 37°C. The second PCA model was built using the FTIR spectra of the T0 samples and the samples stored during 1, 2, 3 and 4 weeks at 4°C. This PCA model, developed from 25 spectra and composed of three principal components, described 94% of the spectral variability and did not allow distinguishing the T0 samples from the samples stored 1, 2, 3 and 4 weeks at 4°C (Figure 7.12c).

Evaluation of the spectra (Figure 7.13) showed that upon storage at 37°C (Figure 7.13a), the peak intensity of the β-turn decreased while the spectral range typical of α-helix was shifted to a higher intensity. Conversely, no spectral difference between both, T0 samples and the samples stored at 4°C during 1, 2, 3 and 4 weeks can be seen (Figure 7.13b).
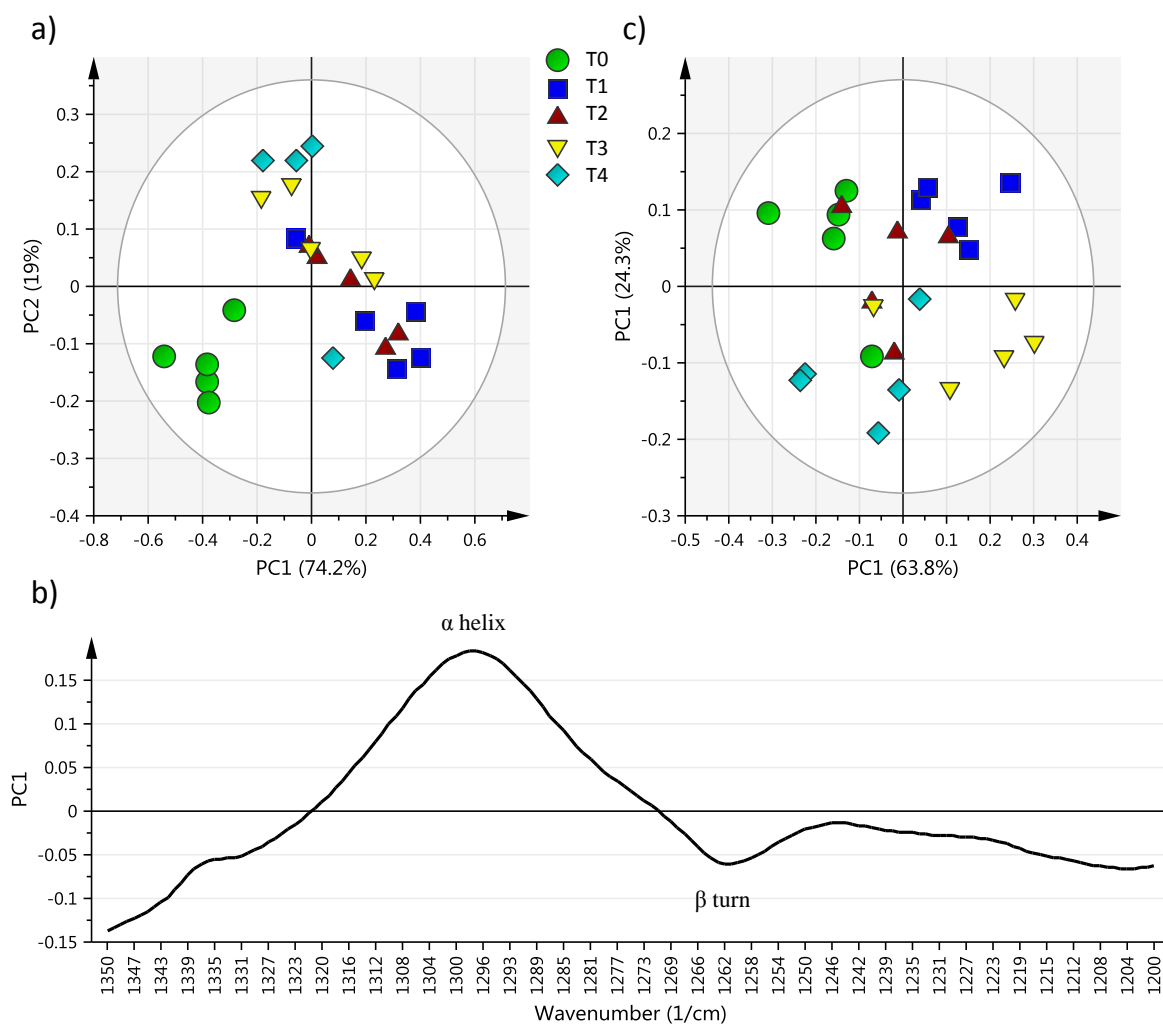
Figure 7.12: PC1 versus PC2 scores plots and PC1 loadings plot obtained after principal component analysis of the FTIR spectra collected on the T0 samples and the samples stored at 37°C or at 4°C (1200-1350cm^{-1} spectral range, amide III). a) PC1 versus PC2 scores plot of T0 samples and the samples stored at 37°C. b) PC1 loadings plot of T0 sample and samples stored at 37°C. c) PC1 versus PC2 scores plot of T0 samples and the samples stored at 4°C.
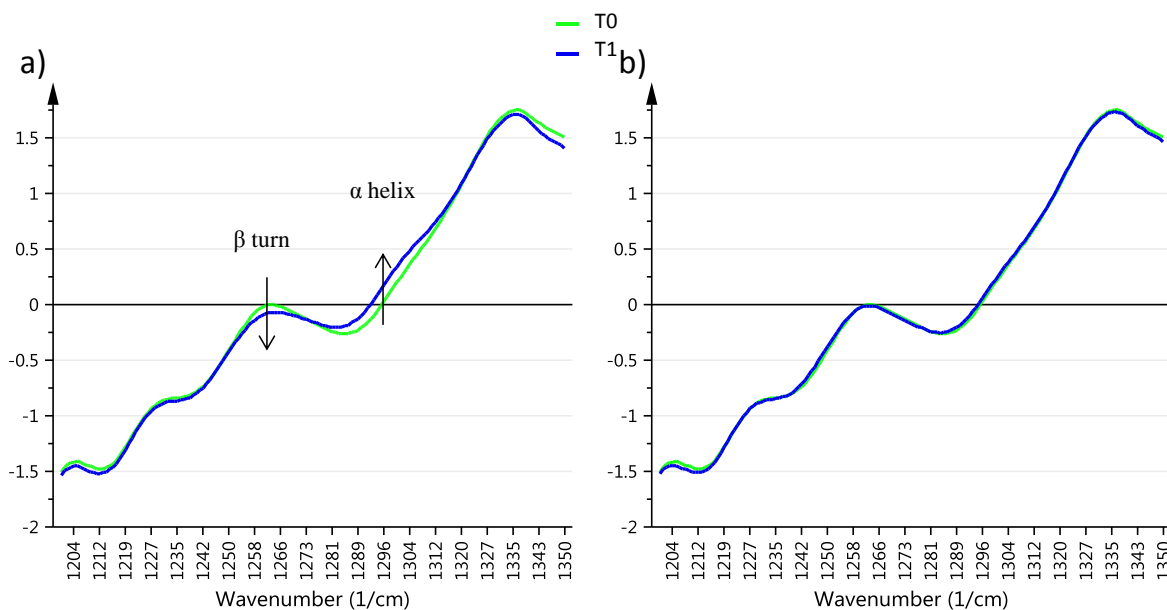
Figure 7.13: a) FTIR spectra of a T0 sample and a sample stored 1 week at 37°C.b) FTIR spectra of a T0 sample and a sample stored 1 week at 4°C.

7.4.   CONCLUSION

This study is, to our best knowledge, the first one combining NIR and FTIR spectroscopy with traditional residual moisture, titration and MDSC analysis to better understand the viability decrease of a freeze-dried live, attenuated virus vaccine during an accelerated stability study. During storage at 37°C, titration of the samples showed that the viability decreased according to a two-phase pattern. Moreover, the residual moisture (evaluated with Karl Fischer and NIR spectroscopy), the glass transition temperature and the relaxation enthalpy also increased according to this two-phase pattern. During storage at 4°C, the virus titer remained constant, no relaxation enthalpy was detected and the residual moisture increased only very slightly.

During storage, the moisture content increase was caused by moisture release from the stopper, equilibrating the moisture content between the stopper and the freeze-dried cake at a temperature-dependent rate. Similarly, the relaxation enthalpy was also found to be different between both storage temperatures. No relaxation enthalpy was detected at 4°C storage whereas at 37°C storage (a temperature close to the formulation Tg) the relaxation

enthalpy was found to increase according to a two-phase pattern. This increase reflected the increased degree of mobility in the amorphous samples during storage due to the moisture release by the stopper.

The measured virus titer decrease at 37°C storage followed the same two-phase pattern as the relaxation enthalpy increase and suggested a link between mobility and virus destabilization. This assumption was supported by the stability of the virus stored at 4°C where no relaxation enthalpy was detected.

Evaluation of the amide A/II band (NIR spectra) revealed that the destabilization of the virus was probably linked to a change in the hydrogen bonds strength between trehalose and the virus proteins. By studying the amide III band (FTIR spectra), it was found that the virus destabilization was coupled to a decrease of β-turn and an increase of α-helix. Together, NIR and FTIR spectroscopy have shown that the relaxation enthalpy (i.e., the molecular mobility) increase upon storage played a role in the stability of the viruses by modifying the strength of the hydrogen bonds between the virus coated proteins and the amorphous trehalose used as stabilizer.

Concluding from all these observations, avoiding an increase in mobility during storage might result in a decreased degradation rate. To achieve the lowest possible mobility increase during storage, an annealing step performed at a temperature of 15 to 20°C below Tg for a short time (from 5h to 20h depending on the formulation) during the secondary drying step of the freeze-drying process might be effective [35, 36].

REFERENCES

[1]   World Health Organization. Guidelines on stability evaluation of vaccines. 2009. Biologicals, 38: 424-434.

[2]   M.J. Pikal Freeze-drying. In: Swarbrick JS, Boylan JC. Encyclopedia of Pharmaceutical Technology. New York: Marcel Dekker, 2002: 1807-33.

[3]   International Conference on Harmonisation (ICH) of technical Requirements for Registration of Pharmaceuticals for human Use, Q5C. Quality of Biotechnological Products: Stability testing of biotechnological/biological products, 1995.

[4]   A. Abdul-Fattah, V.Truong-Le, L. Yee, E. Pan, Y. Ao, D.S. Kalonia, M.J. Pikal. Drying-Induced Variations in Physico-Chemical Properties of Amorphous Pharmaceuticals and Their Impact on Stability II: Stability of a Vaccine. Pharmaceutical Research, 2007; 24(4): 715-727.

[5]   D.T. Brandau, L.S. Jones, C.M. Wiethoff, J. Rexroad, C.R. Middaugh. Thermal stability of vaccines. Journal of Pharmaceutical Sciences, 2003;92: 218-231.

[6]   L. Hansen, R. Daoussi, C. Vervaet, J.P. Remon, T. De Beer. Freeze-drying of live virus vaccines: a review. Vaccine, 2015; 33(42): 5507-5519.

[7]   L. Hansen, S. Pieters, R. Daoussi, J.P. Montenez, C. Vervaet, J.P. Remon, T. De Beer. Near-infrared spectroscopic evaluation of lyophilized viral vaccine formulations. Biotechnology Progress, 2013; 29 (6): 1573-1586.

[8]   L. Hansen, K. Pierre, S. Pastoret, A. Bonnegarde-Bernard, R. Daoussi, C. Vervaet, J.P. Remon, T. De Beer. FTIR spectroscopy for the detection and evaluation of live attenuated viruses in freeze-dried vaccine formulations. Biotechnology Progress, 2015;31(4): 1107-1118.

[9]   L. Zhang, M.J. Henson, S.S. Sekulic. Multivariate data analysis for Raman imaging of a model pharmaceutical tablet. Analytica Chimica Acta, 2005;545: 262-278.

[10]   A. de Juan, R. Tauler. Chemometrics applied to unravel multicomponent processes and mixtures: Revisiting latest trends in multivariate resolution. Analytica Chimica Acta, 2003;500: 195-210.

[11] H. Eastment, and W. Krzanowski. Crossvalidatory choice of the number of components from a principal component analysis. Technometrics, 1982; 24: 73-77

[12] L. Eriksson, E. Johansson, N. Kettaneh-Wold, J. Trygg, C. Wikström, S. Wold. Multi- and Megavariate Data Analysis. Part I: Basic Principles and Applications. Umea: Umetrics, 2006.

[13] E.M. Scott, and W. Woodside. Stability of pseudorabies virus during freeze-drying and storage-effect of suspending media. Journal of Clinical Microbiology, 1976; 4(1): 1-5.

[14] P.M. Precausta, D. Simatos, M. Le Pemp, B. Devaux, F. Kato. Influence of residual moisture and sealing atmosphere on viability of two freeze-dried viral vaccines. Journal of Clinical Microbiology, 1980; 12(4): 483-489.

[15] L.M.C. Allison, G.F. Mann, F.T. Perkins, and A.J. Zuckerman. An accelerated stability test procedure for measles vaccines. Journal of Biological standardization, 1981;9: 185-194.

[16] J.C. Mariner, J.A. House, A.E. Sollod, C. Stem, M. Van Den End, C.A. Mebus. Comparison of the effect of various chemical stabilizers and lyophilization cycles on the thermostability of a vero cell-adapted rinderpest vaccine. Veterinary Microbiology, 1990;21(3): 195-209.

[17] T. De Beer, A. Burggraeve, M. Fonteyne, L. Saerens, J.P. Remon, C. Vervaet. Near infrared and Raman spectoscopy for the in-process monitoring of pharmaceutical production porcesses. International Journal of Pharmaceutics, 2011; 417: 32-47.

[18] M.S. Kamat, R.A. Lodder, P.P. DeLuca. Near-infrared spectroscopic determination of residual moisture in lyophilized sucrose through intact glass vials. Pharmaceutical Research, 1989;6: 961-965.

[19] I.R. Last, K.A. Prebble. Suitability of near-infrared methods for the determination of moisture in a freeze-dried injection product containing different amounts of the active ingredient. Journal of Pharmaceutical and Biomedical analysis, 1993;11: 1071-1076.

[20]   J.A. Jones, I.R. Last, B.F. MacDonald, K.A. Prebble. Development and transferability of near-infrared methods for determination of moisture in a freeze-dried injection product. Journal of Pharmaceutical and Biomedical analysis, 1993;11: 1227-1231.

[21]   M. Savage, J. Torres, L. Franks, B. Masecar, J. Hotta. Determination of adequate moisture content for efficient dry-heat viral inactivation in lyophilized factor VIII by loss on drying and by near infrared spectroscopy. Biologicals, 1998;26: 119-124.

[22]   T.R. De Beer, M. Wiggenhorn, R. Veillon, C. Debacq, Y. Mayeresse, B. Moreau, A. Burggraeve, T. Quinten, W. Friess, G. Winter, J.P. Remon, W.R. Baeyens. Importance of using complementary process analyzers for the process monitoring, analysis, and understanding of freeze-drying. Analytical Chemistry, 2009; 15: 7639-7649

[23]   M.J. Pikal, S. Shah. Moisture transfer from stopper to product and resulting stability implications. Development in Biological standardization, 1992;74: 165-177

[24]   L. Chang, D. Shepherd, J. Sun, D. Ouellette, K.L. Grant, X.C. Tang, M.J. Pikal. Mechanism of protein stabilization by sugars during freeze-drying and storage: native structure preservation, specific interaction, and/or immobilization in a glassy matrix? Journal of Pharmaceutical Sciences, 2005;94(7): 1427-44.

[25]   K. Kawai, T. Hagiwara, R. Takai, T. Suzuki. Comparative investigation by two analytical approaches of enthalpy relaxation for glassy glucose, sucrose, maltose and trehalose. Pharmaceutical Research, 2005; 22(3): 490-495.

[26]   R. Surana, A. Pyne, R. Suryanarayanan. Effect of aging on the physical properties of amorphous trehalose. Pharmaceutical Research, 2004;21(5): 867-74.

[27]   M.K. Haque, K. Kawai, T. Suzuki. Glass transition and enthalpy relaxation of amorphous lactose glass. Carbohydrate Research, 2006;14;341(11): 1884-9.

[28]   L.L. Chang, M.J. Pikal. Mechanisms of protein stabilization in the solid state. Journal of Pharmaceutical Sciences, 2009;98(9): 2886-2908.

[29]   S.P. Duddu, G. Zhang, P.R. Dal Monte. The relationship between protein aggregation and molecular mobility below the glass transition temperature of lyophilized

formulations containing a monoclonal antibody. Pharmaceutical Research, 1997;14(5): 596-600

[30] S. Yoshioka, S. Tajima, Y. Aso, S. Kojima. Inactivation and aggregation of beta-galactosidase in lyophilized formulation described by Kohlrausch-Williams-Watts stretched exponential function. Pharmaceutical Research, 2003;20(10): 1655-60.

[31] S.L. Shamblin, B.C. Hancock, M.J. Pikal. Coupling between chemical reactivity and structural relaxation in pharmaceutical glasses. Pharmaceutical Research, 2006;23(10): 2254-68.

[32] Y. Liu, R.K. Cho, K. Sakuri, T. Miura, Y. Ozaki. Studies on Spectra-Structure Correlations in Near-Infrared Spectra of Proteins and Polypeptides. A Marker Band for Hydrogen-Bonds. Applied Spectroscopy, 1994; 48:1249-1254.

[33] K. Murayama, Y. Ozaki. Two-dimensional near-IR correlation spectroscopy study of molten globule-like state of ovalbumin in acidic pH region: simultaneous changes in hydration and secondary structure. Biopolymers, 2002;67: 394-405

[34] S. Pieters, T. De Beer, J.C. Kasper, D. Boulpaep, O. Waszkiewicz, M. Goodarzi, C. Tistaert, W. Friess, J.P. Remon, C. Vervaet, Y. Vander Heyden. Near-infrared spectroscopy for in-line monitoring of protein unfolding and its interactions with lyoprotectants during freeze-drying. Analytical Chemistry, 2012;84: 947-955

[35] A.M. Abdul-Fattah, K.M. Dellerman, R.H. Bogner, M.J. Pikal. The effect of annealing on the stability of amorphous solids: chemical stability of freeze-dried moxalactam. Journal of Pharmaceutical Sciences, 2007;96(5): 1237-50.

[36] S.A. Luthra, I.M. Hodge, M.J. Pikal. Investigation of the impact of annealing on global molecular mobility in glasses: optimization for stabilization of amorphous pharmaceuticals. Journal of Pharmaceutical Sciences, 2008;97(9): 3865-82.

CHAPTER 8

SPECTROSCOPIC DOSE CLASSIFICATION OF A FREEZE-DRIED LIVE ATTENUATED VIRUS VACCINE

Part of this chapter are published in:

ABSTRACT

This chapter examines the applicability of near-infrared (NIR) spectroscopy to classify freeze-dried live, attenuated virus vaccines according to their dose. Therefore, three different dose presentations (i.e., 125, 50, 25) and a placebo were used. In total, 6 batches were freeze-dried, corresponding to a total of 844 vials (i.e., 243 125-dose vials, 246 50-dose vials, 244 25-dose vials and 111 placebo vials). NIR spectra were collected from each freeze-dried vial and these spectra were first analyzed with principal component analysis (PCA) using the spectral region 7300-4000cm^{-1}, previously demonstrated to allow evaluating freeze-dried live, attenuated virus products. In the PCA scores plot, the 125-dose vials and the placebo vials were well distinguished whereas the 50-dose vials and the 25-dose vials were not well separated.

In a next step, Soft Independent Modelling of Class Analogy (SIMCA) was applied to classify the four dose presentations. Three batches were used to build the model (i.e., the calibration set), two batches were used to test the model (i.e., the test set) and finally, one batch was used to evaluate the robustness of the model. Global correct classification rates of 95.49% and 71.77% were obtained with this model (test set Zoe 4 and Zoe 5 respectively). Afterwards, Orthogonal Partial Least Squares (OPLS) regression modelling was performed allowing the optimization of the spectral range to be used, resulting in an improved SIMCA classification model. A global correct classification rate up to 98.5% was obtained (test set Zoe 4). Finally, in agreement with the European Medicines Agency (EMA) guidelines, the classification model specificity, sensitivity and accuracy was evaluated and a robustness study was performed. This study demonstrated that the classification model was very sensitive to the residual moisture content of the vials to be classified. To conclude, the obtained results suggest that NIR spectroscopy could be used as a fast screening tool to evaluate the dose content of a freeze-dried live, attenuated virus vaccine formulation.

CHAPTER 8

SPECTROSCOPIC DOSE CLASSIFICATION OF A FREEZE-DRIED LIVE ATTENUATED VIRUS VACCINE

8.1.   INTRODUCTION

Vaccines are among the most cost-effective health interventions ever developed. They save millions of lives every year and have lead to the eradication of smallpox, the near eradication of polio and a 75 percent reduction in childhood deaths from measles over the past decade [1].

The live attenuated vaccine is one of the seven different types of vaccines. It contains weakened, attenuated versions of infectious viruses and bacteria and is considered as a good "teacher" of the immune system and is very similar to a natural infection [2]. The instability of live attenuated vaccines in aqueous media is well known [3, 4]. In water, they are susceptible to inactivation by physical (e.g. unfolding) and chemical (e.g. hydrolysis, oxidation, deamidation and the breakage or formation of disulfide bonds) processes which can lead to the disruption of the conformation and function of the structural proteins and glycoproteins [4]. In addition, the lipid bilayer envelope of viruses is extremely susceptible to damage because of their osmotic sensitivity as well as the complex composition of their lipid, carbohydrate and protein components [4, 5].

In order to preserve the potency of live, attenuated vaccines during distribution and long term storage, lyophilization is often used. This process consists of three consecutive steps: sample freezing, primary drying (sublimation) and secondary drying (desorption) [6]. At the end of the freeze-drying process, the overall potency of vaccines is generally determined via cell-based viral plaque assays. This biological method is considered as the gold standard for infective viral particles quantification. In such assays, serial dilutions of the vaccine are used to infect confluent monolayer of adherent cells. After several days of incubation, the cells

are examined in order to find any cytopathic effect. The number of infectious particles can then be calculated from the dilution factor and the number of cytopathic effects detected. Potency assays have the advantage of being time-honored and widely accepted, but are also known to be relatively imprecise and inaccurate, labor-intensive and time-consuming [7-9].

Encouraged by the process analytical technology (PAT) initiative, interest has arisen to develop new fast and non-destructive analytical methods.

Near Infrared (NIR) spectroscopy is a PAT tool that has been demonstrated to be able to evaluate live, attenuated viruses in a freeze-dried vaccine formulation [10]. NIR spectroscopy was able to distinguish between samples prepared using different virus medium volumes or using different pre-freeze-drying treatments. This distinction was possible using two NIR spectral regions: (i) the 7300-4000cm^{-1} region containing the amide A/II band which might reflect information on the coated proteins of the freeze-dried live, attenuated viruses; and (ii) the C-H vibration overtone regions (10,000-7500 and 6340-5500cm^{-1}) which might supply information on the lipid layer surrounding the freeze-dried live, attenuated viruses.

In 2000, approximately 80% of all vaccinations administered globally were produced and supplied as multi-dose products (i.e., products containing more than one dose of medication) [11]. Single-dose formats are more costly than multi-dose products, for three main reasons. The fillings costs of single-dose products are higher and amplified with lyophilized vaccines, single-dose formats need more vaccine overfill per dose than multi-dose products and finally, the packaging costs are higher [12].

The aim of this chapter is to develop and validate an NIR spectroscopic dose classification model able to classify a new freeze-dried live, attenuated virus vaccine vial according to dose. For one vaccine, three different dose presentations (i.e., 125-dose vial, 50-dose vial, 25-dose vial) and a placebo were prepared. Principal Component Analysis (PCA) was first used to evaluate the ability of NIR spectroscopy to distinguish between the freeze-dried formulations containing different virus doses (i.e., 125-dose, 50-dose, 25-dose and placebo).

Soft Independent Modelling of Class Analogy (SIMCA) was then applied to classify the four dose presentations. Once built, the SIMCA model was optimized using Orthogonal Partial Least Squares (OPLS) regression modelling allowing the selection of the optimal spectral range (better than the spectral range (7300-4000cm^{-1}) used in [10]). The model was

afterwards validated according to the European Medicines Agency (EMA) guidelines by evaluating its accuracy, specificity and sensitivity for the classification of new independent observations. In addition, a robustness study was performed by evaluating the ability of the model to classify vials lyophilized in another freeze-drier than the vials used to build the model.

8.2. MATERIALS AND METHODS

8.2.1. Materials

The live, attenuated virus used as vaccine in this study as well as its stabilizer solution, were obtained from Zoetis. The applied four different dose formulations are presented in Table 8.1. The virus medium (i.e., the medium containing the viruses) volume was varied in order to obtain the correct number of doses. The stabilizer solution was kept constant (volume and concentration) in the four formulations. Ultraculture (Lonza, Belgium), a medium free from virus, was used to keep the total volume of the four dose formulations identical. For clarity, the four different virus medium volumes (i.e., x, y, z and 0ml, Table 8.1) used to prepare the different doses were compensated by the addition of an appropriate volume of medium free of virus (i.e., v-x, v-y, v-z and v, Table 8.1) in order to have a total volume of 5ml (Table 8.1). Therefore, the only difference between the dose formulations is the number of virus particles because the volume of "medium" is equal for all dose formulations. Finally, for each dose formulation, samples were prepared with either filtered (0.45µm) virus medium or non-filtered virus medium to evaluate whether cell fragments, that might still be present in the virus medium, interfere with the NIR spectral classification.

Table 8.1: Overview of the studied live, attenuated virus formulations

	Virus medium (ml)	Filtration (0.45µm)	Stabilizer (ml)	Ultraculture (ml)	Total volume (ml)
125-dose vial	x	No	s	v-x	5
125-dose vial	x	Yes	s	v-x	5
50-dose vial	y	No	s	v-y	5
50-dose vial	y	Yes	s	v-y	5
25-dose vial	z	No	s	v-z	5
25-dose vial	z	Yes	s	v-z	5
Placebo vial	0	NA	s	v	5

A total of six batches were freeze-dried and as overviewed in Table 8.2. Five batches were produced at Zoetis and one batch was produced at the Ghent university research lab (UGent). The three first batches produced at Zoetis (Zoe 1, Zoe 2 and Zoe 3) were used as calibration set (i.e., the dataset used to build the model) and the two other batches (Zoe 4 and Zoe 5) were used as independent test sets (i.e., independent dataset used to test and validate the model). The batch produced at the Ghent university research lab (UG) was used as independent test set to evaluate the robustness of the classification model to a freeze-dryer change.

Table 8.2: Overview of the freeze-dried batches

Batches	Batch ID	Batch purpose	Number of samples per dose presentation[1]	Number of titrated samples[1,2]
Zoetis 1	Zoe 1	Calibration set	125 doses NF: 18 125 doses F: 20 50 doses NF: 18 50 doses F: 17 25 doses NF: 18 25 doses F: 19 Placebo: 19 **TOTAL : 129**	125 doses NF: 5/18 125 doses F: 3/20 50 doses NF: 5/18 50 doses F: 3/20 25 doses NF: 5/18 25 doses F: 3/19 Placebo: NA **TOTAL: 24**

Table 8.2: Overview of the freeze-dried batches (continued).

Zoetis 2	Zoe 2	Calibration set	125 doses NF: 19 125 doses F: 16 50 doses NF: 18 50 doses F: 18 25 doses NF: 17 25 doses F: 15 Placebo: 17 **TOTAL: 120**	125 doses NF: 10/19 125 doses F: 3/16 50 doses NF: 10/18 50 doses F: 3/18 25 doses NF: 9/17 25 doses F: 3/15 Placebo: NA **TOTAL: 38**
Zoetis 3	Zoe 3	Calibration set	125 doses NF: 19 125 doses F: 18 50 doses NF: 19 50 doses F: 18 25 doses NF: 19 25 doses F: 18 Placebo: 19 **TOTAL: 130**	125 doses NF: 10/19 125 doses F: 3/18 50 doses NF: 10/19 50 doses F: 3/18 25 doses NF: 10/19 25 doses F: 3/18 Placebo: NA **TOTAL: 39**
Zoetis 4	Zoe 4	Test set	125 doses NF: 17 125 doses F: 18 50 doses NF: 17 50 doses F: 18 25 doses NF: 18 25 doses F: 17 Placebo: 28 **TOTAL: 133**	125 doses NF: 9/17 125 doses F: 3/18 50 doses NF: 9/17 50 doses F: 3/18 25 doses NF: 9/18 25 doses F: 3/17 Placebo: NA **TOTAL: 36**
Zoetis 5	Zoe 5	Test set	125 doses NF: 49 125 doses F: 15 50 doses NF: 41 50 doses F: 22 25 doses NF: 34 25 doses F: 30 Placebo: 18 **TOTAL: 209**	125 doses NF: 10/49 125 doses F: 3/15 50 doses NF: 10/41 50 doses F: 3/22 25 doses NF: 10/34 25 doses F: 3/30 Placebo: NA **TOTAL: 39**

Table 8.2: Overview of the freeze-dried batches (continued).

UGent	UG	Test set (Robustness)	125 doses NF: 20	125 doses NF: 8/20
			125 doses F: 18	125 doses F: 5/18
			50 doses NF: 20	50 doses NF: 6/20
			50 doses F: 20	50 doses F: 5/20
			25 doses NF: 20	25 doses NF: 8/20
			25 doses F: 19	25 doses F: 5/19
			Placebo: 10	Placebo: NA
			TOTAL: 127	**TOTAL: 37**

[1]Filtered (F) and non-filtered (NF)
[2]Each vial has been titrated two times.

8.2.2. Freeze-drying

Five batches were produced at Zoetis (Zoetis 1-5) using a Lyostar 3 (SP scientific, Stone Ridge, NY, USA) and 1 batch was produced at Ghent University (UGent) using a LyoBeta 25 (Telstar, Terrassa, Spain).

All batches were freeze-dried using the same freeze-drying settings, optimized by Zoetis, which cannot be disclosed for confidentiality reasons. All the freeze-dried vials had a visually acceptable cake aspect.

8.2.3. Titration

Titration (potency assay) was done according to Zoetis' internal SOPs. Each titer is expressed in $\log_{10}$ CCID$_{50}$ (Cell Culture Infection Dose 50). Titration provides information about the number of living viral particles contained in each freeze-dried vial. Each analyzed sample was titrated twice.

8.2.4. Residual moisture analysis

The residual moisture content of freeze-dried samples was determined using Karl Fischer titration. After each freeze-drying cycle, the samples were analyzed with a Metrohm 860 KF Thermoprep (oven) coupled to a Metrohm 852 Titrando (Herisau, Switzerland). Three

filtered and three non-filtered vials of each dose formulation and three placebo vials were measured.

8.2.5. NIR spectroscopy

NIR spectra of all freeze-dried samples were collected off-line using a Fourier-Transform NIR spectrometer (Thermo Fisher Scientific, Nicolet Antaris II near-IR analyzer) equipped with an InGaAs detector and a quartz halogen lamp. All NIR spectra were recorded in the 10000-4000 cm^{-1} region with a resolution of 8 cm^{-1} and averaged over 16 scans. One NIR spectrum per freeze-dried sample (in random order) was collected through the bottom of the glass vial using the integrating sphere device immediately after freeze-drying.

8.2.6. Data analysis

NIR spectral data analysis was done using SIMCA 14.0 (Umetrics, Umea, Sweden). Based on a previous study [10], the spectral region 7300-4000cm^{-1}, containing the amide A/II band was evaluated. All collected NIR spectra were mean centered and preprocessed using standard normal variate (SNV) in order to eliminate additive baseline offset variations and multiplicative scaling effects in the spectra which may be caused by possible differences in sample density and sample-to-sample measurement variations.

8.2.6.1. Principal Component Analysis

All collected NIR spectra per batch were first analyzed as one data matrix (**D**) using principal component analysis (PCA), which is an unsupervised multivariate data analysis method allowing to examine whether NIR spectroscopy can distinguish between the different doses. In addition, PCA was also used to understand and explain misclassifications.

PCA produces an orthogonal bilinear data matrix (**D**) decomposition, where principal components (PCs) are obtained in a sequential way to explain maximum variance:

$$D = TP^T + E$$

$$= t_1p'_1 + t_2p'_2 + \ldots + t_Qp'_Q + E$$

Where **T** is the *M x Q* score matrix, **P** is the *N x Q* loading matrix, **E** is the *M x N* model residual matrix, i.e., the residual variation of the data set that it is not captured by the model. **Q** is the selected number of PCs, each describing a non-correlated source of variation in the data set, and **N** is the number of collected spectra at **M** wavelengths [13]. Each principal component consists of two vectors, the score vector **t** and the loading vector **p**. The score vector contains a score value for each spectrum, and this score value informs how the spectrum is related to the other spectra in that particular component. The loading vector indicates which spectral features in the original spectra are captured by the component studied. These abstract, unique, and orthogonal PCs are helpful in deducing the number of different sources of variation present in the data. However, these PCs do not necessarily correspond to the true underlying factors causing the data variation, but are orthogonal linear combinations of them, since each PC is obtained by maximizing the amount of variance it can explain [14].

The number of PCs included in the PCA model was determined by cross validation using the approach of Krzanowski [15]. The data are divided into 7 groups and a model was generated for the data devoid of one group. The deleted group was predicted by the model and the squared differences between the predicted and observed values were summed to form the Predictive Residual Sum of Squares (PRESS). This procedure was repeated 7 times, followed by the summation of all partial PRESS-values in terms of an overall PRESS-value. If a new PC_i enhanced the predictive power compared with the preceding PC_{i-1}, the new PCi was kept in the model [16].

8.2.6.2. Soft Independent Modelling of Class Analogy

Soft Independent Modelling of Class Analogy (SIMCA) was chosen for the development of the classification model based on the NIR spectra from the different dose-vials (125-dose,

50-dose, 25-dose and placebo). As already mentioned (Table 8.2), the batches Zoe 1, Zoe 2 and Zoe 3 were used for calibration of the model. SIMCA [17] is a widely used classification technique which puts more emphasis on similarity within a class than on discrimination between classes [18]. In SIMCA, each class of a training set of observations of known classes is modeled separately by disjoint PCA models. After the separate modelling of each class, a likely class membership of each new observation is predicted.

8.2.6.3. Orthogonal PLS

Orthogonal Partial Least Squares to latent structures (OPLS) is a modification of PLS designed to handle variation in X (i.e., in this study the spectroscopic data matrix) that is orthogonal to Y (i.e., in this study the class membership). OPLS separates the systematic variation in X into two parts, one that is linearly related (and therefore predictive) to Y and one that is uncorrelated (orthogonal) to Y. The predictive variation of Y in X is modeled by the predictive component whereas the variation in X, which is orthogonal to Y, is modeled by the orthogonal components. This partitioning of the X-data provides improved model transparency and interpretability. In this study, the analysis of the loadings plot of the predictive component allowed identifying the spectral contribution responsible for the distinction between the different dose vials. Based on this, the spectral range of the SIMCA classification model was optimized.

8.2.6.4. Evaluation of model performance

The ability of each developed SIMCA model to classify new observations correctly was evaluated using a misclassification table. Such a table shows the proportion of correct classifications of the test set vials (e.g., Zoe 4 and Zoe 5).

From the misclassification table, the number of true positives (TP), true negatives (TN), false positives (FP) and false negatives (FN) can be determined. Afterwards, in order to validate the classification model according to the EMA guidelines [19], the percent classification accuracy, sensitivity and specificity are calculated using the following equations:

% Accuracy: $((TN + TP)/(TN+TP+FN+FP))*100$

% Sensitivity: $((TP)/(TP+FN))*100$

% Specificity: $(TN/(TN+FP))*100$

The sensitivity reflects the model ability to correctly classify the doses whereas the specificity reflects the ability of the model to correctly reject doses when they do not belong to a class. Both are combined to determine the accuracy of the model.

8.3. RESULTS AND DISCUSSION

The results are discussed in three parts: (i) the titer and residual moisture determination of vials from the different batches, (ii) the Principal Component Analysis (PCA) of the NIR spectra and, (iii) the development and validation of the NIR classification model.

8.3.1. Titration and residual moisture analysis

The potency assay performed to analyze the titer of the different dose vials is the only reference method that is currently used to evaluate the viability of the viruses after freeze-drying and during storage. The titration results obtained immediately after freeze-drying are presented in Figure 8.1. The titration results showed that there was no difference between the filtered and non-filtered vials. Secondly, the titers of the UGent batch were lower than the titers of the Zoetis batches. Finally, the titers of the 125-dose vials, the 50-dose vials and 25-dose vials were different within each batch.
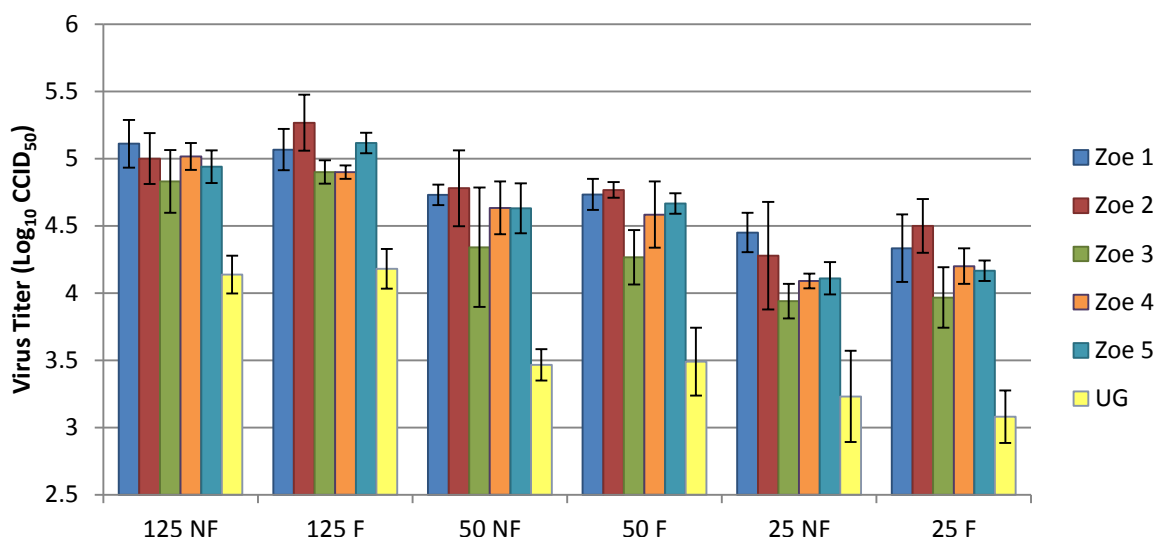
Figure 8.1: Titration results of the different dose vials - filtered (F) and non-filtered (NF) - of Zoetis and UGent batches. Titers are expressed as $\log_{10}$ CCID$_{50}$ (Cell Culture Infection Dose 50). Each vial has been titrated twice and each titer is the mean of several vials (number of titrated vials varies with batch) +/- standard deviation.

The residual moisture content results are presented in Figure 8.2. All evaluated vials had a residual moisture below 2%. Furthermore, for each dose no difference in residual moisture content was detected between filtered and non-filtered vials. Thirdly, the measured 125-dose vials, 50-dose vials and 25-dose vials had similar residual moisture content within each batch. Finally, the residual moisture of batch UGent was higher than the residual moisture of the other batches. This difference might be caused by several reasons; (i) a different degree of supercooling caused by different environmental conditions (i.e., less particles in GMP conditions) leading to differences in cake pore size, (ii) cake rehydration between transport from Ghent to Zoetis were the residual moisture analysis were performed.
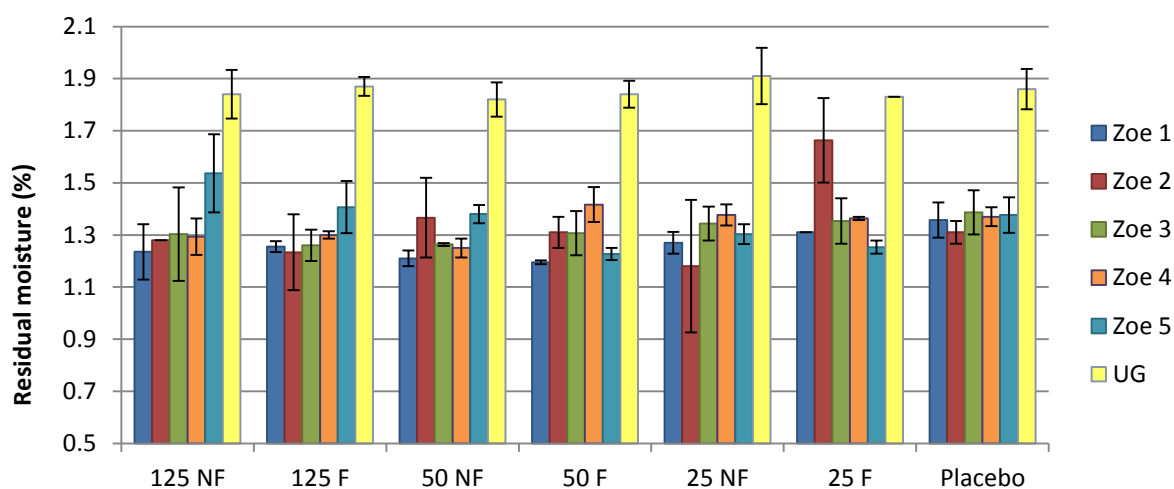
Figure 8.2: Residual moisture content results of the different dose vials - filtered (F) and non-filtered (NF) - of the Zoetis and UGent batches. Residual moisture is expressed in %. Each moisture value is the mean of 3 determinations +/- standard deviation.

8.3.2. Principal Component Analysis of the spectra

The NIR spectra of each batch were first analyzed using principal component analysis (PCA). As mentioned in the material and method section, the 7300-4000 cm^{-1} NIR spectral range was evaluated. This first PCA had multiple aims: (i) to evaluate whether NIR spectroscopy allows distinguishing between the different doses, (ii) to evaluate whether filtration of the virus medium (see materials and methods section) impacts the NIR spectra and (iii) to provide an overview of the data (i.e., indicate groups of observations, trends, outliers and other anomalies). Figure 8.3 shows the scores and loadings plots of three different PCA models developed using the NIR spectra from batch Zoe 1.

The first PCA model developed from the SNV preprocessed spectra of the filtered and non-filtered vials together (i.e., 125 spectra, 1 spectrum per vial) existed of two principal components and described 90.6% of the spectral variability. The PC1 versus PC2 scores plot (Figure 8.3a) did not show differences between the vials in the first PC (explaining 80.4% of the spectral variability). The PC1 loadings plot (data not shown) revealed as main contribution the water band at 5140 cm^{-1} and hence confirmed that there was no difference in residual moisture content between the different dose vials. The second PC (explaining 10.2% of the spectral variability) distinguished the vials according to their dose content (Figure 8.3a). The 125-dose vials and the placebo vials were located at each side of PC2 in the scores plot. However, no clear distinction between the 50-dose vials and the 25-dose vials can be made. The titers of these vials were very close to each others and might explain why NIR spectroscopy did not distinguish between the 50- and 25-dose vials. Finally, no difference between filtered and non-filtered vials was detected with NIR for each dose content.
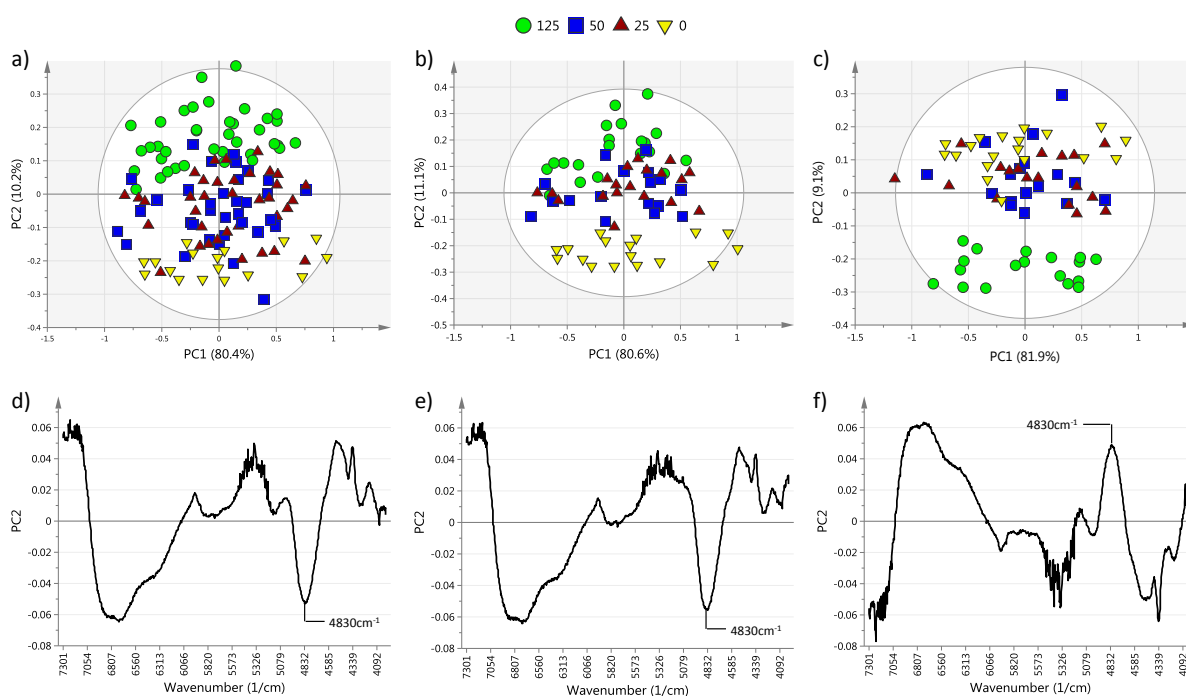
Figure 8.3: PC1 versus PC2 scores and PC2 loadings plot obtained after PCA of the NIR spectra collected from batch Zoe 1. (a, d) scores and loadings plots of the filtered and non-filtered vials together, (b, e) scores and loadings plots of the filtered vials, (c, f) scores and loadings plots of the non-filtered vials.

The second PCA model was developed using the SNV preprocessed spectra of the filtered vials only (i.e., 73 spectra, 1 spectrum per vial) and contained two principal components describing 91.7% of the spectral variability. Interpretation of the PC1 versus PC2 scores plot (Figure 8.3b) led to similar conclusions as for the first PCA model developed for the filtered and non-filtered observations together. The first PC (80.6% of the spectral variability) described the moisture differences between the vials while the second PC (11.1% of the spectral variability) distinguished the vials according to their dose content (except the 50- and 25-dose vials).

A third PCA model was built using the SNV preprocessed spectra of the non-filtered vials (i.e., 72 spectra, 1 spectrum per vial) and described 91% of the spectral variability (two principal components). The first PC (81.9% of the spectral variability) described the moisture differences between the vials. The second PC (covering 9.1% of the spectral variability) distinguished the 125-dose vials but not the 50-dose vials, 25-dose vials and the placebos (Figure 8.3c). The loadings plots of the second PCs of the 3 PCA models (Figure 8.3d, e, f) were similar. Among the different bands involved in the distinction between the dose vials, the clear band at $4830cm^{-1}$ was identified as the amide A/II band. This band was already involved in the distinction between vials composed of different virus volumes (i.e., varying virus medium volume compensated by water instead of Ultraculture) in a previous study [10] and might reflect information on the viral coated proteins. The same PCA was also performed on SNV and 2nd derivative spectra. Nevertheless, the distinction of the different dose vials was not possible using this preprocessing (data not shown).

PCA of the SNV preprocessed spectra of Zoe 1 using the 7300-$4000cm^{-1}$ spectral range has shown that the distinction between the different dose vials was possible for 125-dose vials and the placebo vials. The distinction between the 50-dose vials and 25-dose vials was however not possible. Identical conclusions could be made after PCA of the other batches produced at Zoetis. Furthermore, the PCA demonstrated that filtration had no negative effect on the NIR spectra because: (i) the PCA performed by combining the filtered and non-filtered vials did not distinguish them (Figure 8.3a) and (ii) the filtered vials were better separated than the non-filtered vials. Nevertheless, an exception was found in the PCA of

the filtered vials of batch Zoe 5. The distinction of the different dose formulations was not possible with this batch, which might indicate an issue with the filtration step.

8.3.3. Development and validation of a classification model

The overall aim of this study is to develop a model able to classify new freeze-dried products according to their dose content. Soft Independent Modelling of Class Analogy (SIMCA) and Partial Least Squares Discriminant Analysis (PLSDA) are two frequently used classification methods. One of the required conditions for PLSDA to work reliably is that each class occupies a separate volume in the X-space (i.e., the different classes do not overlap) [16]. The PCA performed in the previous section has shown that the 50-dose vials and the 25-dose vials cannot be easily separated hence making the use of a PLSDA model less appropriate. Based on similarity within a class rather than on discrimination between classes, SIMCA better deals with slightly overlapping classes and hence constitutes a better choice. Therefore, SIMCA was selected as classification model for this study.

In total, five batches produced at Zoetis were available to build and validate (i.e., test) the SIMCA classification model. As mentioned in the material and methods section, the batches Zoe 1, Zoe 2 and Zoe 3 were used to build the model, while Zoe 4 and Zoe 5 were used to validate the model. Filtered and non-filtered vials were combined in the dataset in order to have more observations. This should not negatively influence the classification according to dose since the filtration step had no effect on the virus titer and no negative effect on the spectra, as demonstrated higher.

8.3.3.1. Development of the SIMCA classification model

Based on a previous study [10], the SNV preprocessed spectral range 7300-4000cm^{-1} was selected. Afterwards, the developed SIMCA model was evaluated with an independent test set, i.e., batches Zoe 4 and Zoe 5.

The misclassification table of Zoe 4 is presented in Table 8.3. The 125-dose vials, 50-dose vials, 25-dose vials and placebo vials had a correct classification rates (CCR) of 97.14%, 91.43%, 100% and 92.86% respectively. Globally, this correct classification rate (95.49%) was satisfactory.

Table 8.3: Misclassification table obtained using Zoe 1-2-3 as calibration set and Zoe 4 as independent test set. 7300-4000cm^{-1} spectral range, SNV preprocessed.

	Members	Correct Classification rate (CCR, %)	125-dose vial	50-dose vial	25-dose vial	Placebo	No class
125-dose vial	35	**97.14%**	**34**	0	0	0	1
50-dose vial	35	**91.43%**	0	**32**	3	0	
25-dose vial	35	**100%**	0	0	**35**	0	
Placebo	28	**92.86%**	0	0	2	**26**	
Total	133	**95.49%**	34	32	40	26	1

Similarly, the misclassification table of batch Zoe 5 is presented in Table 8.4. Its 125-dose vials, 50-dose vials, 25-dose vials and placebo vials had correct classification rates (CCR) of 51.56%, 57.14%, 100% and 94.44% respectively. Surprisingly, the CCR obtained for the 125-dose vial and the 50-dose vial were far under the scores obtained for batch Zoe 4 (Table 8.3).

Table 8.4: Misclassification table obtained using Zoe 1-2-3 as calibration set and Zoe 5 as independent test set. 7300-4000cm^{-1} spectral range, SNV preprocessed.

	Members	Correct Classification rate (CCR, %)	125-dose vial	50-dose vial	25-dose vial	Placebo	No class
125-dose vial	64	**51.56%**	**33**	6	8	0	17
50-dose vial	63	**57.14%**	0	**36**	27	0	
25-dose vial	64	**100%**	0	0	**64**	0	
Placebo	18	**94.44%**	0	0	1	**17**	
Total	209	**71.77%**	33	42	100	17	17

The PCA previously performed on the filtered vials of batch Zoe 5, already showed that the distinction of the different dose formulations, 125-dose vial and placebo included, was not possible.

Before refining the SIMCA model, some more investigations of batch Zoe 5 were performed to understand the low correct classification rate of the 125 and 50-dose vials of this batch. A PCA performed on each group of dose vial (i.e., 125-dose vial, 50-dose vial and 25-dose vial,

separately, hence resulting in three PCA models) and their respective scores plots confirmed that the filtered vials of the 125 and 50-dose vial were different from the non-filtered vials (Figure 8.4). This explains the low CCR of the 125 and 50-dose vial obtained with the SIMCA model.

In the first PCA model (125-dose vial, 64 spectra, 1 spectrum per vial) composed of three principal components explaining 96.8% of spectral variability, an obvious difference between the filtered and non-filtered vials (Figure 8.4a) can be observed along PC2 (17.2% of spectral variability). In the second PCA model (50-dose vial, 63 spectra, 1 spectrum per vial) composed of three principal components and explaining 96.8% of spectral variability, a difference between the filtered and non-filtered vials can also be observed (Figure 8.4b) along PC3 (3.56% of spectral variability). In the last PCA model (25-dose vial, 64 spectra, 1 spectrum per vial) composed by three principal components explaining 97.2% of spectral variability, no difference between the filtered and the non-filtered vials can be observed in the PC scores plot (Figure 8.4c). Analysis of the PC2 loadings plot of 125-dose PCA model (Figure 8.4d) identified a peak (4740cm^{-1}) responsible for the difference between the filtered and non-filtered vials. This peak, located in a spectral range related to a fundamental N-H stretch with amide III [20] can be linked to a protein component of the formulation (i.e., virus coated proteins or proteins from the stabilizer solution).
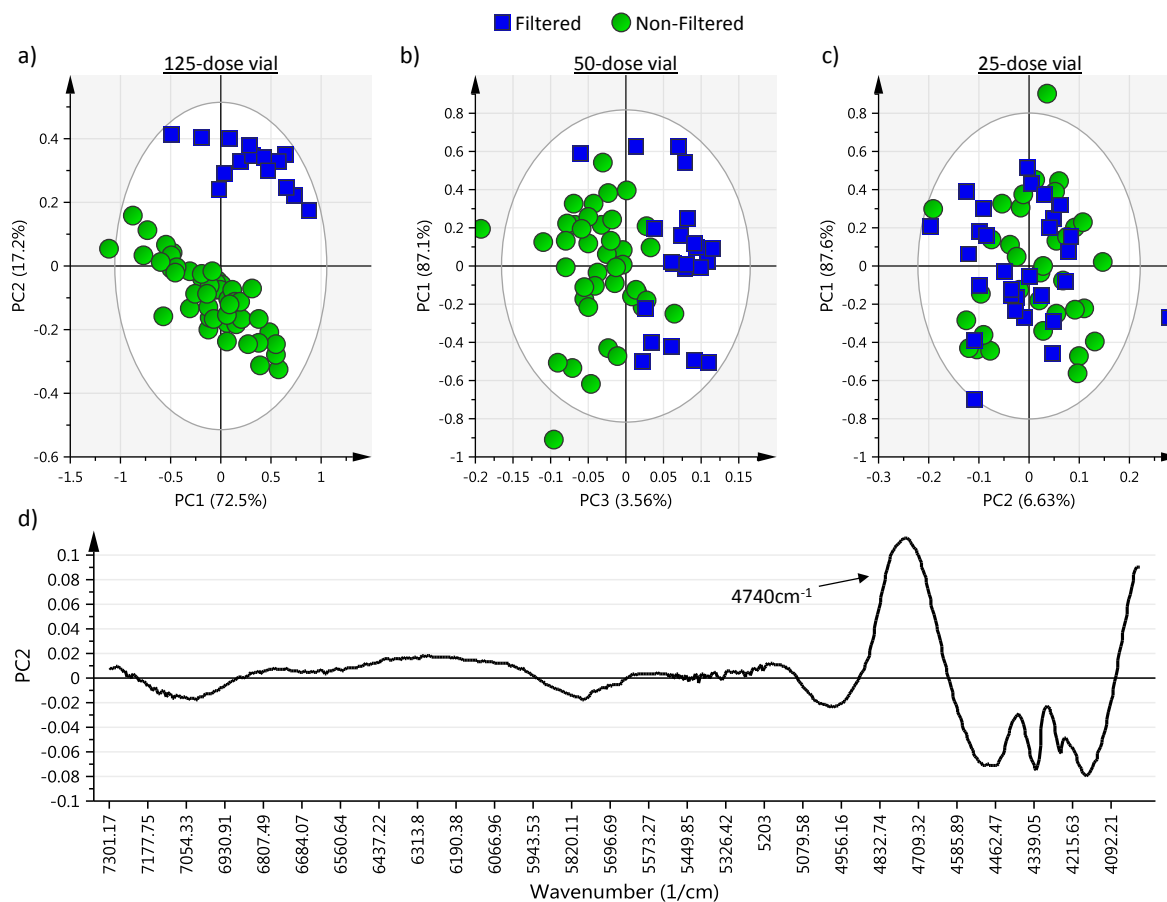
Figure 8.4: PCA of each group of dose vials performed on the NIR spectra collected from batch Zoe 5. (a, b, c) scores plots of the filtered and non-filtered 125-dose, 50-dose and 25-dose vials respectively.(d) PC2 loadings plots of the 125-dose vial.

Although the SIMCA model misclassified the filtered 125 and 50-dose vials of batch Zoe 5 the titration results of these vials did not show any differences between the filtered and non-filtered vials.

8.3.3.2. Model optimization

Model optimization was performed to improve the correct classification rates of the model. Several optimization strategies such as: (i) evaluation of different spectral preprocessing, (ii) evaluation of different spectral range and (iii) decomposition of the model into sub-models were tried. Among these, only the spectral range optimization using OPLS significantly improved the model predictive power and will therefore be discussed further.

Orthogonal Partial Least Squares regression (OPLS) offers the advantage to separate the variation correlated to Y (i.e., the predictive component) and the variation not correlated to Y (i.e., the orthogonal component). By applying OPLS on the SNV preprocessed spectra (7300-4000cm^{-1} spectral range) of all batches produced at Zoetis (5 batches, filtered and non-filtered vials, 654 spectra), the variation correlated to the dose was captured by the predictive component. The developed OPLS model covered 99.2% of the spectral variability and was composed by one predictive component (10.2% of the spectral variability) and six orthogonal components (89% of spectral variability). The scores plot showing the predictive component versus the first orthogonal component allowed clearly distinguishing between the doses (Figure 8.5). The 125-dose vials were well separated from the other dose vials and the distance in the scores plot between the 125-dose vials and the other classes of vials was in agreement with the dose content. Even although slightly overlapping, the 50- and 25-dose vials were better separated than with the PCA model.
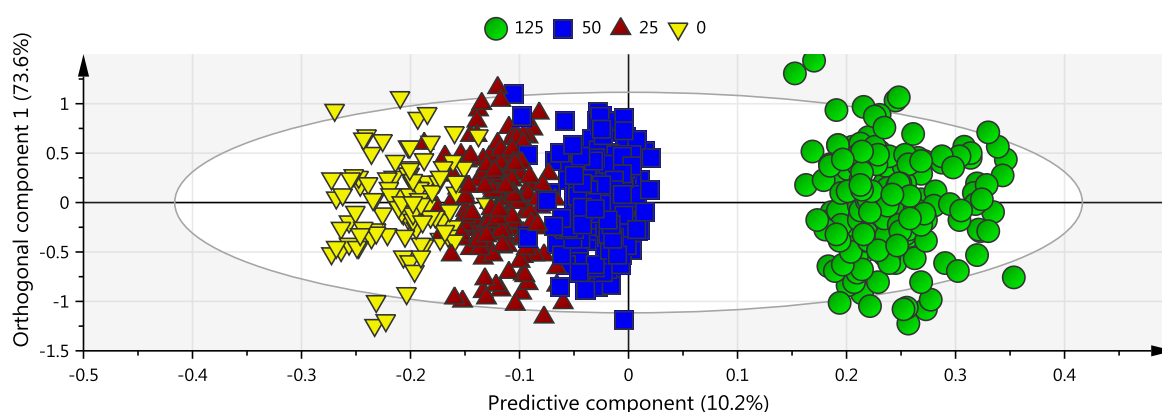
Figure 8.5: Predictive versus first orthogonal component scores plot obtained after OPLS modelling of the SNV pretreated spectra collected from all batches produced at Zoetis.

In order to identify the spectral contribution responsible for the distinction between the different dose vials by the predictive component, the loadings plot of the predictive component was examined (Figure 8.6). As already observed in the loadings plot of the second principal component of the PCA model allowing to distinguish between the different doses (Figure 8.3d), a band at 4830cm^{-1} was clearly co-responsible for distinguishing between the different doses (Figure 8.6). This band corresponds to the amide A/II. The loadings plot of the predictive component also showed two rather noisy regions (7300-7054cm^{-1} and 5700-5200cm^{-1}) having a predictive component value of approximately 0 while

this was not the case in the PCA loadings plot (Figure 8.3d). The loadings plot of the predictive component also showed a region that did not contain any information (4220-4000cm^{-1}).
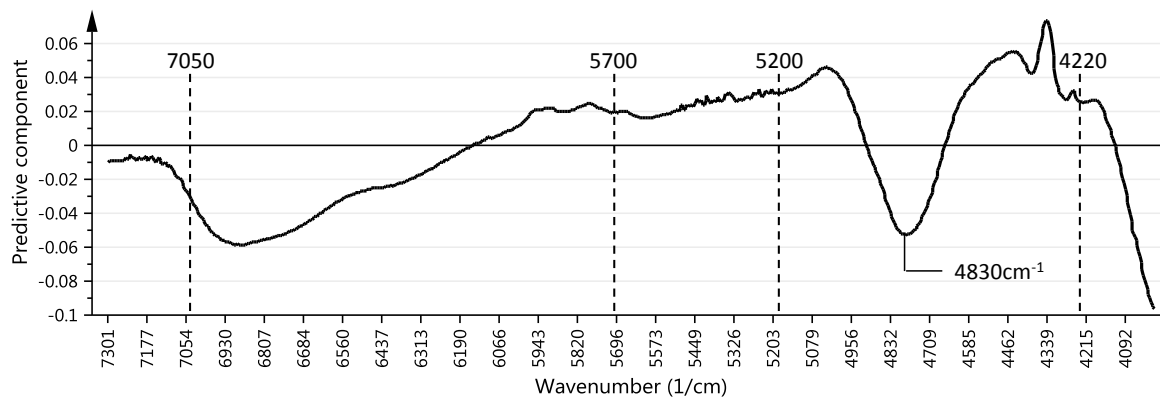
Figure 8.6: Loadings plot of the predictive component obtained after OPLS of the SNV preprocessed spectra and collected from all batches produced at Zoetis.

Based on these findings, a new spectral range more appropriate to separate the dose formulations was concluded: 7050-5700 & 5200-4220cm^{-1}.

To evaluate the effect of this new spectral range on the correct classification rates, a new SIMCA model using Zoe 1, Zoe 2 and Zoe 3 (i.e., 379 spectra, 1 spectrum per vial) was developed.

The misclassification table of Zoe 4, used as independent test set, is presented in Table 8.5. The 125-dose vial, 50-dose vial, 25-dose vial and placebo had a correct classification rate (CCR) of 97.14%, 100%, 97.14% and 100% respectively. Globally, the correct classification rate (98.5%) was almost perfect.

Table 8.5: Misclassification table obtained using Zoe 1-2-3 as calibration set and Zoe 4 as independent test set. 7050-5700 & 5200-4220cm^{-1} spectral range, SNV preprocessed.

	Members	Correct classification rate (CCR, %)	125-dose vial	50-dose vial	25-dose vial	Placebo
125-dose vial	35	**97.14%**	**34**	1	0	0
50-dose vial	35	**100%**	0	**35**	0	0
25-dose vial	35	**97.14%**	0	1	**34**	0
Placebo	28	**100%**	0	0	0	**28**
Total	133	**98.5%**	34	37	34	28

The second independent test set, batch Zoe 5, was also evaluated with the optimized spectral range. To avoid introducing misclassification caused by the filtration step (see higher), only the non-filtered vials were used. Therefore a SIMCA model using the non-filtered vials of batches Zoe 1, Zoe 2 and Zoe 3 was built using the spectral range 7050-5700 & 5200-4220cm^{-1}, SNV preprocessed. Because a new model was built (with the non-filtered vials exclusively), the non-filtered vials from Zoe 4 were also evaluated. The misclassification table of both independent test sets (Zoe 4 and Zoe 5) is presented in Table 8.6.

Table 8.6: Misclassification table obtained using Zoe 1-2-3 as calibration set and Zoe 4 and Zoe 5 as independent test sets. 7050-5700 & 5200-4220cm^{-1} spectral range, SNV preprocessed.

	Zoe 4 non-filtered						Zoe 5 non-filtered					
	Members	CCR, %	125 dose-vial	50 dose-vial	25 dose-vial	Placebo	Members	CCR, %	125 dose-vial	50 dose-vial	25 dose-vial	Placebo
125-dose vial	17	**94.12%**	**16**	1	0	0	49	**100%**	**49**	0	0	0
50-dose vial	17	**100%**	0	**17**	0	0	41	**100%**	0	**41**	0	0
25-dose vial	18	**94.44%**	0	1	**17**	0	34	**88.24%**	0	4	**30**	0
Placebo	28	**100%**	0	0	0	**28**	18	**94.44%**	0	0	1	**17**
Total	80	**97.50%**	16	19	17	28	142	**96.48%**	49	45	31	17

Globally, both test sets were well classified except four 25-dose vials of Zoe 5 which were classified as 50-dose vial. This observation is not surprising considering that both classes still slightly overlap in the OPLS scores plot (Figure 8.5).

8.3.3.3. Classification validation

The above evaluated classification of two independent test sets (i.e., Zoe 4 and Zoe 5) already constitutes an important part of the validation. Nevertheless, referring to the EMA guidelines, qualitative NIR procedures should be validated for a minimum of specificity and robustness [19]. Therefore, the developed classification model in this study (using batches Zoe 1-2-3, 7050-5700 & 5200-4220cm^{-1} SNV preprocessed spectra) was further validated by determining its sensitivity, specificity and accuracy. These parameters were determined using the two independent test sets available for this study (i.e., Zoe 4 and Zoe 5) and are presented in Table 8.7.

Table 8.7: Validation parameters (sensitivity, specificity, and accuracy) obtained using the optimized spectral range (7050-5700 & 5200-4220cm^{-1}) SNV preprocessed: (a) Zoe 1-2-3 filtered and non-filtered combined in calibration set, Zoe 4 filtered and non-filtered combined as independent test set and (b) Zoe 1-2-3 non-filtered as calibration set, Zoe 5 non-filtered as independent test set.

a)	Sensitivity	Specificity	Accuracy
125-dose vial	97.14%	100%	99.25%
50-dose vial	100%	97.96%	98.50%
25-dose vial	97.14%	100%	99.25
Placebo	100%	100%	100%

b)			
125-dose vial	100%	100%	100%
50-dose vial	100%	96.04%	97.18%
25-dose vial	88.24%	99.07%	96.48%
Placebo	94.44%	100%	98.59%

All obtained validation values were above 95% except in two cases. The sensitivity reflects the ability of the model to correctly classify new doses. The model built using the non-filtered vials had a lower sensitivity to detect the 25-dose vials. With all values above 96%, the specificity of the model was excellent. This means that the risk to attribute a dose vial to

a wrong class is very low. Remarkably, both the 125-dose vial and the placebo had a specificity of 100%. Finally, the accuracy values of the models were all above 96%.

The robustness of the model is a measure of its capacity to remain unaffected by small but deliberate variations in method parameters and provides an indication of its reliability during normal usage [21]. The dose classification of the vials from the batch freeze-dried in another freeze-dryer (UGent batch) and having higher residual moisture content was considered as being an interesting case for model robustness evaluation.

Using the model built with batches Zoe 1-2-3 (filtered and non-filtered vials), 7050-5700 & 5200-4220cm^{-1} SNV preprocessed spectra, the correct classification rates obtained using UG as test sets were 0% for all doses and placebos (data not shown). In addition of being lyophilized in another freeze-dryer the vials of UG batch had higher residual moisture content than the vials used in the calibration set (Figure 8.2). Considering that the used spectral range 7050-5700 & 5200-4220cm^{-1} contains a water band at 5100-5200cm^{-1} [22], logically, the classification model is sensitive to the residual moisture content of new vials. In order to be classified, new vials must have a residual moisture included in the residual moisture range of the vials used to build the model. The classification rates of UG could probably be improved by the addition of supplemental batches in the model varying in moisture content and produced using different freeze-dryers. The robustness study has shown that the model was very sensitive to the residual moisture content of the vials to be classified.

8.4. CONCLUSION

This study demonstrates the possibility of NIR spectroscopy to classify freeze-dried live, attenuated virus vaccines according to their dose. A PCA was performed in order to detect trends and possible outliers. Two doses (i.e., 50-dose vial and 25-dose vial) could not clearly be distinguished in the PCA model. Therefore, the SIMCA modelling approach was selected since its ability to better deal with classes that do not occupy a separate volume in the X-space. The optimization of the calibration model was performed by optimizing the spectral range via Orthogonal Partial Least Squares regression. The optimized spectral range 7050-5700 & 5200-4220cm^{-1} contained the amide A/II region which was involved in the separation

of the different dose vials in the PCA but also identified in the predictive component of the OPLS model. The optimized calibration model was able to classify vials of an independent test set with a global correct classification rate of 98.5% (test set Zoe 4). The optimized model was also characterized for its specificity, sensitivity and accuracy following the EMA guidelines. With all values above 96%, the specificity of the model was excellent meaning that the risk to attribute a dose vial to a wrong class was very low. In addition, both the 125-dose vial and the placebo had a specificity of 100%. Finally, the robustness study demonstrated that the classification of new vials was sensitive to their residual moisture content. In order to be classified, new vials must have a residual moisture included in the residual moisture range of the vials used to build the model.

REFERENCES

[1]   World Health Organization, The art of saving a life. Available at: http://artofsavingalife.com/about/ January, 2015. Accessed on February 10, 2015.

[2]   National Institute of Allerfy and Infectious Diseases.Types of vaccines. Available at: http://www.niaid.nih.gov/topics/vaccines/understanding/pages/typesvaccines.aspx. April, 2012 Accessed on February 10, 2015.

[3]   J. Peetermans. Factors affecting the stability of viral vaccines. Development in Biological standardization, 1996; 87:97-101.

[4]   D. Chen, and D. Kristensen. Opportunities and challenges of developing thermostable vaccines. Expert Review Vaccines, 2009; 8(5): 547-557.

[5]   O.S. Kumru, S.B. Joshi, D.E. Smith, C.R. Middaugh, T. Prusik, D.B. Volkin. Vaccine stability in the cold chain: Mechanisms, analysis and formulation strategies. Biologicals, 2014;42: 237-259.

[6]   M.J. Pikal. Freeze-drying. In:Swarbrick JS, Boylan JC. Encyclopedia of Pharmaceutical Technology. New York: Marcel Dekker, 2002:1807-33.

[7]   D.B. Volkin, C.J. Burke, G. Sanyal, C.R. Middaugh. Analysis of vaccine stability. Development in Biological standardization, 1996;87 : 135-142.

[8]   C.J. Burke, T-A. Hsu, D.B. Volkin. Formulation, stability, and delivery of live attenuated vaccines for human use. Therapeutic Drug Carrier Systems, 1999;16 (1): 1-83.

[9]   D.T. Brandau, L.S. Jones, C.M. Wiethoff, J. Rexroad, C.R. Middaugh. Thermal stability of vaccines. Journal of Pharmaceutical Sciences, 2003; 92(2): 218-231.

[10]   L. Hansen, S. Pieters, R. Daoussi, JP. Montenez, C. Vervaet, JP. Remon, T. De Beer. Near-infrared spectrsocopic evaluation of lyophilized viral vaccine formulations. Biotechnology Progress, 2013;29 (6): 1573-1586.

[11]   L. Jodar, P. Duclos, J.B. Milstien, E. Griffiths, M.T. Aguado, C.J. Clemens. Ensuring vaccine safety in immunization programmes – a WHO perspective. Vaccine, 2001;19: 1594-1605.

[12] P.K. Drain, C.M. Nelson, J.S. Lloyd. Single-dose versus multi-dose vaccine vials for immunization programmes in developing countries. Bulletin of the World Health Organization, 2003; 81(10).

[13] L. Zhang, M.J. Henson, S.S. Sekulic. Multivariate data analysis for Raman imaging of a model pharmaceutical tablet. Analytica Chimica Acta, 2005;545: 262-278.

[14] A. de Juan, R. Tauler. Chemometrics applied to unravel multicomponent processes and mixtures: Revisiting latest trends in multivariate resolution. Analytica Chimica Acta, 2003;500: 195-210.

[15] H. Eastment, and W. Krzanowski. Crossvalidatory choice of the number of components from a principal component analysis, Technometrics, 1982;24: 73-77

[16] L. Eriksson, E. Johansson, N. Kettaneh-Wold, J. Trygg, C. Wikström, S. Wold. Multi- and Megavariate Data Analysis. Part I: Basic Principles and Applications. Umea: Umetrics, 2006.

[17] S. Wold. Pattern Recognition, 1976;8: 127-136.

[18] Y. Roggo, P. Chalus, L. Maurer, C. Lema-Martinez, A. Edmond, N. Jent. A review of near infrared spectroscopy and chemometrics in pharmaceutical technologies. Journal of Pharmaceutical and Biomedical Analysis, 2007; 44: 683-700.

[19] The European Agency for the Evaluation of Medicinal Products, Guideline on the use of near infrared spectroscopy by the pharmaceutical industry and the data requirements for new submissions and variations, EMEA/CVMP/QWP/17760/2009 Rev2, 2014.

[20] L.G. Weyer, S.C. Lo. Spectra-Structure correlations in the Near-infrared. In: J.M. Chalmers and P.R. Griffiths (Eds.) Handbook of Vibrational Spectroscopy, John Wiley & Sons, United Kingdom, 2002, 1859-1879.

[21] International Conference on Harmonisation (ICH) of technical Requirements for Registration of Pharmaceuticals for human Use, Q2 (R1), Validation of Analytical Procedures: Text and Methodology, Geneva, 2005.

[22] T. De Beer, M. Wiggenhorn, A. Hawe, J.C. Kasper, A. Almeida, T. Quinten, W. Friess, G. Winter, C. Vervaet, J.P. Remon. Optimisation of a pharmaceutical freeze-dried product and its process using an experimental design approach and innovative process analysers. Talanta, 2011; 83: 1623-1633.

CHAPTER 9

FAST AND NON-DESTRUCTIVE TITER PREDICTION OF A FREEZE-DRIED VIRUS VACCINE FORMULATION USING NIR SPECTROSCOPY: A PRELIMINARY STUDY

ABSTRACT

This chapter evaluates the possibility to predict the titer of a freeze-dried live, attenuated virus vaccine formulation using near-infrared (NIR) spectroscopy. Firstly, the critical dose content allowing to detect titer variations of a live, attenuated virus by NIR spectroscopy was determined. Therefore, three dose presentations (i.e., 125-dose vials, 50-dose vials and 25-dose vials) pre-freeze-drying treated by exposure during 0, 3 or 7 days to room temperature and resulting in different virus titers, were freeze-dried. After freeze-drying, the off-line collected NIR spectra were evaluated using Principal Component Analysis (PCA) and demonstrated that the only suitable dose presentation (allowing the detection of titer variations) was the 125-dose, being the highest dose content. Secondly, a calibration data set existing of NIR spectra of freeze-dried 125-dose vials, exposed 0, 9, 16, 23 or 30 days to room temperature prior to freeze-drying and resulting in different virus titers, was modeled using orthogonal partial least squares (OPLS) and partial least squares (PLS) regression in order to predict the titer of new independent freeze-dried vials. After spectral range and spectral preprocessing optimization, a model with a root mean square error of prediction (RMSEP) of 0.19 $\log_{10}$ $CCID_{50}$ was obtained, indicating good predictive performance of the model.

CHAPTER 9

FAST AND NON-DESTRUCTIVE TITER PREDICTION OF A FREEZE-DRIED VIRUS VACCINE FORMULATION USING NIR SPECTROSCOPY: A PRELIMINARY STUDY

9.1. INTRODUCTION

In order to overcome the limited stability of biopharmaceutical products in aqueous solution, freeze-drying (also called lyophilization) of the formulation has become a well-established technique, often used in the biopharmaceutical industry despite its disadvantages of cost and process time. Briefly, the freeze-drying process consists of three main consecutive steps: freezing, primary drying and secondary drying. During the freezing step, the product temperature is decreased (approx. -40 to -50°C) in order to convert most of the water into ice. Herewith, the solutes are crystallized or transformed into an amorphous system. During primary drying, vacuum is introduced in the freeze-drying chamber hence removing the ice by sublimation. The secondary drying step ends the process by removing the unfrozen water from the amorphous phase by desorption [1].

More and more, the pharmaceutical industry, encouraged by the FDA's process analytical technology (PAT) initiative [2], is investing in analytical methods providing ultra-fast (i.e. real-time) and information-rich data. NIR spectroscopy is a molecular vibrational spectroscopic technique allowing fast and non-destructive measurements without any sample preparation [3]. Implemented in the freeze-dryer using fiber optic probes, NIR spectroscopy has already demonstrated its possibility to in-line monitor critical process [4-6] and product information (e.g. protein unfolding [7]). In addition to the well-known possibility to measure off-line the residual moisture of a freeze-dried product [8-11], the possibility to use NIR spectroscopy to evaluate live, attenuated viruses in freeze-dried samples varying in term of virus medium

volume or pre-freeze-drying treatment has also been demonstrated [12]. This was possible by evaluating two NIR spectral regions: (i) the 7300-4000cm^{-1} region containing the amide A/II band which might reflect information on the coated proteins of the freeze-dried live, attenuated viruses; and (ii) the C-H vibration overtone regions (10,000-7500 and 6340-5500cm^{-1}) which might supply information on the lipid layer surrounding the freeze-dried live, attenuated viruses.

The possibility to evaluate different pre-freeze-drying treated live, attenuated viruses (and hence having different titers) [12] offers several opportunities to develop new applications for the pharmaceutical industry. Among these applications, the prediction of the virus titer based on NIR spectra collected off-line, after freeze-drying and during storage, is of great interest. Indeed, at the end of the freeze-drying process, the overall potency of the vaccine is generally measured by cell-based viral plaque assay. Having the advantage of being time-honored and widely accepted, these assays are also known to be relatively imprecise, labor-intensive and time-consuming [13-15]. In addition, they do not provide any useful information regarding the degradation mechanism that the viruses undergo during the process and during storage.

The aim of this chapter is to evaluate the possibility to predict the titer of new freeze-dried samples based on their NIR spectra. The first phase is dedicated to the determination of the critical dose content of the studied live, attenuated virus vaccine needed to be able to distinguish between different pre-freeze-drying treated live, attenuated viruses (hence resulting in different titers). Three dose presentations (i.e., 125-dose vials, 50-dose vials and 25-dose vials) were pre-freeze-drying treated by exposure during 0, 3 or 7 days to room temperature. After freeze-drying, NIR spectra were collected from these samples and were evaluated by Principal Component Analysis (PCA) using the 7300-4000cm^{-1} spectral region containing the amide A/II band. The objective of the second phase of the study is to develop a calibration model able to predict the virus titer of new freeze-dried vials. Therefore, a calibration model was built using NIR spectra of vials (having the critical dose content as determined in the first phase of the study) prepared by pre-freeze-drying treatment (i.e., exposure during 0, 9, 16, 23 and 30 days to room temperature prior to freeze-drying). Using

the developed model, the possibility to predict the titer of vials coming from an independent test set (i.e., one independent batch) was then evaluated.

9.2. MATERIALS AND METHODS

9.2.1. Materials

The live, attenuated virus used as vaccine in this study as well as its stabilizer solution were obtained from Zoetis. The stabilizer solution was kept constant (volume and concentration) in all formulations.

The chapter is divided into two phases. In phase 1 (i.e., the determination of the critical dose content), the virus dose as well as the virus pre-freeze-drying treatment were varied. In phase 2 (i.e., the evaluation of the possibility to predict the virus titer), the virus dose was kept constant (at the dose at which titer variations could be detected) and only the virus pre-freeze-drying treatment was varied.

The formulations used for phase 1 are presented in Table 9.1. Three different virus dose presentations (i.e., 125-dose vials, 50-dose vials and 25-dose vials) combined with three different pre-freeze-drying treatments were used (i.e., exposure during 0, 3 or 7 days to room temperature).

The virus medium volume was varied in order to obtain the correct number of doses and compensated by Ultraculture (Lonza, Belgium), a medium free from virus, in order to keep the total volume identical among all samples. For clarity, the three different virus medium volumes (i.e., e, f, g ml in Table 9.1) used to prepare the different doses were compensated by the addition of an appropriate volume of medium free of virus (i.e. h-e, h-f and h-g, Table 9.1) in order to have a total volume of 5ml).

Table 9.1: Formulations used in phase 1 of the study.

Stress time (days)	Doses	Virus medium volume (ml)	Stabilizer solution	qsp filling volume, Ultraculture - medium free from viruses (ml)	Total volume (ml)
0	25	e	33% (v/v)	h-e	5
3	25	e	33% (v/v)	h-e	5
7	25	e	33% (v/v)	h-e	5
0	50	f	33% (v/v)	h-f	5
3	50	f	33% (v/v)	h-f	5
7	50	f	33% (v/v)	h-f	5
0	125	g	33% (v/v)	h-g	5
3	125	g	33% (v/v)	h-g	5
7	125	g	33% (v/v)	h-g	5

All symbols (e, f, g and h) represent absolute values in µl.

The formulations used for phase 2 are presented in Table 9.2. A fixed dose (i.e., the dose at which titer variations could be detected) was used during this study. In order to obtain formulations having different titers, the formulations were stressed at room temperature during different periods of time (i.e. 0, 9, 16, 23 or 30 days) prior to freeze-drying. An independent test set was also prepared according to the same procedure (i.e. exposure of the formulation to room temperature before freeze-drying, see also Table 9.2).

Table 9.2: Formulations used in phase 2.

	Stress time (days)	Doses*	Virus medium volume (ml)	Stabilizer solution	*qsp* filling volume, medium free from viruses (ml)	Total volume (ml)
Calibration set	0	125	g	33% (v/v)	h-g	5
	9	125	g	33% (v/v)	h-g	5
	16	125	g	33% (v/v)	h-g	5
	23	125	g	33% (v/v)	h-g	5
	30	125	g	33% (v/v)	h-g	5
Test set	0	125	g	33% (v/v)	h-g	5
	7	125	g	33% (v/v)	h-g	5
	11	125	g	33% (v/v)	h-g	5

All symbols (g and h) represent absolute values in µl
* the dose at which titer variations could be detected (see results).

9.2.2. Freeze drying

All samples used in this study were produced at Zoetis and freeze-dried using a Lyostar 3 freeze-dryer (SP scientific, Stone Ridge, NY, USA). The freeze-drying settings were optimized by Zoetis and cannot be disclosed for confidentiality reasons. All freeze-dried vials had a visually acceptable cake aspect.

9.2.3. Titration

Titration (potency assay) was done according to Zoetis' internal SOP. Each titer is expressed in $\log_{10}$ $CCID_{50}$ (Cell Culture Infection Dose 50). Titration provides information about the number of living viral particles contained in each sample. Each titrated sample was evaluated twice. Three samples per dose and per pretreatment were titrated except for the calibration set (phase 2) where 13 samples per pretreatment were titrated.

9.2.4. Residual moisture analysis

The residual moisture content of the freeze-dried samples was determined via Karl Fischer titration. After each freeze-drying cycle, three samples per dose and per pretreatment were analyzed with a Metrohm 860 KF Thermoprep (oven) coupled to a Metrohm 852 Titrando (Herisau, Switzerland).

9.2.5. NIR spectroscopy

NIR spectra of all freeze-dried samples were collected off-line using a Fourier-Transform NIR spectrometer (Thermo Fisher Scientific, Nicolet Antaris II near-IR analyzer) equipped with an InGaAs detector and a quartz halogen lamp. All NIR spectra were recorded in the 10000-4000cm^{-1} region with a resolution of 8 cm^{-1} and averaged over 16 scans. One NIR spectrum per freeze-dried sample (in random order) was collected through the bottom of the glass vial using the integrating sphere device immediately after freeze-drying.

9.2.6. Data analysis

NIR spectral data analysis was done using SIMCA 14.0 (Umetrics, Umea, Sweden). All collected NIR spectra were mean centered and preprocessed using standard normal variate (SNV) in order to eliminate the additive baseline offset variations and multiplicative scaling effects in the spectra which may be caused by possible differences in sample density and different-sample-to-sample measurement variations. Second derivative with 37 Savitzky-Golay smoothing points was also applied in phases 1 and 2. Second derivative was used for (a) spectral discrimination improvement, as a qualitative fingerprinting technique to accentuate small structural differences between similar spectra and for (b) spectral resolution enhancement.

9.2.6.1. Principal Component Analysis

The collected NIR spectra were firstly analyzed as one data matrix (**D**) using principal component analysis (PCA), an unsupervised multivariate data analysis method allowing to examine whether NIR spectroscopy can distinguish between the different pre-freeze-drying

treatment. PCA produces an orthogonal bilinear data matrix (**D**) decomposition, where principal components (PCs) are obtained in a sequential way to explain maximum variance:

$$D = TP^T + E$$

$$= t_1 p'_1 + t_2 p'_2 + \ldots + t_Q p'_Q + E$$

Where **T** is the *M x Q* score matrix, **P** is the *N x Q* loading matrix, **E** is the *M x N* model residual matrix, i.e., the residual variation of the data set that it is not captured by the model. **Q** is the selected number of PCs, each describing a non-correlated source of variation in the data set, and **N** is the number of collected spectra at **M** wavelengths [16]. Each principal component consists of two vectors, the score vector **t** and the loading vector **p**. The score vector contains a score value for each spectrum, and this score value informs how the spectrum is related to the other spectra in that particular component. The loading vector indicates which spectral features in the original spectra are captured by the component studied. These abstract, unique, and orthogonal PCs are helpful in deducing the number of different sources of variation present in the data. However, these PCs do not necessarily correspond to the true underlying factors causing the data variation, but are orthogonal linear combinations of them, since each PC is obtained by maximizing the amount of variance it can explain [17].

The number of PCs included in the PCA model was determined by cross validation using the approach of Krzanowski [18]. The data are divided into 7 groups and a model was generated for the data devoid of one group. The deleted group was predicted by the model and the squared differences between the predicted and observed values were summed to form the Predictive Residual Sum of Squares (PRESS). This procedure was repeated 7 times, followed by the summation of all partial PRESS-values in terms of an overall PRESS-value. If a new PC_i enhanced the predictive power compared with the preceding PC_{i-1}, the new PCi was kept in the model [19].

9.2.6.2. Partial least squares (PLS) regression

Partial least squares (PLS) regression is a commonly applied multivariate calibration technique. In PLS, a (in our case, spectroscopic) data matrix (**X**) is decomposed taking into account the underlying relationship between **X** and the y-vector. In PCA, the decomposition of the data matrix is performed regardless the y-vector [20].

9.2.6.3. Orthogonal PLS

Orthogonal Partial Least Squares to latent structures (OPLS) is a modification of the PLS method designed to handle variation in X (i.e., in this study the spectroscopic data matrix) that is orthogonal to Y (i.e., in this study the titer). OPLS separates the systematic variation in X into two parts, one that is linearly related (and therefore predictive) to Y and one that is uncorrelated (orthogonal) to Y. The predictive variation of Y in X is modeled by the predictive component whereas the variation in X, which is orthogonal to Y, is modeled by the orthogonal components. This partitioning of the X-data provides improved model transparency and interpretability.

9.2.6.4. Permutation test

In order to check that the built PLS and OPLS model do not only fit the training set well but poorly predict the new observations, a permutation test was used. The idea of this validation is to compare the goodness of fit (R^2) and the goodness of prediction (Q^2) of the original model with the goodness of fit and the goodness of prediction of several models based on data where the Y values have been randomly permuted, while the X-matrix has been kept intact.

9.2.6.5. Evaluation of model performance

The different models were compared by analyzing their root mean square error of prediction (RMSEP) which can be calculated by:

$$(\Sigma(y\ obs - y\ pred)^2 / n)^{1/2}.$$

Low values of this chemometric validation parameter indicate good quantitative model performances.

9.3. RESULTS

The results are divided according to the two phases; (phase 1) the evaluation of the critical dose content allowing to distinguish between the NIR spectra of live, attenuated virus samples differently pre-freeze-drying treated (hence resulting in different titers, see further) and (phase 2) the evaluation of the possibility to predict the virus titer of new freeze-dried vials based on their NIR spectra.

9.3.1. Phase 1: Evaluation of the critical dose content

9.3.1.1. Titration and residual moisture results

Three different virus dose presentations (i.e., 125-dose vials, 50-dose vials and 25-dose vials) combined with three different pre-freeze-drying treatments (i.e., exposure during 0, 3 or 7 days to room temperature prior to freeze-drying), were used in this study. The virus titer and residual moisture results are presented in Figure 9.1. As expected, the titers increased with the dose content and decreased with the number of exposition days to room temperature (Figure 9.1a). For all dose contents (i.e., 125-dose, 50-dose and 25-dose), the formulations exposed 0 and 7 days to room temperature as well as the formulations exposed 0 and 3 days to room temperature resulted in different titers. The formulations exposed 3 and 7 days to room temperature resulted in different titers only for the 25-dose vials.

Similarly, samples of each dose presentation and of each stressing time were also analyzed using Karl Fischer and all residual moisture values were found to be below 1.6% and not to be different from each other (Figure 9.1b).
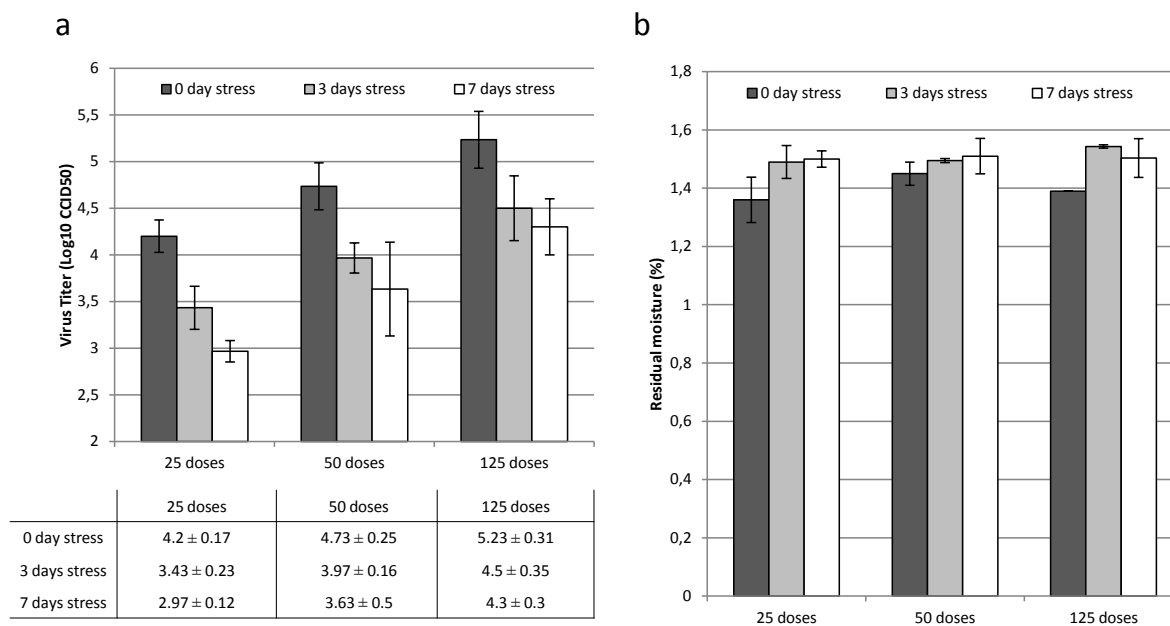
	25 doses	50 doses	125 doses
0 day stress	4.2 ± 0.17	4.73 ± 0.25	5.23 ± 0.31
3 days stress	3.43 ± 0.23	3.97 ± 0.16	4.5 ± 0.35
7 days stress	2.97 ± 0.12	3.63 ± 0.5	4.3 ± 0.3

Figure 9.1: Titration (a) and residual moisture (b) results of the different formulations used in phase 1. Titers are expressed as $\log_{10}$ $CCID_{50}$ (Cell Culture Infection Dose 50) and presented in a table below the titer bar chart. Each titer and residual moisture result is the average of three determinations.

9.3.1.2. Principal Component Analysis

In order to determine the critical dose content allowing to distinguish between the NIR spectra of live, attenuated virus samples differently pre-freeze-drying treated (hence resulting in different titers), each dose content (i.e., 125-dose, 50-dose and 25-dose) was separately analyzed with PCA using the $7300\text{-}4000\text{cm}^{-1}$ spectral range, SNV and 2nd derivative preprocessed.

The PCA model developed from the NIR spectra of the 125-dose vials exposed during 0, 3 and 7 days to room temperature (i.e., 35 spectra, 1 spectrum per vial, 12 vials per exposure time, 1 outlier left out) was composed by 3 principal components and explained 88.2% of the spectral variability. The PC2 (capturing 14.1% of the overall spectral variability) versus PC3 (capturing 7.96% of spectral variability) scores plot (Figure 9.2a) distinguished between the 125-dose vials exposed 0, 3 or 7 days to room temperature. The separation was caused by a combination of both components. Analysis of the PC2 loadings plot (Figure 9.2a) showed that PC2 correlates mainly with the residual moisture content and was in agreement with the Karl Fischer results (i.e., 0 day stressed samples have a bit lower residual moisture

content than 3 and 7 days stress). Analysis of PC3 loadings plot (Figure 9.2b) showed that several peaks were involved in the separation between vials exposed different days to room temperature. Interestingly a peak located in the region of the amide A/II band (4850cm^{-1}) can be observed in the PC3 loadings plot.
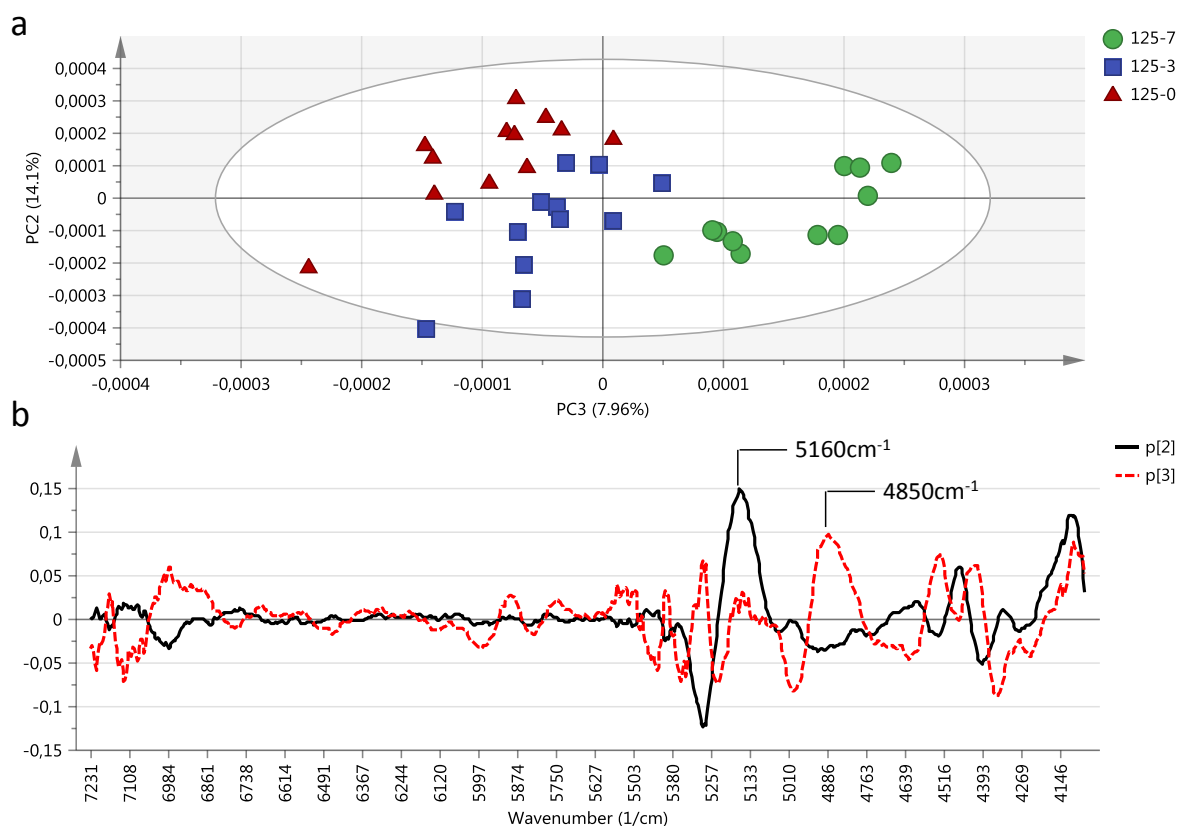

Figure 9.2: Scores and loadings plot of the PCA model built with SNV and 2nd derivative preprocessed NIR spectra of the 125-dose vials exposed during 0, 3 and 7 days to room temperature. (a) PC2 versus PC3 scores plot of the PCA built with the spectral range 7300-4000cm^{-1}. (b) PC2 and PC3 loadings plot of the PCA built with the spectral range 7300-4000cm^{-1}.

Similarly, a PCA was performed on the 50-dose and 25-dose vials exposed during 0, 3 and 7 days to room temperature. The PCA model built with the NIR spectra of the 50-dose vials exposed during 0, 3 and 7 days to room temperature (i.e., 36 spectra, 1 spectrum per vial, 12 vials per exposure time) was composed of 4 principal components and explained 95.8% of the spectral variability. The PC1 versus PC4 scores plot (Figure 9.3) showed that only the 50-dose samples exposed during 7 days to room temperature were separated from the other exposed samples (i.e., 0 and 3 days) according to PC4 (accounting for 2.44% of spectral

variability). Analysis of the PC4 loadings plot showed that the amide A/II band (4850cm^{-1}) was involved in the separation according PC4 (data not shown).
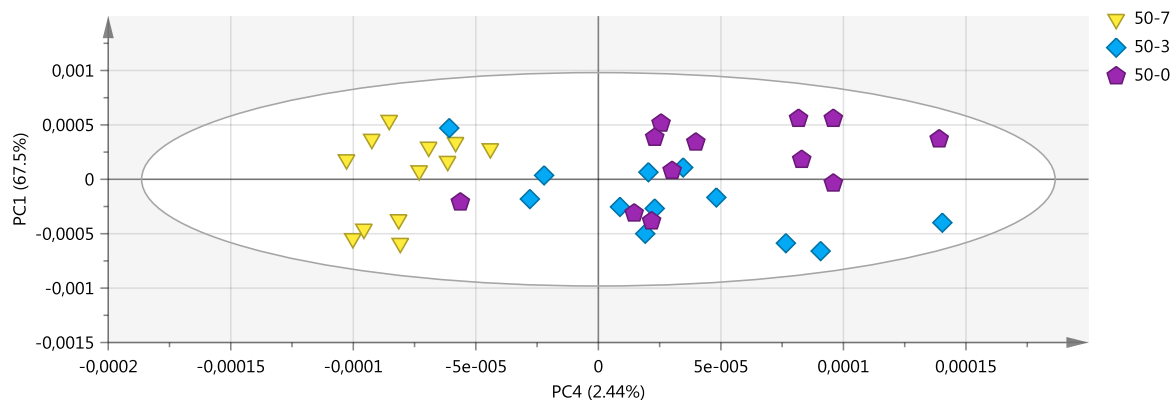

Figure 9.3: PC1 versus PC4 scores plot of the PCA model built with the spectral range 7300-4000cm^{-1} SNV and 2nd derivative preprocessed NIR spectra of the 50-dose vials exposed during 0, 3 and 7 days to room temperature.

The last PCA model, built with the NIR spectra of the 25-dose vials exposed during 0, 3 and 7 days to room temperature (i.e., 36 spectra, 1 spectrum per vial, 12 vials per exposure time), was composed of 4 principal components and explained 95.8% of the spectral variability. No PC combination was able to distinguish between the differently pre-freeze-drying treated vials.

Using the 7300-4000cm^{-1} spectral range, containing the amide A/II band which might provide information on the virus coated proteins [12], it was possible to distinguish all the 125-dose vials according to their pre-freeze-drying treatment. Using the 50-dose vials, it was only possible to distinguish the vials exposed 7 days to room temperature and finally, no distinction between the differently pre-freeze-drying treated 25-dose vials was detected. Therefore, 125-dose vial is the critical dose content allowing to distinguish between the NIR spectra of live, attenuated virus samples differently pre-freeze-drying treated (hence resulting in different titers).

9.3.2. Phase 2: Evaluation of the possibility to predict the virus titer

The aim of phase 2 was to evaluate the possibility of NIR spectroscopy to predict the titer of live, attenuated virus vaccine vials after freeze-drying. Therefore, OPLS and PLS models were developed. Nevertheless, prior the model development, the selection of an adequate calibration set was critical. According to the results presented above (phase 1), the 125-dose vials were selected. Indeed, the 125-dose vials were the only ones in which differently pre-freeze-drying treated live, attenuated viruses (and hence having different titers) could be detected by NIR spectroscopy. In order to have the largest possible titer range, 125-dose formulations were pre-freeze-drying treated by exposure to room temperature during different periods of time (i.e., 0, 9, 16, 23 and 30 days). After freeze-drying, NIR spectra of all vials were collected, the samples of the calibration set (i.e., the dataset used to build the model) were titrated, and their residual moisture was measured. In addition, prior to the development of the prediction model, a PCA was performed in order to verify whether the samples of the calibration set with different titers could be distinguished by NIR spectroscopy.

9.3.2.1. Titration and residual moisture results

The titration and residual moisture results are presented in Figure 9.4. Regarding the obtained titers, the 125-dose vials can be subdivided into 3 groups. The 125-dose vials exposed during 0 days to room temperature (5.09±0.20 (n=13)) constitute the first group. The 125-dose vials exposed during 9 and 16 days to room temperature, with titers of (3.82±0.11 (n=13)) and (3.65±0.18 (n=13)) respectively, form the second group. The third group is composed by the 125-dose vials exposed during 23 and 30 days to room temperature having titers of 2.98 ±0.15 (n=13) and 3.17 ±0.17 (n=13) respectively.

The vials were also analyzed with Karl Fischer and all residual moisture values were found to be below 1.7% and not to be different from each other although a slight residual moisture increase with the number of exposition days to room temperature can be observed. The 125-dose vials exposed 0, 9, 16, 23 and 30 days had a residual moisture of 1.35%±0.11 (n=3), 1.37%±0.07 (n=3), 1.49%±0.12 (n=3), 1.54%±0.07 (n=3) and 1.59%±0.09 (n=3), respectively.
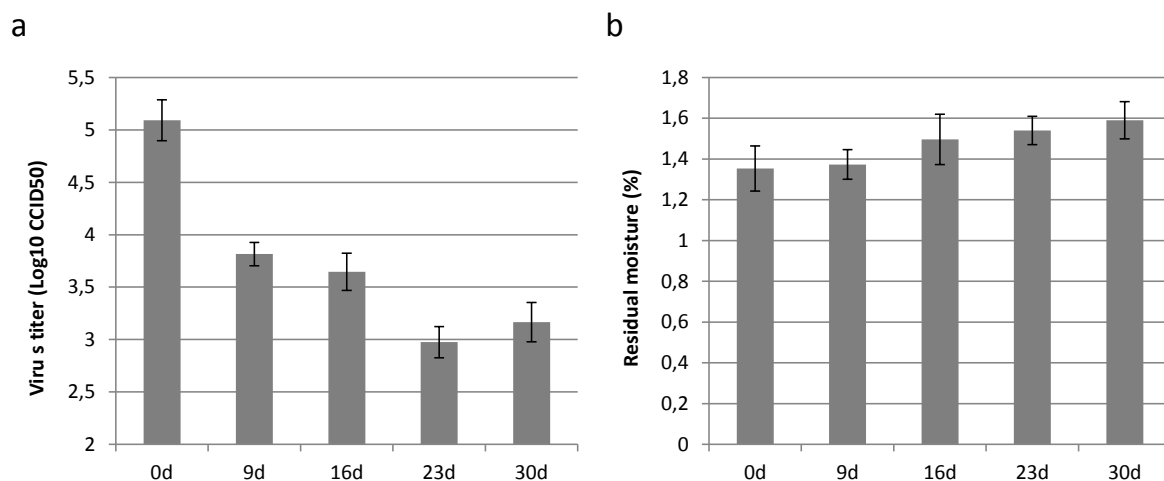
Figure 9.4: Titration (a) and residual moisture (b) results of the different formulations used as calibration set in study 2 (d = exposure day(s) to room temperature). Titers are expressed as $\log_{10}$ CCID$_{50}$ (Cell Culture Infection Dose 50). Each titer is the average of 13 determinations and each residual moisture result is the average of 3 determinations.

9.3.2.2. Principal Component Analysis

Before building the calibration model, two PCA were performed. The objective of the first PCA model was to determine if the slight residual moisture increase detected by the Karl Fischer analysis influenced the NIR spectra. The second PCA model was built in order to verify whether NIR spectroscopy was able to distinguish the vials of the calibration set having different titers (i.e., exposed 30 days, 9 days and 0 day to room temperature).

The fist PCA model was developed using a short spectral region containing the water band (5450-5021cm^{-1}) and SNV preprocessed spectra. The built model combining the 125-dose vials exposed 0, 9 and 30 days to room temperature (i.e., 66 spectra, 1 spectrum per vial, 22 vials per exposure time) was composed by 2 principal components explaining 99.3% of the spectral variability. The PC1 (capturing 94.4% of the spectral variability) scores line plot is presented in Figure 9.5. As can be observed, no variation of PC1 accounting for water is observed, confirming that the NIR spectra are not influenced by the slight residual moisture increase observed by Karl Fischer.
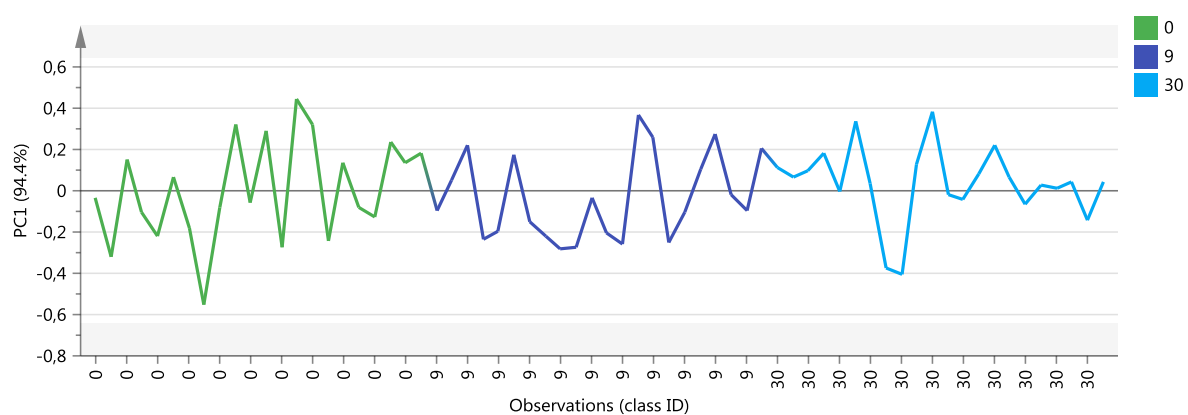
Figure 9.5: PC1 scores line plot of the PCA model built with the SNV preprocessed NIR spectra (5450-5021cm^{-1} spectral range) of the 125-dose vials exposed during 0, 9 and 30 days to room temperature.

The second PCA model was developed using the same spectral range as used in phase 1 (7300-4000cm^{-1}) and SNV combined with 2nd derivative preprocessed spectra. The PCA model combining the 125-dose vials exposed 0, 9 and 30 days to room temperature (i.e., 66 spectra, 1 spectrum per vial, 22 vials per exposure time) was composed by 3 principal components explaining 96% of the spectral variability. The PC2 (capturing 29.7% of the spectral variability) versus PC3 (capturing 8.63% of the spectral variability) scores plot (Figure 9.6) nearly distinguished the differently pretreated formulations. The formulation exposed during 9 days to room temperature was located between the 125-dose vials exposed during 0 and 30 days in the scores plots but slightly overlapped with the two groups. The analysis of the loadings plot was then performed in order to identify the spectral contribution to this separation. The amide A/II band (4850cm^{-1}) was identified and no water band was observed in both PC loadings plots indicating that the residual moisture did not influence the separation of the differently pre-freeze-drying treated viruses.

243
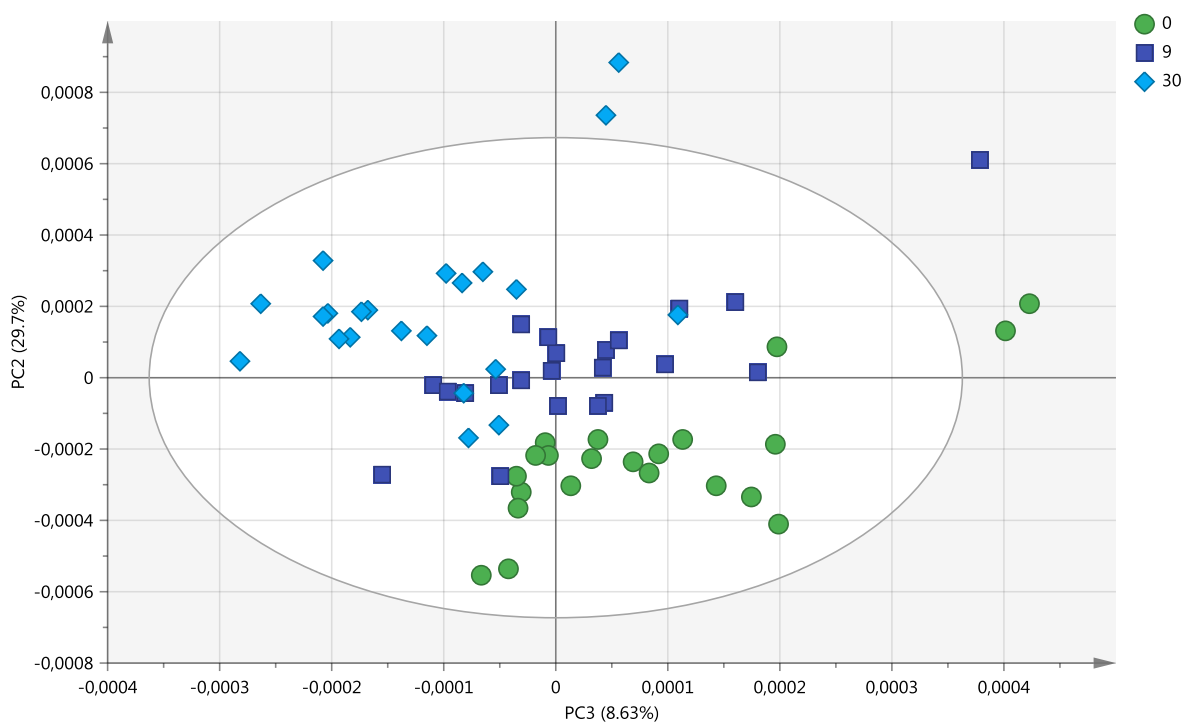
Figure 9.6: Scores plot of the PCA model built with the SNV and 2nd derivative preprocessed NIR spectra (7300-4000cm^{-1} spectral range) of the 125-dose vials exposed during 0, 9 and 30 days to room temperature.

9.3.2.3. Development of the prediction model

An orthogonal partial least squares (OPLS) regression model was first developed and offered the advantage to separate the variation correlated to the titer from the variation uncorrelated to the titer (for further spectral range optimization). Firstly, SNV preprocessed spectra were used but the effect of an additional 2nd derivative preprocessing was also evaluated (see further). Using the spectral range containing the amide A/II band (7300-4000cm^{-1}) demonstrated to be able to separate the different pre-freeze-drying treated samples, the developed OPLS model (62 spectra, 1 spectrum per titrated vial) explained 98.6% of the spectral variability and was composed by 1 predictive component (12.3% of spectral variability) and 4 orthogonal components. The predictive component (12.3% of spectral variability) versus orthogonal component 1 (71% of spectral variability) scores plot distinguished the vials according to the pre-freeze-drying treatment (Figure 9.7).

Figure 9.7: Scores plot of the OPLS model built with the SNV preprocessed NIR spectra (7300-4000cm^{-1} spectral range) of the calibration set.

At first, a permutation test was performed in order to verify that the model did not only fit the training set well, while poorly predicting new observations (see materials and methods section). The permutation plot is presented in Figure 9.8 and shows that the OPLS model was valid for several reasons: (i) the Q^2 values of the twenty permutations were lower than the Q^2 value of the original model, (ii) the Q^2 regression line intersected the y axis below 0 and finally, (iii) the R^2 values of the twenty permutations were lower than the R^2 value of the original model.
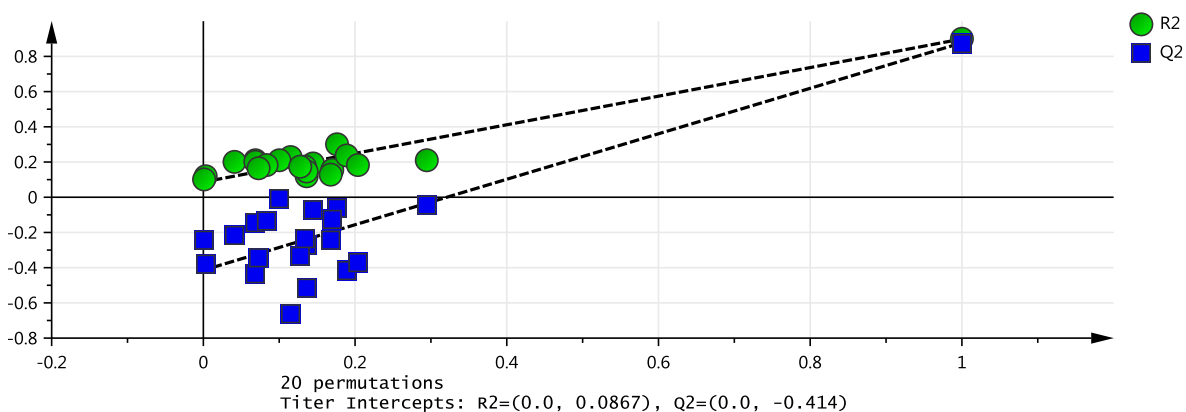
Figure 9.8: Permutation plot of the OPLS model built with the SNV preprocessed NIR spectra (7300-4000cm^{-1} spectral range).

The prediction of an independent test set (i.e., observations that were not used to build the model and coming from another batch) constitutes the best evaluation of the model performance.

The predicted titers and the observed (titrated) titers of the test set are presented in Figure 9.9. With a root mean square error of prediction (RMSEP) of 0.22 $\log_{10}$ $CCID_{50}$, the predicted titers of the test set were close to the titrated values.
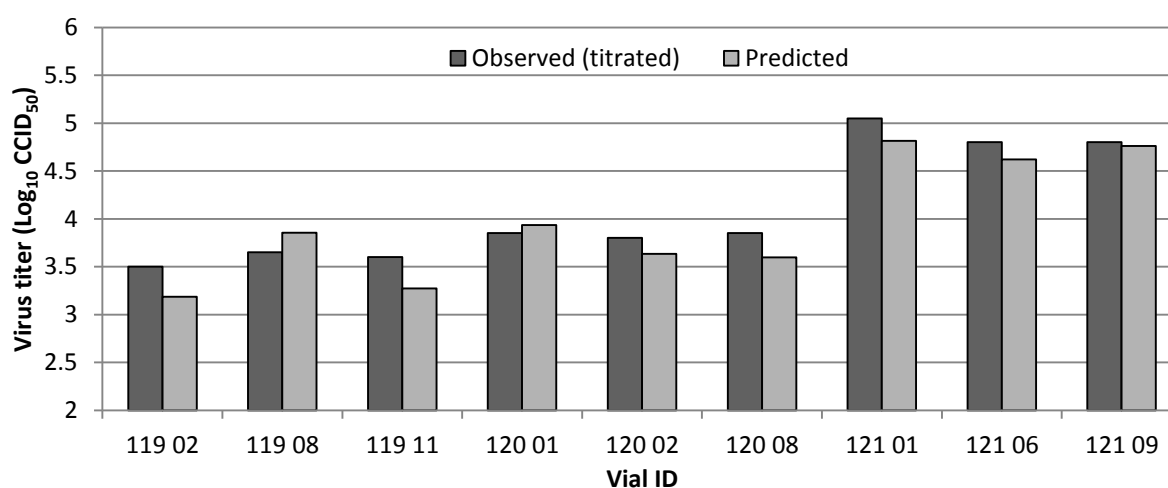
Figure 9.9: Observed and predicted virus titers by the OPLS model built with the SNV preprocessed NIR spectra (7300-4000cm^{-1} spectral range) of the vials coming from the test set. Titers are expressed as $\log_{10}$ $CCID_{50}$ (Cell Culture Infection Dose 50).

Model optimization was performed in order to improve the RMSEP of the model. Several optimization strategies such as: (i) PLS modelling, (ii) use of an additional preprocessing step (i.e. 2nd derivative) or (iii) selection of different spectral ranges were performed. Two supplemental spectral ranges were evaluated based on the loadings plot of the OPLS predictive component; (1) the 5029-4000cm^{-1} spectral range was used in order to avoid the contribution of the water bands, (2) the 5029-4690cm^{-1} spectral range was used in order to only consider the contribution of the amide A/II band. The different spectral ranges are presented in the loadings plot (Figure 9.10) of the predictive component of the OPLS model.
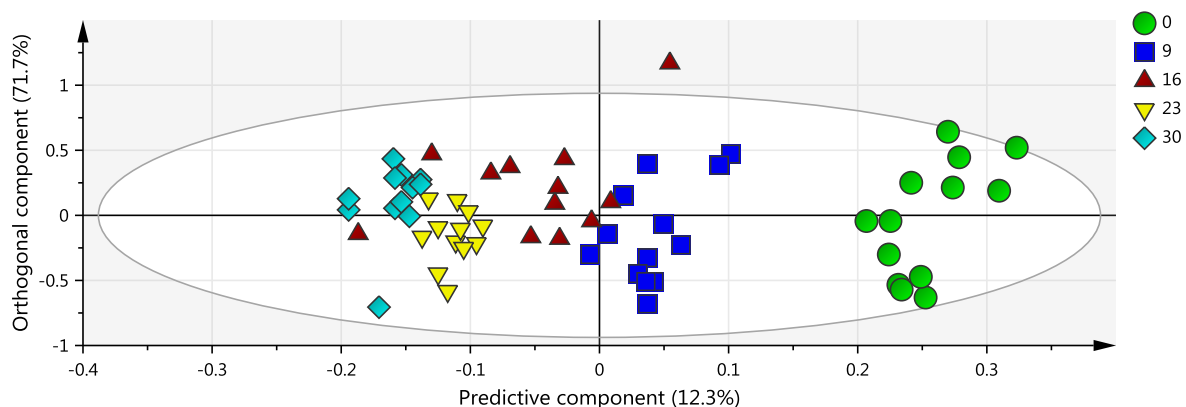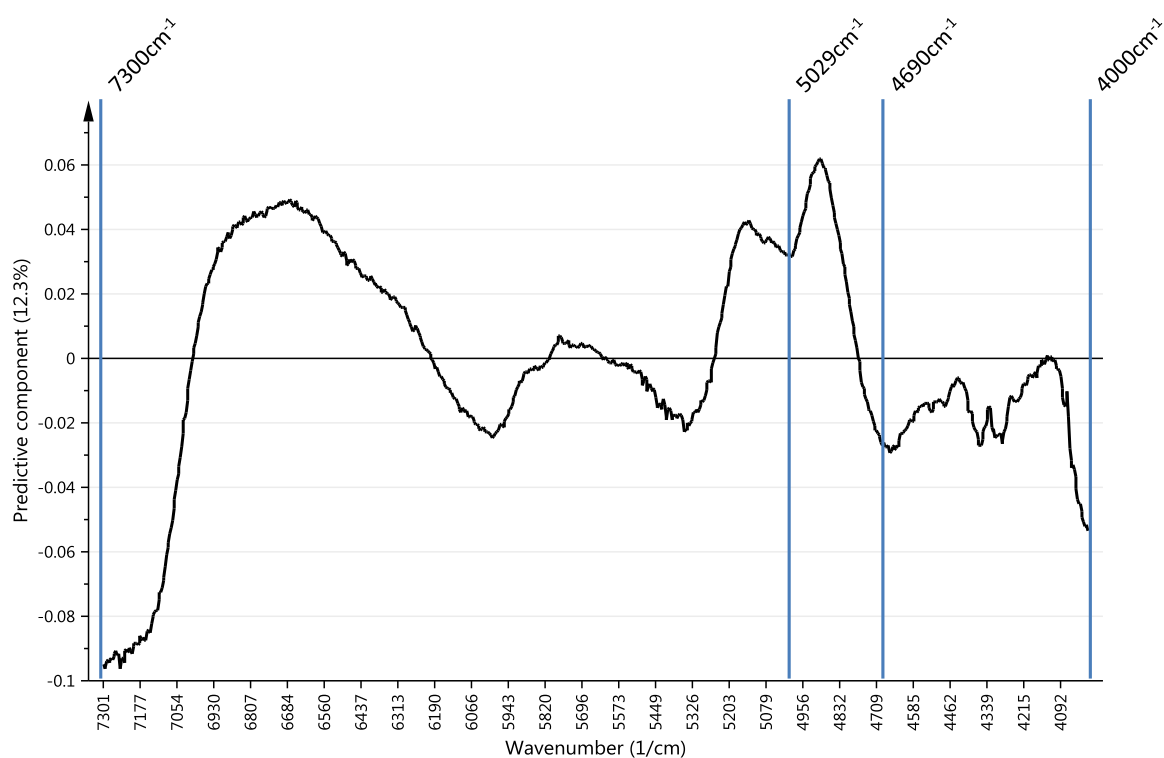
Figure 9.10: Loadings plot of the predictive component of the OPLS model built with the SNV preprocessed NIR spectra (7300-4000cm^{-1} spectral range) of the calibration set. The different spectral ranges evaluated in order to optimize the model are also presented.

The performances of the different resulting optimized models (by PLS modelling, 2nd derivative preprocessing and spectral range selection) are expressed in RMSEP and are presented in Table 9.3. A small RMSEP value indicates good quantitative performance of the model.

As can be seen from Table 9.3, the model type (i.e., PLS or OPLS) had no impact on the performance of the models based on the SNV preprocessed spectra. The additional 2nd derivative did not improve the prediction of an independent test set since the lowest RMSEP values were obtained for the models based on the SNV preprocessed spectra. Moreover, the permutation plots obtained for the models based on the spectra preprocessed with SNV and 2nd derivative showed a low validity of the models (data not shown). Therefore, the SNV preprocessed spectra should be used. Concerning the spectral range, the best RMSEP (0.19 log$_{10}$ CCID$_{50}$) was obtained when using the 5029-4000cm^{-1} spectral range.

Table 9.3: RMSEP values obtained for the different models in order to determine the best predictive model.

Spectral range	Model type	Preprocessing	RMSEP
7300-4000cm^{-1}	OPLS	SNV	0.22
		SNV and 2nd derivative	0.24
	PLS	SNV	0.22
		SNV and 2nd derivative	0.31
5029-4000cm^{-1}	OPLS	SNV	0.19
		SNV and 2nd derivative	0.50
	PLS	SNV	0.19
		SNV and 2nd derivative	0.22
5029-4690cm^{-1}	OPLS	SNV	0.26
		SNV and 2nd derivative	0.47
	PLS	SNV	0.27
		SNV and 2nd derivative	0.50

These results show that NIR spectroscopy is able to predict the titer of a new independent test set with a low RMSEP of 0.19 $\log_{10}$ CCID$_{50}$ using a PLS or an OPLS model, on the condition that the dose content is high enough. In order to further evaluate the suitability of the model for its intended use, the calibration set should be completed with supplemental datasets incorporating batch-to-batch variability.

Nevertheless, the determination of the RMSEP does not suffice to evaluate the risk that every future measurement will be close enough to the unknown true value of the sample. Appropriate validation (e.g., via accuracy profiles [21]) allowing to make a decision related to the validity of a method for future analyses is necessary.

The Société Française des Sciences et Techniques Pharmaceutiques (SFSTP) has developed a validation strategy based on the total error of the procedure (bias + standard deviation) [21]. This approach minimizes the risk to accept an inaccurate calibration method or to reject a capable method. Validation of the calibration model via accuracy profile should also be performed.

9.4. CONCLUSION

The aim of this study was to evaluate the possibility of NIR spectroscopy to predict the titer of new freeze-dried live, attenuated virus vaccine samples. The first phase of this study demonstrated that the 125-dose vials contained the only suitable dose content allowing to distinguish the differently pre-freeze-drying treated formulations (resulting in different titers). The second phase of the study demonstrated that NIR spectroscopy was able to predict the titer of independent vials with an RMSEP of 0.19 $\log_{10}$ $CCID_{50}$. PLS and OPLS models had the same predictive performance when using SNV preprocessed spectra which was the most successful spectral preprocessing method.

This demonstration of the possibility to predict the virus titer of new freeze-dried vials by NIR spectroscopy is promising for the future. Nevertheless, the detection sensitivity of NIR is a drawback for this application and the development of new analytical techniques having better detection sensitivity is needed. Moreover, before its implementation, the current model still needs to be improved by increasing the number of batches in the calibration set (including batch-to-batch variability in the model) and by evaluating more test sets. In addition, a thorough validation of the model via accuracy profiles is required.

REFERENCES

[1]   M.J. Pikal. Freeze Drying.In:Swarbrick JS, Boylan JC. Encyclopedia of Pharmaceutical Technology. New York: Marcel Dekker, 2002:1807-33.

[2]   Food and Drug Administration, 2004. http://www.fda.gov/downloads/Drugs/ GuidanceComplianceRegulatoryInformation/Guidances/ucm070305.pdf.

[3]   T. De Beer, A. Burggraeve, M. Fonteyne, L. Saerens, J.P. Remon, C. Vervaet. Near-infrared and Raman spectroscopy for the in-process monitoring of pharmaceutical production processes. International Journal of Pharmaceutics, 2011; 417: 32-47.

[4]   M. Brülls, S. Folestad, A. Sparén, A. Rasmuson. In-situ near-infrared spectroscopy monitoring of the lyophilization process. Pharmaceutical Research, 2003;20: 494-499.

 [5]   T. De Beer, M. Wiggenhorn, R. Veillon, C. Debacq, Y. Mayeresse, B. Moreau, A. Burggraeve, T. Quinten, W. Friess, G. Winter, JP. Remon, W.R. Baeyens. Importance of using complementary process analyzers for the process monitoring, analysis, and understanding of freeze-drying. Analytical Chemistry, 2009; 15: 7639-7649

[6]   T. De Beer, P. Vercruysse, A. Burggraeve, T. Quinten, J. Ouyang, X. Zhang, C. Vervaet, J.P. Remon, W.R. Baeyens. In-line and real-time process monitoring of a freeze-drying process using Raman and NIR spectroscopy as complementary process analytical technology (PAT) tools. Journal of Phamaceutical Sciences, 2009; 98: 3430-3446.

[7]   S. Pieters, T. De Beer, J.C. Kasper, D. Boulpaep, O. Waszkiewicz, M. Goodarzi, C. Tistaert, W. Friess, J.P. Remon, C. Vervaet, Y. Vander Heyden. Near-Infrared Spectroscopy for In-Line Monitoring of Protein Unfolding and Its Interactions with Lyoprotectants during Freeze-Drying. Analytical Chemistry, 2012; 84: 947-955

[8]   M.S. Kamat, R.A. Lodder, P.P. DeLuca. Near-infrared spectroscopic determination of residual moisture in lyophilized sucrose through intact glass vials. Pharmaceutical Reasearch, 1989;6: 961–965.

[9]   I.R. Last, K.A. Prebble. Suitability of near-infrared methods for the determination of moisture in a freeze-dried injection product containing different amounts of the active ingredient. Journal of Pharmaceutical and Biomedical analysis, 1993;11: 1071-1076.

[10]   J.A. Jones, I.R. Last, B.F. MacDonald, K.A. Prebble. Development and transferability of near-infrared methods for determination of moisture in a freeze-dried injection product. Journal of Pharmaceutical and Biomedical analysis, 1993;11: 1227-1231.

[11]   M. Savage, J. Torres, L. Franks, B. Masecar, J. Hotta. Determination of adequate moisture content for efficient dry-heat viral inactivation in lyophilized factor VIII by loss on drying and by near infrared spectroscopy. Biologicals, 1998;26(2): 119-24.

[12]   L. Hansen, S. Pieters, R. Daoussi, J.P. Montenez, C. Vervaet, J.P. Remon, T. De Beer. Near-infrared spectroscopic evaluation of lyophilized viral vaccine formulations. Biotechnology Progress, 2013; 29 (6): 1573-1586.

[13]   D.B. Volkin, C.J. Burke, G. Sanyal, C.R. Middaugh. Analysis of vaccine stability. Development in Biological standardization, 1996;87 : 135-142.

[14]   C.J. Burke, T-A. Hsu, D.B. Volkin. Formulation, stability, and delivery of live attenuated vaccines for human use. Therapeutic Drug Carrier Systems, 1999; 16 (1): 1-83.

[15]   D.T. Brandau, L.S. Jones, C.M. Wiethoff, J. Rexroad, C.R. Middaugh. Thermal stability of vaccines. Journal of Pharmaceutical Sciences, 2003;92(2): 218-231.

[16]   L. Zhang, M.J. Henson, S.S. Sekulic. Multivariate data analysis for Raman imaging of a model pharmaceutical tablet. Analytica Chimica Acta, 2005;545: 262-278.

[17]   A. de Juan, R. Tauler. Chemometrics applied to unravel multicomponent processes and mixtures: Revisiting latest trends in multivariate resolution. Analytica Chimica Acta, 2003;500: 195-210.

[18]   H. Eastment, and W. Krzanowski. Crossvalidatory choice of the number of components from a principal component analysis, Technometrics, 1982; 24: 73-77

[19]   L. Eriksson, E. Johansson, N. Kettaneh-Wold, J. Trygg, C. Wikström, S. Wold. Multi- and Megavariate Data Analysis. Part I: Basic Principles and Applications. Umea: Umetrics, 2006.

[20] J. Luypaert, D.L. Massart, Y. Vander Heyden. Near-infrared spectroscopy applications in pharmaceutical analysis. Talanta, 2007;72: 865-883.

[21] P. Hubert, J.J. Nguyen-Huu, B. Boulanger, E. Chapuzet, N. Cohen, P.A. Compagnon, W. Dewé, M. Feinberg, M. Laurentie, N. Mercier, G. Muzard, L. Valat, E. Rozet. Harmonization of strategies for the validation of quantitative analytical procedures: A SFSTP proposal–Part III. Journal of Pharmaceutical and Biomedical analysis, 2007;45: 82-96.

SUMMARY AND GENERAL CONCLUSIONS

Freeze-drying is today the preferred method for stabilizing live, attenuated virus vaccines. Despite its wide use in the pharmaceutical industry, freeze-drying formulation and process development of live, attenuated virus vaccines are still performed by trial-and-error experimental work resulting in sub-optimal processes. The stabilization and destabilization mechanisms of the live, attenuated viruses during freeze-drying, are still not fully understood. The molecular complexity of live, attenuated viruses, the multiple destabilization pathways and the lack of analytical techniques allowing the measurement of physicochemical changes in the antigen's structure during and after lyophilization partly explain this lack of knowledge. Therefore, the possibility to apply spectroscopic process analytical tools, in particular NIR and FTIR spectroscopy, to (i) evaluate live, attenuated viruses and their interactions with the stabilizer(s) in freeze-dried samples, (ii) understand virus destabilization mechanisms during storage and (iii) develop practical applications using chemometric models to predict critical end product quality parameters, has been evaluated in this thesis.

In **chapter 2** of this thesis, the freeze-drying process and its used processing equipment is outlined. The freeze-drying process consists of 3 main consecutive steps: freezing, primary drying and secondary drying. During freezing, most of the water is converted into ice. Afterwards, the ice is removed by sublimation (primary drying) and finally, the unfrozen water is removed by desorption (secondary drying).

Although being costly, energy intensive and time consuming, freeze-drying is the preferred stabilization method for biopharmaceuticals. However, despite its wide use and decades of research, the stabilization and destabilization mechanisms of the live, attenuated viruses, the optimal formulation components and process settings are still matter of research. **Chapter 3** reviews the existing knowledge on the freeze-drying process of live, attenuated virus vaccines. The different stresses that viruses may encounter during the different freeze-

drying process steps as well as the mechanisms and strategies (formulation and process) that are used to stabilize them during freeze-drying are overviewed. During freezing, several stresses (intra-virus ice formation, osmolarity change, pH shift, coated protein and lipid layer destabilization) may decrease the live, attenuated virus stability. The selection of an appropriate cryoprotectant and cooling rate are the two main strategies used to avoid these stresses. Information related to the destabilization mechanisms during the drying steps is rather limited. The lipid membrane and the coated viral proteins are the main attributes susceptible to degradation. Both can be protected by the use of stabilizers which stabilize the viruses via the vitrification hypothesis and/or the water replacement hypothesis.

In order to improve product quality and process performance, the pharmaceutical industry is encouraged by the regulatory authorities to implement QbD and PAT principles into their manufacturing processes. **Chapter 4** summarizes the concept of QbD/PAT and addresses some unique considerations coming into play with biotechnological processes and products. The different PAT tools such as Tunable Diode Laser Absorption Spectroscopy (TDLAS), Manometric Temperature Measurement (MTM), Temperature Remote Interrogation System (TEMPRIS), Thermocouples and spectroscopic tools, available to monitor the critical process and product parameters during freeze-drying are overviewed. Their main advantages and disadvantages are also presented. Finally, the measurement principles of the spectroscopic process analytical tools used in this thesis (NIR and FTIR spectroscopy) are described. Several studies related to the product monitoring during freeze-drying have been conducted using both tools and are also presented. The monitoring of residual moisture content as well as the protein behaviour, off-line and in-line, are the most frequent applications of NIR spectroscopic monitoring of freeze-drying. FTIR spectroscopy is recognized to be the tool of choice for analyzing (off-line) the protein secondary structure.

In **chapter 5**, the possibility to use NIR spectroscopy for the distinction between different freeze-dried live, attenuated virus formulations is evaluated. NIR spectra of freeze-dried samples prepared using different virus medium volumes or using different pre-freeze-drying virus treatments (resulting in different virus states) were collected and analyzed using principal component analysis (PCA). Distinction between the formulations varying in terms of 'virus pretreatment' as well as 'virus volume' was possible. Two specific spectral ranges; (1) 7300-4000cm^{-1} containing the amide A/II region (2) 10,000-7500 and 6340-5500cm^{-1}

containing the first and second overtones of CH vibrations allowed this distinction. The possibility to classify new samples according to their pre-freeze-drying virus treatment using a partial least squares discriminant analysis (PLSDA) model was also assessed. Model cross-validation was successful (i.e., correct classification rate of 100%) whereas the prediction of an external independent data test set was not optimal (i.e., correct classification rates of 55.17% and 82.5% depending on the tested formulation).

Once the suitability of NIR spectroscopy to distinguish between freeze-dried samples containing different virus states and virus medium volume was demonstrated, a similar evaluation (using the same strategy) was examined for FTIR spectroscopy in **chapter 6**. FTIR spectra collected on freeze-dried samples varying in virus medium volume, pre-freeze-drying virus treatment or virus dose were analyzed using PCA. Three spectral regions which might provide information on the coated proteins of freeze-dried live, attenuated viruses, being (i) 1700-1600cm^{-1} (amide I band), 1600-1500cm^{-1} (amide II band) and 1200-1350cm^{-1} (amide III band), were evaluated. The amide III spectral range, not influenced by water, was the most appropriate one to distinguish between the different virus medium volume, pre-freeze-drying virus treatment and virus dose samples.

Taking advantage of the findings of chapters 5 and 6, both process analytical spectroscopic techniques (NIR and FTIR) were linked to the results of traditional end product analysis tools **(chapter 7)** in order to better understand freeze-dried live, attenuated virus destabilization mechanisms during storage. Freeze-dried samples stored during four weeks at 4°C or at 37°C were weekly analyzed by NIR and FTIR spectroscopy as well as potency assay, Karl Fischer and modulated differential scanning calorimetry (MDSC).

Stored at 37°C, the virus titer decreased and the relaxation enthalpy increased according a two phase pattern, suggesting a link between mobility and virus destabilization. Evaluation of the amide A/II band (NIR spectra) revealed that the destabilization of the virus was probably linked to a change in the hydrogen bonds strength between trehalose (the stabilizer) and the virus proteins. By studying the amide III band (FTIR spectra), it was found that the virus destabilization was coupled to a decrease of β-turn and an increase of α-helix. Together, NIR and FTIR spectroscopy showed that the relaxation enthalpy (i.e., the molecular mobility) increase upon storage played a role in the stability of the viruses by modifying the strength of the hydrogen bonds between the virus coated proteins and the amorphous

trehalose used as stabilizer. At 4°C, under conditions specified for long term storage, the virus titer remained constant and no relaxation enthalpy was observed.

The aim of **chapter 8** was to develop a model able to classify freeze-dried samples according to their dose content based on off-line collected NIR spectra. Three different dose presentations (i.e., 125, 50, 25) and a placebo were used and 6 batches were freeze-dried. Three batches were used to develop the model (i.e., the calibration set), two batches to test the model (i.e., test set) and finally, one batch to evaluate the robustness of the model. Soft Independent Modelling of Class Analogy (SIMCA) was applied to classify the four dose presentations. Spectral range optimization was performed using Orthogonal Partial Least Squares (OPLS) regression analysis. The optimized calibration model was able to classify vials of an independent test set with a global correct classification rate of 98.5% (test set Zoe 4). The optimized model was also characterized for its specificity, sensitivity and accuracy following the EMA guidelines. Finally, the robustness study demonstrated that the classification of new vials was sensitive to their residual moisture content.

In **chapter 9**, the possibility to predict the titer of a freeze-dried live, attenuated virus vaccine formulation using NIR spectroscopy was assessed. A calibration data set existing of NIR spectra of freeze-dried 125-dose vials, exposed 0, 9, 16, 23 or 30 days to room temperature prior to freeze-drying and resulting in different virus titers, was used as calibration set and modeled using orthogonal partial least squares (OPLS) and partial least squares (PLS) regression. After spectral range and preprocessing optimization, the model was able to predict the titer of new independent freeze-dried 125-dose vials exposed 0, 7 and 11 days to room temperature with a Root Mean Square Error of Prediction (RMSEP) of 0.19 $\log_{10}$ $CCID_{50}$.

Two different live, attenuated virus species were used during this thesis. Species A, formulated in monodose was used in chapters 5, 6 and 7 whereas species B, formulated in multidose was used in chapter 6, 8 and 9.

SAMENVATTING EN ALGEMENE CONCLUSIE

Vriesdrogen (lyofiliseren) is de methode bij uitstek voor de stabilisatie van levend, verzwakte virussen in vaccins. Ondanks hun ruime gebruik in de farmaceutische industrie, gebeurt de formulatie- en procesontwikkeling die gepaard gaat met het vriesdrogen van levend, verzwakte virussen nog steeds via experimentele *trial-and-error*, wat leidt tot suboptimale processen. De stabilisatie en destabilisatie mechanismen voor levend, verzwakte virussen tijdens het vriesdroog proces zijn nog niet volledig ontrafeld. De moleculaire complexiteit van levend, verzwakte virussen, de verschillende oorzaken van destabilisatie en het gebrek aan analytische technieken voor de detectie van fysicochemische veranderingen in de antigen structuur tijdens en na lyofilisatie zijn een gedeeltelijke verklaring voor dit gebrek in kennis. Omwille van deze reden werd de toepasbaarheid van spectroscopische proces analytische technieken, in het bijzonder NIR en FTIR spectroscopie, onderzocht in het kader van (i) de evaluatie van levend, verzwakte virussen en hun interactie met cryo- en lyoprotectanten, (ii) het begrijpen van destabilisatie mechanismen van virussen tijdens langdurige bewaring en (iii) de ontwikkeling van praktische toepassingen, gebruik makende van chemometrische modellen, met als doel het voorspellen van kritische kwaliteitsparameters van het eindproduct.

In **hoofdstuk 2** van deze thesis wordt het vriesdroog proces en materiaal uitgebreid beschreven. Het vriesdroog proces bestaat uit 3 opeenvolgende fases: invriezen, primair drogen en secundair drogen. Tijdens de invriesstap wordt het grootste deel van het water

omgevormd naar ijs. Daarna wordt het gevormde ijs verwijderd via sublimatie (primair drogen) en uiteindelijk wordt het onbevroren water verwijderd via desorptie (secundair drogen). Ondanks de hoge kosten, het enorme energieverbruik en de lange procestijd, is vriesdrogen het voorkeursproces voor het stabiliseren van biofarmaceutische producten. Hoewel, ondanks het wijde gebruik en de vele jaren onderzoek, zijn de stabilisatie en destabilisatie mechanismen van levend, verzwakte virussen, de optimale formulatie samenstelling en proces instellingen nog steeds een belangrijk onderzoeksonderwerp.

Hoofdstuk 3 voorziet een overzicht van de huidige kennis over het vriesdrogen van levende, verzwakte virus vaccins. De verschillende stress factoren die gepaard gaan met de opeenvolgende processtappen en zowel de beschermingsmechanismen als de verschillende strategieën voor stabilisatie, formulatie en proces gerelateerd, tijdens vriesdrogen, worden besproken. Tijdens het invriezen zijn er verschillende stress factoren (intravirale ijsvorming, osmolariteitsveranderingen, pH wijzing, destabilisatie van mantelproteïnen en/of het lipidenmembraan) die de stabiliteit van levend, verzwakte virussen kunnen aantasten. Het toevoegen van een geschikt cryoprotectant of het aanpassen van de invriessnelheid zijn de twee belangrijkste strategieën die worden toegepast om het virus te beschermen tegen deze stress factoren. Informatie gerelateerd aan de destabilisatie mechanismen tijdens de droogstappen zijn beperkt. Het lipidenmembraan en de eiwitten hierin ingebed zijn het meest gevoelig voor degradatie. Beide kunnen beschermd worden door gebruik te maken van lyoprotectanten die het virus stabiliseren volgens de vitrificatie theorie of de watervervang theorie.

Met het oog op het verbeteren van de productkwaliteit en de procesprestaties, wordt de farmaceutische industrie aangemoedigd door de regelgevende instanties om *QbD* en *PAT* te

implementeren in de productieprocessen. **Hoofdstuk 4** geeft een samenvatting van het

QbD/PAT concept en wijdt aandacht aan enkele specifieke overwegingen inzake

biotechnologische processen en producten. De verschillende PAT technologieën zoals

Tunable Diode Laser Absorption Spectroscopy (TDLAS), manometrische temperatuur

metingen (MTM), *Temperature Remote Interrogation System* (TEMPRIS), thermokoppels en

spectroscopische technieken, die toelaten kritische proces- en productparameters te

monitoren tijdens het vriesdrogen, worden besproken, inclusief hun voornaamste voor- en

nadelen. Tot slot wordt een beschrijving gegeven van de meetprincipes van de

spectroscopische proces analytische technologieën, aangewend in deze thesis (NIR en FTIR

spectroscopie). Verschillende studies werden reeds gewijd aan het monitoren van product

karakteristieken, gebruik makende van beide technologieën en deze worden voorgesteld.

Monitoring van het residuele vochtgehalte en het gedrag van proteïnen, zowel *off-line* als *in-line*, zijn de voornaamste toepassingen van NIR spectroscopie bij vriesdrogen. FTIR

spectroscopie daarentegen wordt beschouwd als de methode bij uitstek voor de (*off-line*)

analyse van de secundaire structuur van proteïnen.

In **hoofdstuk 5** werd geëvalueerd of NIR spectroscopie in staat is een onderscheid te maken

tussen verschillende gevriesdroogde levend, verzwakte virus formulaties. NIR spectra van

gevriesdroogde stalen, bereid uit verschillende virus media volumes of gebruik makende van

verschillende pre-vriesdroog behandelingen van het virus (resulterend in een verschillende

staat van het virus) werden opgenomen en geanalyseerd via principale componenten

analyse (PCA). Dit liet toe een onderscheid te maken tussen de formulaties die varieerden in

zowel de voorbehandeling van het virus als in het virus media volume. Twee specifieke

spectrale regio's droegen bij tot dit onderscheid: (1) 7300-4000 cm^{-1}, die de amide A/II regio

bevat en (2) 10 000-7500 en 6340-5500 cm^{-1}, die de eerste en tweede overtoon van CH vibraties bevatten. De mogelijkheid tot classificatie van nieuwe stalen volgens de pre-vriesdroog behandeling van het virus gebruik makende van een partiële kleinste kwadraten discriminantanalyse (PLSDA) model werd ook onderzocht. Cross-validatie van het model was met een correcte classificatiescore van 100% succesvol, de predictie van een externe onafhankelijke data set daarentegen was niet optimaal, met correcte classificatie scores van 55,17% en 82,5%, afhankelijk van de geteste formulatie.

Eenmaal de geschiktheid van NIR spectroscopie werd aangetoond om een onderscheid te maken tussen gevriesdroogde stalen die verschilden in staat van het virus en virus media volume, werd een gelijkaardige evaluatie gebaseerd op dezelfde strategie uitgevoerd voor FTIR spectroscopie in **hoofdstuk 6**. Ook hier werden FTIR spectra van gevriesdroogde stalen, bereid uit verschillende virus media volumes, gebruik makende van verschillende pre-vriesdroog behandelingen van het virus (resulterend in een verschillende staat van het virus) of virus dosis opgenomen en geanalyseerd via PCA. Hiertoe werden drie spectrale regio's onderzocht die mogelijk informatie zouden bevatten over de mantelproteïnen van gevriesdroogde levend, verzwakte virussen, namelijk (i) 1700-1600 cm^{-1} (amide I band), 1600-1500 cm^{-1} (amide II band) en 1200-1350 cm^{-1} (amide III band). De amide III spectrale regio, vrij van storende water signalen, is de meest geschikte regio om een onderscheid te maken tussen de stalen met een verschillend virus media volume, pre-vriesdroog behandeling en virus dosis.

Gebruik makende van de bevindingen uit hoofdstuk 5 en 6, werden beide proces analytische spectroscopische technieken (NIR en FTIR) gelinkt aan de resultaten van de traditionele analysetechnieken op de kwaliteit van het eindproduct (**hoofdstuk 7**), met als finaal doel een

beter inzicht te krijgen in de destabilisatie mechanismen tijdens de bewaring van gevriesdroogde levend, verzwakte virussen. Gevriesdroogde stalen die gedurende 4 weken werden bewaard bij 4°C of 37°C, werden wekelijks geanalyseerd via NIR en FTIR spectroscopie alsook via virale potentie bepalingen, Karl Fischer en gemoduleerde differentiële scanning calorimetrie (MDSC).

Bij de stalen bewaard bij 37°C nam de virus titer af en nam tegelijkertijd de relaxatie enthalpie toe volgens een twee fasen patroon, wat een link suggereert tussen mobiliteit en virus destabilisatie. Evaluatie van de amide A/II band in de NIR spectra onthulde dat destabilisatie van het virus waarschijnlijk is gelinkt aan een verandering in de kracht van de waterstofbindingen tussen trehalose, het protectant, en de mantelproteïnen van het virus. Onderzoek van de amide III band in de FTIR spectra duidt erop dat virus destabilisatie gelinkt is aan een afname van de *β turn* conformatie en een toename in *α helix*. De combinatie van NIR en FTIR spectroscopie toont aan dat de toename in relaxatie enthalpie tijdens bewaring, gelinkt aan de moleculaire mobiliteit, een rol speelt bij het stabiliseren van virussen door het modificeren van de kracht van de waterstofbindingen tussen de virale mantelproteïnen en het amorfe protectant, trehalose. Bij 4°C, specifieke condities voor bewaring op lange termijn, blijft de virus titer constant en werd er geen enthalpie relaxatie vastgesteld.

Het doel van **hoofdstuk 8** was de ontwikkeling van een model dat toelaat om gevriesdroogde stalen te classificeren op basis van hun dosis, gebaseerd op *off-line* gemeten NIR spectra. Drie verschillende doses (125, 50 en 25) en een placebo werden gebruikt en 6 batches werden gevriesdroogd. Drie van deze batches werden gebruikt voor de ontwikkeling van het model, de calibratie set, twee batches dienden om het model te testen, de test set, en, tot slot, de laatste batch werd gebruikt ter evaluatie van de robuustheid van het model.

261

Soft Independent Modelling of Class Analogy (SIMCA) werd toegepast ter classificatie van de vier verschillende doses. Optimalisatie van de spectrale regio werd bekomen via orthogonale partiële kleinste kwadratenregressie analyse (OPLS). Het geoptimaliseerde calibratiemodel was in staat om stalen van een onafhankelijke test set te classificeren met een globale correcte classificatie score van 98,5% (test set Zoe 4). Daarnaast voldeed het geoptimaliseerde model aan de richtlijnen van EMA voor zowel specificiteit, sensitiviteit als accuraatheid. Tot slot, de robuustheidstudie toonde aan dat de classificatie van nieuwe stalen gevoelig is voor hun residuele vochtgehalte.

In **hoofdstuk 9** werd de mogelijkheid onderzocht om de titer te voorspellen van gevriesdroogde levend, verzwakte virus vaccin formulaties via NIR spectroscopie. NIR spectra werden opgenomen van gevriesdroogde stalen (125 doses), die alvorens het vriesdrogen werden blootgesteld aan kamertemperatuur voor 0, 9, 16, 23 of 30 dagen, wat uiteindelijk resulteerde in verschillende virus titers. Deze NIR spectra fungeerden als calibratie set en werden gemodelleerd via orthogonale partiële kleinste kwadratenregressie (OPLS) en partiële kleinste kwadratenregressie (PLS). Na optimalisatie van de spectrale regio en *preprocessing* van de spectra, was het model in staat om de titer te voorspellen van nieuwe, onafhankelijke gevriesdroogde stalen (125 doses) die gedurende 0, 3 of 7 dagen werden blootgesteld aan kamertemperatuur met een gemiddelde kwadratische fout op de voorspelling (RMSEP) van 0,19.

Tijdens deze thesis werd met twee verschillende levend, verzwakte virussoorten gewerkt. Soort A, geformuleerd als monodosis vaccin, werd gebruikt in het kader van hoofdstuk 5, 6 en 7, soort B, geformuleerd als multidoses, werd gebruikt in het kader van hoofdstuk 6, 8 en 9.

BROADER INTERNATIONAL CONTEXT, RELEVANCE, AND FUTURE PERSPECTIVES

The general aim of this thesis was to evaluate the potential of spectroscopic tools as process analytical techniques for the evaluation of live, attenuated viruses in freeze-dried vaccine formulations.

The specific objectives of this thesis are listed below:

- Find out if process analytical techniques can be used to evaluate (and hence understand) live, attenuated viruses and their interactions with other compounds (i.e., stabilizers), in freeze-dried vaccine formulations;
- Using process analytical techniques, increase the understanding of virus destabilization mechanisms during processing and storage;
- Develop and validate chemometric models allowing the prediction of the (or some) end product quality attributes of live, attenuated virus vaccines from fast spectroscopic at-line measurements making some traditional time-consuming off-line end product analyses superfluous.

Three important topics are addressed and confer this thesis an international dimension as well as evaluating and providing new opportunities for the pharmaceutical industry: (i) vaccines (biopharmaceuticals), (ii) freeze-drying and (iii) Process Analytical Technology (PAT).

BROADER INTERNATIONAL CONTEXT

Biopharmaceuticals are considered the key driver of future growth in the pharmaceutical industry [1]. Influential biopharmaceutical companies predict a compound annual growth rate of 4.4% for biopharmaceutical products as contrasted to small-molecule products with a growth rate below 1% [2].

Coming from $33 billion sales in 2005, to $82 billion in 2010 and $109 billion in 2012, IMARC (International Market Analysis Research and Consulting) expects the global biopharmaceutical market to exceed sales worth $166 billion by 2017. The market is currently dominated by monoclonal antibodies (50%), followed by recombinant proteins and vaccines.

The freeze-drying process has become a well-established and preferred stabilization technique for biopharmaceuticals since approximately 46% of the biopharmaceuticals that are currently on the market are freeze-dried (Figure. 11.1) [3].
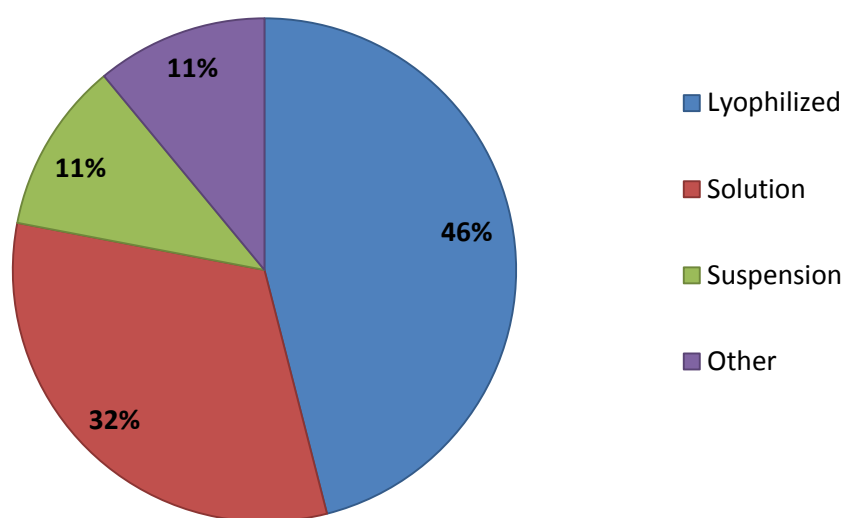

Figure 11.1: FDA-approved biopharmaceuticals grouped according to dosage form. The category denoted "other" includes frozen solution, oral forms (tablets and capsules), depots, gels and emulsions. Adapted from [3].

As mentioned in chapter 3, except the oral polio vaccine (OPV) which is stable in aqueous solution, all live virus vaccines are freeze-dried, emphasizing the importance of this process for the worldwide health. However, the frequent use of freeze-drying does not mean that the processes are optimized. Despite the numerous studies performed, the destabilization mechanisms as well as the optimal protection strategies during lyophilization and storage are still not well known. The lack of knowledge about the virus destabilization mechanisms is attributed to the complex structure of viruses, the multiple degradation routes and the lack of analytical techniques allowing the measurement of physicochemical changes in the

antigen's structure during and after freeze-drying. Quality is generally assessed by off-line time-consuming and less efficient laboratory testing which do not provide direct information to elucidate the mechanisms of destabilization and inactivation of viruses.

Therefore, in order to better understand the virus destabilization mechanisms and consequently improve the formulations and processes, analytical techniques that are able to monitor the product behaviour are needed.

Furthermore, the world of pharmaceutical freeze-drying is entering a new phase and is facing new challenges [4]. Indeed, the spectrum of pharmaceutical applications manufactured by lyophilization has broadened (e.g., nanoparticles, poorly soluble new chemical entities (NCE) or gene delivery systems) allowing for valuable pharmaceutical improvements but also resulting in more complex freeze-dried products. In order to develop optimized formulations and freeze-drying processes, a fundamental understanding of the stabilization mechanisms during the process and during storage is required.

In addition to the development of new types of drugs (which will result in more complex and more challenging freeze-dried products), medicines will also become more personalized, requiring more flexible manufacturing processes [5]. Offering the possibility to steer and control each vial individually, continuous freeze-drying is a possible solution to meet the manufacturing flexibility requirement for personalized medicines.

Conventional batch-wise freeze-drying suffers from some important inherent disadvantages such as:

- High production cost (high energy consumption, large area of space which is very expensive in terms of capital investment and operational/maintenance/exploitation costs) [6];
- Time consuming and labour intensive setup (the process needs to be optimized and validated first at lab-scale, followed by pilot-scale and finally at production scale);
- End product quality variability (uneven heat transfer in the freeze-drying chamber and uncontrolled freezing step at the vial level result in different freeze-drying process conditions in each vial, which might lead to uncontrolled vial-to-vial and batch-to-batch end product variability [7]);
- Lack of flexibility (only large batches can be produced);

- Slow and hence time-consuming and expensive process (the whole cycle may last 1 to 7 days (and even more) depending on the product properties and the dimensions of the vials).

To overcome these disadvantages, a continuous freeze-drying concept [8] is developed and evaluated at the laboratory of Process Analytical Technology where this thesis research was performed. Real-time quality evaluation and control of each freeze-dried vial, using in-line process analyzers, is crucial for the successful implementation of continuous freeze-drying. Therefore, process analytical methodologies have to be developed allowing the continuous monitoring and control of the critical process and product aspects. Furthermore, in-process measurement techniques are needed allowing the visualization and hence understanding of the formulation behaviour during processing (e.g., monitor the influence of the process conditions on the freeze-dried product, visualize the protection ability of stabilizers during processing).

Driven by the needs of the biopharmaceutical industry, the improvement of process understanding and control as well as the introduction of novel lyophilisation equipment will be subjected to more investigation in the coming years. Several process monitoring technologies have been developed for freeze-drying offering the possibility to improve process understanding and control. Especially since the introduction of the Quality by Design (QbD) and PAT concepts, launched by the regulatory authorities (FDA and EMA).

In conclusion, pharmaceutical freeze-drying is starting a new chapter with new challenges but also with new opportunities to "*build quality into (new) products*", one of the most important statements of the PAT concept.

More modestly, this thesis was performed under a close collaboration between Ghent University and Zoetis. Formerly Pfizer Animal Health, Zoetis is an international company which provides animal health products that prevent and treat diseases in livestock and companion animals. Throughout this thesis, the progresses, the obtained results, the experiments to be performed and the remaining challenges were discussed every three months with Belgian Zoetis colleagues as well as colleagues located at different Zoetis sites in the world.

RELEVANCE

Because of the current emphasis on QbD and PAT by the regulatory authorities and the increased complexity of freeze-dried products, it is needed to leave the traditional way of pharmaceutical freeze-drying and to move towards a risk- and science-based approach of freeze-drying process development.

Mainly product behaviour during freeze-drying is uncomprehended, and is partly due to the lack of analytical techniques. Experimental simulations of the in-process product behaviour are currently mainly done via differential scanning calorimetry (DSC) and freeze-drying microscopy measurements. However, these measurements do not fully represent the real process environment and do not reflect all relevant product quality attributes.

Spectroscopic tools such as NIR and FTIR spectroscopy evaluated in this thesis have gained attention as PAT tools in the pharmaceutical industry. Their combination represents a valuable tool to enhance lyophilization process understanding and efficiency, study formulation behaviour, reduce batch losses, reduce the time and costs for process development, reduce the product variability and decrease the time for product release. The freeze-drying process is very time-consuming and complex, and constitutes an important factor on the product cost. Especially, within animal health, where the margins on products are small and therefore any improvement on the cost of goods is crucial to compete in the market. Around 50 % of the veterinary vaccines within Zoetis are based on live attenuated virus strains and therefore an improvement in the freeze-drying process can have huge consequences for all these vaccines. The most important parameters for improvements are the yields of the antigen(s) after the freeze-drying process, the process time and the stability of the lyophilized product. Significant competitive advantages in the market can be obtained by improving these parameters.

The enumeration below summarizes the most important new findings brought by this thesis:

1. NIR and FTIR spectroscopy can be used as analytical techniques to evaluate viruses in freeze-dried vaccine formulations. The implementation of PAT tools, as stimulated by the regulatory bodies (FDA and EMA), to monitor the product behaviour might increase the process understanding and knowledge.

2. The virus behaviour and its interactions with a stabilizer during storage were studied. The obtained results can be used in order to improve the formulations and the process (improved yield and better stability).

3. NIR and FTIR spectroscopy analysis of the freeze-dried product might make some traditional time-consuming off-line end product analysis superfluous (time gain, faster release). The presented applications in this thesis demonstrated that NIR and FTIR spectroscopy might be used as fast screening tools at the end of the freeze-drying process.

FUTURE PERSPECTIVES

The aim of this thesis was to evaluate the potential of spectroscopic tools as process analytical techniques for the evaluation of live, attenuated viruses in freeze-dried vaccine formulations. The obtained results pave the way for new investigations and offer new interesting perspectives but also highlight the shortcomings of the investigated analytical techniques and the need of improvements in order to be able to answer the coming challenges.

The most important needed improvements are listed below:

- Better detection sensitivity in order to:

    o in-line monitor the virus behaviour <u>during</u> freeze-drying

    o increase knowledge of the virus destabilization mechanisms during processing and storage

    o evaluate more complex vaccine products (e.g., containing more than one antigen)

More sensitive new techniques such as; Raman optical activity (ROA), terahertz and fluorescence suppression Raman spectroscopy offer new opportunities to address these challenges and should be evaluated in the future.

- Development of new reference methods for virus characterization in order to:

  o compare the obtained spectra with better reference method than the potency assay (e.g., flow cytometry might be able to evaluate virus antigen fractions in bulks and lyophilized products and is currently under investigation at Zoetis)

However, the possibility to evaluate viruses off-line with NIR and FTIR spectroscopy already offers new opportunities listed below:

- Follow up the accelerated stability study and improve the product stability by:
  o performing an annealing step during secondary drying (i.e., increase the product temperature 15 to 20°C below Tg for a short period of time (from 5h to 20h depending on the formulation)) in order to achieve the lowest possible mobility. Different annealing conditions might be tested (i.e., annealing time and temperature)
  o screen new stabilizers by focusing on their mobility properties
- Implementation of the spectroscopic dose classification application at industrial scale
- Follow up of the titer prediction preliminary study by:
  o including more batches in the calibration model
  o perform robustness study of the calibration model
  o validate the calibration model using accuracy profiles
- Evaluation of other virus species (i.e., other vaccine products)
- Evaluation of the possibility to use NIR and FTIR spectroscopy to evaluate viruses at other steps of the vaccine production process

REFERENCES

[1]   PhRMA. 2011. Medicines in development: Biotechnology. ed.: Pharmaceutical Research and Manufacturers of America, http://www.phrma.org/sites/default/files/1776/biotech2011.pdf; p 1-96. Accessed on 12 September 2015

[2]   Shepard (2012): http://www.gtai.de/GTAI/Content/EN/Meta/Events/Invest/2012/ Reviews/Chemicalhealthcare/Dowloads/Breakfast-seminar-presentation-stephanie-shepard.pdf. Accessed on 12 September 2015

[3]   H.R. Constantino, M.J. Pikal. Lyophilization of Biopharmaceuticals. Arlington (VA): AAPS Press; 2004.

[4]   J.C. Kasper, G. Winter, W. Friess. Recent advances and further challenges in lyophilisation. European Journal of Pharmaceutics and Biopharmaceutics, 2013;85(2): 162-169.

[5]   Personalized Medicine Coalition (2011). Personalized Medicine by the Numbers. Retrieved from http://www.personalizedmedicinecoalition.org/. Accessed on 2 October 2015

[6]   S.W. Baertschi, K. Alsante, R. Reed. Pharmaceutical stress testing: prediction drug degradation, second edition, CRC Press 2011.

[7]   A. Kauppinen, M. Toiviainen, O. Korhonen, J. Aaltonen, K. Järvinen, J. Paaso, M. Juuti, J. Ketolainen. In-line multipoint near-infrared spectroscopy for moisture content quantification during freeze-drying. Analytical Chemistry, 2013; 85 (4): 2377–2384.

[8]   J. Corver. 2013. Method and system for freeze-drying injectable compositions, in particular pharmaceutical. WO2013036107.

CURRICULUM VITAE

Laurent Hansen

PERSONAL INFORMATION

SURNAME:	Hansen
FIRST NAMES:	Laurent Jean Julien
PRIVATE ADRESS:	Lenneke Marelaan 26A/10
	1932 Sint-Stevens-Woluwe
DATE OF BIRTH:	February 9th, 1985
NATIONALITY:	Belgian
EMAIL:	hansen.laur@gmail.com
PHONE:	+32/478 587571

LANGUAGE SKILLS

NATIVE LANGUAGE:	French
OTHER LANGUAGES:	Dutch
	English

EDUCATION

2011- present	Doctoral studies in Pharmaceutical Process Analytical Technology
	Ghent University
2008-2010	Masters degree in biochemistry, cell and molecular biology
	specialized in biotechnology. Graduated magna cum laude.
	Université catholique de Louvain
2004-2008	Bachelor in biological sciences. Graduated cum laude
	Université catholique de Louvain

PUBLICATIONS IN PEER REVIEWED JOURNALS

Freeze-drying of live virus vaccines: A review

Hansen L, Daoussi R, Vervaet C, Remon JP, De Beer T. **Vaccine** *2015, 33(42), 5507-5519.*

FTIR spectroscopy for the detection and evaluation of live attenuated viruses in freeze dried vaccine formulations

Hansen L, Pierre K, Pastoret S, Bonnegarde-Bernard A, Daoussi R, Vervaet C, Remon JP, De Beer T. **Biotechnology Progress** *2015, 31(4), 1107-1118.*

Thermoplastic polyurethanes for the manufacturing of highly dosed oral sustained release matrices via hot melt extrusion and injection molding

Claeys B, Vervaeck A, Hillewaere X. K.D, Possemiers S, Hansen L, De Beer T, Remon JP, Vervaet C. **European journal of Pharmaceutics and Biopharmaceutics**. *2015, 90, 44-52.*

Release characteristics of polyurethane tablets containing dicarboxylic acids as release modifiers – a case study with diprophylline.

Claeys B, De Bruyn S, Hansen L, De Beer L, Remon JP, Vervaet C. **International Journal of Pharmaceutics**. *2014, 477, 244-250.*

Near-infrared spectroscopic evaluation of lyophilized viral vaccine formulations

Hansen L, Pieters S, Montenez JP, Daoussi R, Vander Heyden Y, Vervaet C, Remon JP, De Beer T. **Biotechnology Progress***. 2013, 29 (6), 1573-1586.*

Raman spectroscopy and multivariate analysis for the rapid discrimination between native-like and non-native states in freeze-dried protein formulations.

Pieters S, Vander Heyden Y, Roger JM, D'Hondt M, **Hansen L***, Palagos B, De Spiegeleer B, Remon JP, Vervaet C, De Beer T.* **European journal of Pharmaceutics and Biopharmaceutics** *2013 85(2), 263-271.*

PRESENTATIONS AT CONFERENCES

Oral presentations

Hansen L, Pieters S, Montenez JP, Daoussi R, Vander Heyden Y, Vervaet C, Remon JP, De Beer T. Evaluation of lyophilized viral vaccine formulations using near-infrared spectroscopy

  - 16th Forum of Pharmaceutical Sciences (May 7th 2012, Blankenberge, Belgium).

  - EuPAT 5 (8th to 10th May 2012. Ghent, Belgium)

Hansen L, Pieters S, Montenez JP, Daoussi R, Vander Heyden Y, Vervaet C, Remon JP, De Beer T. Near-infrared spectroscopic evaluation of lyophilized viral vaccine formulations

  - 7th Annual PSSRC Meeting (4th to 6th July 2013, Lille, France)

  - 17th Forum of Pharmaceutical Sciences (October 17th 2013, Spa, Belgium)

Hansen L, De Wolf L, Pierre K, Daoussi R, Vervaet C, Remon JP, De Beer T. Spectroscopic dose classification and prediction of a freeze dried live attenuated virus vaccine.

  - International Conference on Lyophilization and Freeze-Drying (6th to 10th July 2015, Barcelona, Spain)

Poster presentations

Hansen L, Pieters S, Montenez JP, Daoussi R, Vander Heyden Y, Vervaet C, Remon JP, De Beer T. Evaluation of lyophilized viral vaccine formulations using near-infrared spectroscopy

- EuPAT 5 (8th to 10th May 2012. Ghent, Belgium)

- Freeze Drying of Pharmaceutical and Biologicals Conference (7th to 10th August 2012, Breckenridge, USA)

Hansen L, Pieters S, Montenez JP, Daoussi R, Vander Heyden Y, Vervaet C, Remon JP, De Beer T. Near-infrared spectroscopic evaluation of lyophilized viral vaccine formulations

- Knowledge for Growth, FlandersBio's jaarlijkse life science conventie (May 30th 2013, Ghent, Belgium)
- International Conference on Lyophilization and Freeze Drying (2nd to 4th October 2013, Sao Paulo, Brazil)

Poster award (outstanding poster presentation)

Hansen L, Daoussi R, Vander Heyden Y, Vervaet C, Remon JP, De Beer T. Evaluation of FTIR spectroscopy as a tool to detect live attenuated viruses in a freeze dried vaccine formulation

- Knowledge for Growth, FlandersBio's jaarlijkse life science conventie (May 8th 2014, Ghent, Belgium)

Hansen L, De Wolf L, Pierre K, Daoussi R, Vervaet C, Remon JP, De Beer T. Spectroscopic dose classification and prediction of a freeze dried live attenuated virus vaccine.

- International Conference on Lyophilization and Freeze Drying (6th to 10th July 2015, Barcelona, Spain)

ATTENDED COURSES AND WORKSHOPS

Course: Design of Experiment, February 2011, Ghent (Belgium)

Course: Multivariate data analysis, March 2011, Ghent (Belgium)

Course: Differential Scanning Calorimetry (DSC) Training course, November 2011, TA instruments, Zellik (Belgium)

Course: Modulated Differential Scanning Calorimetry (MDSC) Training course, November 2011, TA instruments, Zellik (Belgium)

Course: Fundamentals of Technology transfer, November 2011, UGent doctoral school (transferable skills), Ghent (Belgium)

Course: Leadership foundation, March 2012, UGent doctoral school (transferable skills), Ghent (Belgium)

Course: Insights in Lyophilisation, Current Best Practices & New research Trends, May 2012, Antwerp (Belgium)

Course: Clinical trials : study design, implementation and reporting , September 2013, UGent doctoral school (specialized course), Ghent (Belgium)

Training: Infrared spectroscopy & Chemometrics, February 2014, CRA-W, Gembloux (Belgium)

Course: Project management, January 2015, UGent doctoral school (transferable skills), Ghent (Belgium)

Workshop: Quality by Design & Infrastructure design and organization, July 2015, International Society of Lyophilization – Freeze Drying, Barcelona (Spain)